GALECTINS-1 AND -3 FUNCTIONS IN MÜLLER GLIA DURING RETINAL DEVELOPMENT AND DEGENERATION

PhD Thesis

Joshua Luis

Institute of Ophthalmology

University College London

DECLARATION

This dissertation is the result of my own work unless specifically indicated in the text. It has not been previously submitted, in part or whole, to any university or institution for any degree, diploma, or other qualification.

Signed: _____  _____

Date: _____21st September 2022 _____

Joshua Luis

ACKNOWLEDGEMENTS

It has been a huge pleasure to be part of the Müller laboratory group during my PhD. I feel very lucky to work with talented scientists who are also my good friends. Karen, Celia, Rachel, and Will have made the last few years immensely enjoyable and were there for me during a time of videoconferences and social distancing.

I am deeply grateful to have had two exceptional supervisors to guide me through my PhD. Professor Astrid Limb has been a constant source of support and advice. In addition to being a knowledgeable and experienced supervisor, Astrid always made herself available and had my best interests at heart. My second supervisor, Professor Sir Peng Khaw, has been a constant source of inspiration. I feel privileged to have been able to exchange ideas with him on a regular basis, as he never fails to broaden my perspective on science, healthcare, and patient advocacy.

I would like to thank Fight for Sight and Moorfields Eye Charity for their support in funding my PhD studies. It has been an invaluable experience for me, and I hope that I can continue to contribute to the visual sciences as I progress through my career.

Lastly, I could not have done any of this without the unwavering support and encouragement from my family. Having my parents and Aysha by my side is the greatest gift I could have asked for.

ABSTRACT

Within the retina, Müller glial cells (MGCs) are central regulators of metabolic homeostasis during normal function and during pathogenic states. MGCs are major producers of Galectins (Gal) -1 and -3, carbohydrate-binding proteins which have been found to be key regulators of various cellular processes. This study aimed to investigate the potential roles of Gal-1 and -3 during inflammatory stimuli, as well as during models of retinal development and degeneration.

Treatment of MIO-M1 cells with the pro-inflammatory cytokine IL-1 resulted in significant upregulation of Gal-1 ($p<.01$) and the sialylation enzyme ST3 beta-galactoside alpha-2,3-sialyltransferase 1 ($p<.01$), whereas treatment with TGF-β significantly reduced the production of Gal-3 ($p<.001$) but had no significant effect on ST6 beta-galactoside alpha-2,3-sialyltransferase 1 ($p>.05$). Inhibition of Gal-3 by siRNA increased the rate of MIO-M1 cell proliferation ($p<.001$). TGF-β2 treatment increased the rate of migration of MIO-M1 cells ($p<.01$), but this effect was nullified following Gal-3 siRNA inhibition. During retinal organoid development, Gal-1 mRNA and protein expression peaked between days 10 and 30, whilst Gal-3 mRNA and protein expression increased steadily to peak at the end of the experimental period of 90 days.

Using an experimental model of intraocular pressure elevation, Gal-3 protein expression was found to be upregulated in anterior chamber tissues including the iridocorneal angle and iris. Additional studies in a rodent model of optic neuropathy showed that MGC derived extracellular vesicles were effective in partially restoring retinal function at 2 weeks after treatment ($p<.001$). This effect, however, was not maintained at 4 weeks ($p>.05$), for which further investigations are merited.

Although the current study has provided a better understanding of the roles of Galectins during retinal development and degeneration, additional studies are warranted to elucidate the wider roles of Gal-1 and -3 during retinal degenerative diseases and explore any potential therapeutic applications of these molecules.

IMPACT STATEMENT

Degenerative retinal diseases include a wide range of conditions which globally represent a large burden of disease. Whilst various treatments are currently available for these diseases, our understanding of the molecular mechanisms which govern their progression remains incomplete. Müller glial cells are the major type of support cell within the retina, responsible for maintaining normal retinal function as well as coordinating protective responses during periods of stress or injury. Of particular significance is the discovery that certain species, such as the zebrafish, can regenerate their retinal tissue following injury, in processes which centre around Müller glial cells.

Galectins are a group of proteins which bind to specific sequences of sugar molecules. They are present throughout different human tissues and have been recently found to be important mediators of diseases such as cancer, inflammation, and fibrosis. Recent studies have found Müller glial cells to be a main source of Galectins within the retina, furthermore, the concentration of Galectins was significantly increased during retinal degeneration in human and zebrafish tissues. On this basis, the overall object of this study was to investigate the possible roles of Galectins -1 and -3 in the retina, within a wider context of developing Müller cell-derived therapies for degenerative retinal diseases.

Using the immortalised human Müller cells line, Moorfields-Institute of Ophthalmology Muller-1 lineage (MIO-M1), the present study showed that Galectin -1 and -3 production was modified by major cytokines released during retinal degeneration. Furthermore, Galectin-3 appeared to influence the growth, migration and contraction of Müller glial cells, possibly through the activation of cytokine signalling pathways within these cells. These are novel findings which further our current understanding of Galectins and their influence on MGC activities at a molecular level.

An important part of this study focused on the *in vitro* expression of Galectins -1 and -3 within retinal organoids derived from pluripotent stem cells. Retinal organoids are a landmark discovery in recent years, where stem cells cultured under specific conditions develop into highly organised retinal structures in culture. Expression of Galectins -1 and -3 was found to be precisely regulated throughout the different

stages of retinal organoid development and showed evidence of responding to external signalling molecules, similar to that observed with Müller cells in culture upon stimulation with pro-inflammatory cytokines. These findings highlight an under-recognised role for these molecules during retinal development, which in turn has potential implications for future studies on regenerative therapies.

Lastly, this study investigated whether extracellular vesicles derived from MGCs were able to partially restore retinal function as that observed with intact Müller cells. Using a NMDA model of optic neuropathy, a marked improvement of retinal function was observed following two weeks after intravitreal injection of these vesicles. However, this effect was transient as it was no longer observed after 4 weeks. These observations strongly suggest that a more refined protocol should be further explored to induce retinal repair with extracellular vesicles as a promising therapeutic modality.

In summary, the results from this study have provided novel insights into the roles of Galectin-1/-3 and extracellular vesicles within the retina. These findings further our understanding of the immensely complex processes involved in retinal development and degeneration, which in turn helps to make Müller cell-based neuroprotective and retinal regenerative treatments an ever-closer reality.

CONTENTS

LIST OF TABLES

LIST OF FIGURES

List of Abbreviations and Acronyms

AMD	Age-related macular degeneration
BDNF	Brain-derived neurotrophic factor
BRB	Blood retinal barrier
CBP	Carbohydrate binding proteins
CNS	Central nervous system
CNTF	Ciliary neurotrophic factor
DR	Diabetic retinopathy
ECM	Extracellular matrix
EGF	Epidermal growth factor
EHP	Elevated hydrostatic pressure
ELISA	Enzyme-linked immunosorbent assay
ELM	External limiting membrain
EMT	Epithelial Mesenchymal Transformation
ERG	Electroretinogram
ERK	Extracellular signal-regulated kinase
ESC	Embryonic stem-cell
EV	Extracellular vesicle
FGF	Fibroblast growth factor
GABA	Gamma-aminobutyric acid
Gal	Galectin
GFAP	Glial fibrillary acidic protein
GON	Glaucomatous optic neuropathy
HGF	Hepatic growth factor
HPMC	Hydroxypropyl methylcellulose
IHC	Immunohistochemistry

IL	Interleukin
ILM	Inner limiting membrane
INL	Inner nuclear layer
IOP	Intraocular pressure
LGALS	Lectin, galactoside-binding, soluble
MAPK	Mitogen-activated protein kinase
MGC	Müller glial cell
NFL	Nerve fibre layer
NGF	Nerve growth factor
NMDA	N-methyl-D-aspartate
NT-3/4	Neurotrophin-3/4
NTG	Normal tension glaucoma
OCT	Optic coherence tomography
ONH	Optic nerve head
ONL	Outer nuclear layer
OPL	Outer plexiform layer
PCR	Polymerase chain reaction
POAG	Primary open angle glaucoma
PSC	Pluripotent stem-cell
PTEN	Phosphatase and tensin homolog
PVR	Proliferative vitreoretinopathy
RGC	Retinal ganglion cells
RO	Retinal organoid
RPE	Retinal pigmented epithelium
SAG	Smoothened agonist
SMA	Smooth muscle actin

STAT	Signal transducer and activator of transcription
STR	Scotopic threshold response
TGF	Transforming growth factor
TM	Trabecular meshwork
TNF	Tumour necrosis factor
VEGF	Vascular endothelial growth factor

1. INTRODUCTION

1.1 Müller Glial Cells and Their Role Within the Retina

1.1.1 Structure and Function of the Retina

The vertebrate retina is a highly specialised tissue capable of converting light stimuli into meaningful neuronal signals. Incident light passes through the neuroretina to the photoreceptors, where it is detected and transduced into electrical signals; these signals are then encoded by a complex network of neurons before being transmitted to the brain. There is a strong spatial-temporal relationship as the signal generated from the outermost photoreceptors travel inward through the different sublayers of the neuroretina. Consequently, the structural organisation of the neuroretina is closely associated with its function.

As the initiating event of vision, phototransduction occurs at the outer segments of cone and rod photoreceptors, where large numbers of disks replete with visual opsins are densely stacked (Figure 1-1). The highly sensitive process of phototransduction demands a constant supply of energy, as evidenced by the abundance of mitochondria within the directly connected inner segment. Immediately proximal to the inner segment lies the external limiting membrane (ELM), formed from cell bodies of photoreceptors and Müller glial cells (MGCs). The ELM delineates the border of the outer nuclear layer (ONL), which contains the nuclei of the photoreceptors; followed by the outer plexiform layer (OPL), which contains the axons of the photoreceptors and their synapses with bipolar cells. In contrast to most cells of neuronal origin, photoreceptors possess the unusual property of being relatively depolarised in the absence of stimuli, only becoming hyperpolarised following activation of the phototransduction cascade. As a consequence, bipolar cells

divide into “ON” and “OFF” subtypes and perform the task sorting photoreceptor signals they receive at the OPL.

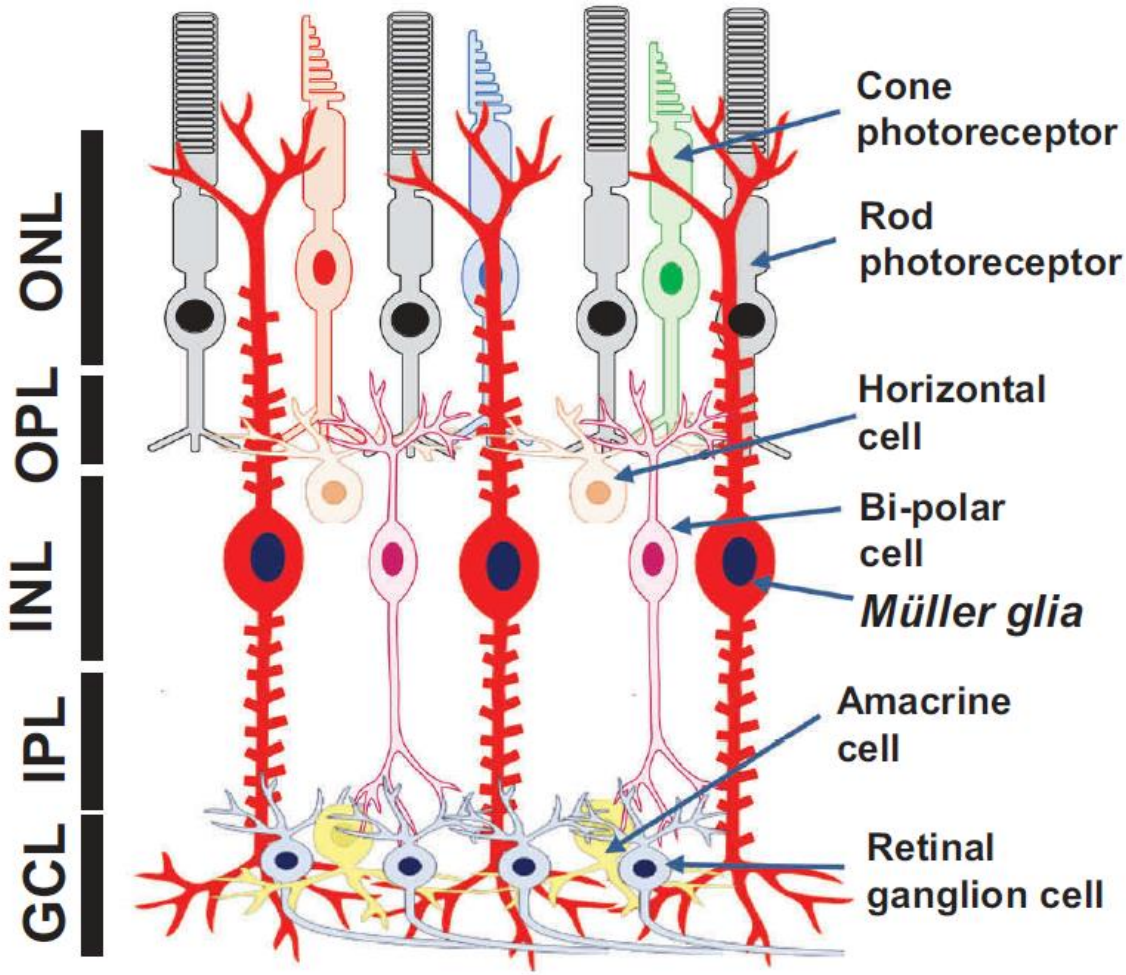

Figure 1-1 Structure and distribution of cell types within the retina. Müller glial cells span across the depth of the retina, and form the central support of neurovascular units. (Eastlake, Luis, and Limb 2019) OPL/IPL, outer/inner plexiform layer; ONL/INL, outer/inner nuclear layer; GCL, ganglion cell layer.

Neighbouring the OPL, the inner nuclear layer (INL) contains the nuclear bodies of several cell types, including bipolar, amacrine, horizontal and Müller Glial Cells (MGCs). Much of the visual signal encoding is performed by the neurons in this sublayer through a complex network of interconnections, which ultimately synapse with retinal ganglion cells (RGCs) within the inner plexiform layer (IPL). The RGCs are positioned across the ganglion cell layer (GCL) and project toward the optic disc via the nerve fibre layer (NFL). The terminal end

feet of MGCs together with astrocytes form the inner limiting membrane (ILM), which delineates the inner boundary between the neuroretina and the vitreous.

To accurately perform phototransduction, visual signal encoding and transmission, cells of the neuroretina require a tightly controlled microenvironment. This includes a suitable electrochemical gradient, a sufficient supply of metabolites and neurotransmitters, as well as the presence of appropriate trophic factors to maintain the specialisation and integrity of this highly organised tissue. MGCs are the major cell type responsible for these supportive functions within the healthy retina, as well as for the wide range of responses during pathological states.

1.1.2 Müller Glial Cell Morphology and Function

Müller Glial Cells are the principal glial cell type in the vertebrate retina and are positioned radially across the neuroretina (Figure 1-1). The somata of MGCs are located within the INL, from which processes extend in both directions to form constitutive parts of the ILM and ELM. Similar to other parts of the central nervous system (CNS), MGCs are central to the neurovascular units found within the retina, which allows them to envelope almost all neighbouring cells and structures into a columnar structure (Hawkins and Davis 2005). The adaptability of MGC morphology is a reflection of their function, as significant variation exists between different regions within the retina (Bringmann et al. 2006). It is this versatility that allows MGCs to perform their large repertoire of supportive functions (Newman and Reichenbach 1996).

MGCs continuously facilitate the exchange of ions and molecules between retinal vasculature, neurons, vitreous, and subretinal space via their extensive connections (Bringmann et al. 2013). This is in part due to the copious expression of water (aquaporin 4) and rectifying potassium (K+) channels on their surface, which play their respective roles in maintaining fluid balance and

the resting potential; both of which are essential requirements for proper neuronal firing (Newman 1993).

In contrast to the high metabolic demands of neurons which depend on their many mitochondria for aerobic metabolism, MGCs primarily rely on anaerobic glycolysis for their energy source. This property serves a dual purpose; firstly, it leads to the export of lactate to support the more energy efficient oxidative metabolism in neurons and photoreceptors (Poitry-Yamate, Poitry, and Tsacopoulos 1995); secondly, it contributes to the remarkable resistance MGCs exhibit to low energy states and helps to explain their improved preservation following retinal damage as compared to other cell types (Bringmann et al. 2006). In addition to providing metabolites for the neurons they serve, MGCs also continuously recycle the neurotransmitters glutamate and gamma-aminobutyric acid (GABA), both of which are converted to glutamine via the glutamine synthetase pathway and released for re-use by neurons (Biedermann, Bringmann, and Reichenbach 2002). The coupling of these crucial metabolic pathways between neurons and MGCs is an essential feature of normal retinal function, which becomes even more important at times of metabolic stress. For example, a transient rise in extracellular K+ concentration causes glycogenolysis in MCGs, demonstrating their capacity for adaptive energy supplementation in response to neuronal discharge (Reichenbach et al. 1993).

Other functions of MGCs include production of antioxidants such as glutathione; release of neurotrophic factors such as brain-derived neurotrophic factor (BDNF) to maintain neuronal integrity and differentiation; provision of an alternate retinal isomerase pathway for cone photoreceptors in the visual cycle; phagocytosis of cell debris; and an intriguing recent finding of an optical fibre-like property that minimises scatter of incident light (Franze et al. 2007). MGCs are intricately in tune with the retinal microenvironment and are central to the maintenance of homeostasis within the retina. Many of the MGC functions outlined above have been elucidated following studies of retinal

dysfunction, where the presence of certain stressors become too great for MGCs to control. The pathophysiology of retinal diseases is diverse and immensely complex, but reactive gliosis caused by excessive stress to MGCs is a common finding in a wide range of disease states. As such, understanding MGC reactive gliosis is essential in providing the insight required to develop potential treatment strategies.

1.1.3 Reactive Gliosis

The definition of reactive gliosis continues to evolve as its mechanisms become better understood. In general, reactive gliosis refers to a wide range of coordinated glial cell responses in the CNS following injury; however, the term itself is typically used to imply the proliferation of glial cells leading to scar formation in the CNS (Graca, Hippert, and Pearson 2018). The most consistent feature for detecting gliotic MGCs is the upregulation of intermediate filaments vimentin, glial fibrillary acidic protein (GFAP), synemin and nestin, which provide structural support to the hypertrophied MGCs and play an important part in stabilising damaged retinal structures (Lundkvist et al. 2004). These intermediate filaments may have further distinct roles in the gliotic process; specifically, GFAP is expressed intracellularly, nestin appears to extend into the subretinal space and contribute to scar formation, and synemin is more closely related to vascular structures (Bertaud, Qin, and Buehler 2010). In addition to gliosis causing striking structural alterations in MGCs and surrounding neural cells, metabolic pathways can also be profoundly affected.

The retina is subject to high levels of oxidative stress during normal function, due in large part to incoming light energy and high turnover of oxidative metabolites (Youssef, Sheibani, and Albert 2011). In some cases, this is further exacerbated by genetic predisposition, exogenous damage such as cigarette smoke, and mitochondrial dysfunction (Masuda, Shimazawa, and Hara 2017). Oxidative stress is increasingly recognised as a major

contributing factor in a number of retinal diseases, such as age-related macular degeneration (AMD), glaucoma, diabetic retinopathy (DR) and retinal vascular disorders (van Reyk, Gillies, and Davies 2003; Jarrett and Boulton 2012).

MGCs upregulate antioxidant production including glutathione and heme oxygenase-1 (HO-1) in the presence of increased oxidative stress (Ulyanova et al. 2001). An increased autophagic response also occurs in the presence of hydroquinone, an oxidative stress inducing aromatic organic phenol present at high concentrations in cigarette smoke (Ramirez et al. 2017). Although MGCs are relatively resistant to oxidative stress, at higher thresholds, a proliferative and dedifferentiating response can occur (Jadhav, Roesch, and Cepko 2009). As the source of injury increases, the overall viability of MGCs is reduced, and degeneration of surrounding neurons can be observed (Sardar Pasha et al. 2017). These findings highlight the ability for MGCs to respond to stressors in a calibrated manner, depending on their nature, severity, and duration.

Another key feature of retinal damage is the elevation of glutamate levels. At high concentrations, glutamate is particularly toxic to neurons such as RGC and bipolar cells, where hypoosmotic swelling plays a major role in causing neuronal death (Vogler et al. 2013). MGCs are much more resistant to glutamate toxicity and respond by increasing the uptake of glutamate and the production of neurotrophins BDNF, nerve growth factor (NGF), neurotrophin-3 (NT3) and NT4 to promote the survival of neurons and photoreceptors (Taylor et al. 2003). However, chronic glutamate excitotoxicity has been associated with apoptotic RGC loss and the pathogenesis of axonal injury, retinal ischaemia and glaucoma (Section 1.3.3).

The initial reactive glial response to damage is largely neuroprotective, where regular MGC functions become augmented in the presence of appropriate triggers and stressors as described previously. However, secreted cytokines such as interleukin-1 (IL-1) and tumour necrosis factor (TNF-α) contribute to the increased vascular permeability and leakiness of the blood retinal barrier

(BRB), which in turn causes an influx of extravasated proteins and immune cells (Bringmann et al. 2006). Clinically, these consequences manifest as oedema, haemorrhage and inflammation. In more severe cases of MGC reactivity, MGCs can dedifferentiate and acquire a progenitor-like phenotype which is capable of migration into damaged areas of the retina to proliferate. The mechanisms which enable this proliferation are similar to those found during retinal development and are thought to be essential for the regenerative properties seen in zebrafish retina. It should be noted that only a proportion of MGCs re-enter the cell cycle at this stage. This subpopulation tends to express lower levels of GFAP, whereas MGCs which do not re-enter the cell cycle tend to express higher levels of GFAP (Fischer and Reh 2003). Whether these different subpopulations are inherently dissimilar, or simply a divergence from the same population following exposure to different conditions is not entirely clear.

Following the proliferative and reparative phase, usually occurring within one or two weeks, tissue remodelling begins. In the zebrafish, the process of tissue remodelling initially forms a border for the damaged region in an attempt to restore structure and function where possible (Lahne et al. 2020). In cases of severe damage, scar formation usually occurs, in order to recreate a permanent barrier for the retinal microenvironment such as the case in retinal detachment (Lewis et al. 2010). Within the CNS, this scar forming process appears to be coordinated by astrocytes in a signal transducer and activator of transcription-3 (STAT-3) dependent manner (Wanner et al. 2013). Although the formation of fibrotic scars is effective in protecting the retina against further infiltration of unwanted protein and immune cells, depending on the nature of damage, fibrosis can also lead to associated loss of function, as damaged neurons are not replaced.

The complex array of gliotic changes show localised responses within a population of MGCs, as recent evidence demonstrated striking differences between the metabolic profiles of adjacent individual cells (Pfeiffer et al.

2020). An additional layer of complexity exists in that the gliotic scar can vary drastically between different species, further highlighting the heterogeneity of this process (Bringmann et al. 2006). Consequently, a major focus of research in recent years has involved the understanding of the specific molecular mechanisms of reactive MGCs during gliosis, particularly those that control whether a gliotic process ultimately results in tissue regeneration or significant inflammation and scarring.

1.1.4 Müller Glial Cells in Retinal Degeneration

Teleost fish possess the extraordinary ability to completely regenerate their retina following damage, a phenomenon that has not been observed in mammals (Bernardos et al. 2007). MGCs have been shown to be responsible for this regenerative capacity, and the underlying mechanisms are closely related to those found in MGCs during the development of the retina. Indeed, each cell within the columnar unit centred around a MGC is thought to originate from a common progenitor (Reichenbach and Bringmann 2010).

Dying photoreceptors release TNF-α, which has shown to be a requirement for the induction of MGC proliferation in the zebrafish (Nelson et al. 2013). In addition to upregulating cell cycle specific genes responsible for proliferation, TNF-α also upregulates the *ascl1a* gene. The Ascl1a protein potentiates canonical Wnt signalling through *dkk1b* inhibition, resulting in the translocation of β-catenin in a signalling pathway that has been shown to be necessary for MGC dedifferentiation (Gorsuch and Hyde 2014). The β-catenin pathway also influences Sox2, an important transcription factor in the maintenance of retinal progenitors (Zhang and Cui 2014).

Intravitreal injection of the neurotoxin ouabain is an established model of inducing retinal regeneration in the zebrafish. In this model, the INL and GCL are rapidly damaged within the first three days after toxin injection, accompanied by a considerable increase in retinal thickness (Fimbel et al. 2007). Subsequently, regeneration of retinal structures and function occurs

over a short period of weeks. A recent proteomics study conducted in the host laboratory investigated the differential protein regulation in the degenerating and regenerating zebrafish retina following ouabain injection (Eastlake et al. 2017). The majority of identified proteins were unsurprising, considering the retinal damage inflicted. These included proteins related to energy and lipid metabolism, antioxidant synthesis, cytoskeletal remodelling and chromatin components. However, among the most highly expressed proteins during retinal degeneration, Galectin-1 stood out as a protein whose function was not well understood, and not previously described to be associated with retinal degeneration. In fact, the relatively new field of Galectins is rapidly expanding, and may be a key player in our objective to understand the pivotal determinants of gliosis associated retinal degeneration.

1.2 Galectins

Galectins (Gal) are carbohydrate binding proteins (CBP) with high affinity to ß-galactosides, which belong to the phylogenetically conserved family of lectins. To date, fifteen mammalian Galectins have been discovered and named in the order of their discovery; of these, eleven have been identified in humans (Arthur et al. 2015). Galectins are widely distributed across different organisms, whilst significant variability exists in their expression between distinct species, tissues and subcellular compartments.

Understanding of the functions of Galectins has grown steadily over the past decade. This has been made possible by substantial advancements in the field of glycobiology, which has resulted in a rapidly increasing number of Galectin related publications. As a result, our understanding of carbohydrates has expanded beyond their traditional function as substrates of energy. Instead, we now recognise that carbohydrates, as well as their related molecules such as Galectins, participate in much more complex systems which mediate intra- and inter-cellular signalling and regulation.

1.2.1 Molecular Properties of Galectins

Galectins can broadly be divided into three categories: prototypic, tandem repeat and chimeric (Figure 1-2). Prototypic Galectins include Gal-1, -2 and -7, which contain one carbohydrate recognition domain (CRD) and form homodimers upon binding to their glycoconjugates; tandem repeat Galectins include Gal-4, -8, -9 and -12, which contain two different CRDs; whilst Gal-3 is the only chimeric Galectin capable of forming pentamers (Johannes, Jacob, and Leffler 2018). The distinctive structures of Galectin molecules make them ideally suited for cross-linking glycans of either the same type, as in the case of homodimers and pentamers, or of different types, as in the case of tandem repeat Galectins.

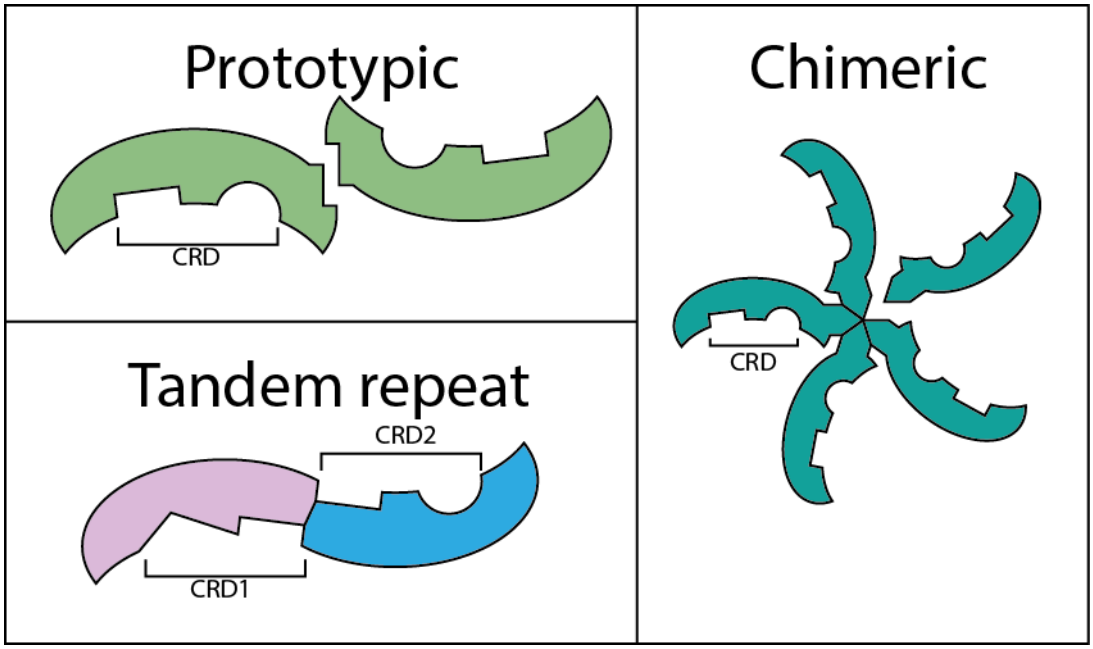

Figure 1-2 Classification of Galectins. Galectins are divided into three subtypes; prototypic Galectins contain a single CRD, and form homodimers, tandem repeat Galectins contain two distinct CRDs within the same molecule, whereas chimeric Galectins contain a single CRD but forms pentamers. CRD, carbohydrate recognition domain (Johannes, Jacob, and Leffler 2018).

Whilst Gal-1 and Gal-3 are widely distributed throughout the human body, other Galectins appear to be more tissue specific (Cruzat et al., 2018). For instance, Gal-7 expression is restricted to stratified epithelia (Magnaldo et al., 1998), Gal-5 is specific to erythrocytes (Gitt et al., 1995), Gal-12 is found in adipocytes (Yang et al., 2011), and Gal-4 and -6 are primarily found in the gastrointestinal tract (Gitt et al., 1998). Gal-1, -3, -7, -8 and -9 have been found to be distributed within ocular tissues including the cornea, trabecular meshwork, lens, and retina (Sugaya et al. 2015; Fautsch, Silva, and Johnson 2003; Gonen, Donaldson, and Kistler 2000; Uehara, Ohba, and Ozawa 2001). During states of ocular disease, the expression of these Galectins and their corresponding glycoconjugates undergo significant changes.

Crucial to the function of Galectins is the specific binding which occurs between their carbohydrate recognition domains (CRDs) and the corresponding glycans (Camby et al. 2006). The CRD regions of Galectins are formed of a β-sheet sandwich structure which consists of two antiparallel β-

sheets. Glycan binding occurs on the concave β-sheet surface, which can be further divided into five sub-regions designated A-E; the central C sub-region is specific for ß-galactose, whilst the adjacent sub-regions correspond to sugars or functional groups attached to the ß-galactose residue (Figure 1-3) (Chan et al. 2018; Nagae et al. 2009). This particular arrangement is crucial for carbohydrate binding and is responsible for the majority of molecular interactions between Galectins and their binding targets.

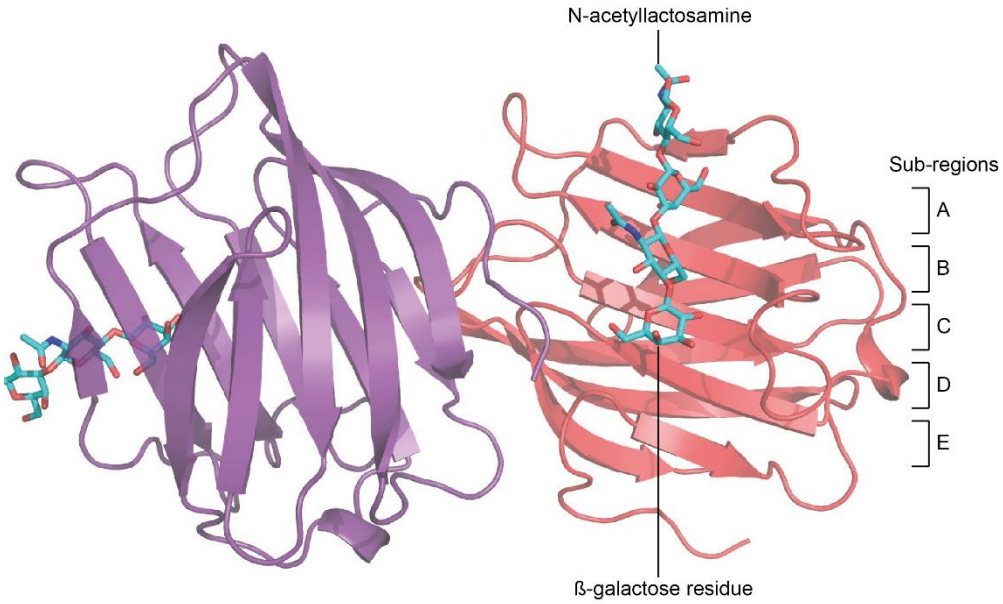

Figure 1-3 Prototypic Gal-9 dimer complex. The N-acetyllactosamine are represented by ball-and-stick models; binding occurs on the concave β-sheet surface of Gal-9, where the terminal ß-galactose residue binds to the central C subregion. (Nagae et al. 2009)

Each Galectin CRD recognises a specific region of a corresponding ß-galactose containing glycan, also known as the glycan determinant. Whilst a Galectin CRD may be able to accommodate a large number of similar molecular structures, its affinity for a specific glycan determinant is greater by orders of magnitude. The identification of glycan determinants specific to each CRD has proven to be an arduous undertaking, in part due to the multitudinous nature of glycans, which is further compounded by the lack of accessible and reliable carbohydrate sequencing techniques.

To date, a number of interactors have been identified to possess the appropriate glycan determinants for various Galectins. In general, these interactors are mainly localised in the extracellular matrix and cell membranes, as well as membranes found in intracellular structures such as exosomes, endosomes and lysosomes (Obermann et al. 2017). Galectins are secreted from cells via a non-classical pathway which remains incompletely understood (Popa, Stewart, and Moreau 2018); this is particularly important as the intracellular and extracellular functions of Galectins appear to be distinct and are sometimes opposing (Johannes, Jacob, and Leffler 2018).

1.2.2 The “Sugar Code”

Glycans are formed by the covalent attachment of monosaccharides and polysaccharides to organic molecules; this process is ubiquitous in nearly all known biological systems. The ability for CBPs to recognise and bind to their glycan determinant forms the foundation of the “sugar code” concept; which stipulates that information is stored and communicated through differential glycosylation states of a protein or lipid in addition to the underlying molecule itself (Gabius et al. 2004). As a result, many consider monosaccharides to be the third alphabet of life, alongside nucleotides and amino acids (Gabius 2018). In order to achieve the intended interactions with Galectins, corresponding glycan determinants must be encoded via appropriate glycosylation. For proteins, this is a post-translational modification process which takes place primarily in the Golgi apparatus. More specifically, O-glycosylation is carried out by the polypeptide-GalNAc-transferases (GALNT) enzyme family, whereas N-glycosylation of mucins is carried out by the N-acetylglucosaminyltransferase (MGAT) enzyme family (Boscher, Dennis, and Nabi 2011). Whilst Galectins are able to bind to both O-glycosylated and N-glycosylated proteins, high affinity binding generally requires N-glycosylation; Gal-8 is an exception to this as it binds with high affinity to both types (Nielsen et al. 2018).

In contrast to proteins and nucleic acids which possess linear primary structures, monosaccharide units are able to form glycosidic linkages in several different positions. This allows glycans to take the form of complex branching chains. It has been estimated that a hexasaccharide has over 10^{12} theoretically possible configurations (Laine 1994), with the number of physiologically functional glycan determinants estimated to be around 3000 (Cummings 2009). Traditional pull-down experiments have identified a large number of potential molecules which interact with Galectins, although the binding affinity for these molecules are not provided in these experiments (Kamili et al. 2016). More modern techniques using extensive glycan libraries have yielded better results, which have revealed a strong preference for the majority of Galectin family members towards polylactosamine (polyLacNAc).

1.2.3 Galectin Functions and Cellular Activation Pathways

Human Galectins are encoded by the lectin, galactoside-binding, soluble (*LGALS*) family of genes, the structures of these genes including their promoter regions have been well characterised (Chiariotti et al. 2002). A rapidly growing number of studies have demonstrated *LGALS* genes to be differentially expressed in a range of systemic and organ specific diseases, such as cancer, diabetes and inflammation. As Galectins become established as disease biomarkers, there has been increasing interest in the molecular mechanisms governing their expression. Cytokines such as TNF-α, transforming growth factor (TGF-β) and the interleukin (IL) family are of particular interest, and recent studies have revealed their activity both upstream and downstream of Galectins.

Galectins are the only CBPs in animals that can be found in both the intracellular and extracellular compartments (Leffler et al. 2002). Since proteins in the extracellular matrix (ECM) are richly glycosylated, glycans found on ECM proteins were some of the earliest Galectin interactors to be identified (He and Baum 2006). For instance, Gal-1 has been shown to

interact with a number of ECM components including vitronectin, laminin and osteopontin to influence ECM assembly and turnover. At the same time, Gal-1 has also been shown to interact with cell-surface molecules including β-1 integrin (Moiseeva, Williams, and Samani 2003). These findings strongly suggest that Gal-1 serves a role in anchoring cell surface glycans to the ECM. Additional experiments have demonstrated these interactions to have downstream effects on cell adhesion, migration, and proliferation. One of the key pathways involved in this process is the mitogen-activated protein kinase /extracellular signal-regulated kinase (MAPK/ERK) pathway, where not only does Gal-1 influence extracellular activation, but intracellular Gal-1 also appears to interact with proteins of the Ras family to further modulate cell growth and proliferation (Blazevits et al. 2016). In addition to the ECM, Galectins have been shown to directly interact with surface glycans of circulating cells and their effects on cells of the immune system have been particularly well studied, as detailed in later sections (Thiemann and Baum 2016).

Amongst members of the Galectin family, Gal-3 is unique in its capacity to self-associate into pentamers through its N-terminal domain. This characteristic ability to crosslink multiple ligands is crucial for Gal-3 to perform its functions, many of which are thought to involve the stabilisation of cell surface receptors in order to modulate their function. Key examples of these functions include vascular endothelial growth factor (VEGF) and basic fibroblast growth factor (bFGF) signalling, where Gal-3 has pro-angiogenic effects which are dependent on both the activity of its CRD as well as its ability to oligomerise (Markowska, Liu, and Panjwani 2010). In addition, the focal adhesion kinase/protein tyrosine kinase 2 (FAK/PTK2) receptor also appears to be crucial in mediating the effect of Gal-3. Although the exact interplay between Gal-3, VEGF and FAK/PTK2 has not been completely elucidated, strong evidence suggests that these pathways are closely related (Chen et al. 2012).

Another common feature of Gal-3 function is its association with lipid membranes. When found extracellularly, Gal-3 has been shown to facilitate phagocytosis of apoptotic cells; whilst intracellular Gal-3 tends to accumulate around disrupted vesicular membranes and aid their clearance (Caberoy et al. 2012). Furthermore, in contrast to its extracellular function, intracellular Gal-3 appears to have anti- apoptotic properties in a pathway involving B-cell lymphoma 2 protein (Bcl-2) (Yang, Hsu, and Liu 1996).

It was initially thought that the extracellular functions of Galectins depended on their carbohydrate binding properties whereas their intracellular functions did not (Arthur et al. 2015). However, more recent studies have found notable exceptions to this generalisation. Nevertheless, the molecular insights of Galectins underscore their versatility as they appear to take part in a diverse range of functions.

1.2.4 Galectins in Systemic Diseases

In contrast to other carbohydrate binding proteins which have relatively restricted functions, for instance selectins and toll-like receptors, Galectins perform a number of different roles. To some extent, this complexity is a reflection of the varied functions of their ligand oligosaccharides, insofar as the ability to participate in seemingly unrelated intra- and inter-species biological interactions (Varki 1993). One compelling theory at present proposes that the distinctive patterns of protein glycosylation expressed by different groups of cells form an important aspect of their microenvironment. Together with the production and secretion of a specific mixture of Galectins into the extracellular milieu, these two factors act in concert to influence important processes including cell-ECM interactions, receptor-ligand signal modulation and the trafficking of immune cells (Thiemann and Baum 2016).

Since its discovery as the most highly upregulated gene during heart failure, Gal-3 has emerged as a crucial molecule in the pathogenesis of cardiovascular disease (Sharma et al. 2004). In addition to becoming a

promising biomarker for disease diagnosis and monitoring (Amin, Amin, and Wijaya 2017), the contribution of Gal-3 to disease progression has also been verified in a number of animal models (Suthahar et al. 2018). The presence of Gal-3 in cardiac diseases causes changes in cell cycle regulation, macrophage recruitment and fibroblast activation, which together result in cardiac remodelling and ultimately loss of cardiac function (Zhong et al. 2019).

Within several types of tumours, the expression of Gal-1, -3 and -9 has been associated with different clinical phenotypes (Bartolazzi 2018). Whilst a higher concentration of Gal-1 has been shown to consistently correlate with more aggressive cancer progression, the roles of Gal-3 and Gal-9 appear to be more variable (Camby et al. 2006). These effects have been shown to be mediated through alterations in cell proliferation and invasion (Inohara, Akahani, and Raz 1998), tumour neovascularisation, as well as immunomodulation (Chou et al. 2018).

Interactions between Galectins and the immune system were some of the first discoveries made in the exploration of their functions. This is in part due to the remarkable similarity between the antigen-antibody system and the specificity with which CBPs such as Galectins bind to their corresponding glycan determinants. Indeed, Gal-3 was initially named Mac-2 as it was found in macrophages at high concentrations (Lakshminarayan et al. 2014). Gal-3 has predominantly been associated with detrimental effects during inflammation; for instance, serum concentrations of Gal-3 and Gal-3 binding protein (G3BP) are increased in patients with Behçet's disease (Lee et al. 2007), although more recent data suggest that the upregulation of Gal-3 may be playing a protective role (Lee et al. 2019). Other Galectins such as Gal-2, -9 and -10 also participate in the regulation of T cells and their associated cytokines, as reviewed in detail elsewhere (Arthur et al. 2015).

Gal-1 has been shown to have potent immunosuppressive functions via multiple mechanisms of action. Firstly, Gal-1 is an established inducer of T cell apoptosis (Perillo et al. 1995); secondly, Gal-1 plays an important role

during normal development and maturation of T cells, including regulatory T cells via the upregulation of forkhead box P3 (FOXP3) (van der Leij et al. 2004; Juszczynski et al. 2007); and lastly, Gal-1 has been shown to induce IL-10 production and to inhibit IFN-γ production in both CD4+ and CD8+ T cells (Perillo et al. 1995). These effects were particularly evident in tumours, which suggests that elevated Gal-1 concentrations contribute to neoplasm related immunosuppression.

Tissue fibrosis is a common converging pathway for a number of disease processes following injury, characterised by accumulation of ECM, tissue contraction and loss of function. It has recently emerged that Gal-3 is a central regulator of fibrosis, as evidenced by studies in the lung, kidney, and liver (Li, Li, and Gao 2014). The pathogenesis of pulmonary fibrosis has been investigated in particular detail, where Gal-3 was found to regulate TGF-β, reduce phosphorylation and nuclear translocation of β-catenin but had no effect on Smad2/3 phosphorylation (Nishi et al. 2007). Research in idiopathic pulmonary fibrosis has also demonstrated the ability for Gal-3 to induce epithelial mesenchymal transition and myofibroblast activation via TGF-β1 (Mackinnon et al. 2012), with later studies demonstrating similar results in atrial fibrosis (Shen et al. 2018). These findings are further substantiated by animal models of Gal-3 downregulation which attenuates tissue fibrosis, in a process accompanied by a decrease in TGF-β and alpha smooth muscle actin (α-SMA) expression (Henderson et al. 2006). One hypothesis for this observation is that the crosslinking effect of Gal-3 on N-glycosylated TGF-β receptors via alpha-1,6-mannosylglycoprotein 6-beta-N-acetylglucosaminyltransferase (MGAT5) activity may stabilise and potentiate TGF-β signalling (Partridge et al. 2004).

The ophthalmic field has made significant contributions to our understanding of Galectins as a whole; the exquisitely organised structure of the eye renders it an ideal organ to further investigate these molecules. The following sections explore the current knowledge on the involvement of Galectins in ocular

disease (Table 1-1, Figure 1-4). It is worth keeping in mind that much of the research in this field can potentially be translated to other organs.

Functions Galectins-1 and -3 within the Eye

	Molecule	Effects	References
Cornea	Gal-1	Reduce inflammatory response in Pseudomonas aeruginosa infections	(Suryawanshi et al. 2013)
	Gal-3	Anchors Mucins -1 and -16	(Argueso et al. 2009)
		Promotes cell migration and wound healing	(Cao, Said, et al. 2002; Saravanan et al. 2009)
		Reduced in dry eye diseases	(Soria et al. 2018)
		Increased in inflammatory corneal diseases	(Hrdlickova-Cela et al. 2001)
	Gal-7	Promotes re-epithelialisation	(Cao, Said, et al. 2002)
Glaucoma	Gal-3	Upregulated in the TM and ONH	(Belmares et al. 2018; Fautsch, Silva, and Johnson 2003)
		Present in higher concentrations in the aqueous humour	(Tripathi et al. 1994)
		Promotes RGC loss	(Abreu et al. 2017)
	Gal-3	Anchors cells within the TM	(Diskin et al. 2009)
Ocular immunology	Gal-1	Contributes to ocular immune privilege	(Ishida et al. 2003)
		Ameliorates EAU	(Toscano et al. 2006)
		Downregulates IL-1b, -16 and MCP-1	(Romero et al. 2006)

	Gal-3	Causes microglial inflammation	(Burguillos et al. 2015)
		Enhances phagocytosis	(Karlsson et al. 2009)
	Gal-8	Ameliorates EAU	(Sampson et al. 2015)
		Increases the number of regulatory T cells	(Sampson et al. 2016)
	Gal-9	Contributes to ocular immune privilege	(Shimmura-Tomita et al. 2013)
Neovascular diseases	Gal-1	Activates VEGFR2	(Markowska, Liu, and Panjwani 2010)
		Promotes choroidal neovascularisation	(Wu et al. 2019)
		Upregulated in proliferative diabetic retinopathy	
	Gal-3	Activates and stabilises VEGFR2	(Markowska, Jefferies, and Panjwani 2011)
	Gal-8	Promotes lymphangiogenesis	(Chen et al. 2016)
Epithelial mesenchymal transformation	Gal-1	Mediates adhesion of the photoreceptor layer to the interphotoreceptor matrix	(Uehara, Ohba, and Ozawa 2001)
		Over-expression correlates with RPE differentiation and migration	(Eastlake et al. 2018; Alge et al. 2006)
	Gal-3	Causes clustering of CD147 and intergrin-β1	(Priglinger et al. 2013)

Table 1-1 Functions of Galectins in ocular diseases. EAU, experimental autoimmune uveitis; IL, interleukin; MCP, monocyte chemotactic protein; ONH, optic nerve head; RGC, retinal ganglion cell; RPE, retinal pigmented epithelium; TM, trabecular meshwork; VEGFR, vascular endothelial growth factor receptor.

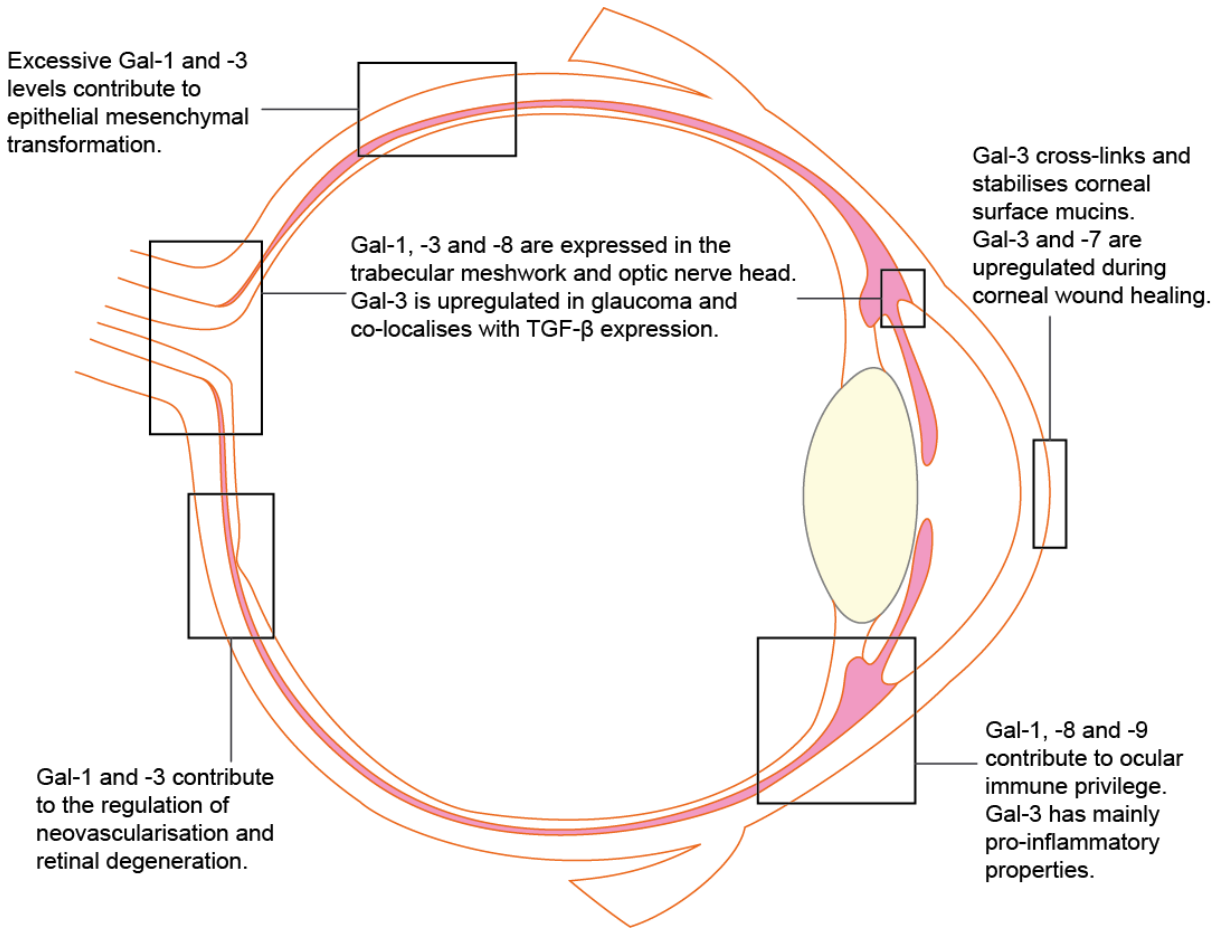

Figure 1-4 Roles of Galectins within the eye. Schematic diagram showing the main known roles of Galectins within the different cellular structures of the eye.

1.2.5 Galectins in Ocular Diseases

1.2.5.1 Galectins in Corneal Diseases

A major role of Gal-3 in the cornea relates to its interactions with the glycocalyx, a layer of large glycoproteins covering the apical surface of the corneal epithelium, composed mainly of mucins. Gal-3 associates closely with Mucins -1 and -16, acting as an anchor to these proteins and the underlying epithelial cells and to each other (Argueso et al. 2009; Uchino 2018). The glycocalyx has hydrophilic properties and mediates several important functions, including mechanical impairment of pathogens, tear film stabilisation, and lubrication during blinking.

The extracellular domains of mucins can extend up to 500nm from the plasma membrane and are highly glycosylated; in fact, the carbohydrate content of mucins can account for over 70% of their molecular weight in some cases (Taniguchi et al. 2017). Due to the high proportion of serine and threonine residues in these molecules, the majority of carbohydrate conjugates in mucins are O-glycans whereas relatively few N-glycans are present. Both O-glycans and N-glycans have been demonstrated to bind to Gal-3, and the interactions between mucins and Gal-3 is critical in the overall integrity of the glycocalyx (Argueso et al. 2009; Guzman-Aranguez and Argueso 2010). The ability for Gal-3 to stabilise ocular surface mucins is largely attributed to its ability to self-associate to both the C- and N-terminal domains which facilitates the formation of large complexes (Ahmad et al. 2004; Argueso 2013). Studies which inhibited alpha-1,6-mannosylglycoprotein 6-beta-N-acetylglucosaminyltransferase-1 (MGAT1) function led to impaired stability of surface MUC16 and weakening of the glycocalyx (Taniguchi et al. 2017). This effect was shown to be mediated through modulation of the interaction between MUC16 and Gal-3, and to increased stress in the endoplasmic reticulum leading to the unfolded protein response.

In addition to mucins, a number of other binding partners have been identified for Gal-3. CD147 (also known as EMMPrin and basigin) is a particularly important molecule found to co-localise with Gal-3 in areas of ulceration and gelatinolytic activity in human cornea tissue (Cruzat et al. 2018). Gal-3 appears to cause clustering of CD147 to initiate cell-cell detachment and induces the expression of matrix metalloproteinases (Mauris et al. 2014). Additionally, Gal-3 bind selectively to clusterin, another important molecule in the maintenance of ocular surface integrity (Fini et al. 2016). Gal-3 has also been demonstrated to promote cell migration and wound healing, via α3β1 integrin and activation of focal adhesion kinase and Rac1 GTPase (Saravanan et al. 2009).

Clinical studies have demonstrated that Gal-3 expression is reduced in the conjunctival epithelium of patients with dry eye disease and meibomian gland dysfunction (Soria et al. 2018). Conversely, Gal-3 protein levels are increased in the tears of patients with ocular inflammatory conditions such as sarcoidosis and adenoviral conjunctivitis, but not in healthy subjects or those with non-inflammatory conditions such as corneal degeneration (Hrdlickova-Cela et al. 2001). Taken together, these findings suggest that Gal-3 is an integral part of the milieu of extracellular molecules found in the corneal epithelium; and that its presence is important for the maintenance of a healthy ocular surface. However, it remains unclear whether elevated Gal-3 concentrations within the tear film has a pathogenic role in inflammatory conditions, or it is simply a reflection of the presence of inflammatory cells such as macrophages, which are known to express Gal-3 abundantly.

Additional evidence shows that Gal-3 may be exploited as a binding partner by Herpes Simplex Virus type 1 (HSV-1), as part of the initial HSV-1-glycocalyx interaction necessary for the intracellular translocation of HSV-1 (Woodward, Mauris, and Argueso 2013). In this context, it has been demonstrated that an intact glycocalyx where the majority of Gal-3 has already been bound to mucins, the available sites for HSV-1 binding is dramatically reduced. This may help to explain the propensity for HSV-1 to cause corneal infection following epithelial injury, as the healing edge of areas of corneal wound exhibit increased concentration of Gal-3 molecules. In the context of Pseudomonas aeruginosa corneal infections, Gal-1 treatment has been shown to reduce the pro-inflammatory Th17 cell response, whilst promoting the activities of Th2 and IL-10 (Suryawanshi et al. 2013). Further characterisation of the role of Galectins in other forms of infective keratitis would contribute to our understanding of the role of Galectins in corneal infection and inflammation.

Gal-7 is known to play an important role in promoting cell-ECM interactions, as evidenced by microarray cDNA sequencing in a model of corneal excimer

laser injury, which revealed significant upregulation of this molecule during wound healing (Cao, Wu, et al. 2002). Enhanced expression of Gal-7 was confirmed by subsequent experiments, which also found that Gal-8 and -9 are upregulated following corneal cauterisation (Chen, Cao, et al. 2015). Further studies in mouse models of corneal re-epithelialisation have found that Gal-3 is concentrated in areas of migrating epithelium, whereas Gal-7 is upregulated throughout the epithelium (Cao et al. 2003). In addition, Gal-$3^{-/-}$ mice have shown significantly lower wound closure rates than wild type animals, whereas Gal-$1^{-/-}$ mice did not show such effect. Interestingly, the application of exogenous Gal-7 but not of Gal-3 was able to stimulate corneal re-epithelialisation in Gal-$3^{-/-}$ mice (Cao, Said, et al. 2002). In this case, the fact that exogenous Gal-3 did not have a rescue effect on Gal-$3^{-/-}$ mice raises the possibility that Gal-3 must be present intracellularly to contribute significantly to normal wound healing.

1.2.5.2 Galectins in Glaucoma

Glaucoma is a heterogeneous group of disorders which share the hallmark features of RGC loss and ONH remodelling. In most forms of glaucoma, increased intraocular pressure is the prominent aetiological factor, and remains the only modifiable risk factor targeted in clinical practice (Weinreb, Aung, and Medeiros 2014). The molecular processes which occur in the TM and ONH remodelling as well as RGC cell degeneration remain incompletely understood and constitute major areas of current glaucoma research. Galectins, in particular Gal-3, have been implicated in both pathogenic processes.

The rate at which aqueous fluid drains out of the anterior chamber is regulated by cells of the TM and their modifications of the surrounding extracellular matrix. TGF-β2 has been demonstrated to be an important factor involved in TM fibrosis (Kang et al. 2013), as evidenced by elevated concentrations of this cytokine in the aqueous humour of patients with primary open angle

glaucoma (Tripathi et al. 1994). Concurrently, there is evidence of Gal-3 upregulation in the TM and the ONH of human glaucomatous eyes (Fautsch, Silva, and Johnson 2003; Belmares et al. 2018), and given the known significance of Gal-3 involvement in fibrogenesis of other organs (Suthahar et al. 2018), it would be invaluable to elucidate the interaction between Gal-3 and TGF-β in the context of glaucoma.

One potential explanation for the upregulation of Gal-3 in glaucoma is through its interactions with matricellular proteins, as suggested by *in vitro* studies showing that inhibition of Gal-3 in sarcoma cells promotes their adhesion and migration on laminin 111, a process that is dependent on the activation of the phosphoinositide 3-kinases (PI-3K) dependent pathway (Melo et al. 2011). TGF-β2 also positively regulates matricellular protein activity; in the TM, it is well-documented that TGF-β2 signalling activates p38 and Smad 2/3 pathways to regulate the production of a number of important matricellular proteins including secreted protein acidic and cysteine rich (SPARC) (Rhee et al. 2003), thrombospondins-1 and -2, tenascins-C and -X, and osteopontin (Rhee et al. 2009; Chatterjee, Villarreal, and Rhee 2014). The accumulation of Gal-3 and various matricellular proteins could lead to significant ECM remodelling and therefore increased TM outflow resistance as observed in primary open angle glaucoma (Melo et al. 2011).

Gal-1 and -8 have been found throughout the human trabecular meshwork and Schlemm's canal (Fautsch, Silva, and Johnson 2003). *In vitro*, TM cells strongly adhered to Gal-8 coated wells, but not to Gal-1 or Gal-3 coated wells. This is thought to be mediated by the binding between Gal-8 and β1 integrins present on TM cell membranes; and more specifically, the CRD region of Gal-8 appears to be selective for the 3-sialylated glycans contained within β1 integrins (Diskin et al. 2009).

In addition to its potential role in fibrosis, Gal-3 has also been implicated in the pathogenesis of glaucomatous RGC loss. This is illustrated by findings that Gal-3 knockout mice exhibit a higher rate of RGC survival following optic

nerve crush injury (Abreu et al. 2017). Furthermore, electron microscopy analysis of degenerating RGCs shows increased cellular fragmentation in Gal-3-/- mice, which suggests that there is incomplete clearance of damaged RGCs (Abreu et al. 2017). The current hypothesis for this effect is attributed to Gal-3 mediated microglia activation, substantiated by existing evidence in the CNS that Gal-3 dependent microglial activation results in inflammatory neurodegeneration (Siew et al. 2019).

1.2.5.3 Galectins in Immune Mediated Eye Diseases

In its normal state, the intraocular microenvironment is a well-established site of immune privilege. The immunosuppressive effects are achieved through a combination of synergistic mechanisms including the blood-retinal barrier and locally released molecules (Mochizuki, Sugita, and Kamoi 2013). There is accumulating evidence that Gal-1 is one such molecule which contributes to this effect, in accord with its immunomodulatory functions elucidated in other organs. Within the retina, the role of Gal-1 was further confirmed by experiments using retinal pigmented epithelial cells from Gal-$1^{-/-}$ mice which exhibited significantly dampened immunosuppressive properties (Ishida et al. 2003). In addition to inducing T-cell apoptosis, Gal-1 has also been shown to inactivate microglia in the CNS, which has downstream effects of decreasing the production of important pro-inflammatory cytokines such as TNF-α and monocyte chemotactic protein-1 (MCP-1) (Starossom et al. 2012). It is interesting to note that the immunosuppressive properties exhibited by Gal-1 appear to require cell-cell contact and do not occur over long distances (Fajka-Boja et al. 2016).

During experimental autoimmune uveitis, recombinant Gal-1 (rGal-1) has been shown to ameliorate inflammation, via diversion of the Th1 pre-dominant response towards Th2 and Treg mediated anti-inflammatory state (Toscano et al. 2006). This finding was further validated using a rodent model of endotoxin-induced uveitis, where rGal-1 had a similar anti-inflammatory effect.

This was reflected in the downregulation of cytokines present in ocular tissue and included IL-1b, IL-6 and MCP-1. (Zanon Cde et al. 2015) Interestingly, anti-Gal-1 antibodies have been found in patients with autoimmune and toxoplasma retinochoroiditis, which correlated with disease progression (Romero et al. 2006).

Another Galectin which has been shown to have immunoregulatory effects within the eye is Gal-8. Using a murine model of experimental autoimmune uveitis, intraperitoneal treatment with exogenous Gal-8 has been shown to increase the number of regulatory T cells, as well as increase their cytotoxic T-lymphocyte-associated protein 4 (CTLA-4) and IL-10 expression. This is accompanied by a decrease in the production of T-helper 1 (TH1) and TH17 cells (Sampson et al. 2015). These immunomodulatory effects were later confirmed *in vitro*; where Gal-8 stimulated Treg conversion occurred via the binding of Gal-8 to TGF-β and IL-2 receptors which led to downstream activation of Smad3 and STAT5 signalling (Sampson et al. 2016).

In addition to Gal-1 and Gal-8, Gal-9 has also been shown to contribute to the immune privileged status of the eye. Gal-9 is constitutively expressed in a number of ocular tissues, including the corneal epithelium, corneal endothelium and iris-ciliary body (Shimmura-Tomita et al. 2013). The immunosuppressive properties of Gal-9 have been attributed to its binding to T-cell immunoglobulin and mucin domain (Tim)-3 receptor, leading to apoptosis of effector T-cells but not regulatory T-cells (Sehrawat et al. 2009). In support of these findings, the expression of Gal-9 was found to be significantly lower in corneal tissue obtained following graft rejection as compared to successful grafts; and the blockade of Gal-9 increased corneal graft destruction in mice (Sugaya et al. 2015). This effect was seen in animal models of allergic conjunctivitis, where Gal-9 blockade resulted in an increase in severity (Fukushima et al. 2008). Furthermore, in the context of Thyroid-associated ophthalmopathy, the interaction between Gal-9 and Tim3 caused downstream suppression of the protein kinase B/nuclear factor kappa B (NF-

kB) pathway, resulting in an inhibitory effect on TLR mediated inflammation which shares NF-kB signalling (Luo et al. 2017).

In contrast to the anti-inflammatory properties of Galectins mentioned above, Gal-3 has predominantly shown pro-inflammatory functions. Endogenous Gal-3 from microglia appears to act as a ligand for toll-like receptor 4 (TLR4), which contributes to microglial inflammation and subsequent detrimental effects (Burguillos et al. 2015); binding of Gal-3 to TLR4 is dependent of the CRD region of Gal-3, which then increases Gal-3 self–association. These findings are comparable to a study of Huntington's disease, where both human and mouse subjects with the disease exhibited higher concentrations of Gal-3 in the brain and plasma, which was found to be microglia driven and occurred before any clinically measurable motor impairment (Siew et al. 2019). The upregulation of Gal-3 in CNS microglia appeared to be nuclear factor kappa B (NF-kB) mediated, whilst the downstream pro-inflammatory effects were driven by intracellular but not extracellular Gal-3. Increased intracellular Gal-3 was localised to areas of lysosomal damage and resulted in pyrin domain-containing 3 (NLRP3) inflammasome activation and upregulation of IL-1β (Uchino et al. 2018). Furthermore, Gal-3 exhibits opsonin properties to enhance phagocytosis and aid clearance (Karlsson et al. 2009). Although the immunological role of Gal-3 in the retina is less well understood in comparison to the CNS, there is increasing evidence that some of the detrimental mechanisms are shared. As such, Gal-3 is likely to significantly contribute to the pathogenesis of ocular inflammatory conditions (Karlsson et al. 2009).

1.2.5.4 Galectins and Ocular Neovascularisation

Over the last few decades, VEGF has emerged as a key regulator of blood vessel formation, particularly in the context of tumorigenesis and ocular diseases (Ferrara and Adamis 2016). Blocking the actions of VEGF within the eye has dramatically shifted our approach to controlling the clinical

consequences of pathological neovascularisation in diseases such as diabetic retinopathy, age-related macular degeneration (AMD) and retinal vein occlusion.

In more recent years, Galectins -1 and -3 have been noted to interact with VEGF signalling and modify its effects; in particular, Gal-3 appears to stabilise VEGFR2 on the plasma membrane and prevent its internalisation (Markowska, Jefferies, and Panjwani 2011). Both Gal-1 and Gal-3 increase the proliferation and capillary tube formation of human endothelial cells, Gal-1 and Gal-3 individually activate VEGFR2 (Markowska, Liu, and Panjwani 2010), whereas the combination of these two Galectins leads to VEGFR1 activation (D'Haene et al. 2013). Upregulation of Gal-1 has also been observed in a mouse model of laser induced choroidal neovascularisation (CNV). It is of interest that deletion of the *LGALS1* gene in this model suppressed VEGFR2 expression and attenuated CNV formation, fibrosis and markers of epithelial-to-mesenchymal transition (EMT) (Wu et al. 2019). Gal-1 inhibition by specific inhibitors has also shown to attenuate retinal angiogenesis in animal models of retinal neovascularisation (Yang et al. 2017; Wu et al. 2019).

Whilst both Gal-1 and -3 increase the proliferation and capillary tube formation of human vascular endothelial cells resulting in new blood vessels formation (Ridano et al. 2017; Markowska, Liu, and Panjwani 2010), Gal-8 has been shown to act specifically on human lymphatic endothelial cells and to promote lymphangiogenesis in a pathway involving integrin VEGF-C, and podoplanin. (Chen et al. 2016)In diabetic retinopathy, both IL-1β and Gal-1 are upregulated following stimulation by advanced glycation end products (AGE) via the activation of TLR4 signalling (Kanda et al. 2017), whilst expression of Gal-1 is downregulated by the glucocorticoid receptor via dual specificity phosphatase (DUSP) 1 (Hirose et al. 2019). A recent study of epiretinal membranes from patients with PDR confirmed Gal-1 to be upregulated, in correlation with VEGF expression and microvessel density (Abu El-Asrar et al.

2020). Vitreous samples from patients with PDR also showed increased Gal-1 expression, although this was not found to be correlated with VEGF levels (Kanda et al. 2015).

Interestingly, the widely adopted VEGF-A blocker Aflibercept is able to eliminate the pro-angiogenic effect of Gal-1, which appears to depend on the glycosylation state of Aflibercept (Kanda et al. 2015). Moreover, this dual effect has not been seen in similar studies using bevacizumab, a structurally different anti-VEGF. This observation may help to explain the variation in clinical efficacy seen between different anti-VEGF agents (Ridano et al. 2017). In clinical practice, a major challenge in anti-VEGF therapy is the large degree of variability seen in individual patient responses even when the same anti-VEGF agent is used; to date, attempts to explain this phenomenon through genetic studies have been largely unfruitful (Hagstrom et al. 2014). Given the evidence presented for the interaction between VEGF glycoconjugates and Galectins, the glycosylation state of the retinal VEGF and its receptor may be an underappreciated factor in the variable responses observed with anti-VEGF therapies (Wdowiak et al. 2018).

1.2.5.5 Role of Galectins in Epithelial Mesenchymal Transformation (EMT)

Constitutive Gal-1 expression is important for the adhesion of the photoreceptor layer to the interphotoreceptor matrix; as evidenced by the observation that experimental injection of an anti-Gal-1 antibody induces retinal detachment and vacuolation (Uehara, Ohba, and Ozawa 2001). Gal-1 excess is correlated with retinal pigmented epithelium (RPE) dedifferentiation and migration as reported in proliferative vitreoretinopathy (PVR), in which Gal-1 in retinectomy tissues showed upregulation when compared to controls (Eastlake et al. 2018). Furthermore, addition of exogenous Gal-1 to *ex vivo retinectomy samples* in culture inhibit the attachment and migration of PVR cells (Alge et al. 2006), whereas silencing the *LGALS1* gene inhibited TGF-β1

mediated EMT (Wu et al. 2019). Taken together, these data suggest that Gal-1 acts as an anchor for the RPE cell layer in the normal retina but is released in higher concentrations in the context of PVR pathogenesis, possibly in an effort to limit the aberrant migration of RPE cells.

Gal-3 inhibits RPE migration and attachment via the clustering of CD147 and integrin-β1 (Priglinger et al. 2013). *In vitro* studies have demonstrated that these effects are mediated via activation of the ERK/MAPK pathway (Alge-Priglinger et al. 2011), and that they are dependent on the activities of alpha-1,6-mannosylglycoprotein 6-beta-N-acetylglucosaminyltransferase A (MGAT5) (Priglinger et al. 2016). Following modification by MGAT5, the N-glycans conjugated to epidermal growth factor (EGF) and TGF-β receptors undergo cross-linking by Gal-3, thus stabilising the receptors and prolonging their expression (Partridge et al. 2004). The activity of MGAT5 appears to be a rate limiting step in cytokine signalling. As such, manipulation of this glycosylation enzyme as well as Gal-3 availability form attractive potential strategies in controlling aberrant EMT (Abu El-Asrar, Missotten, and Geboes 2011).

1.2.5.6 Galectins in Retinal Development and Regeneration

During organ development, there is evidence that the spatial-temporal distribution of different members of the Galectin family change over time; in addition, striking changes also occur in terms of their subcellular localisation (Kaltner et al., 2002). The zebrafish has proven to be a particularly informative model for studying embryogenesis, owing partly to the availability of its complete genome. A number of Galectin-like molecules are expressed by the zebrafish (Vasta et al., 2004); in particular, Drgal1-L2, a teleost fish Galectin structurally and functionally similar to mammalian Gal-1, was found to be expressed in the notochord during embryogenesis (Ahmed et al., 2004). Blocking Drgal1-L2 during zebrafish development resulted in skeletal and trunk defects (Ahmed et al., 2009). This work was also extended to the mammalian neural stem cells and olfactory system (Puche et al., 1996),

where some studies demonstrate Gal-1 to stimulate stem cell proliferation (Sakaguchi et al., 2006), whilst other studies suggest a role for Gal-1 in axonal degeneration via the p75(NTR) neurotrophin receptor (Plachta et al., 2007). Gal-3 has also been shown to modulate gliogenesis within the mouse CNS via BMP signalling (Al-Dalahmah et al., 2020). Within the pig retina, Gal-3 has been isolated during development, exhibiting an increase in concentration during the first 6 months of life (Kim et al., 2009). In this case, the production of Gal-3 appears to originate from Müller cells, although its mechanism of action remains to be elucidated.

As indicated above, it is well known that the teleost fish retina has the capability to endogenously regenerate following injury (Lenkowski and Raymond, 2014). This phenomenon has been ascribed to Müller glial cells being the source of progenitors which replenish the damaged photoreceptors and neurons (Bernardos et al., 2007). A study in teleost fish showed that the Drgal1-L2 protein is upregulated following retinal injury and that this coincides with retinal regeneration (Eastlake et al., 2017). Furthermore, knockdown of Drgal1-L2 diminished the regenerative process of rod photoreceptors within the zebrafish (Craig et al., 2010). In rodent models, Gal-3 is upregulated in Müller cells during retinal degeneration, whilst Gal-3 knockout mice exhibited attenuated retinal degeneration in a mouse model of cerebral hypoperfusion (Manouchehrian et al., 2015). Given the established role of Müller cells in the regeneration of the teleost fish retina, the coinciding upregulation of Galectins warrants further investigation in the pursuit of Müller cell based retinal therapies (Eastlake et al., 2019).

1.2.6 Potential Clinical Applications of Galectins

As the functions of Galectins become better understood, there is a growing interest in developing specific inhibitors for the purposes of scientific exploration and potential therapeutic use. This has proven to be a challenging task, given the multivalent nature of Galectins and their ability to self-

associate. In addition, it is difficult to design molecules to specifically inhibit the shallow groove in the CRD region of Galectins, whilst achieving high specificity within a family of molecules which share highly conserved CRD amino acid sequences. Nevertheless, a variety of approaches to developing Gal-1 and -3 inhibitors appear to be yielding promising results (Blanchard et al. 2016).

Clinical applications for Galectins are being pursued in areas which are thematically analogous to their functions as outlined in this review. Notably, a recent phase 2 clinical trial has been started for the use of TD139, an inhibitor of Gal-3, in the treatment of idiopathic pulmonary fibrosis (Chan et al. 2018); whilst GR-MD-02, another Gal-3 inhibitor, has been investigated in early clinical trials targeting psoriasis and fibrotic non-alcoholic steatohepatitis (Harrison et al. 2016; Ritchie et al. 2017); and other studies in cancer and heart failure are also yielding promising results (Bartolazzi 2018). Several commercial organisations have been actively pursuing therapeutic applications of Galectin inhibitors in various clinical settings over the past few years (Blanchard et al. 2016). The outcome of these studies could provide crucial insights into the potential for targeting Galectins during major disease processes.

Amongst the various potential applications of Galectins in ocular diseases, glaucoma is a particularly interesting disease, as it encompasses several major themes of Galectin function, including regulation of signalling molecules, cell cycle regulation, and fibrosis.

1.3 Pathogenesis of Glaucoma

Glaucoma is a major cause of visual loss worldwide, second only to reversible causes of uncorrected refractive error and cataract (Quigley and Broman 2006; Burton et al. 2021). A variety of clinical presentations and disease aetiologies can ultimately lead to glaucomatous optic neuropathy (GON), characterised by degeneration of retinal ganglion cells (RGC) and optic nerve head (ONH) remodelling. In addition to these two disease-defining processes, intraocular pressure (IOP) is also a crucial factor to consider in the management of glaucoma, although it should be noted that a significant proportion of patients with glaucoma present with IOP values within the normal population range (Weinreb and Khaw 2004). Understanding the causal relationships between IOP, ONH remodelling, and RGC degeneration in the aetiology of glaucoma is key to the formulation of successful treatment strategies. As such, the following section summarises our current understanding of these important interactions.

1.3.1 Intraocular Pressure

Cross-sectional studies have demonstrated IOP within the general population to follow an approximately Gaussian distribution with an exaggerated central peak and modest skew towards higher pressures (Chan et al. 2017; Bonomi et al. 1998). The original suggestion that Glaucoma can be defined simply by IOP of 21mmHg or higher has been fundamentally refuted (Leydhecker, Akiyama, and Neumann 1958). In modern glaucoma research, there is agreement across different study cohorts that utilising IOP values alone to diagnose glaucoma offers poor sensitivity and specificity (Tielsch et al. 1991; Chan et al. 2017). This diagnostic challenge is further compounded by the finding that glaucoma prevalence varies significantly between different regions and ethnic groups (Tham et al. 2014). Nevertheless, IOP is unquestionably a crucial aetiological factor in the pathogenesis of glaucoma, as evidenced by the non-linear increase in glaucoma risk as IOP rises (Chan et al. 2017), as

well as the observation that IOP reduction in patients with ocular hypertension leads to a decrease in their risk of developing primary open angle glaucoma (POAG) (Kass et al. 2002; 'The Advanced Glaucoma Intervention Study (AGIS): 7. The relationship between control of intraocular pressure and visual field deterioration.The AGIS Investigators' 2000) and is associated with a lower risk of visual field progression (Garway-Heath et al. 2015).

Currently, medical and surgical approaches to reduce intraocular pressure are the only approved clinical treatment strategies in the treatment of glaucoma (Kass et al. 2002). Although the exact mechanisms through which higher IOP causes GON remains incompletely understood, there is accumulating evidence that the crucial disease instigating processes occur within the ONH.

1.3.2 Optic Nerve Head Remodelling

Amongst the pathogenic features of glaucoma, remodelling of the ONH appears to be the most specific. Indeed, elevated IOP often results in ocular hypertension without causing GON, whilst RGC degeneration can occur in a range of non-glaucomatous optic neuropathies. As such, there is broad agreement that certain pathogenic processes which occur within the ONH are specific in causing glaucoma. Current evidence suggests that key mechanisms include reduced axoplasmic flow within RGC axons, impairment of optic nerve head blood supply, as well as mechanical and metabolic stress leading to reactive gliosis and apoptosis of RGCs (Morgan 2000).

In the healthy human retina, over 1 million RGC axons converge at the ONH, traversing perpendicular to the lamina cribrosa before acquiring myelin sheaths to form the optic nerve. RGC axons within the ONH have very high energy requirements, as evidenced by high concentrations of cytochrome C oxidase in pre-laminar and lamina cribrosa regions, which decreases dramatically as the RGC axons acquire myelin sheaths (Balaratnasingam et al. 2009). The lamina cribrosa is a specialised porous collagenous plate which provides structural rigidity to the ONH. Situated between RGC axons and the

lamina cribrosa are astrocytes, the major glial cell type found in this region, which provide structural and metabolic support to the RGCs, both directly and via their continuous interactions with the extracellular environment (Morgan 2000; Burgoyne et al. 2005).

The ONH is constantly subject to static and dynamic biomechanical forces, in part determined by IOP in its anterior aspect and intracranial pressure (ICP) in its posterior aspect (Baneke et al. 2020). In a healthy subject, this creates a translaminar pressure gradient of around 3.5mmHg per 100µm, which appears to cause a restricting effect to RGC axons even during physiological conditions (Hollander et al. 1995). The translaminar pressure gradient is particularly sensitive to postural changes, diurnal variation, as well as disease states where IOP may be increased, or ICP decreased (Ren et al. 2010). As the translaminar pressure gradient increases, axonal transport through the lamina cribrosa becomes progressively more compromised, which interferes with the distribution of key molecules such as neurotrophic factors (Quigley et al. 2000), and the normal turnover and migration of mitochondria (Hollander et al. 1995).

Another important aspect of the ONH structure is the blood supply to this region. Indeed, impaired blood flow is currently thought to be the principal pathogenic factor for normal tension glaucoma (NTG) (Trivli et al. 2019). This may be due to the observation that short ciliary arteries which supply the ONH appear to be particularly vulnerable to changes in ocular perfusion pressure when compared to the central retinal artery. As such, adequate ocular perfusion pressure is crucial to normal ONH function, particularly considering the highly metabolically active unmyelinated RGC axons. Ocular perfusion pressure is defined as the difference between systemic blood pressure and IOP; therefore, an overall reduction of ocular perfusion can result from both systemic hypotension and ocular hypertension (Choi et al. 2007). In addition, cohort studies have also demonstrated conditions such as migraines and primary vascular dysregulation to be independent risk factors for NTG

(Mozaffarieh and Flammer 2013). A common theme in these disorders of vascular autoregulation appears to be endothelial dysfunction, which is associated with elevated serum Endothelin-1 levels (Moore et al. 2008).

Astrocytes are the predominant glial cells found in the ONH. Similar to glial cells in other parts of the CNS, astrocytes act as the central columns within their respective neurovascular units (Liu et al. 2018). Astrocytes are intimately coupled to adjacent RGCs, blood vessels, and extracellular matrices to allow for adjustments to local changes, both rapidly and long-term. At times of excess stress, studies have demonstrated ONH astrocytes to become reactive and decrease their expression of glial fibrillary acidic protein (GFAP), a finding which consistently coincides with morphological changes, axonal transport delay and astrocyte swelling (Balaratnasingam et al. 2008). There is evidence to suggest that astrocytes are also capable of remodelling the collagenous lamina cribrosa over time (Hernandez 2000); indeed, studies have shown that in glaucomatous eyes, pores within the lamina cribrosa become more tortuous than in healthy subjects over time (Wang et al. 2018). Whilst this has not been unequivocally proven, it is likely that in chronic GON, the constant necessity for astrocytes to undergo remodelling of its cytoskeleton and adjacent connective tissues eventually results in the pathognomonic appearance of cupped optic discs.

In summary, the ONH is a nexus for biomechanical forces and metabolic activity in the posterior globe. These potential sources of injury are counterbalanced by the protective mechanisms in the healthy subject but can become overwhelming in individuals who are susceptible to GON. Whilst the contribution of the various pathogenic mechanisms outlined in this section may depend on the glaucoma subtype and patient factors, the pathways ultimately converge to cause degeneration of RGCs, and therefore irreversible loss of vision.

1.3.3 Degeneration of Retinal Ganglion Cells

Maintenance of healthy RGCs requires the availability of essential metabolic substrates, specific trophic factors as well as prompt removal of environment stressors (Levkovitch-Verbin 2015). This is especially important in GON, as RGC degeneration is irreversible, in a manner comparable to other neurodegenerative diseases within the CNS. Indeed, a degree of RGC loss is inevitable during the normal ageing process, reflected by an estimated 0.7 decibels of sensitivity lost per decade as measured by Humphrey visual fields testing (Anderson et al. 2005).

Neurotrophins belong to a family of highly conserved proteins which includes nerve growth factor (NGF), BDNF, neurotrophin-3 (NT-3) and neurotrophin-4 (NT-4) (Huang and Reichardt 2001). BDNF appears to be particularly important for RGC survival, as it is found to be expressed in the superior colliculus and travel through RGC axons via retrograde transport. Neurotrophins exert their effects through two independent classes of receptors: the Trk family of high-affinity tyrosine kinase, which include the TrkA, TrkB, and TrkC receptors, and the low-affinity p75 neurotrophin receptor (p75NTR) (Meldolesi 2017). In general, downstream targets of TrK receptor activation result in pro-survival signalling via the MAPK/ERK and PI3K pathways, whereas p75NTR activation induces a mixture of proapoptotic pathways via JNK and a variety of other pathways including NF-κB.(Chao 2003)

Deprivation of neurotrophins such as BDNF is thought to contribute to the activation of MAPK pathways that promote apoptosis (Levkovitch-Verbin 2015). At the same time, animal models of glaucoma have demonstrated a decrease in the expression of the anti-apoptosis BCL-2 family of genes (Levkovitch-Verbin, Makarovsky, and Vander 2013). The BCL-2 family of genes are key regulators of the intrinsic apoptosis pathway, which tends to become activated through metabolic stress and mitochondrial instability (Kilbride and Prehn 2013). Together, these factors cause downstream

activation of effector caspases and result in RGC death via apoptosis. Moreover, studies have increasingly revealed important roles played by other constituents of the neuroretina, including MGCs, microglia and the complement cascade (Almasieh et al. 2012).

1.3.4 Experimental Models of Glaucoma

Establishing representative pre-clinical models of disease is an essential step in the development of effective therapies. This is challenging in glaucoma, a disease with complex aetiology which remains incompletely understood. In general, animal-based glaucoma models are much more costly but offer more complete pathophysiological representation, whilst *in vitro* models are simpler to design and perform but encapsulate comparatively limited fractions of glaucoma pathogenesis. Innovation and refinement of glaucoma models is an area of intense active research, and although significant progress has been made in recent years, several major hurdles exist in both animal-based and *in vitro* approaches.

1.3.4.1 *In Vivo* Glaucoma Models

A number of different animal models of glaucoma have been developed across different species (Bouhenni et al. 2012). These include spontaneously occurring strains, genetic modification techniques (Harada et al. 2019), and methods to induce intraocular pressure elevation (Biswas and Wan 2018). Although spontaneous and genetic models can offer insight into the underlying aetiology of glaucoma, inducible models are often preferred due to the availability of controls in untreated animals. The first animal experiments were conducted in primates and rabbits (Quigley and Addicks 1980); these gradually gave way to rodent models due to their ease of upkeep and cost-effectiveness as well as the evolution of animal research regulations.

A further advantage of rodent glaucoma models is the similarities between their anterior chamber anatomy and aqueous dynamics to humans (Pang and

Clark 2007). One of the earliest rat glaucoma models utilised hypertonic saline injection into the episcleral veins to induce sclerosis of the trabecular meshwork thereby decreasing aqueous outflow (Morrison et al. 1997). This was followed by models which use laser photocoagulation of the trabecular meshwork (TM) and injection of viscoelastic and/or microsphere beads to block drainage of aqueous through the TM (Levkovitch-Verbin et al. 2002).

When performing the anterior chamber microsphere injection technique, significant differences can exist within the same species. This has been demonstrated in mice, where higher IOP elevation was achieved in the C57BL/6 mouse strain, as well as younger animals, which reflected in a higher degree of RGC damage and axial elongation in these groups (Cone et al. 2010). A recent review of the microbeads model summarised the differences in the techniques employed (Morgan and Tribble 2015); notably, the types of microspheres used include latex, polystyrene and ferromagnetic materials, and the rats used included Norway Brown, Wistar, Sprague Dawley and Albino Swiss strains. Despite these challenges, the ferromagnetic microsphere models remain popular among glaucoma researchers due to advantages such as the ability to maintain a clear visual axis which allows for imaging studies to be carried out with minimal interference.

One clear advantage of models of induced intraocular pressure elevation is that these models replicate a larger proportion of the glaucoma pathogenic process. However, there are also important limitations to these models; firstly, any neuropathic damage as a result of intraocular pressure elevation would be a secondary finding, and therefore subject to variations; secondly, species which are the most accessible for animal research are rodents, which lack the distinct collagenous lamina cribrosa found in primates (Morrison, Cepurna Ying Guo, and Johnson 2011); thirdly, as explored in previous sections, a significant proportion of patients with glaucoma do not present with particularly high intraocular pressures (Section 1.3.1); and finally, the methods used to elevate intraocular pressure may have effects which are not representative of

human glaucoma aetiology, such as inflammation and ischaemia. However, despite these differences, much of the axonal degeneration seen in the rodent is not dissimilar to that seen in primates, suggesting that the lamina cribrosa may not be an essential part of the neurodegenerative changes seen in glaucoma associated with high IOP (Morrison et al. 1995).

Given these limitations, animal models of optic neuropathy are also frequently used in glaucoma research. Such models include physical and pharmacological methods of damaging the optic nerve. Physical models such as crushing or severing of the optic nerve are analogous to injuries which cause rapid and severe damage, as seen in trauma, ischaemic optic neuropathy, or acute angle closure attack (Tang et al. 2011). Alternatively, injections of N-methyl-d-aspartate (NMDA) can be used to induce excitatory neurotoxicity, which subsequently results in the apoptosis of RGCs, the crucial irreversible pathogenic event of glaucoma (Niwa et al. 2016). Whilst these models do not offer insight into anterior chamber dynamics or optic nerve head remodelling, they tend to be highly accurate and repeatable for investigating RGC degeneration.

Choosing appropriate animal models in glaucoma research requires consideration of the merits and limitations of each model to best suit the scientific question investigated. In particular, it is important to consider the “Three Rs” guidance on animal welfare in scientific research when making this choice, namely that the use of animals should be replaced, reduced and refined when possible (Fenwick, Griffin, and Gauthier 2009). To this end, there is a growing interest in the development of *in vitro* models of glaucoma to substitute and supplement human and animal research.

1.3.4.2 *In Vitro* Glaucoma Models

In vitro models tend to utilise *ex vivo* tissue or immortalised cell-lines to simulate IOP increase found in glaucoma. A major advantage of this approach is the ability to precisely control the degree of elevated hydrostatic pressure

(EHP) to simulate (Aires, Ambrosio, and Santiago 2017). Several studies have found detrimental effects of EHP on immortalised RGC cells, including increased apoptosis, which appears to be driven predominantly by the intrinsic/mitochondrial pathway (Ju et al. 2009). A particular interesting finding in an experiment using *ex vivo* rat retina was that RGCs appear to be relatively resistant to slow pressure increases, whilst short pulses of the same magnitude resulted in disproportionately greater RGC damage. This may partially explain the devastating effect a sudden rise in IOP may have, as seen in acute angle closure attacks; it also helps to explain the converse observation, where significant portion of individuals with ocular hypertension do not develop GON despite persistently high IOPs (Ingensiep et al. 2022).

EHP experiments using *ex vivo* rat retina containing glial and microglial cells revealed increased expression of pro-inflammatory cytokines such as IL-6, whilst blockade of TNF-α and IL-1β demonstrated protective effects (Madeira et al. 2015). These altered patterns of pro-inflammatory cytokine expression are comparable to those found in glaucomatous states, although further inferences of their effects are somewhat limited by the lack of circulating immune cells within these *in vitro* models.

In vitro models are particularly well-suited for investigations which target a narrow network of signalling pathways, as a variety of techniques can be applied both in terms of pathway activation and blockade, as well as data acquisition and analysis. There is, however, a critical weakness in these models, as cells have the tendency to behave differently *in vitro* outside of their normal microenvironment. Therefore, generalisations of *in vitro* findings to animal and human disease should be carried out with caution.

In 2012, a ground-breaking discovery allowed the growth of three-dimensional organoids *in vitro* from human stem cells (Nakano et al. 2012). More specifically, this technique was applicable to the eye, as protocols became established to form retinal organoids which replicated the intricate laminated structure of the retina. These organoids provide an appealing compromise

between *in vitro* and animal models, as they are able to recapitulate the structure and microenvironment of the retina. The application of retinal organoids in glaucoma research is still a relatively new field. Nevertheless, even at these early stages, encouraging advances have been made such as protocols which preferentially increased RGC yield and neurite extension (Fligor et al. 2018).

1.4 Development of Cell Based Therapies

The retina is particularly well-suited for the development of cell-based therapies for several reasons. Firstly, the majority cell types within the retina are derived from a common neuronal lineage; secondly, the retina is arranged into well-defined layers which contain distinct cell types (Heavner and Pevny 2012); and thirdly, *in vivo* visualisation of the retina and its sublayers, up to a cellular resolution, is possible throughout any therapeutic period (Burns et al. 2019). A multitude of cell-based approaches have been employed with the goal of preventing and treating ocular diseases. Broadly speaking, these approaches can be divided into the induction of endogenous regeneration, replacement therapy utilising exogenous sources of cells, and application of cell-derived products for neuroprotection (Figure 1-5, Figure 1-6).

1.4.1 Endogenous Regeneration

Regeneration of the retina is a phenomenon that has been well described in fish and amphibians, including the zebrafish, where cell lineage tracing attributed the source of the regenerated cells to MGCs present in the inner nuclear layer of the central retina (Raymond et al. 2006). Unfortunately, whilst a population of MGCs with neural stem cell characteristics has been identified in the adult human retina (Bhatia et al. 2009), retinal regeneration has not been observed to occur naturally in humans. As such, considerable research has focused on identifying the fundamental mechanisms which allow for the re-population of retinal cells.

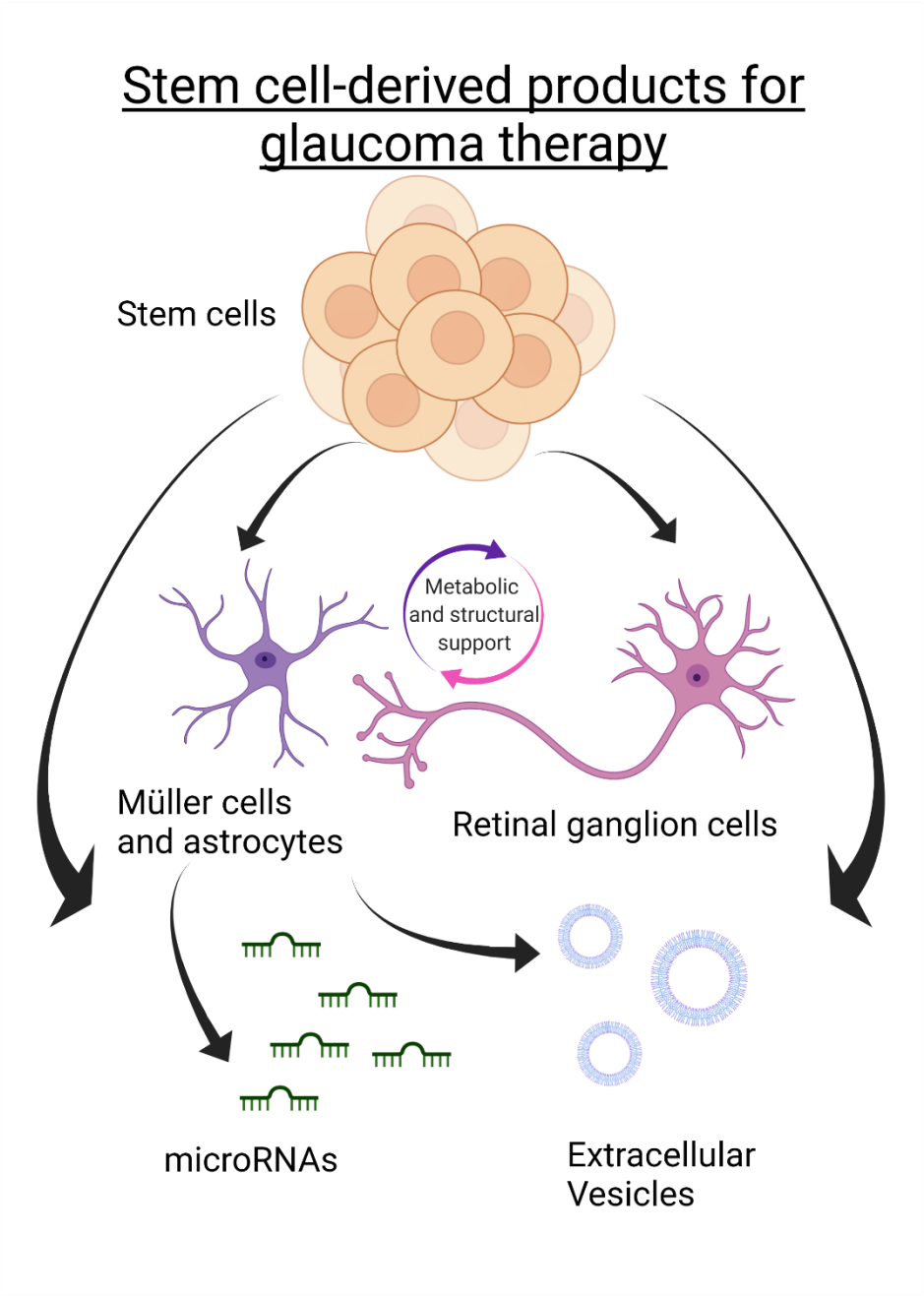

Figure 1-5 Stem cell-derived products for glaucoma therapy. Embryonic and Induced Pluripotent stem cells have been demonstrated to be capable of differentiating into Müller cells, astrocytes and retinal ganglion cells in vitro. Animal experiments have demonstrated beneficial effects resulting from the direct implantation of these cells, whilst other recent studies have explored the potential therapeutic effects of products such as microRNAs and extracellular vesicles derived from various sources.

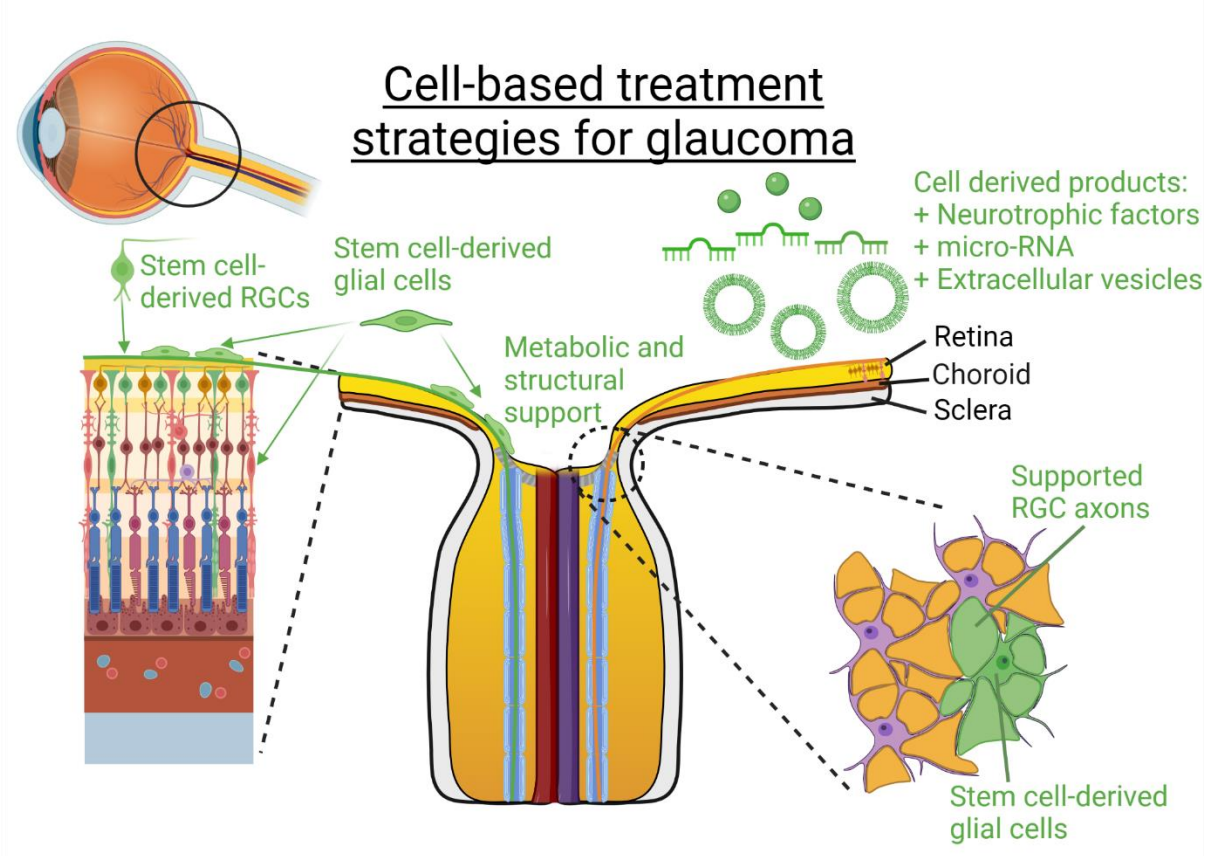

Figure 1-6 Treatment strategies for cell-based therapies in glaucoma. Cell replacement strategies aim to insert stem cell-derived glial cells and retinal ganglion cells (RGCs) into their normal anatomical locations, whereas the implantation of glial cells into locations adjacent to RGCs has been shown to promote visual benefit. Furthermore, the injection of cell-derived products such as neurotrophic factors, micro-RNAs and extracellular vesicles are more recently developed modalities of neuroprotection.

A host of differentially expressed factors by zebrafish MGCs following injury has been identified using both genetic and proteomic methods (Qin, Barthel, and Raymond 2009; Eastlake et al. 2018). Of particular importance are the presence of factors such as *stat3*, *ascl1,* and its downstream target *lin-28,* in allowing the re-entry of MGCs back into the cell cycle (Nelson et al. 2012). Activation of these intracellular pathways is thought to be due, at least in part, to the paracrine release of cytokines including TNF-α and TGF-β (Yafai et al. 2014), as well as growth factors such as EGF-1 and FGF (Wan et al. 2014).

The detailed interactions of these pathways during the regenerative process have been extensively reviewed elsewhere (Goldman 2014). Although investigations in this area have substantially advanced our knowledge of

intracellular mechanisms during retinal injury in different species, endogenous retinal regeneration has not yet been achieved in adult mammals. A major hurdle preventing the development of RGC replacement therapy is the sheer distance covered by the axons of RGCs during their projection to the brain. A typical RGC axon measures 50 mm in length, which is some 10,000 times the width of its cell body (Yu, Cringle, et al. 2013). In other words, if the diameter of a RGC axon (0.5-1 µm) was scaled-up to the width of an average road, its projection would proportionally be 200 kilometres. As such, precise methods of axonal guidance must be developed in order for such therapies to restore functional visual circuits between the retina and the brain.

1.4.2 Cell Replacement Therapies

An alternative approach to treat degenerative retinal conditions is to prepare functional cells *in vitro*, followed by implantation into the damaged tissue. Although current technologies can derive therapeutic cells to closely match damaged cells, designing a method of delivery which promotes integration within the retinal circuit has proven to be exceptionally difficult (Stout and Francis 2011). This is further complicated by the finding that evidence previously thought to demonstrate structural integration were in fact due to cytoplasmic material exchange (Santos-Ferreira et al. 2016; Pearson et al. 2016). Nevertheless, several studies have demonstrated functional recovery following treatment despite a lack of integration of transplanted cells (Becker et al. 2016). Currently, a variety of approaches are being developed to achieve functional cell replacement. These can broadly be divided according to the type of source cell used, as described in the following sections.

1.4.2.1 Embryonic Stem Cells and Induced Pluripotent Stem Cells

Embryonic stem cells (ESC) are derived from the inner cell mass of the blastocyst and have the ability to differentiate to any cell type from the three germ layers, mesoderm, endoderm and ectoderm (Yamanaka et al. 2008).

Discovered more recently, induced pluripotent stem cells (iPSC) can be generated from adult cells by the overexpression of ‘Yamanaka factors’ which include Oct3/4, Sox2, Klf4 and cMyc (Takahashi, Okita, et al. 2007; Takahashi, Tanabe, et al. 2007). Various human fibroblasts, keratinocytes and hematopoietic cells have been used to generate stable iPSC lines which show characteristics similar to ESCs (Wernig et al. 2007; Guenther et al. 2010).

The use of human ESCs (hESCs) has been explored for use in a wide range of retinal degenerative conditions. Established protocols include the differentiation of RPE for AMD-based therapies (da Cruz et al. 2018), and the generation of retinal progenitors which express markers for differentiated rod and cone photoreceptors following injection to the rodent eye (Zhou et al. 2015). More recently, studies have shown that ESCs can be differentiated to generate RGCs using either chemically defined or CRISPR-engineered protocols (Sluch et al. 2015; Zhang et al. 2020; Langer et al. 2018; Kobayashi et al. 2018). Using a reporter stem cell line, RGCs expressing brain-specific homeobox/POU domain protein 3B (BRN3B) and BRN3C can be FACS sorted from adherent hESC-differentiated retinal tissue and grown on scaffolds to guide axonal outgrowth (Sluch et al. 2015). These cells survived in culture and could be generated rapidly within 4 weeks. They exhibited axonal outgrowth, and were viable when transplanted into the adult rat retina (Zhang et al. 2020).

Both hESC and hiPSC have been used to generate 3D retinal organoids that are shown to closely mimic *in vivo* development (Nakano et al. 2012; Volkner et al. 2016; Cui et al. 2020). This differentiation protocol developed by Nakano and Sasai (Nakano et al. 2012) has provided an easy-to-follow method for reliably generating laminated neuroretinal tissues. Adapted by many other laboratories (Volkner et al. 2016; Lane et al. 2020; Sridhar et al. 2020; Eastlake et al. 2019), this novel strategy has paved the way for modern retinal research, including development, disease pathogenesis, and regenerative medicine. Retinal organoids are physiologically and metabolically functional,

where photoreceptors (Kim et al. 2019) and RGCs (Hallam et al. 2018) have been demonstrated to produce electrophysiological responses to light activity. RNA-Seq analysis of retinal organoids has identified multiple RGC subtypes, which highlights their cellular diversity during *in vivo* development (Langer et al. 2018). One recent study demonstrated that RGCs derived from retinal organoids formed by hiPSC survived for up to a month and improved function following injection into the vitreous of mice with optic neuropathy (Rabesandratana et al. 2020).

Differentiation of photoreceptor precursors was found to be increased in retinal organoids by the addition of COCO, an antagonist of the Wnt, Notch, TGF-β, and BMP pathways (Pan et al. 2020; Kruczek et al. 2017). The generation of RGCs using this method has proved more challenging, as there is a short competence window for the differentiation of RGCs during early retinal development. Furthermore, the number of RGCs decreases over time in retinal organoid cultures (Aparicio et al. 2017), whilst photoreceptor numbers increase (Volkner et al. 2016). There is some *in vivo* evidence that the addition of microRNAs such as miR-125b, miR-9, and Let-7 can increase the production of RGCs, in addition to promoting progenitor cell competence (La Torre et al. 2012). Additionally, it may also be possible to regulate RGC differentiation by mitophagy-dependent metabolic reprogramming via glycolysis (Esteban-Martinez and Boya 2018). Regulation of differentiation pathways such as Shh, TGF-β, Notch and Wnt signalling have also shown to control RGC differentiation in mammalian retinas (Walshe, Leach, and D'Amore 2011; Silva, Ercole, and McLoon 2003; Zhang and Yang 2001), whilst the addition of netrin-1 to retinal organoid culture medium has shown to enhance RGC neurite outgrowth (Fligor et al. 2018). An *in vitro* approach using retinal organoids provides the perfect platform to discover and refine RGC differentiation techniques; as such, a robust protocol may be available in the not-too-distant future.

In some cases, methods to isolate cells from stem-cell derived retinal organoids may be more advantageous than trying to develop protocols to promote direct differentiation. RGCs are especially well suited for this, as they can be produced more rapidly due to being one of the first cell-types to develop in retinal organoids (Fligor et al. 2018). In summary, ESC and iPSC-based methodologies are ideal for the development of cell-based disease models and therapies for glaucoma and other retinal diseases.

1.4.2.2 Mesenchymal Stem Cells

Mesenchymal stem cells (MSCs) are adult stem cells that can be derived from the bone marrow or umbilical cord. They are considered multipotent and have the capacity to differentiate towards cells of mesodermal lineage such as osteocytes, adipocytes and chondrocytes (Pittenger et al. 1999). Recently, some studies have shown that MSCs have the capacity to differentiate into neural lineages by the activation of Wnt/β-catenin, Notch and Shh pathways (Kondo et al. 2011; Leite et al. 2014; Yu, Liu, et al. 2013; Long et al. 2017; Huang et al. 2014) and addition of growth factors including EGF, bFGF and Hepatic growth factor (HGF) (Li et al. 2019; Huat et al. 2014; Bae et al. 2011). The secretome of MSCs comprise of a wide range of cytokines and growth factors including IL6, IL8, BDNF, Ciliary neurotrophic factor (CNTF), NGF, PDGF, LIF, NT-3, TGF-β2, and FGF2 (Baberg et al. 2019; Petrenko et al. 2020; Teixeira et al. 2017), and inflammatory factors including TNFα and IL-1β (Martire et al. 2016; Guo et al. 2007).

MSCs have been extensively explored for their therapeutic use in the treatment of glaucoma. Intravitreal injections of MSCs in glaucoma-induced rodent eyes align along the ILM and can survive for several weeks resulting in increased RGC survival (Johnson et al. 2010). A study compared the injection of human MSCs with their MSC-derived extracellular vesicles (EVs) into a rat optic nerve crush model. The results showed sustained neuroprotection of RGCs by whole cell treatment as compared to EVs alone, suggesting cellular

based-therapies might confer better sustained neurotrophic support to the retina (da Silva-Junior et al. 2021). MSCs have also been engineered to produce high levels of BDNF, and transplantation studies into hypertensive rat eyes demonstrated significant neuronal protection (Harper et al. 2011). Presently, few MSC-based therapies have reached clinical trial stages. Unfortunately, a recent study showed no significant changes in visual function as measured by electroretinogram (ERG) in two patients with open-angle glaucoma, and one patient was removed due to retinal detachment complications (Vilela et al. 2021), which suggests that additional refinement is required for this type of cell therapy. Two further clinical trials using bone marrow derived stem cells to treat optic nerve damage are currently in the recruitment phase (NCT01920867, NCT03011541).

1.4.2.3 Müller Glial Cells

Müller glia cells (MGCs) are the main glial cell type in the retina. They span radially across all neuroretinal layers to form contacts with all cells of the neurovascular unit (Section 1.1). MGCs with stem cell characteristics have been identified in the adult human eye. These cells can be isolated from post-mortem tissues and spontaneously become immortalised *in vitro* (Limb et al. 2002; Lawrence et al. 2007). Isolated human MGCs express characteristic stem cell markers such as SOX2, PAX6, βIII-tubulin and notch 1 and depending on culture supplementation, can be induced to become photoreceptor or retinal ganglion cell precursors (Singhal et al. 2012; Jayaram et al. 2014).

Extensive research has been conducted on the potential for MGCs in the treatment of glaucoma. In a rodent model of NMDA-induced retinal ganglion cell depletion, transplantation of human MGC derived RGC precursors into the vitreous space resulted in a partial recovery of RGC function as judged by the negative scotopic threshold response (nSTR) of the electroretinogram (Singhal et al. 2012). These cells aligned along the inner limiting membrane,

however little to no integration was observed (Singhal et al. 2012). Other studies have shown that rodent primary RGCs and progenitor-derived RGCs survive transplantation and become orientated along the host axons towards the ONH (Hertz et al. 2014), although there was limited evidence for substantial RGC integration and extension of axons through the ONH. One study found that following ablation of RGCs by intravitreal injection of NMDA to the feline eye, transplantation of MGCs into the intravitreal space resulted in partial recovery of visual function (Becker et al. 2016). However, transplanted MGCs did not attach directly to the retina as seen in rodent studies, but instead formed aggregates, suggesting that the vitreous may constitute a barrier for cell attachment onto the retina in the larger eye. As highlighted previously, RGC integration and axonal projection remain major hurdles for this type of therapy.

Isolation of MGCs has been performed successfully from human iPSC derived retinal organoids *in vitro*. Subsequent intravitreal transplantation of organoid derived MGCs into a rat model of RGC depletion has been demonstrated to induce a partial recovery of visual function (Eastlake et al. 2019). This study validates MGC implantation as a method of providing neuroprotection, and allogenic transplant studies are currently under way. There are important risks to consider when applying these cells to human therapies however, such as the need for traceability, elimination of potential pathogens, and histocompatibility. Nevertheless, it is evident that MGCs are highly specialised cells to function within the retina, whilst being a versatile source of cells for a variety of potential therapeutic applications (Eastlake, Lamb, et al. 2021).

1.4.3 Neuroprotection

Retinal regeneration has proven to be an immensely difficult goal with attention in recent years shifted somewhat to strategies of neuroprotection. As we gain deeper understanding of the pathogenesis of glaucoma, various experimental approaches have emerged aimed at inhibiting detrimental

pathways or enhancing endogenous protective mechanisms to prevent GON (Pardue and Allen 2018). Although there is a large body of data to support the neuroprotective effects of neurotrophins and antioxidants, effective delivery into the eye remains a significant hurdle preventing the translation of our current knowledge into clinical practice. Particularly as direct injection of soluble neurotrophins into the vitreous is not a practical approach, given the short half-life of these molecules, and the potential drawbacks associated with repeated injections (Ghasemi et al. 2018).

Cell-based therapy as an approach to deliver neuroprotective molecules offers several potential advantages to bypass issues associated with methods which deliver single molecules. Firstly, cells can act as a vehicle to deliver a wide range of factors into the retina simultaneously; secondly, the bioavailability of neuroprotective molecules can potentially be prolonged through continuous production by implanted cells; and finally, cells are naturally homeostatic and responsive to spatial-temporal changes in their microenvironment (Eastlake, Luis, and Limb 2019). Of course, developing an effective cell-based neuroprotective therapy has its own unique challenges, such as the choice of cell source, accurate and precise differentiation protocols, immunosuppression, and effective transplantation techniques.

1.5 Cell-Derived Products

1.5.1 Neurotrophins

The dependence of RGCs on neurotrophic factors is evident during optic nerve development (Meyer-Franke et al. 1995), as well as in the adult tissue, where RGC survival is reliant upon the retrograde delivery of neurotrophic signals from targets within the CNS (Iwabe et al. 2007). In rodent models, adeno-associated viral delivery of bFGF and BDNF can promote RGC survival following glutamate insult (Schuettauf et al. 2004), whilst CNTF treatment significantly reduced RGC loss (Ji et al. 2004). There is also compelling evidence for RGC neuroprotection by the neurotrophin nerve growth factor (NGF) (Chen, Wang, et al. 2015; Lambiase et al. 2009).

Despite this promising data, there remain concerns over the duration of any therapeutic effects from direct delivery of these neurotrophins, whereas whole cell transplant-based strategy may offer a longer-lasting solution. In support for this hypothesis, rat and human bone marrow derived MSCs induced to secrete high levels of BDNF, GDNF and VEGF, were found to exert a marked neuroprotective effect in a rodent optic nerve transection model following intravitreal injection (Levkovitch-Verbin et al. 2010). An alternative approach has incorporated the use of a polymeric capsule containing immortalized pigment epithelial cells transfected with the human CNTF gene (Thanos et al. 2004). These devices have been demonstrated to be capable of sustained CNTF secretion and delivery to the posterior chamber for up to 1.5 years following implantation (Sieving et al. 2006; Zhang et al. 2011). Randomised phase I and II clinical trials are currently ongoing to evaluate the safety and efficacy of these devices in patients with primary open-angle glaucoma (NCT01408472, NCT02862938).

In order to realise the potential of neurotrophic factors in the future management of glaucoma, a safe, stable, and continuous system for their delivery remains a major challenge. Furthermore, despite deprivation of

neurotrophic factors being characteristic of the glaucomatous retina, prolonged delivery of BDNF and TrkB receptor to axotomized optic nerve was unable to maintain long-term RGC survival (Di Polo et al. 1998). It is likely therefore, that neurotrophin secretion constitutes a part, but not all of the efficacy of whole-cell transplantation, as the roles of additional paracrine signals continue to be elucidated.

1.5.2 MicroRNA and Extracellular Vesicles

MicroRNAs (miRNA) are endogenous, small, non-coding RNAs. Their primary function is the post-transcriptional regulation of protein-coding gene expression by binding to the targeted messenger RNA (mRNA), which leads to the inhibition of translation or mRNA degradation. Through this system of interference, miRNA have been demonstrated to play pivotal roles in cell proliferation, differentiation, and apoptosis (Cai et al. 2012; Zhang et al. 2012). Several miRNAs have shown potential for RGC neuroprotection. These include miR-141-3p, which indirectly inhibits pro-apoptotic Bax and caspase-3 signalling pathways via targeting of docking protein 5 (DOK5)(Zhang et al. 2019); miR-93-5p, which was found to protect RGCs in culture from NMDA-induced cell death (Li et al. 2018); and miR-200a, which was found to preserve the thickness of the nerve fibre layer in a mouse model of glaucoma (Peng et al. 2019).

In recent years, significant research interest in neuroprotective strategies has focused upon the phosphatase and tensin homolog (PTEN) gene, the master inhibitor of the pro-regenerative mTOR/PI3K/Akt pathway (Park et al. 2008). In nervous tissue this pathway is responsible for the regulation of axon formation and extension during development, and the regeneration of peripheral nerve axons (Saijilafu et al. 2013). Numerous miRNAs have been found to target PTEN and subsequently activate the mammalian target of rapamycin (mTOR) pathway including miR-214 (Bera et al. 2017), miR-1908 (Xia et al. 2015), miR-494 (Wang et al. 2010), and miR-21 (Sayed et al. 2010).

In a model of glaucoma, inhibitors of miR-149 were shown to be neuroprotective of RGCs along with an associated upregulation of the PI3K/Akt pathway (Nie et al. 2018).

Over the past decade, secreted extracellular vesicles (EVs) comprising of cytosol enclosed in a lipid bilayer membrane have been identified as a major mode of intercellular communication (Klingeborn et al. 2017), and some populations of EVs were found to be highly enriched in nucleic acids, particularly mRNAs and micro-RNAs (Nolte-'t Hoen et al. 2016). In the context of glaucoma, a recent study reported evidence of RGC axon regeneration using a heterogenous EV population isolated from the L-cell fibroblast line in an optic nerve crush model (Tassew et al. 2017). In addition, MSC derived EVs have also been found to significantly enhance survival of RGC and regenerate their axons, while partially preventing RGC axonal loss in rodent models (Mead and Tomarev 2017; Pan et al. 2019; Mead, Ahmed, and Tomarev 2018; Mead, Amaral, and Tomarev 2018). Furthermore, delivery of miRNAs via Schwann cell-derived exosomes into cultured neurons were found to promote neuritogenesis (Ching, Wiberg, and Kingham 2018).

Since EVs are capable of delivering their cargo directly into target cells, EVs derived from healthy cells may potentially have a comparable therapeutic potential as the cells themselves. Cell-derived EVs also contain a range of miRNAs to potentially activate multiple anti-apoptotic and pro-survival pathways simultaneously. As evidence accumulates for their neuroprotective efficacy, low-immunogenicity, and high-stability, EVs appear to be promising candidates as an adjunctive therapy to IOP-lowering medications, and thus, a potential future treatment for glaucoma.

1.6 Project Aims

The overall aim of the project was to investigate the role of Gal-1 and -3 during retinal development, rodent models of glaucoma, and MGC responses to retinal inflammation. The overall study was divided into three sections based on the different approaches used, for which the following aims were formulated:

1. To identify factors which may regulate the gene and protein expression of Gal-1 and -3 by MGCs, as well as to examine the potential effects of Gal-1 and -3 on MGC functions, including proliferation, migration and contraction. The potential interactions of Gal-1 and -3 with intracellular pathways were also examined. These studies were undertaken using the MGC line MIO-M1 previously established in the host laboratory.
2. To investigate the expression of Gal-1 and -3 as well as their corresponding sialylation enzymes during retinal development, utilising retinal organoids derived from pluripotent stem cells. This part of the research also aimed to investigate whether expression of these molecules within developing retinal organoids was modified by pro-inflammatory cytokines.
3. To evaluate various models of experimental glaucoma and to investigate the potential use of MGC derived extracellular vesicles for their therapeutic potential. The expression of Gal-1 and -3 in these models was also examined.

2. MATERIALS AND METHODS

2.1 Moorfields and Institute of Ophthalmology - Müller 1 (MIO-M1) Cells

The majority of *in vitro* experiments in this project were conducted using the Moorfields Institute of Ophthalmology Müller 1 (MIO-M1) cell line isolated in the host laboratory as previously described (Limb et al., 2002). MIO-M1 cells are MGCs derived from cadaveric human retinal tissue which express MGC markers and became spontaneously immortalised. Cells were cultured in Dulbecco's Modified Eagle Medium (DMEM, Cat No. 31966-047; Gibco, Life Technologies, Carlsbad, CA, USA) containing high glucose, GlutaMAX™, and pyruvate. This was supplemented with penicillin at 20U/ml and streptomycin at 20µg/ml (Cat No. 15070-063; Gibco, Life Technologies) as well as Foetal Calf Serum (FCS; Biosera, Boussens, France) at concentrations of 10% for maintenance and 2% during experiments. The cells were incubated at 37°C and 5% CO_2, passage numbers between 20 and 30 were used during this project.

Cells were grown in T75 flasks during maintenance, T25 flasks for RNA and protein extraction, 24 well plates for immunocytochemistry, and 96 well plates for hexosaminidase assays. Cell passaging was carried out when a confluent layer of cells was present in a T75 flask, typically around 7 days after seeding. During passaging, the culture media was aspirated and 2ml of TrypLE™ Express Enzyme (Cat No. 12604-013; Gibco, Life Technologies) added. The flask was then incubated at 37°C and 5% CO_2 for 5 minutes to detach the cells. After this incubation, 5mls of PBS was added to wash and transfer the cell suspension into a 15ml falcon tube, and then centrifuged for 5 minutes at 1500 RPM to obtain a cell pellet. The supernatant was then aspirated, and the cell pellet re-suspended in 1ml PBS. In general, the cells were divided equally into four T75 flasks during maintenance.

For experiments, cell counting was performed by diluting 50µl of the resuspended cells in 50µL Trypan Blue solution (Cat No. T8154; Sigma Aldrich, Dorset, UK). The seeding numbers for different experiments are shown in Table 2-1. Live cells were counted using a haemocytometer under an inverted microscope in order to obtain accurate and consistent seeding numbers.

MIO-M1 Cells Seeding Densities

	Surface area	Seeding density	Growth Medium
T75 flask	75 cm^2	6 x 10^5	15 mL
T25 flask	25 cm^2	2 x 10^5	5 mL
6 well plate	9 cm^2	8 x 10^4	2 mL
24 well plate	2 cm^2	2 x 10^4	0.8 mL
96 well plate	0.32 cm^2	3 x 10^3	100 µL

Table 2-1 Seeding densities for MIO-M1 cells during experiments of this study.

2.2 Cryopreservation

Surplus cells were re-suspended in cryopreservation media containing 10% Dimethyl Sulfoxide (DMSO, Cat No. D4540, Sigma Aldrich), 40% FCS, and 50% DMEM with penicillin and streptomycin. This was placed in a cryovial placed in an isopropanol freezing container at -80°C for 24 hours and then transferred to a long-term container at -80°C. Thawed cells were cultured for at least one passage before being used in experiments.

2.3 Cytokine Treatment of Müller Glial Cells

MIO-M1 cells were cultured in the presence of a number of cytokines, including recombinant Tumour Necrosis Factor-α (TNF-α; Cat no 300-01A, Peprotech; UK), human recombinant Interleukin-1 (IL-1; Cat no 200-01B, Peprotech), human recombinant Transforming Growth Factor-β1 (TGF-β1;

Cat no 100-21, Peprotech) and TGF-β2 (Cat no 100-35B, Peprotech). Incubation with cytokines was carried using 10nM concentrations of these proteins and initiated at 80% confluency of MIO-M1 cells. Lyophilised cytokines were reconstituted in sterile 0.1% Bovine Serum Albumin (BSA; Acros Organics, Thermo Fisher Scientific; Pittsburgh, PA, USA) in phosphate buffered saline (PBS) and stored at -20°C as per the manufacturer's instructions. Cells were incubated with cytokines for a period of 24 hours for mRNA analyses, and for 48 hours for protein analyses.

2.4 Small Interfering RNA Transfection

Small interfering RNA (siRNA) transfection of MIO-M1 cells was carried out using oligonucleotide duplexes from OriGene (Maryland, U.S.). Three specifically designed duplexes were used for each target gene (Table 2-2). *In silico* analysis was carried out to ensure that siRNA sequences used did not contain off-target. A non-targeting siRNA duplex was used as control (Cat no. SR30004, Origene, U.S.)

Small interfering RNA sequences

Target	Sequence
LGALS1-A	rArGrGrUrGrGrCrUrCrCrUrGrArCrGrCrUrArArGrArGrCTT
LGALS1-B	rArGrCrUrGrCrCrArGrArUrGrGrArUrArCrGrArArUrUrCAA
LGALS1-C	rGrCrArArCrCrUrGrArArUrCrUrCrArArArCrCrUrGrGrAGA
LGALS3-A	rCrGrCrArUrGrCrUrGrArUrArArCrArArUrUrCrUrGrGrGCA
LGALS3-B	rArCrGrCrUrUrCrArArUrGrArGrArArCrArArCrArGrGrAGA
LGALS3-C	rUrGrArArUrUrArCrCrUrGrUrCrUrCrArArUrArUrGrUrCAA

Table 2-2 Small interfering RNA sequences used within the study for Gal-1 and -3. Three siRNA duplex constructs were used to target each protein.

Following optimisation of the procedure (section 3.2.1), subsequent experiments used a combination of all three siRNA duplexes at a total

concentration of 10nM. Transfection was carried out using a proprietary transfection agent siTran (Cat no. TT320001, Origene, U.S.), at a siTran/siRNA ratio of 2uL/ng. This mixture was first dissolved in a transfection buffer (Cat no. TT30005, Origene, U.S.), vortexed and allowed to stand for 10 minutes before being added to the culture media. For the purposes of various experiments within this study, MIO-M1 cells were cultured with the siRNA for 24 hours and 48 hours prior to RNA and protein analysis, respectively; and for 48 hours prior to re-seeding for purposes of migration and contraction assays. Retinal organoids were cultured with siRNA for 24 hours prior to cytokine related studies.

2.5 Retinal Organoid Differentiation

Retinal organoids within this study were derived from the RC-9 line of human embryonic stem cells (RCe013-A, Roslin Cells Limited, Edinburgh, U.K.). For the purposes of stem cell maintenance, RC-9 cells were cultured in Stem Pro (ThermoFisher, U.K, Cat. No. 10639011), with 1:2000 FGF (ThermoFisher, U.K, Cat. No. PHG0367). Differentiation of these ESC cells into retinal organoids is based on protocols developed by Nakano et al. (Nakano et al. 2012) and has been described previously (Eastlake et al. 2019). For detachment, confluent RC-9 cells were washed in PBS, then covered with TryplE (ThermoFisher, U.K.) containing 0.5mg/ml DNase (Sigma-Aldrich, U.K.) and 10μM ROCKi (Y-27632, Millipore, Watford, U.K.) for 1 minute. The cells were then transferred into a 15ml falcon tube and centrifuged at 500rpm for 5 minutes to obtain a cell pellet. Cells were then resuspended and seeded into a low adhesion v-bottomed 96-well plate at a density of 9000 cells/well, in 100μL culture medium, consisting of Glasgow Minimum Essential Medium (GMEM) with L-glutamine with 20% knock-out serum (ThermoFisher, U.K.), 1mM sodium pyruvate (ThermoFisher, U.K.), 0.1mM nonessential amino acids (ThermoFisher), 50units/mL penicillin/streptomycin (ThermoFisher, U.K.), 50μM β-mercaptoethanol (ThermoFisher, U.K.), 20μM ROCKi and 3μM Wnt antagonist (Millipore, Watford, U.K.). A further 100μL of this media solution

was added on day 2, followed by 100µL media exchanges on day 5 and day 8. On day 12, the embryoid bodies (EBs) formed were transferred into separate wells of squared 25-well, low-adhesion plates, and the media was changed to 750µL GMEM with L-glutamine, 20% knock-out serum (KOSR), 10% foetal calf serum (FCS) 1mM sodium pyruvate, 0.1mM nonessential amino acids, 50units/mL penicillin/streptomycin, and 50µM β-mercaptoethanol, 1% Matrigel and 100nM smoothened agonist (SAG; Millipore, Watford, U.K.); media exchange was performed on day 15. From day 18, media exchanges were performed twice weekly with Dulbecco's modified Eagle's medium/F12-glutamax containing 10% FCS, 1% penicillin/streptomycin/amphotericin (ThermoFisher, U.K.), 1% N2 supplement (ThermoFisher, U.K.), and 0.5 µM retinoic acid (Sigma-Aldrich, U.K.). Dissection was performed on appropriate retinal organoids between day 30 and day 35 under microscopy using microsurgical instruments in order to isolate viable retinal mantles. All plates were maintained at 37°C, 5% CO_2, and atmospheric O_2.

2.6 Cell Proliferation Assays

Müller cell proliferation was determined using the hexosaminidase assay. Hexosaminidase is a ubiquitous lysosomal enzyme, the total activity of which is directly proportional to the number of cells in a homogenous population. This method was first introduced by Landegren (1984) for the quantification of T cells and its applicability in MIO-M1 cells is demonstrated in section 3.1.1. Of note, in the original study, the absorbance values obtained from hexosaminidase assays were found to be directly proportional to both the number of cells and the length of incubation.

The substrate 4-nitrophenyl-N-acetyl-ß-D glucosaminide (Cat No. N9376; Sigma Aldrich) was used for the hexosaminidase assay. This was dissolved in sodium citrate solution (pH 5.0) at a concentration of 0.25%, and then added to 0.5% Triton X-100 solution (Cat No. X100; Sigma Aldrich). In order to assess the number of cells at a specific time point using the hexosaminidase

assay, growth media from cells cultured in 96 well plates were aspirated. The wells were washed twice with 200µl PBS, and 60µl of substrate solution was added. The plates were then incubated between 30 minutes and 2 hours at 37°C, following which the reaction was blocked with 90µl of 0.1M glycine-NaOH buffer solution (pH 10.4). The final absorbance was measured using a Safire UV-VIS spectrophotometer (Tecan, Mannedorf, Switzerland) at 405nm wavelength with a refence of 620nm. The value obtained was normalised to the control of each experiment; individual passages were triplicated as a minimum and repeated over no fewer than three passages.

2.7 Cell Migration Assay

Wound scratch assays were used to examine the rate of migration for cells as described previously (Bobadilla et al. 2019). Accordingly, MIO-M1 cells were grown to 90% confluence on a 24-well plate under conditions as specified within each experiment. A sterile 200µL pipette tip was used to produce a vertical scratch within each well. The wells were washed twice with PBS, which was then replaced with growth media, with cytokine or growth factor supplement as specified in each experiment. An inverted microscope was used to photograph a portion of the scratch within the cells prior to incubation, and after 24 hours, a further photograph was taken at the same location. The area without cells was measured using ImageJ software (Java, USA), and change between baseline and at 24 hours were calculated to determine percentage (%) values.

2.8 Collagen Gel Contraction Assay

Collagen contraction gels were prepared using a mixture of 600 µL of rat tail collagen, 95µL concentrated medium mix consisting of 70 µL 10x DMEM (Sigma-Aldrich, UK), 7µL L-glutamine, and 18µL NaHCO3 (Gibco, Life technologies, UK). The mixture was then titrated to pH 7.0 using approximately 56µL 1M NaOH. 5 x 10^4 MIO-M1 cells diluted in 60µL 1x DMEM was added and mixed gently. 150µL of the resultant mixture was then

cast into glass bottom MatTek dishes (MatTek Corporation, MA, USA) quickly before collagen polymerisation occurred. The MatTek dishes containing freshly cast gels were placed in a 37˚C incubator for 10 minutes in order for the collagen to polymerise and set. Following this, the bottom of the gel was gently detached from the dish and growth medium added as per experimental conditions.

2.9 Gene Expression Analysis

2.9.1 RNA Extraction

The isolation of RNA was performed using the RNeasy Plus Mini Kit (Cat No. 74134; Qiagen, Hilden, Germany) containing proprietary buffers RLT plus, RW1 and RPE. Following cell incubation in T25 flasks, the media was aspirated and washed once using PBS. This was followed by the addition of 350µl of RLT plus buffer containing 1% ß-mercaptoethanol to cover the monolayer of cells and stored at -20°C overnight.

The next day, RNA extraction was performed following the manufacturer's instructions including the use of gDNA elimination and RNeasy spin columns. The final RNA elution was carried out using 30µl of nuclease free water, and the final RNA concentration was measured by spectrophotometry (Nanodrop-1000, Thermo Fisher Scientific, Pittsburgh, PA, USA).

2.9.2 Reverse Transcription

Reverse transcription (RT) was carried out using the SuperScript® IV First-Strand Synthesis System (Cat No. 18091050, Thermo Fisher Scientific). A 200µl reaction tube contained 500ng or 1µg RNA, 1µl 50µM Oligo d(T)18 primer (Cat No. 18418-012; Life Technologies), 1µl 10mM dNTP mix (Cat No. U151A; Promega, Madison, WI, USA), and nuclease free water to reach a final volume of 13.5µl. This initial reaction mix was briefly vortexed and centrifuged, then heated to 65°C for 5 minutes using a thermal cycler

(Mastercycler® Pro: vapo protect; Eppendorf, UK) to allow for annealing to occur, followed by at least 1 minute at 4°C. Next, 4µl 5x SSIV buffer, 1µl DTT buffer, 0.5µl RNasin® Plus RNase inhibitor (Cat No. N2611; Promega) and 1µl SuperScript® IV reverse transcriptase enzyme were added to the initial reaction mixture. This mixture was again briefly vortexed and centrifuged, followed by incubations at 55°C for 10 minutes and 80°C for 10 minutes. Of note, the RT reaction mixture was kept on ice between individual steps, and the quantity of RNA was kept consistent within each experiment. In cases where reverse transcription was not performed directly following RNA extraction, the RNA was stored at -80°C and thawed on ice.

2.9.3 Quantitative Polymerase Chain Reaction

Quantitative polymerase chain reactions (qPCR) were carried out using SYBR® Green JumpStart™ Taq ReadyMix™ (Cat no. S4438, Sigma-Aldrich, UK), according to manufacturer's instructions. This consisted of 10µL SYBR green reagent, 0.25µL indicator dye, and 10ng cDNA made up to 9.75µL using Nuclease free water. Reactions were carried out on MicroAmp® Optical 96-Well Reaction Plates (Cat no. N8010560, Thermo Fisher), and each condition was repeated in triplicate. QuantStudio™ 6 Flex Real-Time PCR System (Applied Biosystems, Massachusetts, USA) was used as the thermo cycler. Each 96-well plate was sealed with an adhesive film to avoid evaporation and centrifuged prior to placing in the thermo cycler machine.

Thermo cycling was programmed to initially hold at 50°C for 2 minutes and then 95°C for 10 minutes. Then, 40 cycles of PCR steps were performed, which each consisted of 95°C for 15 seconds and then 60°C for 1 minute. Following this, a melt curve step of 95°C for 15 seconds, 60°C for 1 minute and a dissociation stage of 95°C for 15 seconds were carried out. Data was collected between the 60°C and 72°C stage of each cycle.

Primers used in the quantitative polymerase chain reaction (qPCR) were designed using Primer-BLAST(https://www.ncbi.nlm.nih.gov/tools/primer-

blast/) to produce amplicons which are shorter than 200 base-pairs in length. Optimisation of primer concentrations was carried out to ensure qPCR efficiency. This consisted of performing qPCR using combinations of forward and reverse primers at concentrations between 50nM and 300nM, using both control cDNA and nuclease free water as no-target controls (NTC). Confirmation of qPCR efficiency was carried out using the melt curve, where successful amplification of cDNA resulted in a single peak, whilst NTC samples produced no significant peaks (Figure 2-1). A concentration combination of forward and reverse primers which demonstrated good amplification efficiency was chosen for each primer pair. In cases where most or all concentration combinations were efficient, 200nM was chosen for both forward and reverse primers. Primers used in this project are listed in Table 2-3.

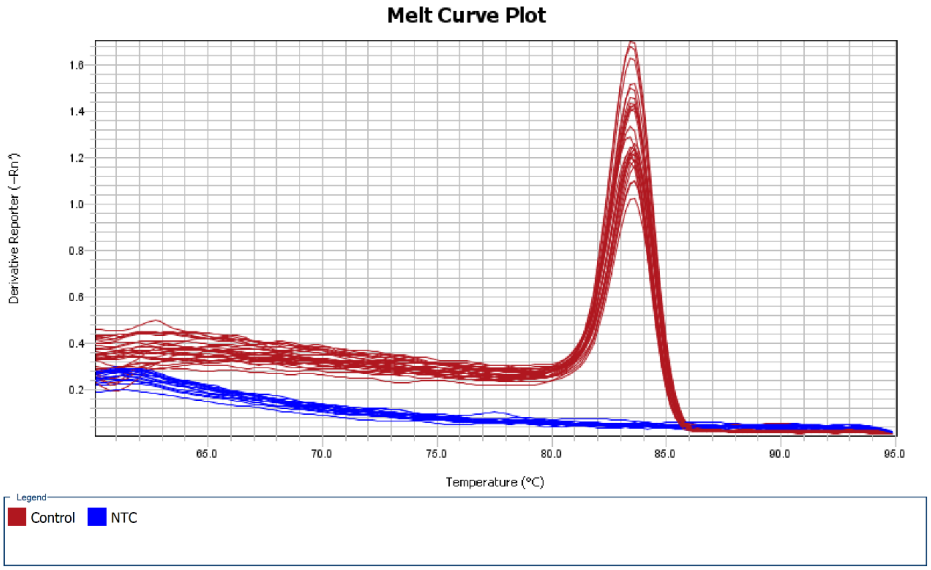

Figure 2-1 Example of confirmatory melt curve to demonstrate a single peak for control cDNA (red lines), and no significant peaks for no-target control (NTC) samples (blue lines). In this particular case, all concentrations of primers tested demonstrated acceptable qPCR efficiency.

Quantitative PCR Primers

Target		Sequence	Product Length (bp)
GAPDH	Forward	GTCTCCTCTGACTTCAACAGCG	131
	Reverse	ACCACCCTGTTGCTGTAGCCAA	
Gal-1	Forward	AAGCTGCCAGATGGATACGAA	76
	Reverse	CGTCAGCTGCCATGTAGTTGA	
Gal-3	Forward	TGATTGTGCCTTATAACCTG	172
	Reverse	ATGACTCTCCTGTTGTTCTC	
ST3Gal1	Forward	GAAACTCCAGCGTGTCTCCA	176
	Reverse	CATAGGCTGAGTGACCGTCC	
ST6Gal1	Forward	CTACCACCCGCTGCTCTATG	89
	Reverse	GTGTGGCTTTTCCAAGCAGG	
TGF-β1	Forward	GAGAAGAACTGCTGTGTGCG	134
	Reverse	GTGTCCAGGCTCCAAATATAG	
TGF-β2	Forward	CAGGAGTGGCTTCACCACAAAG	160
	Reverse	TGGCATATGTAGAGGTGCCATCA	
TGF-β3	Forward	TCGACATGATCCAGGGACTG	96
	Reverse	CCACTGAGGACACATTGAAACG	

Table 2-3 Quantitative PCR primers used; amplification efficiency was confirmed for all primer pairs.

Data obtained from the thermo cycler were analysed using the ΔΔCt method. This consisted of firstly ensuring the triplet replicates for each condition showed consistency and excluding spurious data points. Ct values were then determined based on a threshold level indicating significant amplification. Each Ct value was then normalised to the house keeping gene, Glyceraldehyde 3-phosphate dehydrogenase (GAPDH) to produce the ΔCt value. Following this, ΔCt values of experimental samples were normalised to corresponding control samples to produce ΔΔCt values. Final fold change values were then calculated using the formula:

$$Fold\ change = 2^{-\Delta\Delta Ct}$$

2.9.4 RNA Sequencing

RNA Sequencing was carried out by UCL Genomics laboratory (UCL, London, UK), which included sample preparation and processing. RNA integrity was confirmed using Agilent's 2200 Tapestation. Samples were processed using the KAPA mRNA HyperPrep Kit (p/n KK8580) according to manufacturer's instructions. Briefly, mRNA was isolated from total RNA using Oligo dT beads to pull down poly-adenylated transcripts. The purified mRNA was fragmented using chemical hydrolysis (heat and divalent metal cation) and primed with random hexamers. Strand-specific first strand cDNA was generated using Reverse Transcriptase in the presence of Actinomycin D. This allows for RNA dependent synthesis while preventing spurious DNA-dependent synthesis. The second cDNA strand was synthesised using dUTP in place of dTTP, to mark the second strand. The resultant cDNA is then "A-tailed" at the 3' end to prevent self-ligation and adapter dimerisation. Full length xGen adaptors (IDT), containing two unique 8bp sample specific indexes, a unique molecular identifier (N8) and a T overhang were ligated to the A-Tailed cDNA. Successfully ligated cDNA molecules were then enriched with limited cycle PCR (12 cycles).

Libraries to be multiplexed in the same run were pooled in equimolar quantities, calculated from Qubit and Bioanalyser fragment analysis. Samples were sequenced on the HiSeq 3000 instrument (Illumina, San Diego, US) using a 75bp paired read run with a corresponding 8bp UMI read.

Run data were demultiplexed and converted to fastq files using Illumina's bcl2fastq Conversion Software v2.19. Fastq files were then aligned to the human genome UCSC hg38 using RNA-STAR 2.5.2b then UMI deduplicated using Je-suite (1.2.1). Reads per transcript were counted using FeatureCounts and differential expression was estimated using the BioConductor package SARTools, a DESeq2 wrapper.

The normalisation and differential expression analysis was performed by DESeq2, within a package called SARTools. The results were pre-filtered into up regulated and down regulated genes (2.5-fold change; p<5%).

Bioinformatic analysis of RNA-seq data was conducted using the online platform iDEP90 (http://ge-lab.org/idep/) which conducts differential expression and pathway analysis. Analyses of read count data were conducted using iDEP 0.91, hosted at http://ge-lab.org/idep/.

2.10 Protein analysis

2.10.1 Immunostaining of Adherent Cells and Ocular Tissues

For cells to effectively adhere, 13mm microscope slide coverslips were placed in 24 well plates and pre-coated with 250µl Matrigel (Cat No. E6909; Sigma Aldrich) for 2 hours. Following removal of excess Matrigel, cells were seeded as previously described.

At the end of each experimental period, the media was aspirated from the wells, and 4% paraformaldehyde (PFA) was used to fix the cells for 5 minutes. Excess PFA was then removed and the wells washed 3 times with PBS and covered in blocking solution containing Tris-buffered saline (TBS), 0.3% Triton and 5% donkey serum at room temperature for 1 hour. This blocking solution

was then replaced by a primary antibody containing blocking solution, and incubated overnight at 4°C. On the following day, the wells were washed 3 times for 5 minutes with PBS, then incubated in donkey derived secondary antibody labelled with Alexa-Fluor fluorochoromes (Jackson ImmunoResearch Laboratories, PA, USA) diluted in blocking solution for 3 hours at room temperature. The cells were washed a further 3 times, and stained with 4', 6-diamidino-2-phenylidole (DAPI; Cat No. D9542; Sigma Aldrich) diluted at 1:5000 in PBS for 2 minutes, then washed with PBS and MiliQ water for 1 minute each. Finally, the coverslips were removed from the 24 well plates and mounted to microscope slides using Vectashield (Vector Laboratories, CA, USA), and sealed with nail varnish. Antibody titres are included in appendix 8.1)

2.10.2 Immunohistochemical Staining of Retinal Organoids

At specified timepoints, the media was aspirated from wells and replaced with 4% paraformaldehyde (PFA) for 10 minutes to fix the retinal organoids, then replaced with 30% sucrose for storage. Organoids were embedded in optimal cutting temperature (OCT) compound and frozen prior to sectioning using a Leica cryostat at a thickness of 8-10µm, the sections were transferred onto microscopy slides (Superfrost plus, VWR, U.K., Cat. No. 631-0108P). For immunostaining, microscopy slides were washed with TBS, then covered in "carbo free" blocking solution (Vector Laboratories, CA, USA, Cat. No. SP-5040-125) for 1 hour. This blocking solution was then replaced by a primary antibody containing blocking solution, and incubated overnight at 4°C. On the following day, the slides were washed 3 times for 5 minutes with PBS, then incubated in donkey derived secondary antibody labelled with Alexa-Fluor fluorochoromes (Jackson ImmunoResearch Laboratories, PA, USA) diluted in blocking solution for 3 hours at room temperature. The slides were washed a further 3 times, and stained with 4', 6-diamidino-2-phenylidole (DAPI; Cat No. D9542; Sigma Aldrich) diluted at 1:5000 in PBS for 2 minutes, then washed with PBS and MiliQ water for 1 minute each.

2.10.3 Image Acquisition and Manipulation

Fluorescence images were acquired on a confocal laser scanning microscope (Leica Stellaris 5, Leica, Germany), using 10x, 20x, and 40x objectives. Oil immersion was used to obtain 40x images. Exposure times for each fluorescence filter and microscope settings were adjusted appropriately and kept constant within experiments. Image processing and manipulation was carried out using Leica Application Suite X (LASX, Leica, Germany).

2.10.4 Protein Extraction from Cultured Cells

At the end of the incubation period specified for each experiment, a cell pellet was obtained using procedures outlined above (section 2.1). Protein extraction was then performed immediately by adding 100µl radio immunoprecipitation assay (RIPA) lysis buffer (Cat No. R0278; Sigma Aldrich) containing 3mM sodium orthovanadate, 1mM phenylmethane sulphonyl fluoride (PMSF), 0.5mM dithiothreitol (DTT) and 10µl protease inhibitor cocktail (Cat No. P8340; Sigma Aldrich) to each cell pellet obtained from T25 flasks. A homogenous suspension was achieved via pipetting and vortex, this mixture was then placed on ice for 5 minutes to complete cell lysis. Centrifugation at 10,000 rpm for 5 minutes was then carried out, and supernatant collected which contained the proteins of interest, these were stored at -20°C.

2.10.5 Determination of Protein Concentration in Cell Lysates

The concentration of proteins contained in cell lysates were measured using the Thermo Scientific Pierce BCA protein assay kit (Cat No. 23225; Life Technologies). Triplicates of samples and duplicates of standards, blanks, and zero wells were prepared according to the manufacturer’s instructions using a 96 well plate. The BCA reagent was prepared and added to each well, and then incubated at 37°C for 30 minutes. Following the incubation period, the absorbance of each well was measured at 562nm with reference to

690nm using a Safire UV-VIS spectrophotometer (Tecan). Following normalisation to the blank readings in each experiment, the concentration of each protein sample was then calculated using a standard curve constructed from the wells with known standard concentrations.

2.10.6 Western Blotting Assay

Protein gel electrophoresis was carried out using the NuPAGE® system (Invitrogen), consisting of 15 well 4-12% Bis-Tris polyacrylamide gels (Cat No. NP0336; Thermo Fisher Scientific) and MES sodium dodecyl sulphate (SDS) running buffer (Cat No. NP0002; Thermo Fisher Scientific) chosen due to the relatively low molecular weight of Gal-1 (13kDa).

For each sample, 10µg of protein made up to 9.75µl was added to 3.75µl of 4x lithium dodecyl sulfate (LDS) sample loading buffer (Cat No. NP0007; Thermo Fisher Scientific) and 1.5 µl of 10x reducing agent (Cat No. NP0009; Thermo Fisher Scientific). The loading protein mixture was briefly vortexed, centrifuged, then denatured 80°C for 10 minutes into primary structures.

The polyacrylamide gels were loaded into XCell SureLock™ Mini-Cells (Thermo Fisher Scientific) as per manufacturer's instructions, forming an inner compartment containing 200ml MES buffer and 500µl antioxidant (Cat No. NP0005; Thermo Fisher Scientific), and an outer compartment containing 600ml MES buffer. 15µl of each sample was then loaded into individual wells, flanked by 5µl of coloured 11-245 kDa protein ladder (Cat No. P7712; New England Biolabs, Ipswich, MA, USA). Finally, the electrodes were connected, and the gel resolved at 180V for 35 minutes.

2.10.7 Protein Gel Transfer

Protein transfers were performed using 0.45µm polyvinylidene fluoride (PVDF) membranes (Cat No. IPFL00010; Merck Millipore, Darmstadt, Germany). The transfer membranes were cut to size, then covered in methanol for 2 minutes, rinsed in distilled water, and then placed in transfer buffer (Cat No. NP0006;

Thermo Fisher Scientific) containing 15% methanol and diluted in distilled water. The transfer process was carried out using a semi-dry process, where thick filter paper (Cat No. 1703968; Bio-Rad Laboratories, West Berkley, CA, USA) pre-soaked in transfer buffer were placed outside of the transfer membrane toward the anode, and the protein gel, towards the cathode of a Trans-Blot® SD Semi-Dry Transfer Cell (Bio-Rad Laboratories). Care was taken to remove any pockets of air in this arrangement, and that the gel and transfer membrane were in full contact. The transfer process was then performed at 10V for 30 minutes.

2.10.8 Protein Immunodetection

The PVDF membranes containing the transferred proteins were placed in 10ml of blocking solution containing 0.1% Tween-20 (Cat No. 003005; Thermo Fisher Scientific), 5% milk and 5% FCS diluted in TBS for 1 hour at 37°C. The membrane was then incubated in further blocking solution containing the primary antibody for the protein of interest (Section 8.1) overnight at 4°C on a shaker.

On the next day, the membrane was washed 3 times using 0.1% Tween-20 diluted in TBS for 30 minutes each, then incubated in blocking solution containing 1:5000 of the corresponding secondary species-specific antibody conjugated to horseradish peroxidase (Jackson ImmunoResearch Laboratories Inc., PA, USA) for 1 hour at room temperature. The membrane was washed 3 times further for 30 minutes each, after which it was covered in a chemiluminescent substrate (Cat No. WBLUR0500; Millipore Corporation, Billerica, MA, USA) for 2 minutes. The degree of luminescence was assessed by X-ray film (Cat No. AUT-300-040D; Thermo Fisher Scientific) development carried out in a dark room.

In order to visualise additional proteins, PVDF membranes were stripped up to twice using TBS containing 5mM NaCl and 200mM glycine at pH 2.5 for 30

minutes on a shaker. The membranes were then incubated with antibody for a different protein of interest at 4°C overnight.

2.10.9 Enzyme-linked Immunosorbent Assay

Anterior chamber Gal-3 protein concentration levels were quantified using commercially available enzyme-linked immunosorbent assay (ELISA) kits (Cat no. NBP2-76724, Novus Biologicals, USA). Samples were stored at -80°C immediately following acquisition. For the purposes of ELISA, samples were thawed and centrifuged for 2 minutes at 10,000 RPM, diluted and processed according to manufacturer's instructions. Optical density was measured at the end of the procedure and the corresponding concentration determined via a standard curve.

2.11 Experimental Models of Elevated Intraocular Pressure and Glaucoma: Animal Husbandry, Anaesthesia, and Intraocular Pressure Measurement

The use of animals was approved by the local ethics committee at University College London, Institute of Ophthalmology, and the U.K. Home Office. All animals were maintained according to U.K. Home Office regulations for the care and use of laboratory animals (Scientific Procedures Act 1986, Licence no. PA021D07F). Wild-type Lister Hooded rats aged between 8 and 10 weeks were used for the NMDA neurotoxicity model, and wild-type Brown Norway rats aged 6-8 months were used for the ferromagnetic bead model of glaucoma. All animals were given unrestricted access to food and water and kept under 12-hour light/dark cycles with no changes to standard animal husbandry protocols.

For anaesthesia, reversible agents were used for surgical procedures; this consisted of Ketamine (Narketan; 45 mg/kg) and Medetomidine Hydrochloride (Domitor; 0.375 mg/kg) to induce anaesthesia, and Atipamezole (Antisedan; 2.5 mg/kg) for reversal. For ERG measurements, non-reversible anaesthesia

was used, consisting of Ketamine (Narketan; 60 mg/kg) and Xylazine (Rompun; 7.5 mg/kg). Recovery from both investigative and surgical procedures was carried out in animal cages placed on heated mats until the return of normal activities under monitoring. During recovery, subcutaneous injections of 0.9% saline were given at 1ml/kg and topical carbomer gel was applied to both eyes for lubrication.

IOP was measured between 9am and 11am using a rebound tonometer as calibrated to the rat eye (iCare, Tonolab), an average of five valid measurements was taken as per manufacturer's instructions.

2.11.1 Anterior Chamber and Intravitreal Injections

Ferromagnetic microbeads (5 µm diameter, BcMag aldehyde terminated magnetic microbeads; Bioclone Inc) were sterilised by three washes with 70% ethanol, followed by three washes with sterile saline, and then resuspended at 10mg/ml.

For anterior chamber injections, anaesthetised animals were placed onto a 3D printed custom-made rat holder which secured the rodent's teeth and allowed for movement and rotation around all axes (Figure 2-2). Local Anaesthesia using proxymetacaine hydrochloride 0.5% (Bausch & Lomb, UK) was administrated to both eyes and the rat was then placed under the visual axis of an operating microscope. A 30-gauge needle was then used to create a paracentesis, following which a 30-gauge Hamilton needle was used to deliver 20µl of the ferromagnetic microbeads and/or 2% hydroxypropyl methylcellulose (HPMC).

For intravitreal injections, the same animal preparation procedures were followed as above, with the addition of phenylephrine hydrochloride 2.5% (Bausch & Lomb, UK) and tropicamide 1% (Bausch & Lomb, UK) administered to the operated eye for dilation. Following this, a coverslip was placed over the cornea and held in place with 2% HPMC as coupling fluid in order to visualise the entry point and advancement of the delivery needle.

Injections were performed using 32G Hamilton syringes, and the point of entry was 1mm posterior to the limbus, with the needle trajectory pointed towards the optic nerve head. The needled was then advanced slowly under microscopical visualisation, and the contents delivered by an assistant, a 30 second delay was used before withdrawal to minimise possible fluid reflux. For the induction of RGC excitatory neurotoxicity, each injection consisted of a 2µL mixture of 80 µM NMDA and 80 mg/ml triamcinolone diluted in 0.9% sterile saline. For the injection of EVs, each injection consisted of 3 x 10^9 EVs diluted in 2µL of 0.9% sterile saline.

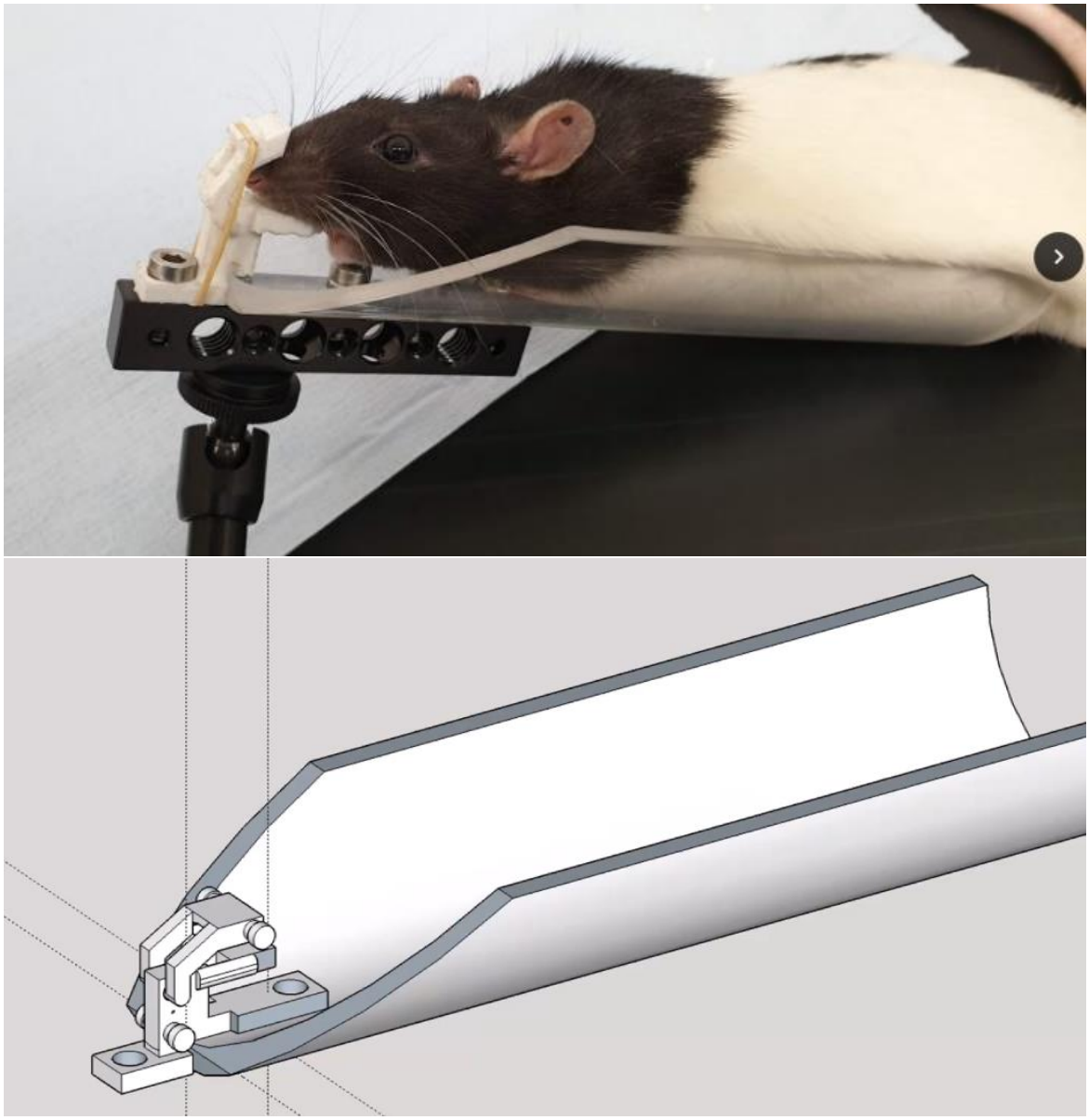

Figure 2-2 3D printed custom rat holder for surgical procedures, the animal's teeth is secured under mild tension, and the holder can be rotated in all 3 axes. Top – CAD rendering; Bottom – 3D printed holder with anaesthetised animal in place.

2.11.2 Scotopic Electroretinograms

Animals were dark-adapted overnight in preparation for scotopic electroretinograms (ERGs), and all procedures were conducted under dim red-light illumination. Following anaesthesia as described above, both eyes were anaesthetised using proxymetacaine hydrochloride 0.5% (Bausch & Lomb, UK) and dilated using phenylephrine hydrochloride 2.5% (Bausch & Lomb, UK) and tropicamide 1% (Bausch & Lomb, UK). Once fully anaesthetised, each animal was placed on a heated stage at the centre of a Faraday cage enclosed Ganzfeld stimulator (Diagnosys, UK). A ground electrode was placed just above the tail, two reference electrodes posterior to each eye, and two positive electrodes with looped gold contacts on each cornea using topical carbomer gel as coupling fluid. Adjustment of the electrode contacts on the corneas were performed to ensure electrode resistance of below 5kΩ.

The protocol used to obtain scotopic ERGs has been previously described (Jayaram et al. 2014). Stimulus intensity between -4.75 and -3.5 log.cd.s.m^{-2} were used, as these have previously been shown to be the most sensitive regions for the detection of scotopic threshold response values. Interflash intervals ranged from 2 to 20 s, with 3–30 recordings per step depending on the light intensity. Responses were filtered using low-frequency cut-off (0.312 Hz) and a high-frequency cut-off (500 Hz).

2.12 Extracellular Vesicle Extraction

All EVs used in the experiments within this study were extracted and purified by a collaborating scientist within the laboratory. Specific techniques regarding the purification, quantification, and characterisation of these EVs have been described in detail previously (W. Lamb, PhD Thesis, UCL Repository, 2021).

In brief, MGCs cultures were grown to 80% confluence under standard conditions, and then washed three times in particle-depleted PBS. Cultures were then incubated for 48 hours in vesicle-free media, which was collected,

and centrifuged at 300 x g for 10 minutes. The supernatant was recovered, and the pellet discarded. Centrifugation was repeated at 2,000 x g for 15 minutes, and 10,000 x g for 30 minutes. Supernatant was then passed through a 0.22 µm filter (Corning®, U.K.), and then transferred to an ultracentrifugation tube, where it was layered on top of a 5 mL cushion of 30% sucrose solution (Sigma-Aldrich, MA, United States). The solution was then centrifuged at 100,0000 x g for 120 minutes at 4 °C, whereby the supernatant was discarded, and the sucrose layer containing the vesicles collected (~6mL). Vesicles were washed in 10 mL of 1X PBS, passed through a 0.22 µm filter for a second time, and finally pelleted by centrifugation at 100, 000 x g for 120 minutes at 4 °C. The pellet was resuspended in 500 µL of sterile, particle-depleted PBS.

The concentration and size profile of small EV preparations were quantified by nanoparticle tracking analysis (NTA). Measurements were made using a NanoSight LM10 instrument equipped with a 405 nm LM12 module and EM-CCD camera (NanoSight, Malvern Panalytical Ltd, Malvern, UK). For each sample, 5 videos of 30 seconds were taken for processing. The Brownian motion of each particle was tracked between frames and the size was calculated by using the Stokes-Einstein equation.

2.13 Statistical analysis

For RT-PCR and western blotting, densitometry measurements of X-ray film images were carried out on captured images using ImageJ software (Java, USA), and normalised to ß-actin in each experiment. All experiments were repeated in at least three different cell passages.

Experimental data was stored and processed on Excel (Microsoft Corp., USA). GraphPad Prism version 5.01 (GraphPad Software Inc., La Jolla, CA, USA) was used for Student's t-test and the generation of graphs. SPSS version 24.0 (SPSS Inc, Chicago, IL, USA) was used for regression analysis and one-way analysis of variance (ANOVA) including post hoc Bonferroni

correction. A p value of less than 0.05 was considered statistically significant, all error bars in this study represent the standard error of the mean (SEM).

3. GALECTIN INTERACTIONS WITH MÜLLER GLIAL CELLS

3.1 Introduction

As reviewed in the previous section (Section 1.2.2), Galectins have been shown to play important roles in a wide range of cellular events including proliferation, apoptosis, differentiation, and migration. Available data within retinal tissues is somewhat limited in comparison to other organs (Section 1.2.4). Nevertheless, Galectins, in particular Gal-1 and -3, have been found to be upregulated in crucial pathogenic processes such as excessive glial proliferation, epithelial mesenchymal transformation and RGC degeneration. Given that proteomic and mRNA expression studies have identified MGCs to be major producers of Galectins within the retina (Craig et al. 2010; Eastlake et al. 2017), the main aim of this chapter was to explore the potential involvement of Galectins in cellular processes typically observed in reactive gliosis.

Reactive gliosis is a complex phenomenon involving a diverse group of cellular pathways, which act together to limit tissue injury and restore function where possible (Section 1.1.3). Within the retina, the intricate processes involved in reactive gliosis are principally regulated by Müller glial cells (MGCs). Key features of reactive MGCs during gliosis include increased proliferation, migration, dedifferentiation, and contraction. Significant parallels can be drawn from these processes and the established functions of Gal-1 and -3 within other organs. As such, the experiments in this chapter were designed to investigate whether Gal-1 and -3 would influence the cellular function of MGCs *in vitro* to exhibit features of gliosis, as well as whether these Galectins interact with gliosis associated signalling pathways.

MIO-M1 cells *in vitro* were previously found to express Gal-1 and -3 at relatively high levels without external stimulus; therefore, the first step in this

set of experiments was to establish a method of downregulating the production of these molecules. For this purpose, a methodology using siRNA duplex transfection was tested for its ability to reduce Gal-1/3 mRNA and protein expression within target MGC cells. Refinements were made to this technique to ensure minimal cellular injury and adequate rate of transfection.

An important aspect of Galectin related research has been the identification of its binding targets. As lectins are defined by their ability to bind specific carbohydrate molecules, the majority of Gal-1/-3 related effects are thought to be mediated through the binding of their corresponding glycan determinants (Section 1.2.1). Galectins share a central galactose binding domain, and the majority of Galectin family members demonstrate a high binding affinity towards polylactosamine (polyLacNAc, Section 1.2.2). Furthermore, specific polyLacNAc modifications also influence the strength of Galectin binding, for example, α2-6 sialylation inhibits all Galectin interactions except Gal-3, whereas α2-3 sialylation affects Gal-2, -3, -4 and -7 binding but has no impact on Gal-1 (Stowell et al. 2008). The characterisation of the degree of α-2,3 and α-2,6 sialylation can be achieved through the quantification of α-2,3- and α-2,6- sialyltransferase 1 mRNA expression, as well as the use of plant lectins Maackia amurensis (MAL) and Sambucus nigra agglutinin (SNA), which demonstrated specific binding affinity to α-2,3 and α-2,6 sialylation respectively.

During reactive gliosis, characteristic cellular changes occur, including proliferation, migration, and contraction. These observed effects during gliosis are controlled by a complex network of intracellular pathways, which become activated during various stages of reactive gliosis. Established gliotic pathway including the JAK/STAT, SMAD, and ERK pathways (Kang and Hebert 2011). These pathways can be activated by a range of cytokines, including TNF-α, IL-1, FGF, and TGF-β. The activation of these pathways requires upstream cytokines such as TNF-α and IL-1. In animals such as the zebrafish where retinal regeneration can be observed, developmental pathways such as

Wnt/β-catenin also appear to be activated in addition to pro-inflammatory pathways (Lenkowski et al. 2013). Whilst there are clear parallels between the known functions of Gal-1 and -3 within the retina, limited evidence currently exists to describe their participation in the aforementioned intracellular pathways.

3.1.1 Objectives

The specific objectives of this chapter were as follows:

- To establish and validate a method of Gal-1/-3 expression downregulation within MIO-M1 cells by introducing siRNA duplexes via a transfection reagent.
- To investigate the effects of Gal-3 on the proliferation, migration, and contraction of MIO-M1 cells using the Hexosaminidase, scratch, and collagen gel contraction assays respectively.
- To investigate the effect of cytokines on Gal-1 and -3 mRNA production within MIO-M1 cells using quantitative PCR and immunohistochemical methods.
- To investigate potential interactions between Gal-1/-3 and intracellular pathways and their upstream cytokines using western blots to demonstrate protein phosphorylation.

3.2 Results

3.2.1 Silencing of Galectins -1 and -3 Expression: Optimisation of Galectin siRNA Transfection in Müller Glial Cells

To determine the optimal conditions for siRNA transfection of MIO-M1 cells, a set of experiments was conducted utilising different concentrations of siRNA oligonucleotide duplex, transfection agent, and cell confluence based on manufacturer's recommendations.

During initial experiments, MIO-M1 cells were incubated for 4 hours at siRNA concentrations of 0.1nM, 1nM and 10nM (Figure 3-1), and siTran/siRNA ratio of 10µL/ng. Using 0.1nM siRNA, only a very small proportion (<5%) of cells were shown to be transfected as judged by visible red TYE-563 fluorescence; whilst using 1nM siRNA, almost all cells (>95%) exhibited fluorescence with para-nuclear predominance. At 10nM siRNA concentration, diffuse fluorescent staining of all cells as well as significant morphological changes and areas of cell membrane damage were observed. The cell membrane disruption observed was likely to be secondary to the presence of the transfection agent. On this basis, the next set of experiments investigated the possibility of reducing the quantity of transfection agent used.

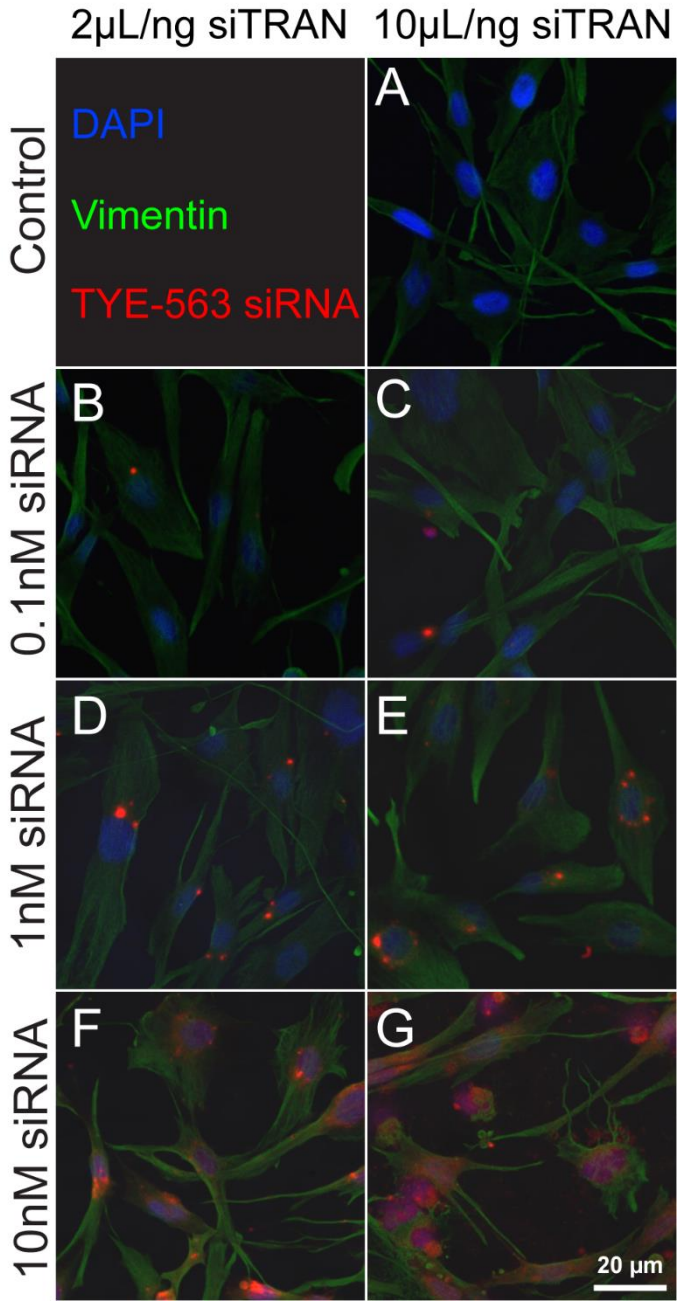

Figure 3-1 MIO-M1 cells incubated for 4 hours with TYE-563 labelled siRNA and siTran. At siTran/siRNA ratio of 10µL/ng, higher concentrations of siRNA resulted in increased intracellular TYE-563 fluorescence (C, E, G) when compared to vehicle control (A); however, at 10nM concentration of siRNA, there are significant morphological changes and evidence of cellular membrane damage (G). When siTran/siRNA ratio was reduced to 2µL/ng, a similar dose-related pattern of TYE-563 fluorescence is seen (B, D, F), without any evidence of cellular damage at 10nM siRNA (F).

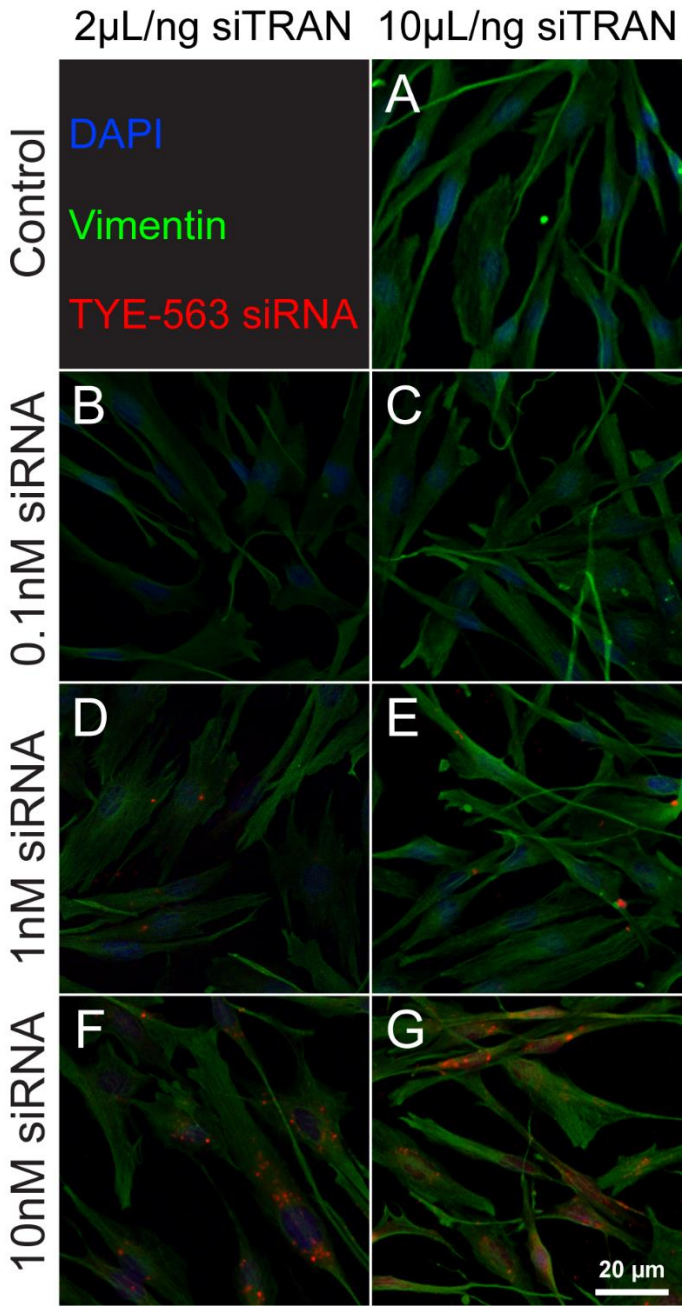

Figure 3-2 MIO-M1 cells incubated for 24 hours with TYE-563 labelled siRNA and siTran. Compared to 4 hours of incubation, a similar pattern of TYE-563 fluorescence is present at increasing concentrations of siRNA (C, E, G) when compared to vehicle control (A), although there is a general reduction of TYE-563 at lower siRNA concentrations (B, C, E, F). The cellular damage and membrane disruption can still be seen at 10nM siRNA when using 10µL/ng siTran (G), whereas the MIO-M1 cells were able to retain good cell morphology as well as TYE-563 fluorescence when 2µL/ng siTran was used.

To test the effects of lowering transfection reagent concentrations, MIO-M1 cells were incubated for 4 hours at siRNA concentrations of 0.1nM, 1nM and 10nM and siTran/siRNA ratio of 2µL/ng (Figure 3-1). A dose-dependent pattern similar to the higher ratio was present at 0.1nM and 1nM siRNA concentrations. At 10nM, in addition to almost all cells exhibiting TYE-563 uptake and multiple para-nuclear foci in most cells, no evidence of significant cellular toxicity was observed. Furthermore, when the incubation period was extended to 24 hours (Figure 3-2), there was a general decline in the degree of TYE-563 fluorescence when transfecting with 0.1nM and 1nM siRNA concentrations. In contrast with that observed when 10nM siRNA was used for transfection, MIO-M1 cells transfected with 2µL/ng siTran exhibited normal cell morphology in addition to enhanced retention of TYE-563 fluorescence. Interestingly, the significant change in cell morphology seen at 4 hours for 10nM siRNA concentration and 10µL/ng siTran had resolved at 24 hours. Nevertheless, 2µL/ng siTran/siRNA ratio was chosen for all subsequent experiments in order to avoid any potential adverse effects of cell membrane disruption, however transient these may be.

3.2.2 Gene and Protein Expression of Gal-1 and -3 by Müller Glial Cells Following siRNA Treatment

As three siRNA duplex constructs were designed for each target gene, individual siRNA oligonucleotides duplexes were first examined for their efficacy in downregulating Gal-1 mRNA expression at 24 hours following treatment using qPCR (Figure 3-3, A). A duplex containing a random genetic sequence confirmed to have no target was used as control.

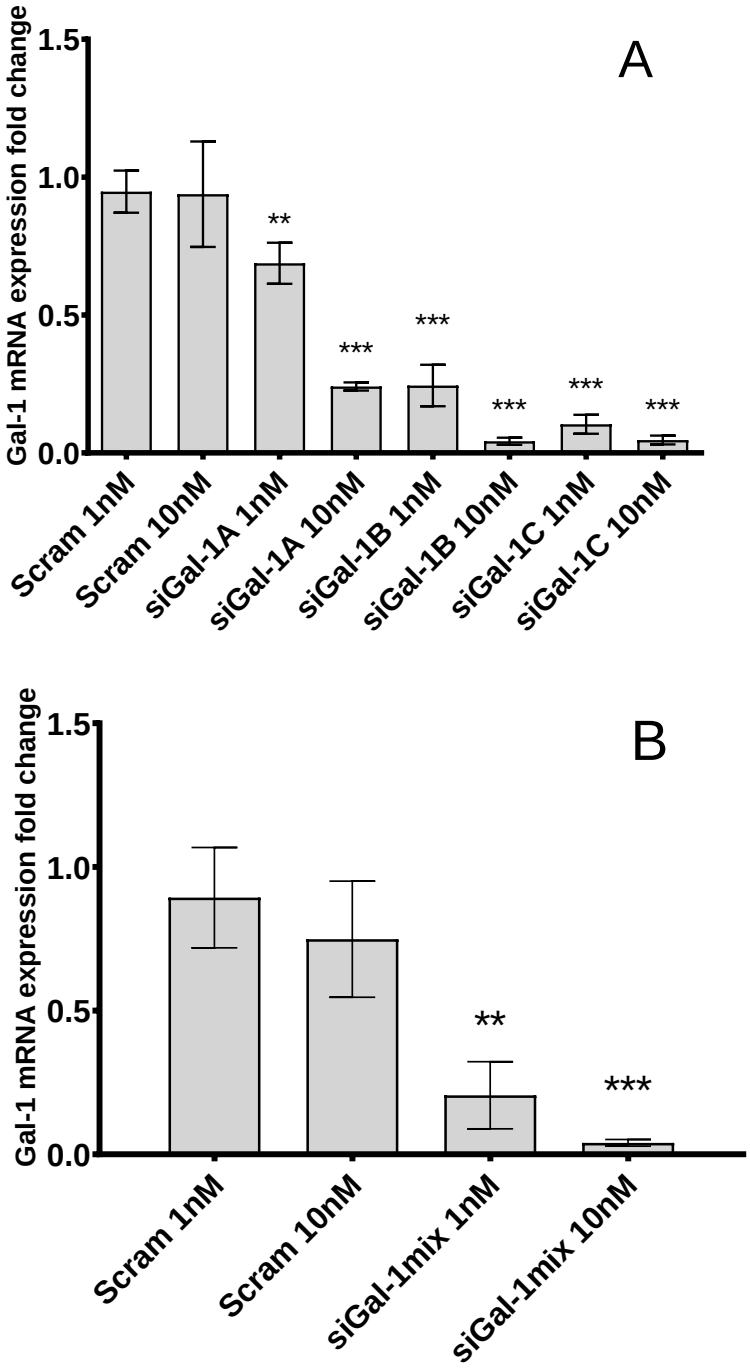

Figure 3-3 Downregulation of Gal-1 mRNA expression using siRNA as assessed by qPCR at 24 hours. (A) Individual oligonucleotides were able to achieve significant dose-dependent downregulation, although duplex A appeared to be less effective than duplexes B and C. (B) A mixture of all three duplexes was able to achieve >95% mRNA downregulation when used at 10nM. All mRNA expression levels were normalised to untreated cells. * - p<0.05, ** - p<0.01, *** - p<0.001.

Compared to control siRNA used at 1nM concentration, duplex constructs A, B, and C used at the same concentration achieved 26% ($p=0.008$), 70% ($p<0.001$), and 84% ($p<0.001$) downregulation of mRNA expression, respectively. Compared to control siRNA used at 10nM concentration, duplex constructs A, B, and C used at the same concentration achieved 69% ($p<0.001$), 90% ($p<0.001$), and 89% ($p<0.001$) downregulation of mRNA expression, respectively. A combination of all three duplex constructs prepared to silence Gal-1 achieved downregulation of mRNA expression of 69% ($p=0.001$) at 1nM and 95% ($p < 0.001$) at 10nM (Figure 3-3, B).

Three individual siRNA duplex constructs designed to downregulate Gal-3 were also tested. At 3nM, individual duplex constructs A, B, and C achieved Gal-3 mRNA downregulation of 79%, 97%, and 98% (all $p<0.001$, Figure 3-4, A), respectively. A combination of all three duplex constructs against Gal-3 achieved mRNA downregulation of 76% ($p=0.001$) at 1nM and >99% ($p<0.001$) at 10nM (Figure 3-4, A).

To further establish the duration of siRNA silencing effect on mRNA expression, a combination of all three duplex constructs against Gal-3 at 10nM concentration was used, and the mRNA expression of Gal-3 was measured over the following 10 days (Figure 3-4, B). Compared to day 0, over 97% downregulation of Gal-3 mRNA expression was maintained at days 1, 2, 4 and 7 ($p<0.001$ at all points). At day 10, the degree of Gal-3 mRNA downregulation was still significant at 77% ($p<0.001$), although diminished as compared to the previous days.

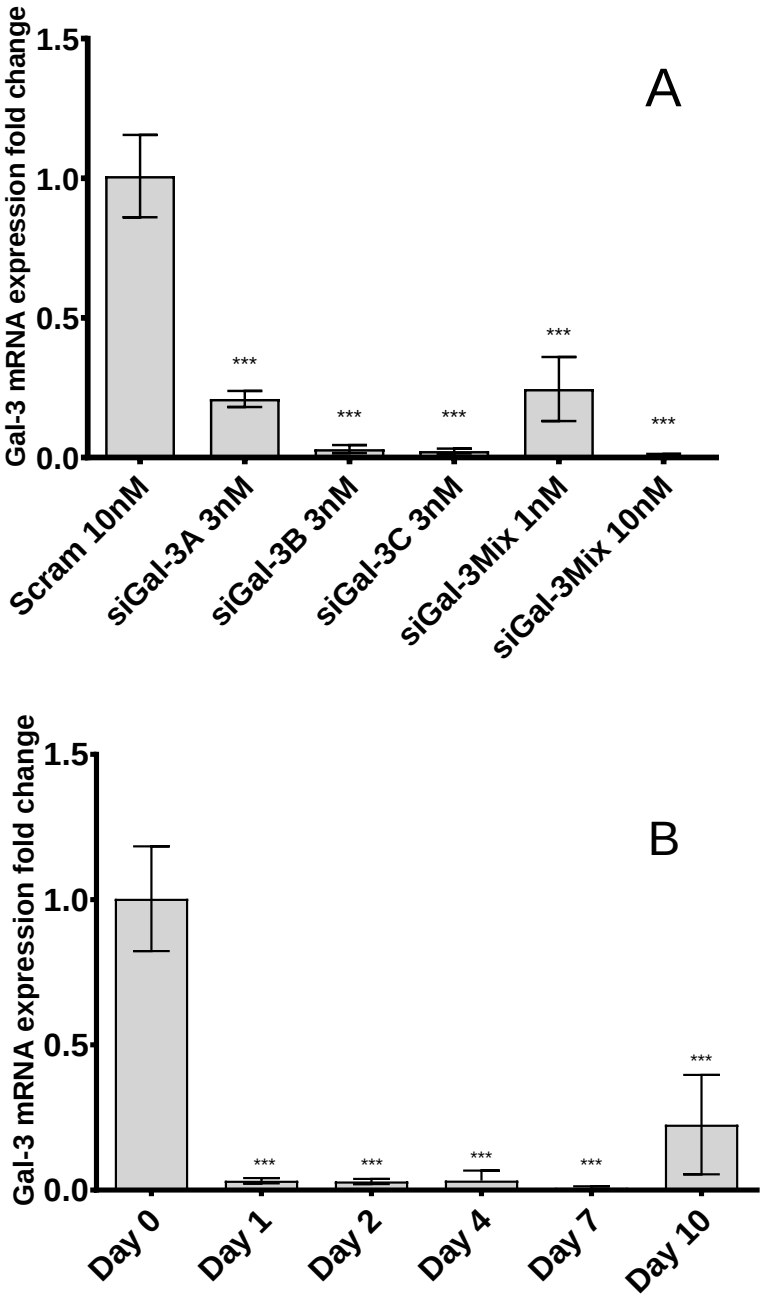

Figure 3-4 Downregulation of Gal-3 mRNA expression using siRNA as assessed by qPCR. (A) Individual oligonucleotides were able to achieve significant dose-dependent downregulation at 24 hours, although duplex A appeared to be less effective than duplexes B and C. (B) The effect of mRNA downregulation was maintained at >95% efficiency for 7 days, at day 10, Gal-3 mRNA expression was still significantly down regulated by around 75%. * - p<0.05, ** - p<0.01, *** - p<0.001.

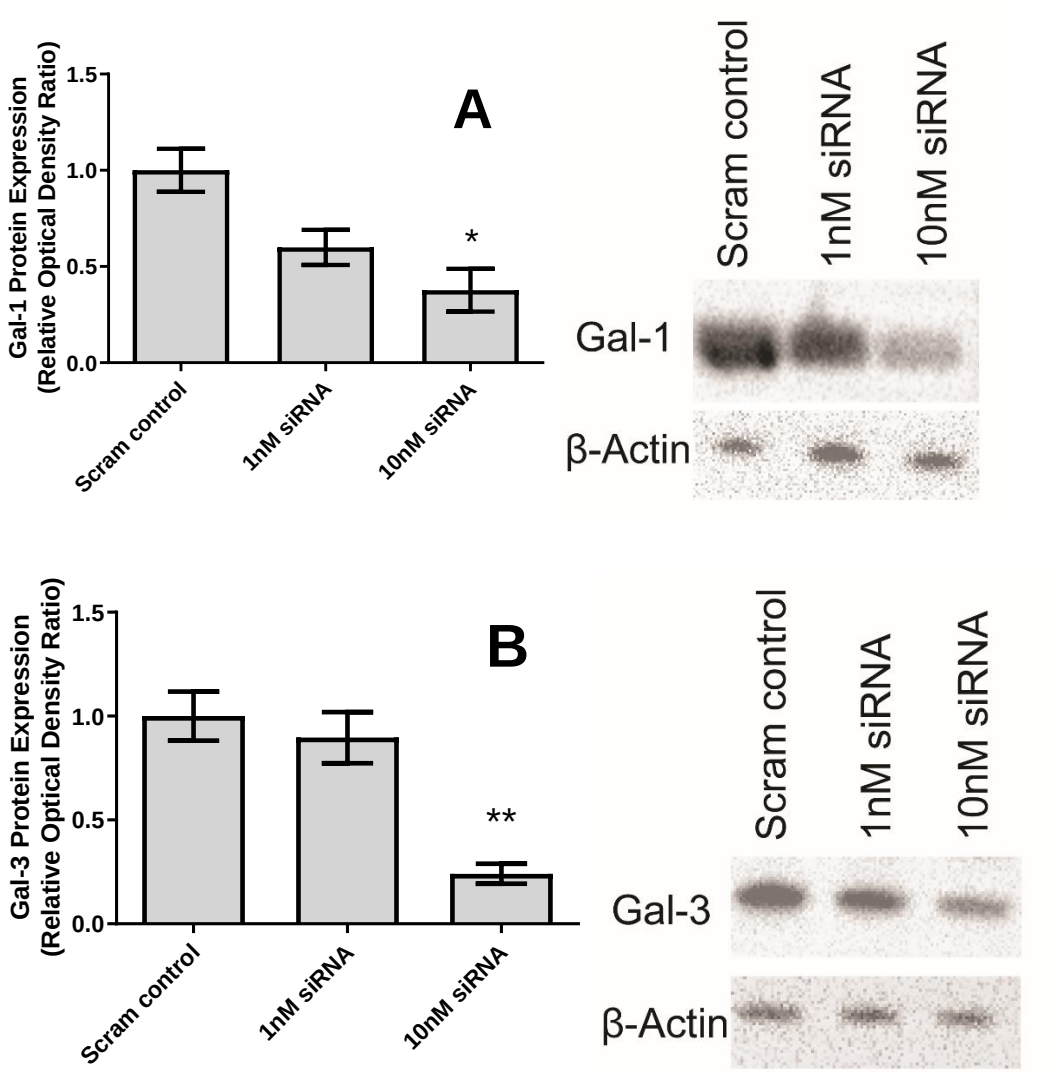

Figure 3-5 Downregulation of Gal-1 (A) and -3 (B) protein expression by siRNA constructs as assessed by western blotting. 10nM siRNA mixtures were able to achieve significant downregulation of Gal-1 (>50%) and -3 (>70%) proteins in cell lysates at day 3. Representative blots are shown including β-Actin as normalising controls. N = 3, * - p<0.05, ** - p<0.01.

Further to the downregulation of Gal-1/-3 mRNA by siRNA constructs, protein analysis of cell lysates using western blotting also demonstrated the downregulation of Gal-1 and -3 (Figure 3-5). At 48 hours following incubation with the siRNA construct mixture against Gal-1, MIO-M1 cell lysates following incubation with 1nM mixture of siRNA constructs did not result in significant downregulation of protein expression ($p=0.06$), whereas siRNA construct mixture used at 10nM was able to achieve a significant downregulation (61%, $p=0.01$) of protein expression. The effects of siRNA constructs for Gal-3 were similar as those for Gal-1, as the 1nM siRNA construct mixture did not achieve significant downregulation of protein expression ($p=0.71$). In contrast, siRNA mixture used at 10nM resulted in a significant downregulation (75%, $p=0.0035$) of Gal-3 protein expression.

3.2.3 Effects of Galectin-3 and Cytokines on the Proliferation of Müller Glial Cells

The effect of various cytokines on the rate of MIO-M1 proliferation was assessed using the hexosaminidase assay. TNF-α and IL-1 caused a significant decrease in the rate of proliferation of MIO-M1 cells, whereas TGF-β1/2 had no significant effect (Figure 3-5). The effect of Gal-3 inhibition on the proliferation of MIO-M1 cells was investigated using siRNA. For this purpose, MIO-M1 cells were incubated with a triple siRNA duplex construct mixture at 10nM for 48 hours prior to the addition of TGF-β1 or -β2. Incubation of the Gal-3 siRNA mixture resulted in a significantly higher rate of proliferation, which was not significantly affected by the addition of TGF-β1 or -β2.

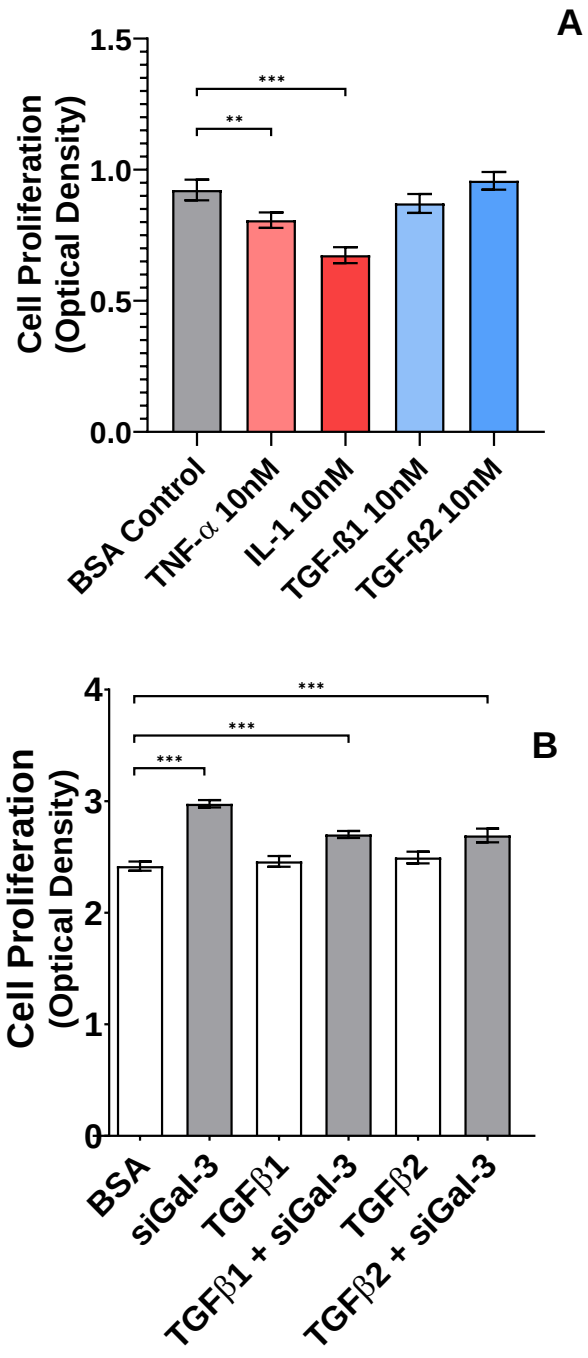

Figure 3-6 Cell proliferation as measured by hexosaminidase assay. TNF-α and IL-1 appeared to decrease the rate of proliferation in MIO-M1 cells and TGF-β1/2 had no significant effect (A). Inhibition using siGal-3 resulted in a higher rate of proliferation, which was not affected by the presence of TGF-β1/2 (B). ** - p<0.01, *** - p<0.001

3.2.4 Effects of Galectin-3 and Cytokines on the Migration of Müller Glial Cells

Effects on MIO-M1 cell migration was assessed using a scratch assay. The degree of cell migration was measured by the difference in the cell-free area immediately following a linear scratch to the monolayer of cells and 48 hours thereafter. Figure 3-7 illustrates typical appearances of assays at the end of the 48-hour experimental period.

Incubation of the cells with either TGF-β1 or –β2 during the 48-hour period following the scratch resulted in an increase in the rate of migration of MIO-M1 cells as compared to control (Figure 3-7, B).

The effect of Gal-3 inhibition on the migration of MIO-M1 cells was investigated using siRNA. For this purpose, 90% confluent MIO-M1 cells were incubated with a triple siRNA duplex construct mixture at 10nM for 48 hours prior to administering the linear scratch and the addition of TGF-β1 or -β2.

Inhibition of Gal-3 expression using siRNA did not result in any significant change in the rate of migration when compared to the scrambled siRNA construct control. However, when Gal-3 siRNA inhibition was performed prior to the addition of TGF-β1 or -β2, the pro-migratory effect of TGF-β was significantly diminished (Figure 3-7, B).

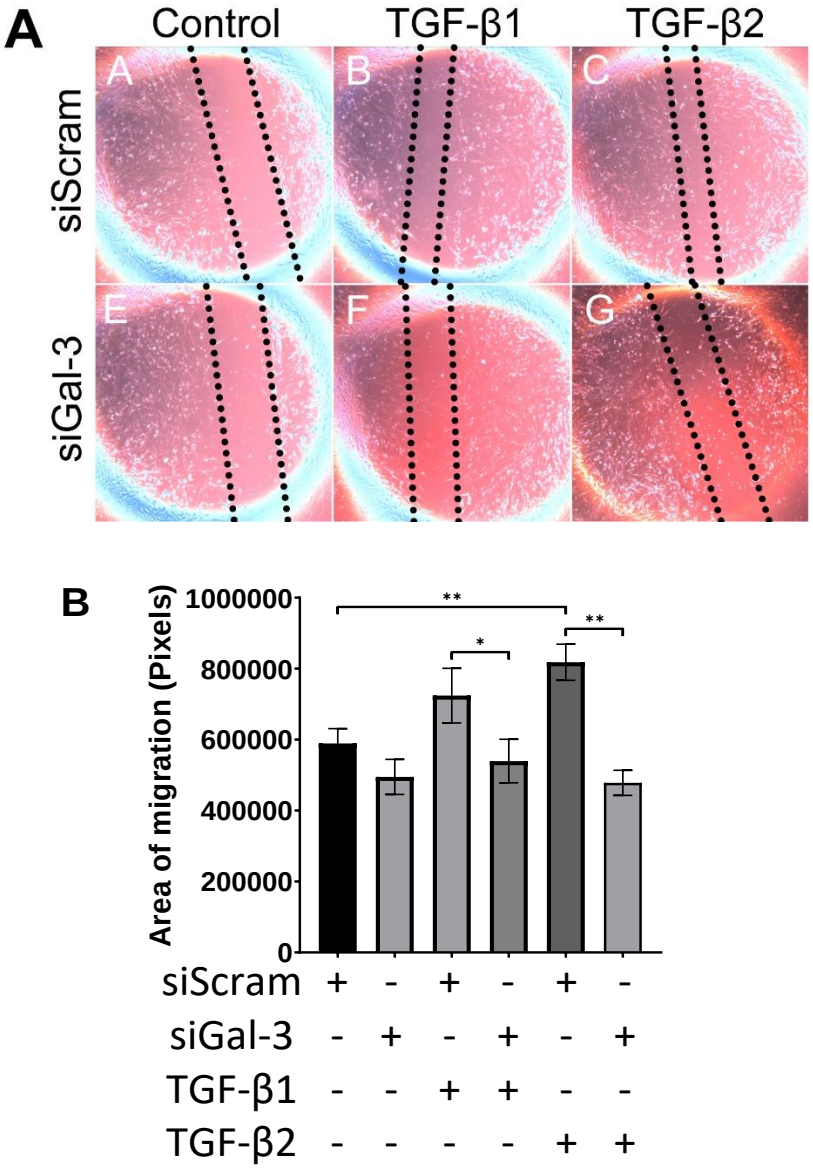

Figure 3-7 Effects of TGF-β1 or -β2 on MIO-M1 cell migration as assessed by a scratch assay. (A) Representative scratched cultures and the regions assessed for migration. (B) TGF-β1 and -β2 significantly increased the rate of migration of MIO-M1 cells. Inhibition of Gal-3 via siRNA treatment did not result in any significant change in the rate of migration when compared to control (scrambled siRNA). When Gal-3 inhibition was performed prior to the addition of TGF-β1 or -β2, there was a significant decrease in cell migration when compared to TGF-β treatment alone. * - p<0.05, ** - p<0.01, *** - p<0.001

3.2.5 Effects of Galectin-3 and Cytokines on the Contraction of Müller Glial Cells

Effects on MIO-M1 cell contraction was assessed using the collagen gel contraction assay, as illustrated in Figure 3-8B. The degree of gel contraction was measured by the percentage decrease in the total area of collagen gels between the start of each experiment and the end of 7-day incubation period.

Samples incubated with TGF-β1 were found to exhibit significantly increased contraction when compared to control. However, when MIO-M1 cells underwent treatment with a triple siRNA duplex construct mixture against Gal-3 at 10nM for 72 hours prior to the initiation of the scratch assay, no significant differences in contraction were found when TGF-β1 was added (Figure 3-8, A). In this case, the control sample underwent incubation with scrambled siRNA duplex constructs prior to the collagen gel contraction assay.

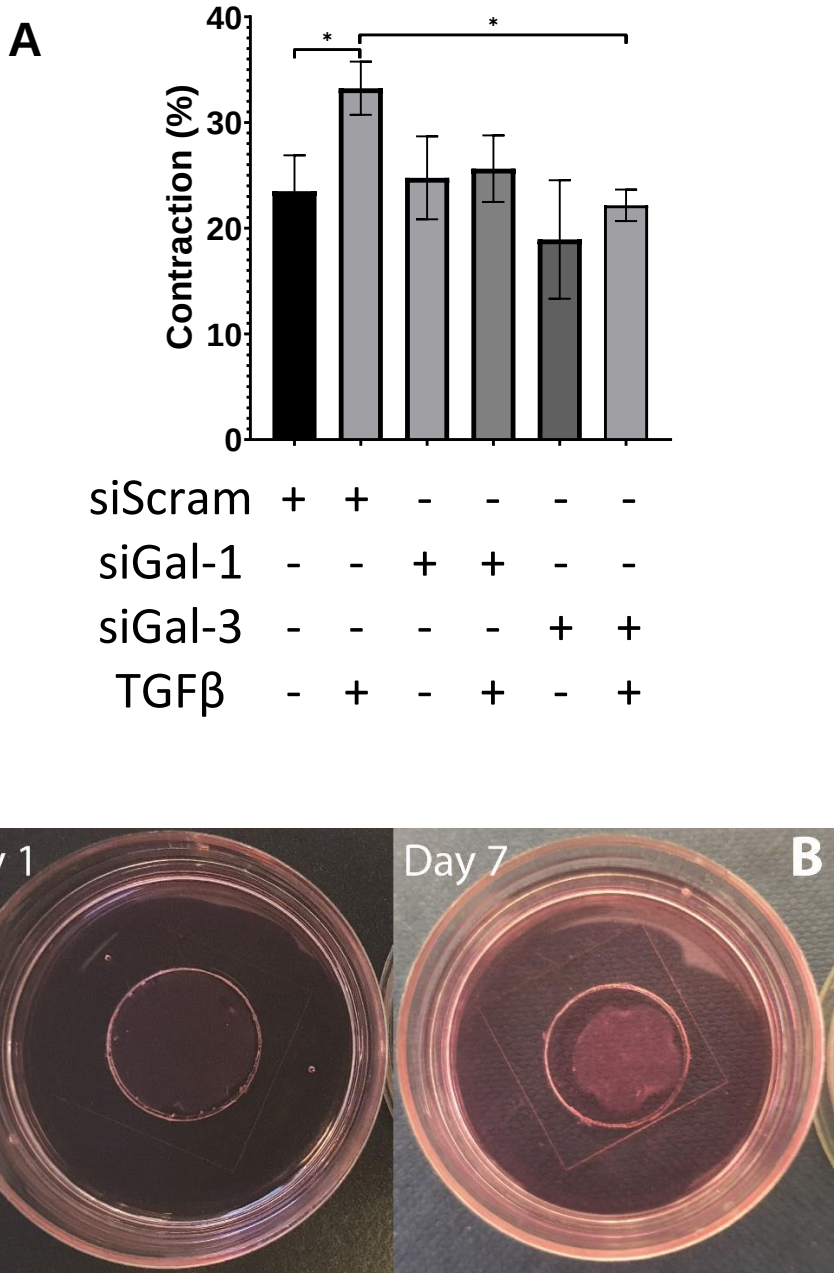

Figure 3-8 Effects on MIO-M1 cell contraction was assessed using the collagen contraction assay. (A) TGF-β1 significantly increased the rate of contraction of MIO-M1 cells. Inhibition of Gal-1 or -3 via siRNA treatment did not result in any significant change in rate of migration when compared to control. When Gal-3 inhibition was performed prior to the addition of TGF-β1, no significant increase in tissue contraction was noted when compared to Gal-3 inhibition alone. (B) Example of sample at day 1 and day 7. * - p<0.05, ** - p<0.01

3.2.6 Cytokine Regulation of Galectins and Sialylation Enzyme Expression by Müller Glial Cells

The effect of cytokines on gene and protein expression of Gal-1 and -3 within MIO-M1 cells were examined using qPCR and immunocytochemical methods respectively. TNF-α, IL-1, TGF-β1 and -β2 were added to the culturing media of MIO-M1 cells at 10nM for 24 hours. The concentration and duration of cytokine treatment was previously tested in the host laboratory to ensure acceptable cell morphology and viability.

Treatment with IL-1 and TNF-α caused significant increases in Gal-1 mRNA expression within MGCs, whilst treatment with TGF-β1 or TGF-β2 had no significant effect on the mRNA expression of this molecule (Figure 3-9, A, B). Interestingly, treatment of MGCs with IL-1 also resulted in a significant increase in mRNA expression of the sialylation enzyme *ST3GAL1*, but TNF-α and TGF-β1/2 had no such effect (Figure 3-9, B). The ability for IL-1 to increase Gal-1 protein expression was demonstrated via immuno-cytochemical staining, where at 48 hours following incubation with IL-1, MIO-M1 cells demonstrated a significant increase in the intensity of staining for Gal-1 (Figure 3-9, C).

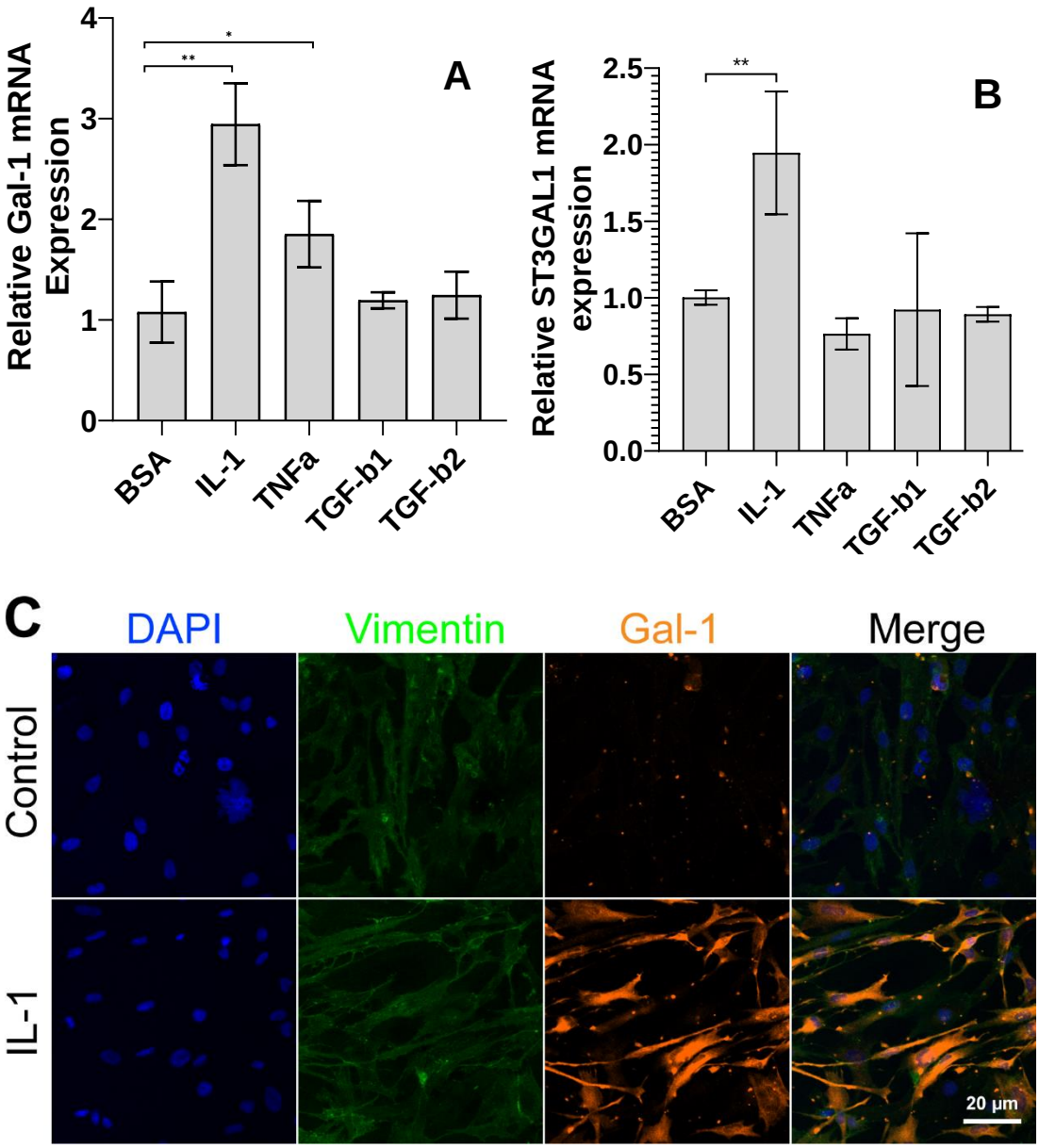

Figure 3-9 Immune-cytochemical staining of MIO-M1 cells. (A) mRNA expression of Gal-1 and (B) ST3GAL1 following treatment with various cytokines. Treatment with IL-1 and TNF-α at 10nM caused an increase in Gal-1 expression, whilst other cytokines including TGF-β1/2 had no significant effect. IL-1 treatment also resulted in a significant increase in mRNA expression of the sialylation enzyme ST3GAL1. (C) Gal-1 is present in aggregates within the cytosol of MIO-M1 cells at rest, IL-1 treatment caused significant upregulation of Gal-1 protein expression. Exposure of Gal-1 fluorescence was adjusted for IL-1 treated image intensity. * - p<0.05, ** - p<0.01.

In terms of the regulation of Gal-3 expression, treatment of MIO-M1 cells with TNF-α or TGF-β resulted in significant downregulation of mRNA coding for this molecule, which was confirmed for both the -β1 and -β2 isoforms of TGF-

β after 24 hours incubation of the cells (Figure 3-10, A). IL-1 treatment did not demonstrate any significant effects. Furthermore, mRNA coding for *ST6GAL1* did not show any significant changes following treatment with any of the cytokines tested, and variation between experimental repeats for this particular enzyme was relatively high (Figure 3-10, B). The ability for TGF-β to decrease Gal-3 protein expression was demonstrated via immune-cytochemical staining, where at 48 hours following incubation with TGF-β, MIO-M1 cells demonstrated a significant decrease in intensity for Gal-3 (Figure 3-10, C).

Given that TGF-β significantly downregulated the production of Gal-3, an additional qPCR experiment was carried out to further explore whether Gal-3 may have a reciprocal effect on TGF-β production. To investigate this, a combination of 3 siRNA duplex constructs at 10nM against Gal-3 was incubated with MIO-M1 cells, as described above, in order to achieve downregulation of Gal-3 protein. At 48 hours following incubation, the mRNA expression of TGF-β isoforms was examined using qPCR. This showed no significant changes in any of the three isoforms of TGF-β (Figure 3-11).

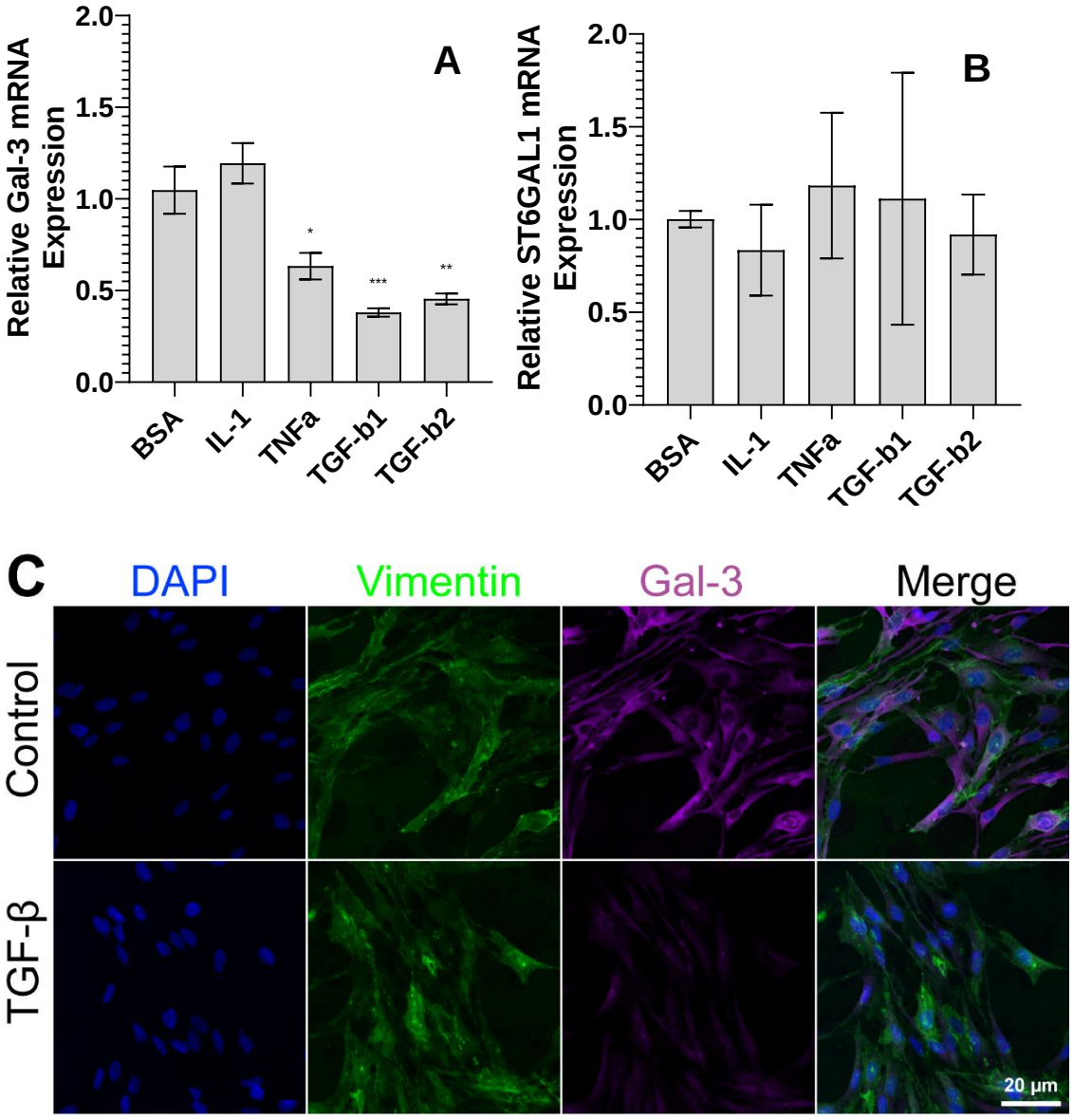

Figure 3-10 (A) Treatment with TGF-β resulted in significant downregulation of Gal-3 mRNA, which was confirmed for both TGF-β1 and TGF-β2 at 24 hours after incubation. (B) ST6GAL1 did not show any significant changes following treatment with cytokines, however, variation between experimental repeats were relatively high. (C) TGF-β1 treatment also caused significant downregulation of Gal-3 protein expression as shown by immunocytochemical staining. * - p<0.05, ** - p<0.01, *** - p<0.001.

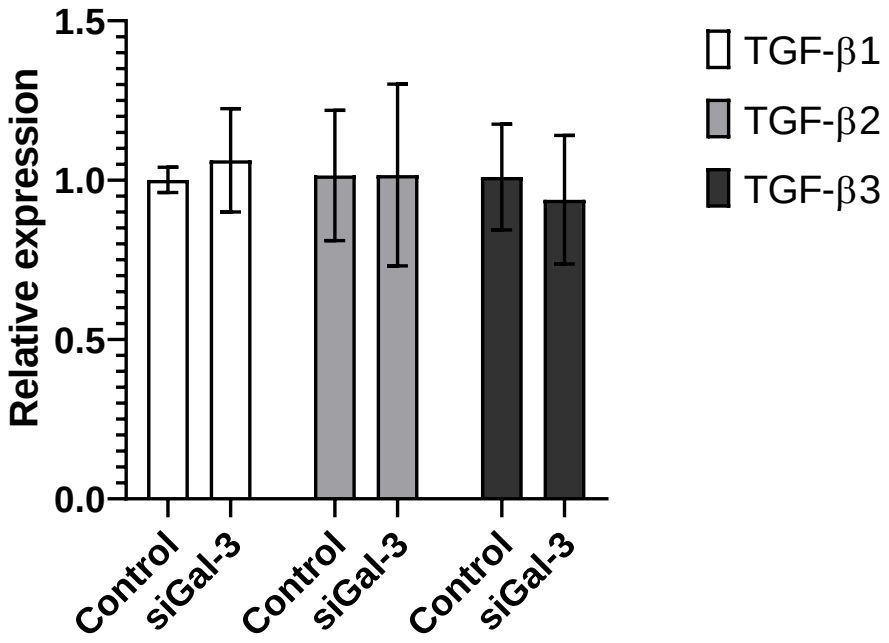

Figure 3-11 Downregulation of Gal-3 using siRNA treatment at 10nM did not result in any significant change in the expression of all three isoforms of TGF-β. P>0.05.

3.2.7 Interaction of Galectin-1 and -3 with Gliosis Associated Intracellular Pathways

Cytokine induced activation of intracellular pathways were investigated in combination with Gal-1/-3 inhibition. STAT3 protein phosphorylation was found to be significantly increased following treatment with TNF-α at 10nM for 30 minutes (Figure 3-12, A). In contrast, inhibition of Gal-1 for 72 hours using triple siRNA duplex construct mixture resulted in significantly reduced STAT3 protein phosphorylation. Interestingly, TNF-α treatment following Gal-1 siRNA resulted in significantly increased STAT3 phosphorylation when compared to Gal-1 siRNA alone but decreased compared to TNF-α treatment alone (Figure 3-12, A). Inhibition of Gal-3 or treatment with IL-1 did not appear to have any significant effect on STAT3 phosphorylation.

In their resting state, there was almost no detectable Smad phosphorylation found within MIO-M1 cells. Treatment of these cells with TGF-β for 30 minutes significantly increased Smad phosphorylation (Figure 3-12, B). However, this TGF-β associated effect was significantly dampened in cells which underwent Gal-3 inhibition using triple siRNA duplex construct mixture for 72 hours prior (Figure 3-12, B).

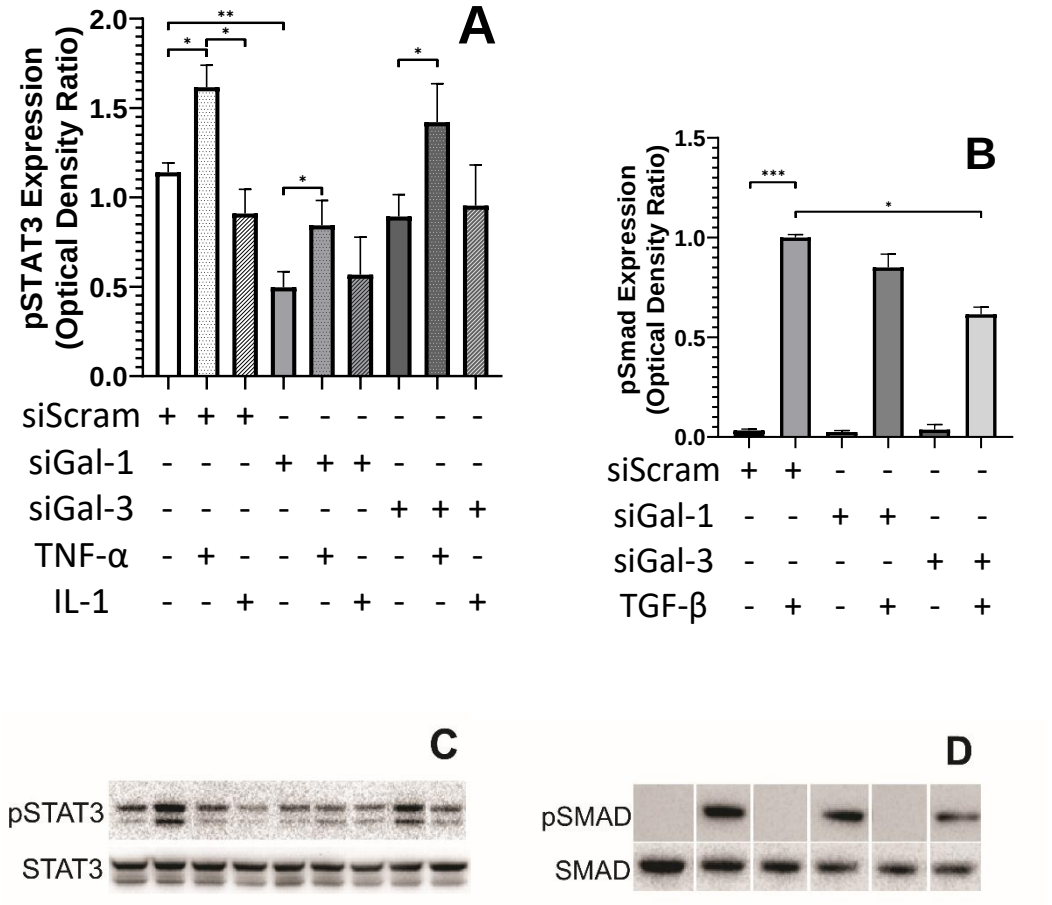

Figure 3-12 (A) STAT3 phosphorylation (pSTAT) was significantly decreased following siRNA inhibition of Gal-1. TNF-α treatment increased STAT3 phosphorylation after 30 minutes, this effect was reduced following siRNA inhibition of Gal-1. (B) Smad phosphorylation (pSmad) was significantly increased following TGF-β treatment, this was significantly dampened following siRNA inhibition of Gal-3. (C, D) Representative immunoblots showing phosphorylated and total STAT3 and SMAD proteins respectively. * - p<0.05, ** - p<0.01

Cytokines TNF-α or IL-1 were used at 10nM to treat MIO-M1 cells for 30 minutes; subsequent western blot showed no significant changes in phosphorylation of the p44/42 of the ERK pathway. Furthermore, inhibition of Gal-1 or -3 with siRNA duplex construct mixtures for 72 hours also resulted in no significant changes in p44/42 phosphorylation (Figure 3-13, A).

Incubation of MIO-M1 cells with a Wnt antagonist for 30 minutes resulted in a decrease in the activation of β-Catenin, as quantified by non-phosphorylated β-Catenin (Figure 3-13, B). Inhibition of Gal-3 within these cells by incubation of siRNA duplex construct mixture for 72 hours also resulted in significant downregulation of β-Catenin activation. Furthermore, the combination of both Gal-3 siRNA inhibition and Wnt antagonist did not achieve any additional decrease in β-Catenin protein phosphorylation when compared to the use of either reagent alone (Figure 3-13, B).

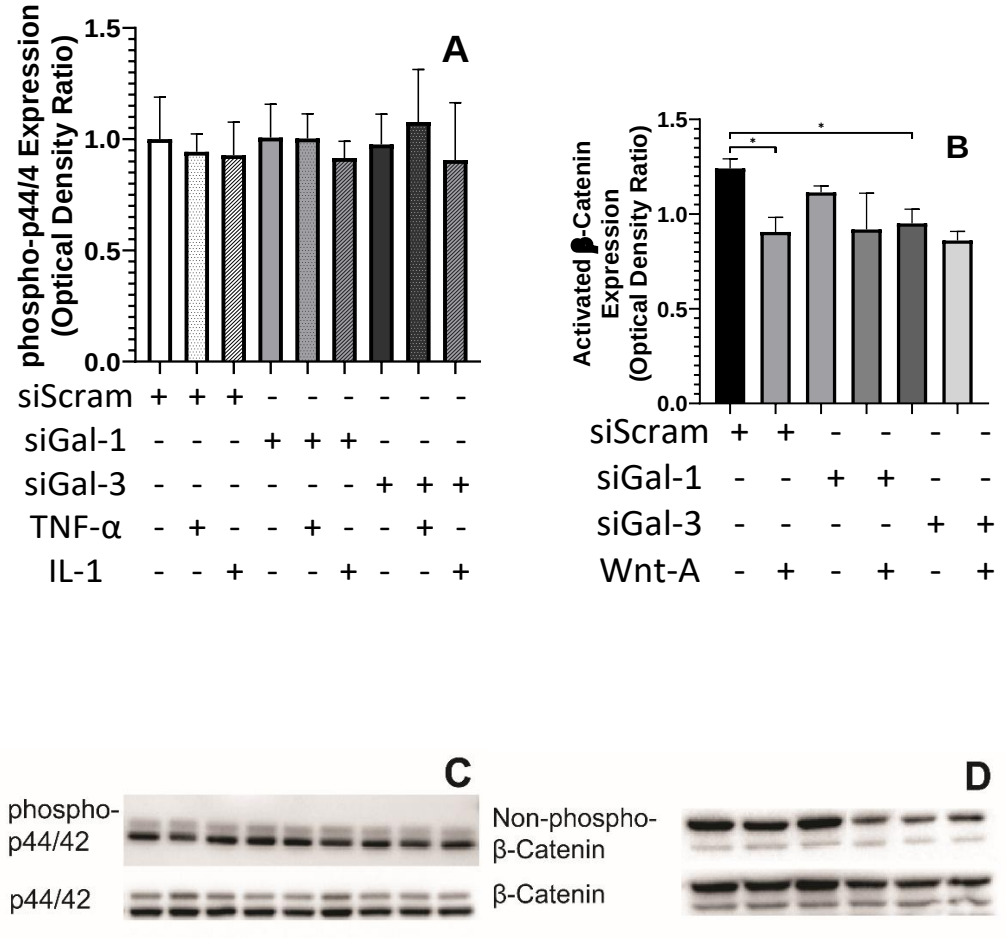

Figure 3-13 (A) p44/42 phosphorylation (phospho-p44/42) did not change significantly following siRNA inhibition of Gal-1 or -3, nor treatment with cytokines TNF-α or IL-1 after 30 minutes. (B) β-Catenin activation (dephosphorylation) was significantly reduced following treatment with Wnt antagonist (Wnt-A) as well as Gal-3 inhibition; these effects did not appear to be additive. (C) Representative immunoblots showing phosphorylated and total p44/42. (D) Representative immunoblots showing non-phosphorylated and total β-Catenin. * - p<0.05.

3.3 Discussion

3.3.1 siRNA Transfection

It was possible to establish an effective and reliable method of downregulating mRNA expression of Gal-1 and -3 proteins using siRNA transfection techniques. Excessively high concentration of the transfection agent (siTran) resulted in visible cell stress, which was likely due the disturbance of cell membranes. As such, the optimal siRNA concentration of 10nM and siTran/siRNA ratio of 2µL/ng were chosen.

When a combination of three siRNA duplexes was used, it was possible to achieve >95% and >99% mRNA downregulation of Gal-1 and -3 respectively. Significant downregulation was also confirmed on western blotting. Notably, the degree of protein downregulation was less than mRNA expression. This is most likely due to the slower turnover of proteins within cells, whereas mRNA molecules were likely to have been degraded much more rapidly. Further experiments using longer periods of siRNA inhibition may be able to confirm this.

3.3.2 Galectin Regulation of Müller Glial Cell Proliferation

The regulation of cell proliferation is a central process in both health and disease. Gal-1 and -3 have been shown to modulate the proliferation of various cell types (Section 1.2), although their effects on MGCs proliferation have not yet been investigated. The current results showed that MIO-M1 cells incubated in the presence of TNF-α or IL-1 exhibited a reduced rate of proliferation, whereas TGF-β did not have a significant effect.

In contrast, downregulation of Gal-3 by siRNA inhibition led to increased Müller glial cell proliferation, and this effect was not modified by TGF-β1 nor TGF-β2. This showed that Gal-3 actively influences the proliferation of MIO-M1 cells, independent of cytokine activity, which is in keeping with existing studies, primarily in the context of malignancies, where Gal-3 appears to

perform the dual function of suppressing proliferation and acting as a chemoattractant for cells of the immune system (Gonnermann et al. 2020).

It is important to highlight that the current experiments were conducted on MIO-M1 cells, which is an immortalised line of human MGCs. As such, MIO-M1 cells spontaneously divide *in vitro*, in contrast to resting MGCs within the human retina do not. Therefore, data on the potential effects on the proliferation of MIO-M1 cells cannot necessarily be extrapolated to MGCs *in vivo*. In order to verify the effects of various cytokines and Gal-1 shown in this chapter, further *in vivo* studies would be required.

3.3.3 Galectin Regulation of Müller Glial Cell Migration and Contraction

TGF-β has been well-documented to increase cell migration in a wide range of conditions (Mitsuhiro, Eguchi, and Yamashita 2003). The current study showed that both TGF-β1 and -β2 were effective in increasing Müller cell migration after 24 hours in culture, whilst inhibition of Gal-3 expression by siRNA did not result in any significant change in the rate of migration of these cells. Interestingly, addition of TGF-β1 or TGF-β2 to Gal-3 silenced Müller cells did not cause any changes in the rate of cell migration. The contraction assay showed similar findings to the migration assay, in that TGF-β caused a significant increase in the rate of contraction whilst inhibition of Gal-3 by siRNA appeared to nullify these changes.

Taken together, from the present findings, it could be suggested that TGF-β-dependent migration and contraction of MGCs during pro-inflammatory processes may be dependent on Gal-3 expression. This is in keeping with similar studies on fibrotic conditions in other tissues such as the lungs (Henderson et al. 2006; Mackinnon et al. 2012). In the retina, these findings may be particularly relevant in diseases characterised by uncontrolled migration and/or contraction, such as proliferative vitreoretinopathies and epithelial mesenchymal transformation (Priglinger et al. 2016). In addition,

whilst the current results are specific to MGCs, if these findings could be reproduced to other cell types, they may also be applicable to ophthalmic conditions involving fibrosis of other ocular tissues, such as corneal and conjunctival scarring and glaucoma.

3.3.4 Cytokine Regulation of Galectins and Sialylation Enzyme Expression in Müller Glial Cells

The expression levels of Gal-1 and -3 have been reported by numerous studies to be modified in response to environmental stressors (section 1.2). Whilst there is a wide range of external factors that may influence cellular functions, the presence of various pro-inflammatory cytokines is a common finding during retinal degenerative processes. As such, selective cytokines of relevance to retinal disease were tested for their potential ability to regulate Gal-1/3 production.

Both, IL-1 and TNF-α, were found to upregulate Gal-1 when incubated with MIO-M1 cells in culture. IL-1 elicited a greater response when compared to TNF-α at the same concentration (10nM). This finding is in keeping with previous studies, which have implicated Gal-1 as a major molecule in the pathogenesis of diabetic retinopathy (Kanda et al. 2015), a disease which is characterised by high levels of IL-1 (Wooff et al. 2019). Similarly, TNF-α is also a major pro-inflammatory cytokine produced during a wide range of pathogenic processes including gliosis. These findings support the hypothesis that Gal-1 may participate in MGC coordinated gliotic processes involving IL-1 and TNF-α signalling (Manouchehrian et al. 2015).

The upregulation of Gal-1 by IL-1 was also shown by immunocytochemical staining of MGCs, which revealed characteristic scattered aggregates of this molecule within the untreated MIO-M1 cells in culture. Following the addition of IL-1, cells showed a dramatic increase in the overall level of Gal-1 protein expression, with intense cytoplasmic distribution in addition to scattered aggregates. This may either be a reflection of increased Gal-1 production, or

an indication that Gal-1 may play specific roles within the cytoplasm following the exposure of Müller cells to IL-1.

Furthermore, IL-1 also caused a significant increase in the sialylation enzyme *ST3GAL1* mRNA expression levels. *ST3GAL1* encodes for ST3 beta-galactoside alpha-2,3-sialyltransferase 1, the principal enzyme responsible for the modification of proteins by α2,3-sialylation, a sialylation pattern that binds preferentially to Gal-1 (Sections 1.2.1). As such, these results suggest that when exposed to IL-1, MIO-M1 cells may not only produce more Gal-1 protein, but perform more α2,3-sialylation on the proteins produced to provide binding targets for Gal-1 as well.

Both isoforms of TGF-β as well as TNF-α were found to significantly downregulate Gal-3 mRNA expression. The effect of TGF-β was more pronounced as confirmed by immunocytochemical staining, although *ST6GAL1* mRNA expression was not significantly altered by the cytokines tested, IL-1, TNF-α, TGF-β1 and -β2, to the MIO-M1 cells in culture. However, firm conclusions from these results cannot be made as there was a high degree of variation between experiments. *ST6GAL1* encodes for ST6 β-galactoside α-2,6-sialyltransferase 1, a key sialyltransferase enzyme found to be significantly upregulated in a range of conditions such as cancer, where it is thought to facilitate major pathological mechanisms such as proliferation, migration and invasion (Garnham et al. 2019). Since the production of this enzyme was not significantly modified by the pro-inflammatory cytokines, it may be possible that selective responses to inflammatory signals by different members of the α-2,6-sialyltransferase family may occur.

Since TGF-β was effective in downregulating Gal-3 expression, siRNA inhibition of Gal-3 was used to examine whether Gal-3 levels might counter-regulate TGF-β in a negative or positive feedback loop. The incubation of MIO-M1 cells with siRNA duplex constructs targeting Gal-3 did not reveal any changes in TGF-β expression in MGCs. These observations are in contrast with other studies in tissue fibrosis, for instance in atrial fibrosis, where Gal-3

was found to activate TGF-β related pathways (Shen et al. 2018; Mackinnon et al. 2012). This difference might therefore be ascribed to cell specificity, as the previous studies examined the effect of these molecules within fibroblasts within the lung.

3.3.5 Involvement of Galectin-1 and -3 in the Activation of Intracellular Pathways by Cytokines

Experiments in this chapter revealed potential involvement of Gal-1 and -3 in the activation of various intracellular pathways. Firstly, inhibition of Gal-1 appeared to downregulate STAT3 phosphorylation when compared to MIO-M1 cells treated with scrambled siRNA duplex constructs. STAT3 is one of the key intracellular pathways involved in inflammation and has been shown to be activated by TNF-α, as shown in this study, as well as IL-6 and TGF-β, as shown by others (Chakraborty et al. 2017).

The finding that Gal-1 silencing RNA in this study was able to diminish STAT3 phosphorylation implies Gal-1 may contribute to the activation of STAT3 in MGCs. In addition, TNF-α was found to upregulate both STAT3 phosphorylation and Gal-1 production, which would suggest that Gal-1 may be an intermediary which potentiates STAT3 phosphorylation. If this is the case, the inhibition of Gal-1 may prove to be a viable treatment strategy to dampen STAT3 related effects which result from TNF-α activation.

There is extensive evidence that the TGF-β family of proteins are important players in the pathogenesis of fibrosis (Walton, Johnson, and Harrison 2017). The majority of these pro-fibrotic effects are thought to be mediated through the Smad-2/3 pathway. In quiescent fibroblasts, TGF-β is thought to be responsible for their differentiation into active myofibroblasts, causing tissue contraction via the secretion of α-SMA. The ocular specific isoform, TGF-β2, has been shown to perform important roles within the healthy retina, including the promotion of immune privilege, and regulation of neuroprotection (Chen et

al. 2020). However, higher concentrations of TGF-β are thought to lead to uncontrolled inflammation and fibrosis.

The present results demonstrated that MIO-M1 cells exhibit low levels of phosphorylated Smad during resting state, which increased significantly following incubation with TGF-β. However, in cells where Gal-3 mRNA silencing had already been performed, the level of Smad phosphorylation was decreased as compared to cells treated with scrambled mRNA when both were incubated with TGF-β. These findings suggest that Gal-3 may be an important regulator of TGF-β induced Smad signalling. However, unlike the findings above regarding TNF-α, Gal-1 and STAT3, TGF-β has been shown to downregulate Gal-3 in MIO-M1 cells (Section 3.2.6). In this case, it is possible that existing retina derived TGF-β downregulates Gal-3 production within MGCs; however, when exogenous sources of Gal-3 are available, such as invading macrophages, Smad activation becomes much more pronounced.

The ERK/MAPK pathway is classically associated with the regulation of cell proliferation (Blazevits et al. 2016). However, despite findings from earlier experiments in this chapter that various cytokines as well as Gal-3 affect the proliferation of MGCs, no significant differences in p44/42 phosphorylation was found when cells were silenced for Gal-1/-2 or cultured with any of the cytokines. One possible explanation for this finding could be that the observed proliferative effects of these molecules were mediated through an alternative pathway, such as JAK/STAT.

Finally, the β-Catenin pathway was examined, which revealed that Gal-3 inhibition decreased β-Catenin activation (dephosphorylation), to a similar degree as the Wnt antagonist used in the experiments. Furthermore, the effect of these two reagents did not appear to be additive. The Wnt/β-Catenin pathway has been shown to be crucial during retinal development (Fujimura 2016), and more recent evidence suggest that the activation of this pathway also exhibits important neuroprotective properties (Kassumeh et al. 2021). The findings from this current chapter suggests that Gal-3 inhibition

downregulated β-Catenin pathway activation in MGCs, and therefore may play a role in inhibiting its corresponding effects.

The effects of Gal-1 and -3 on intracellular activation of transcription factors and their interaction with cytokines revealed in this chapter raise interesting questions, both in terms of possible mechanisms as well as potential therapeutic strategies. Existing literature have revealed both cell surface and intracellular binding partners for Galectins, additionally, it would be informative to ascertain whether these effects are dependent on the carbohydrate binding properties of these Galectins.

3.3.6 Summary

These *in vitro* experiments have elucidated potential roles for Gal-1/3 to interact with cytokine activated intracellular pathways within MGCs. These interactions in turn may be important regulators of cellular processes such as proliferation, migration and contraction, during both normal and pathological states.

4. GALECTINS IN RETINAL DEVELOPMENT *IN VITRO*

4.1 Introduction

The discovery of stem cell derived retinal organoids was a landmark breakthrough (Eiraku et al. 2011), which dramatically transformed the approach to modern ophthalmological research (Kruczek and Swaroop 2020). As reviewed previously (section 1.3.4.2), retinal organoid based experimental models have the potential to overcome many of the shortcomings associated with traditional in vitro models. This is especially relevant for studying retinal development, as cells within retinal organoids *in vitro* arise in a fashion similar to *in vivo* growth. Given the available evidence of the involvement of Gal-1 and -3 in retinal development in organisms such as the zebrafish (section 1.2.5.6), this chapter aimed to characterise their expression in retinal organoids.

4.1.1 Differentiation of Retinal Organoids

Various differentiation protocols for retinal organoids currently exist, while refinements and modifications are continuously being adapted and improved. Specific protocols have been developed to derive retinal organoids from a wide range of different cell lines, ranging from embryonic stem cells to induced pluripotent stem cells (Wahlin et al. 2017; Nakano et al. 2012). Although existing studies have been able to produce retinal organoids containing characteristic laminated retinal mantle structures reliably, there exists a degree of variation in yield. As such, the first important step for retinal organoid-based investigations was to standardise the process of retinal organoid differentiation, with special attention paid to the culturing conditions and the need for organoid dissection.

4.1.2 Expression of Galectin-1 and -3 within Retinal Organoids

Galectins-1 and -3 have been demonstrated to be expressed by MGCs, as well as other cell types within the retina (Section 1.2.4). Whilst most existing studies within the retina have investigated the function of these proteins during various disease processes, relatively little is known of their role during retinal development. Work in the zebrafish has revealed that absence of Drgal1-L2, a protein functionally similar to mammalian Gal-1 can lead to developmental abnormalities in the CNS (Section 1.2.5.6). However, the exact mechanisms of action for these findings have yet to be elucidated, and their relevance in the human retina remains to be confirmed.

Furthermore, as altered expression of Gal-1 and -3 following the addition of exogenous cytokines to MGCs in culture was previously shown, investigation of the effects of cytokines during organoid development may provide important information on their role in Gal expression during organoid development. Specifically, it would be important to understand whether Gal-1 and -3 production within organoids in response to exogenous cytokines may be similar to the response seen in MGC monoculture *in vitro*.

4.1.3 Objectives

The specific objectives of this chapter were as follows:

- To establish and validate a protocol for the differentiation of retinal organoids.
- To quantify the gene expression of *LGALS1* and *LGALS3* within CD29+/CD44+ MGCs during the first 90 days of retinal organoid development using RNA-Seq data.
- To explore any associations between *LGALS1* and *LGALS3* with gene expression of their associated sialylation enzymes *ST3GAL1* and *ST6GAL1*, respectively.
- To characterise the protein expression of Gal-1 and -3 along with α2,3- and α2,6-sialylation using immunohistochemical staining methods.
- To explore the potential effects of exogenous cytokines on the morphology of retinal organoids and Gal-1/-3 production.

4.2 Results

4.2.1 Validation and Refinement of the Retinal Organoid Differentiation Protocol

Following the seeding of RC-9 stem cells into non-adherent 96-well plates, the cells aggregated into spheroid embryonic bodies (EBs) within the first 24 hours (row 1, Figure 4-1). These EBs enlarged steadily over the first 12 days, at which point they were transferred into squared 25-well, low-adhesion plates. In a significant proportion of EBs (between 30-40%), curved protrusions formed at the edge between days 12 and 25. These formations acquire a distinctive, laminated appearance, typically consisting of a visible hyper-reflective band (row 2, Figure 4-1). These structures are the originations of the neuroretinal rim, which then evaginate from the EBs to form prominent lobes around day 30. On average, retinal mantles appeared in 30%-40% of embryonic bodies, with a significant proportion of these displaying multiple mantles by day 30.

Dissection of the neuroretinal tissue from their attached EBs is a crucial part of the retinal organoid differentiation process. This was performed using microsurgical scissors, with the aim of separating a piece of neuroretinal tissue with as little undifferentiated stem cell containing tissue as possible (row 3, Figure 4-1). Viable pieces of neuroretinal tissue tend to appear translucent under light microscopy, in contrast to the much denser appearances of stem cell aggregates. Each piece of separated neuroretinal tissue was then placed in individual wells in a squared well plate and allowed to further develop into a retinal organoid (row 4, Figure 4-1). Particular attention was paid to dissect slightly away from the base of retinal mantles, so as to minimise the amount of non-retinal tissue carried over to the new wells. In almost all of cases following dissection, edges of dissected retinal tissues folded inwards to reform a spheroid structure.

In the majority of cases, edges of the divided neuroretinal tissue closed upon themselves and the organoids reorganised into globular structures following dissection (organoids C&D, Figure 4-1), before further developing into multilobulated structures by day 90. However, it should be noted that the size and quality of the neuroretinal outpouching at the point of dissection appears to be crucial in the subsequent development of viable retinal organoids. As can be seen in organoids A&B in Figure 4-1, the neuroretinal outpouching of organoid A did not have the characteristic laminated hyper-reflective structure, whereas in the case of organoid B, the neuroretinal outpouching appeared to be under-developed at the point of dissection. In both cases, development of the retinal organoids following dissection was unsatisfactory and did not resemble characteristics of retinal organoids at days 60 and 90, as seen in C&D of Figure 4-1. In general, segments of retinal tissue that were larger and better developed prior to dissection gave rise to more representative retinal organoids, which continued to enlarge and grow multiple lobes between days 30 and 90. Conversely, tissues which contained less well-developed retinal material tended to demonstrate a minimal increase in size and reduced definition of the characteristic lamination seen in healthy retinal organoids.

For the purposes of subsequent experiments within this chapter, only organoids which exhibited satisfactory appearances as described above were included in the study.

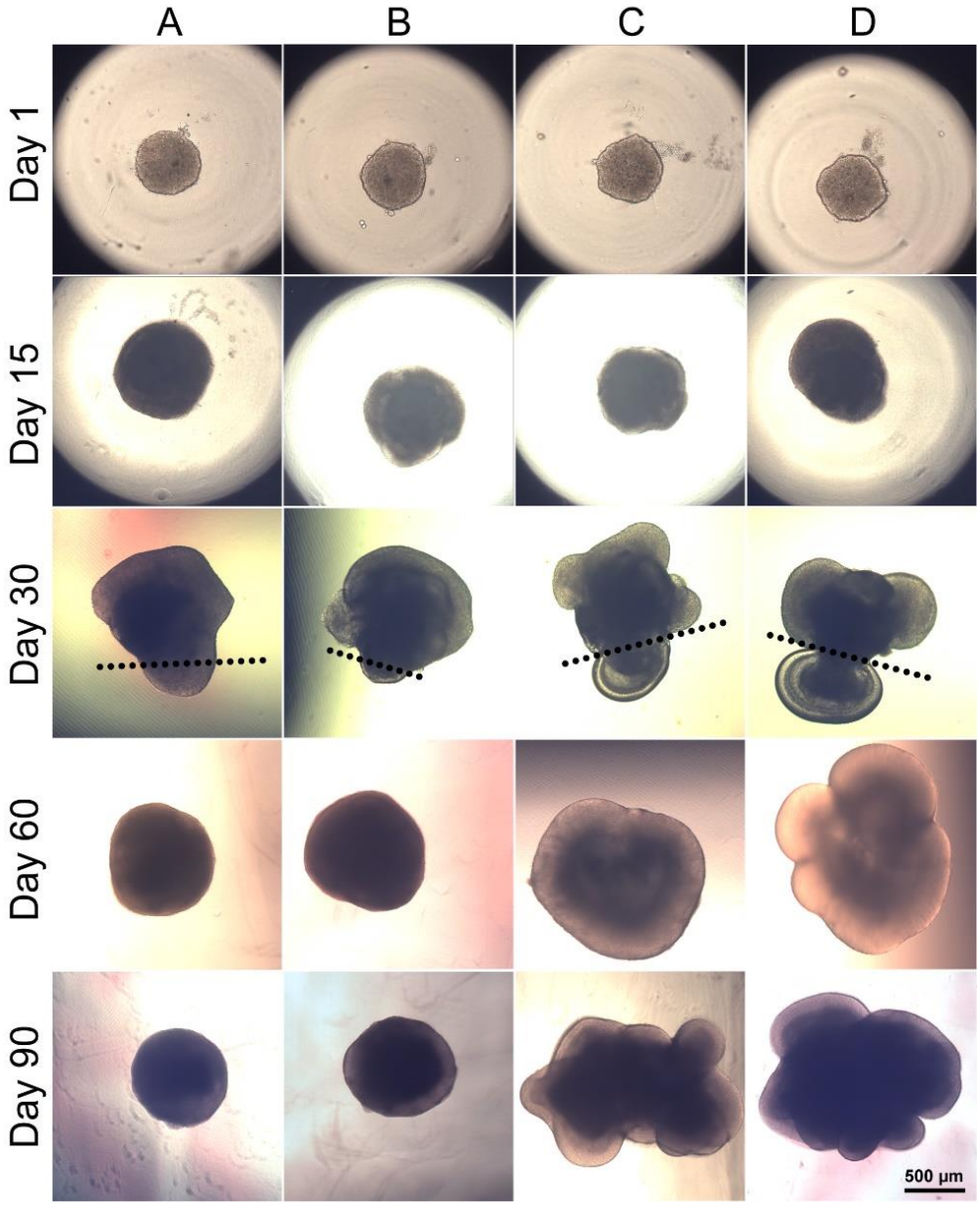

Figure 4-1 Low magnification light microscopy images illustrating the development of retinal organoids during 90 days of maturation. Each column represents a unique embryoid body. Dissection of neuroretinal tissue away from their embryoid bodies was carried out between days 30-35, along the axis denoted by the dotted line. Retinal organoids A&B did not progress to form satisfactory retinal organoids, most likely due to insufficient and/or poorly developed neuroretinal material at the time of dissection. In contrast, organoids C&D exhibited prominent mantles formed of neuroretinal material at the time of dissection and developed into characteristic multilobulated retinal organoids.

4.2.2 Gal-1 and -3 mRNA Expression During Retinal Organoid Development

Previous studies in the host laboratory performed RNA-Seq analysis from MGCs isolated from retinal organoids at various stages of retinal development (Eastlake 2020, manuscript in preparation). Data was taken from this source and analysed to quantify the gene expression of *LGALS1* and *LGALS3* as well as mRNA of related sialylation enzymes to determine potential associations.

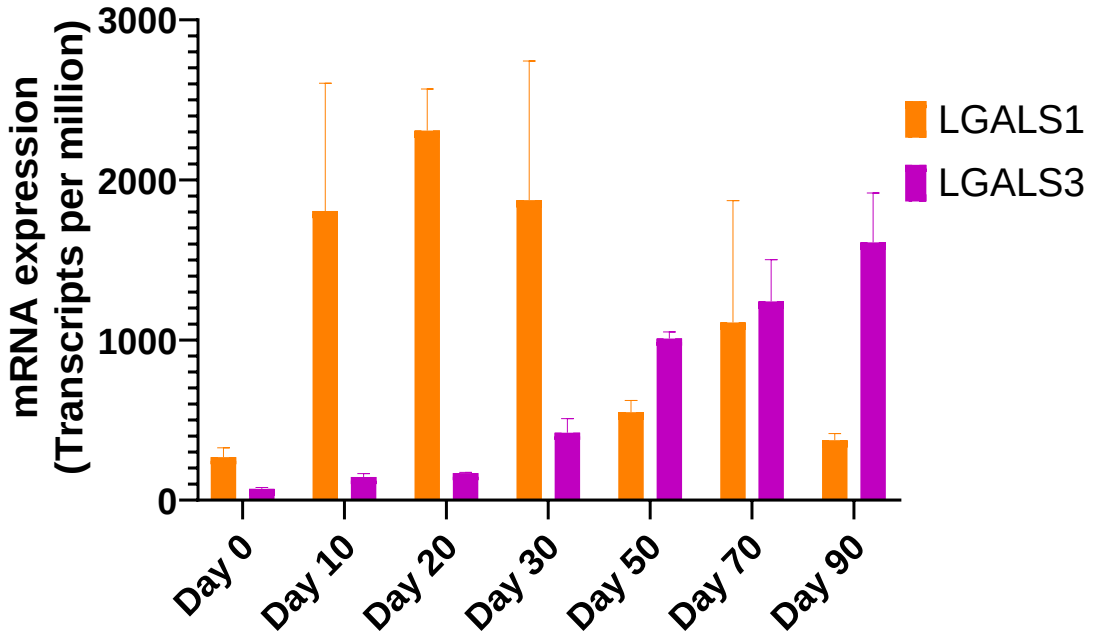

Figure 4-2 Gal-1 and -3 mRNA (LGALS1 and LGALS3 respectively) expression levels in CD29+/CD44+ cells isolated from retinal organoid at various stages of retinal differentiation. Data at Day 0 was obtained from undifferentiated RC-9 stem cells.

RC-9 stem cells undergo a process of retinal organoid differentiation that develop to fully formed retinal organoids from day 25 onwards. MGCs isolated at various stages of organoids maturation up to 90 days, showed significant changes in Gal-1 and -3 mRNA expression (*LGALS1* and *LGALS3* respectively) over time (Figure 4-2). Undifferentiated RC-9 stem cells at day 0 showed relatively low levels of both Gal-1 and -3 mRNA expression. Gal-1 mRNA expression rose quickly during early organoid development and peaked between days 10 and 30, and then again at day 70 of organoid

development. There was, however, a large variation in Gal-1 expression during the various time points examined. In contrast, Gal-3 expression showed less variation and increased steadily as the organoids formed and reached maximum mRNA expression levels towards the end of the 90-day organoid examination period.

It was also possible to investigate the mRNA expression levels of sialylation enzymes within the organoid derived MGCs. *ST3GAL1* expression levels closely correlated with *LGALS1* levels, being low in the undifferentiated RC-9 stem cells and peaking around day 20-30 of organoids formation (Figure 4-3, A). In contrast, examination of *ST6GAL1* expression showed inversed correlation with *LGALS3* expression, being very high in undifferentiated RC-9 stem cells, decreasing dramatically during the first 20 days of organoid differentiation and remained at relatively low levels throughout the remainder of the 90-day retinoid differentiation period (Figure 4-3, B).

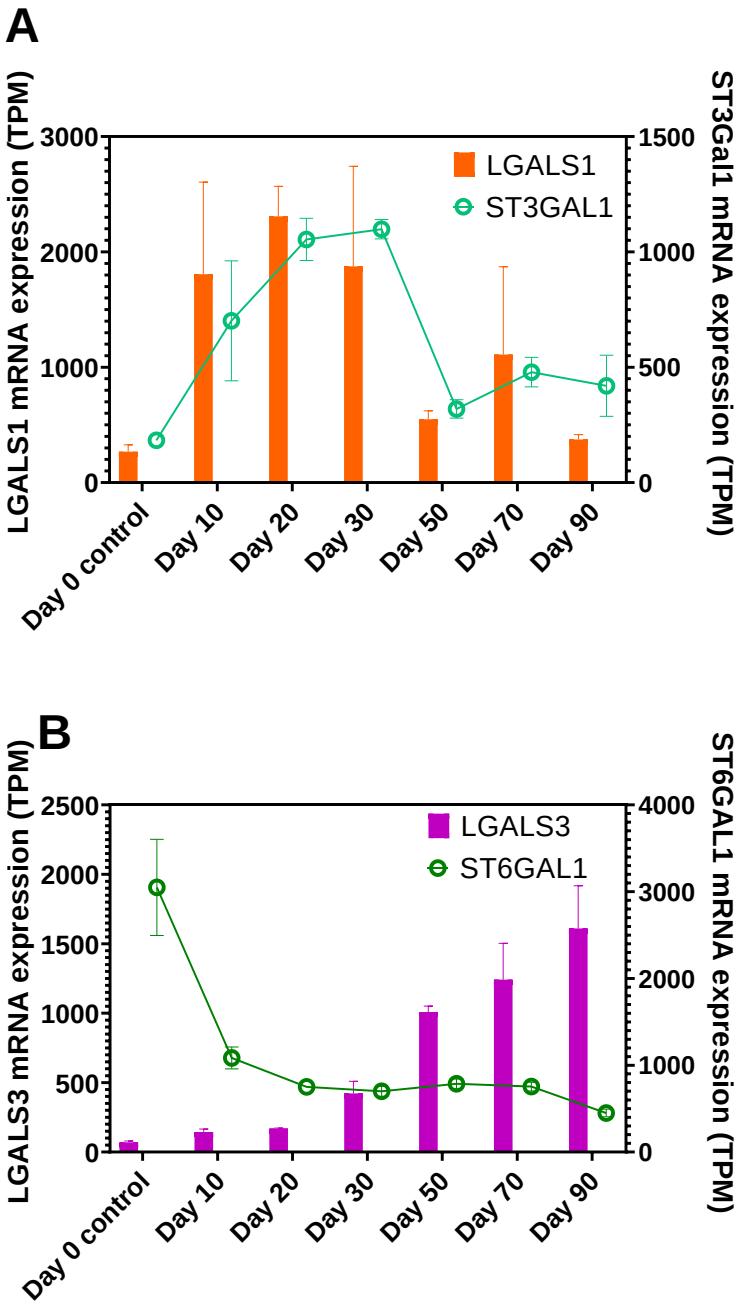

Figure 4-3 Sialylation enzyme mRNA expression levels plotted against Gal-1 and -3 mRNA expression levels. (A) ST3GAL1 expression closely correlated with LGALS1 expression, starting at low levels in RC-9 stem cells and peaking around day 20-30. (B) ST6GAL1 expression correlated inversely with LGALS3 expression, starting at high levels in RC-9 stem cells and decreasing dramatically during the first 20 days of differentiation.

4.2.3 Immunodetection of Galectin Proteins within Retinal Organoids at Various Stages of Maturation

Immunohistochemical staining of retinal organoid sections was performed at different stages of retinal organoid differentiation and maturation *in vitro*. *Maackia amurensis* (MAL) lectin-II binds specifically to α2,3-sialyl acid groups, which are conjugated by the *ST3GAL* family of enzymes including *ST3GAL1*. For this reason, it was chosen as a co-stain used concurrently with a Gal-1 antibody (Figure 4-4). Gal-1 fluorescence intensity appeared to increase from day 15 to day 30 and remained at similar intensities through days 60 and 90. Whilst fluorescence from MAL binding was observed at all time points, no significant differences in MAL fluorescence were apparent between different time points of retinal organoid development and maturation.

Sambucus nigra agglutinin (SNA) is a lectin that binds specifically to α2,6-sialyl acid groups, which are conjugated by the *ST6GAL* family of enzymes including *ST6GAL1*. It was therefore chosen as a co-stain for retinal organoids concurrently with a Gal-3 antibody (Figure 4-5). The intensity for staining for Gal-3 gradually increased through organoid differentiation and maturation, and reached maximum at day 90. However, as seen with MAL immune-fluorescence, fluorescence from MAL binding was observed at all time points but no significant differences in SNA fluorescence were apparent between different time points of retinal organoid culture.

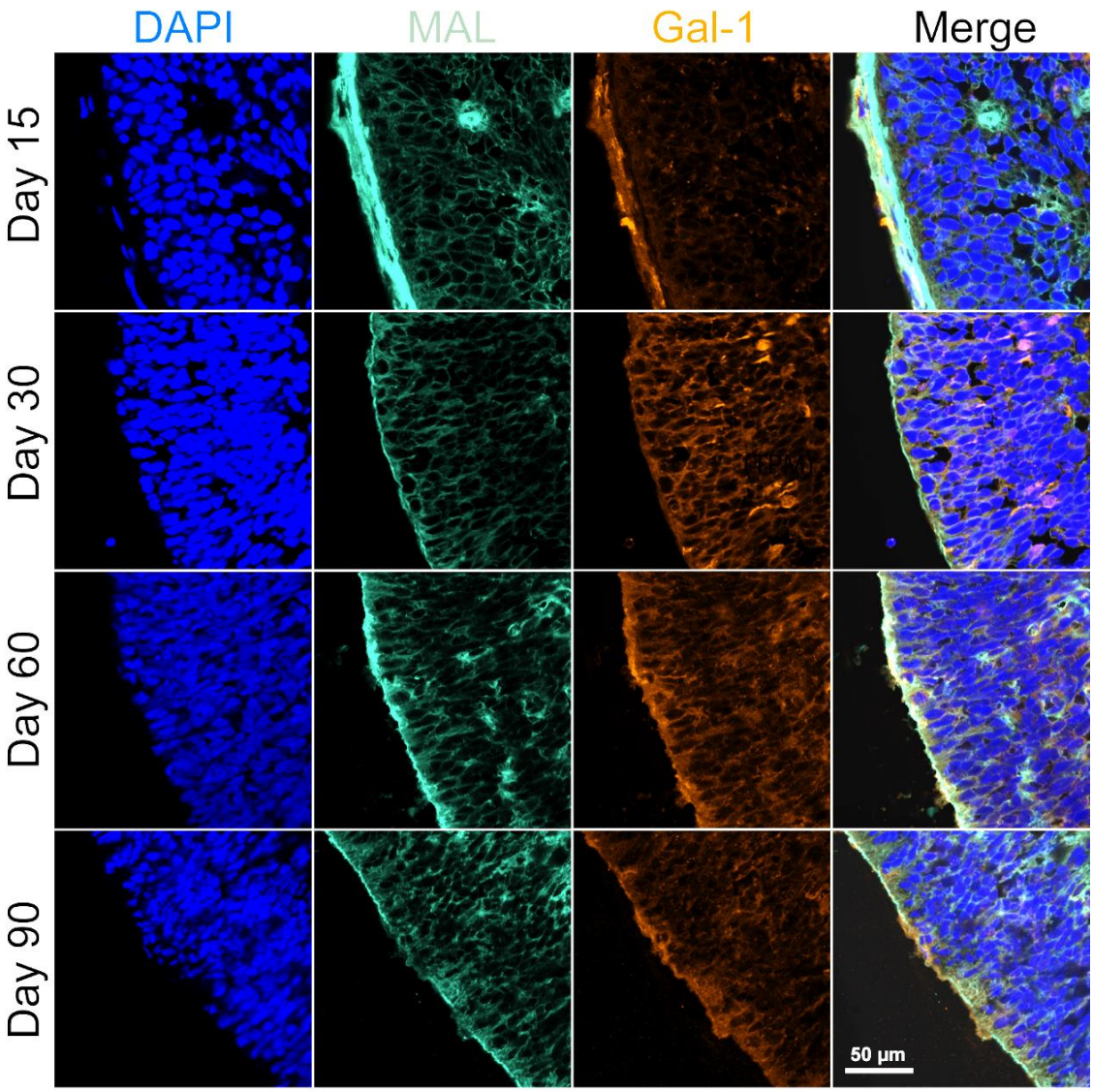

Figure 4-4 Maackia amurensis (MAL) lectin-II was used to stain for tissue α2,3-sialylation concurrently with a Gal-1 antibody. Cell density increased throughout the differentiation period and became progressively more elongated radially to form retinal mantles. Gal-1 fluorescence intensity appeared to increase from day 15 to day 30 and remained at similar intensities through days 60 and 90. However, no significant differences in MAL fluorescence were apparent at different time points of retinal organoid development. (n=5 per time point)

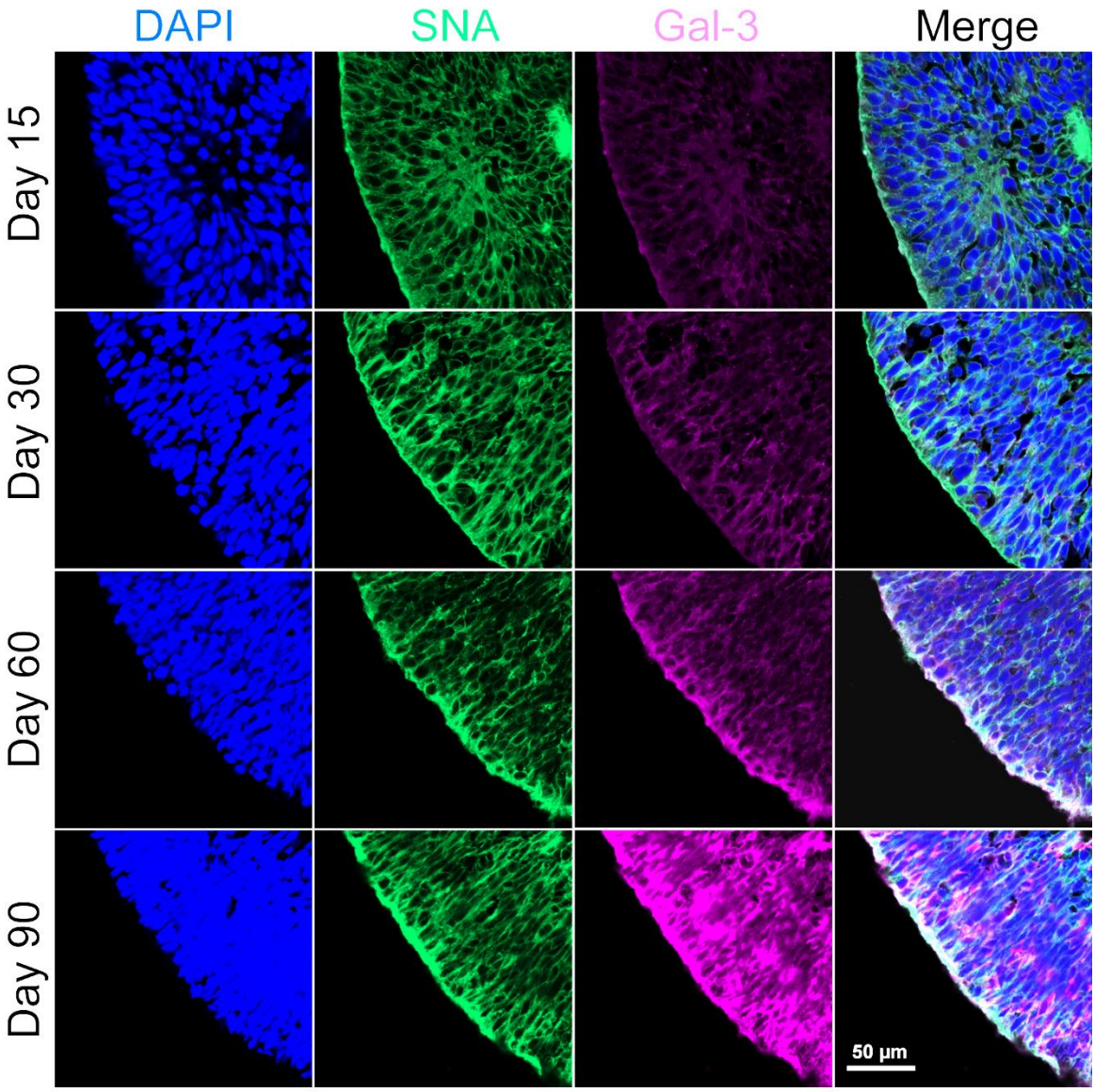

Figure 4-5 Sambucus nigra agglutinin (SNA) was used to stain for tissue α2,6-sialylation concurrently with a Gal-3 antibody. Gal-3 fluorescence increased through the organoid differentiation period and reached maximum intensity at day 90. However, no significant differences in SNA fluorescence were apparent at different time points of retinal organoid development. (n=5 per time point)

4.2.4 Effect of Cytokines on Gal-1 and -3 Expression within Mature Retinal Organoids

Mature retinal organoids following 75 days of *in vitro* development were used to investigate the effect of exogenous cytokines on the expression of Gal-1 and -3. Retinal organoids were cultured for 5 days in their regular maintenance media with the addition of individual cytokines. Each treatment group contained 11 to 13 organoids, derived from 2 separate experimental batches.

Treatment with IL-1 appeared to have a detrimental effect on the retinal organoids and resulted in areas of tissue degeneration as evident by a loss of normal tissue structure and a lack of DAPI nuclear staining in these areas. No significant differences were seen following treatment of TGF-β1 or -β2.

Treatment with TNF-α appeared to induce thinning of the retinal mantles within retinal organoids, as evidenced in Figure 4-6 and Figure 4-9. Further analysis of retinal mantle thickness showed no statistically significant differences between the groups, although there appeared to be a trend for the TNF-α treated group to possess thinner retinal mantles (Figure 4-8). For the purposes of this analysis, between 11 and 13 organoids were examined per group, and retinal mantle thickness measurement was carried out at the centre of the largest retinal mantle of each organoid.

Vimentin was found to be distributed throughout the retinal organoids, exhibiting characteristic radial distribution within the retinal structures. Gal-1 appeared to be more highly expressed in the central aggregates of cells within retinal organoids. In addition, IL-1 treated organoids exhibited significantly increased expression of Gal-1 in areas where retinal degeneration was more prominent.

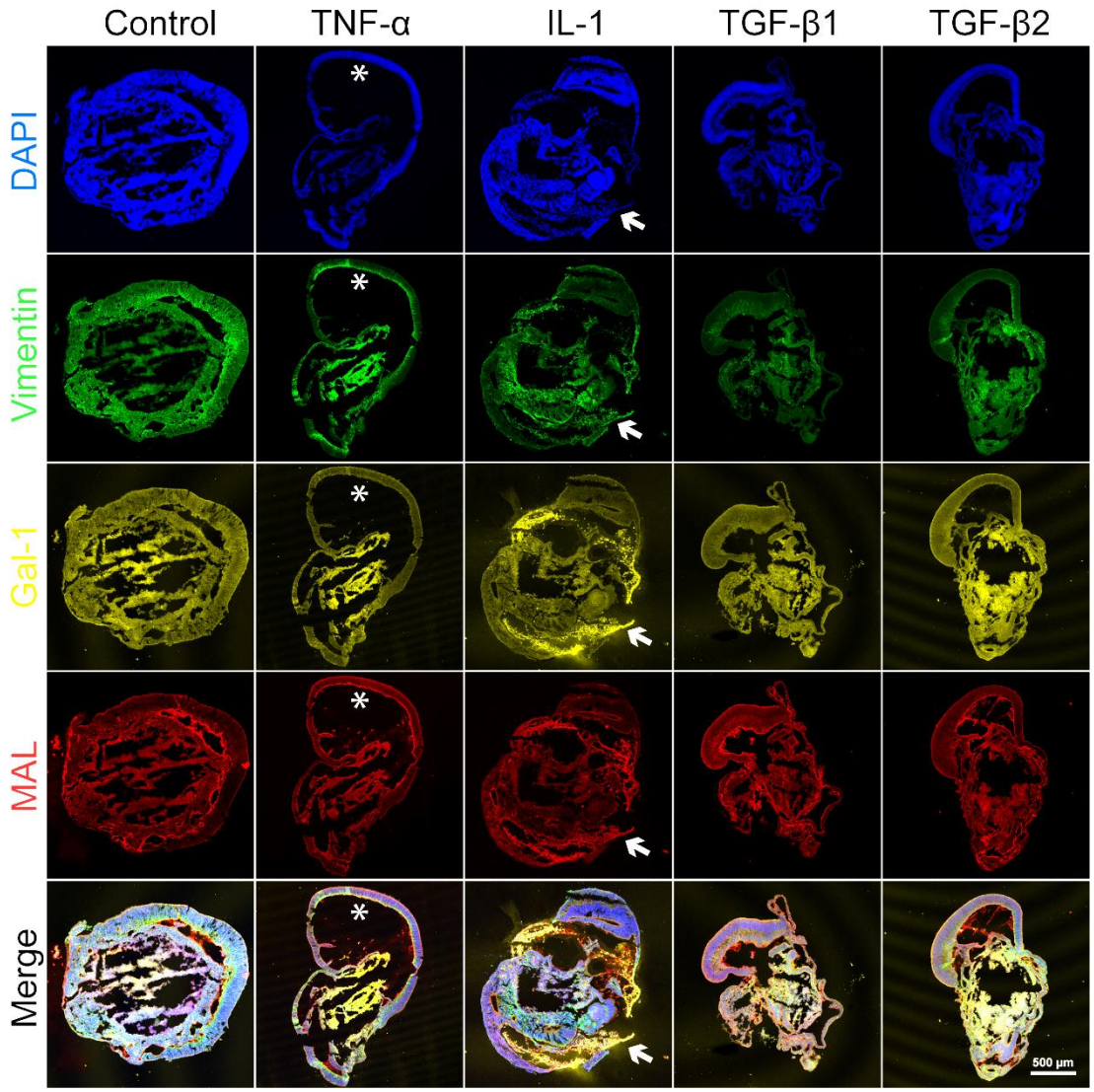

Figure 4-6 Effects of cytokines on Gal-1 expression within retinal organoids. (*) TNF-α treatment resulted in significant thinning of retinal mantles within retinal organoids. Gal-1 was found to be present throughout the organoids, but its expression was significantly higher in areas of retinal degeneration following IL-1 treatment. MAL binding appeared to be higher on the inner boundaries of retinal mantles, as well as in the areas of retinal degeneration following IL-1 treatment, which co-localised with Gal-1 expression (arrows). (n=11-13 per group)

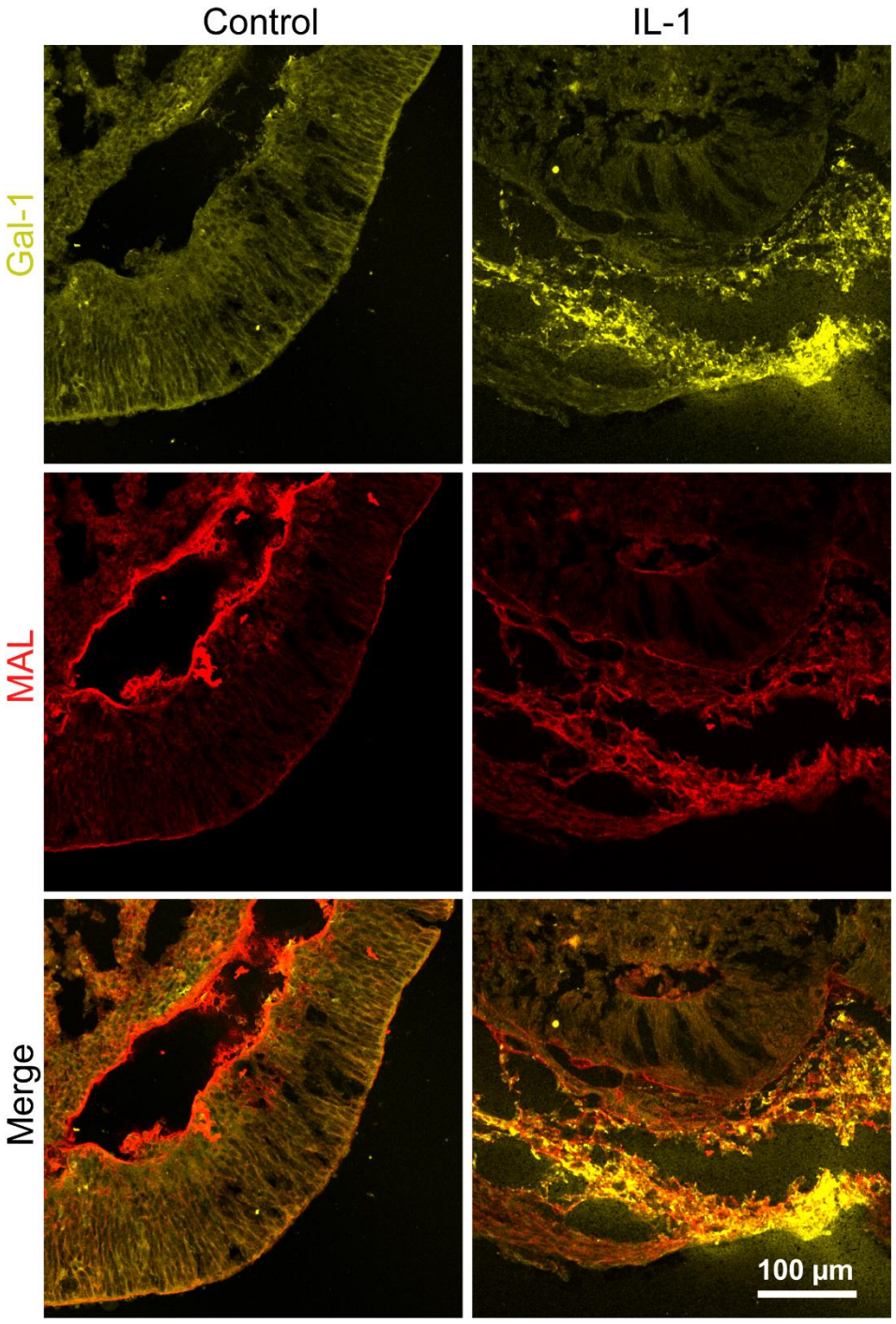

Figure 4-7 High magnification images showing increased binding of MAL to the inner boundaries of retinal mantles, as well as to areas of retinal degeneration following IL-1 treatment. This binding co-localised with increased Gal-1 expression.

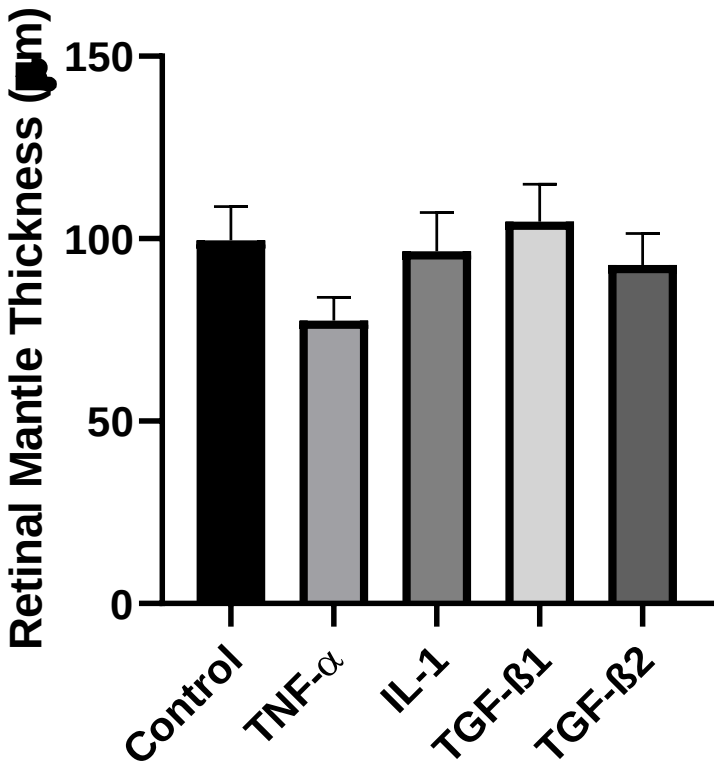

Figure 4-8 Thickness of retinal mantle thickness within retinal organoids at day 75 following 5-day treatment with cytokines, TNF-α, IL-1, TGF-β1 and -β2. No statistically significant differences were found between the groups (p=0.31, ANOVA, n=11-13 per group).

MAL binding was observed throughout the organoids and showed increased intensity on the inner border of the retinal mantles in all organoids. However, increased binding of MAL was observed in degenerated areas of the retinal mantles following incubation of these organoids with IL-1. This increase in MAL staining co-localised with the distribution of increased Gal-1 expression (Figure 4-6). These findings were also confirmed on higher magnification images (Figure 4-7).

As seen with Gal-1, examination of Gal-3 protein expression within mature organoids showed that this molecule was widely expressed throughout retinal organoids. TNF-α treatment resulted in thinning of the retinal mantles, and IL-1 treatment resulted in areas of retinal degeneration, as noted previously (Figure 4-9). Treatment with TGF-β1 or -β2 resulted in significant

downregulation of Gal-3 protein expression, whilst TNF-α treatment also appeared to have a downregulating effect, although to a lesser extent. High magnification images confirmed these findings (Figure 4-10) and demonstrated increased concentration of Gal-3 expression in the outer portion of retinal mantles. SNA staining appeared to follow the outline of cellular membranes, whilst no significant differences in SNA staining were found following TGF-β.

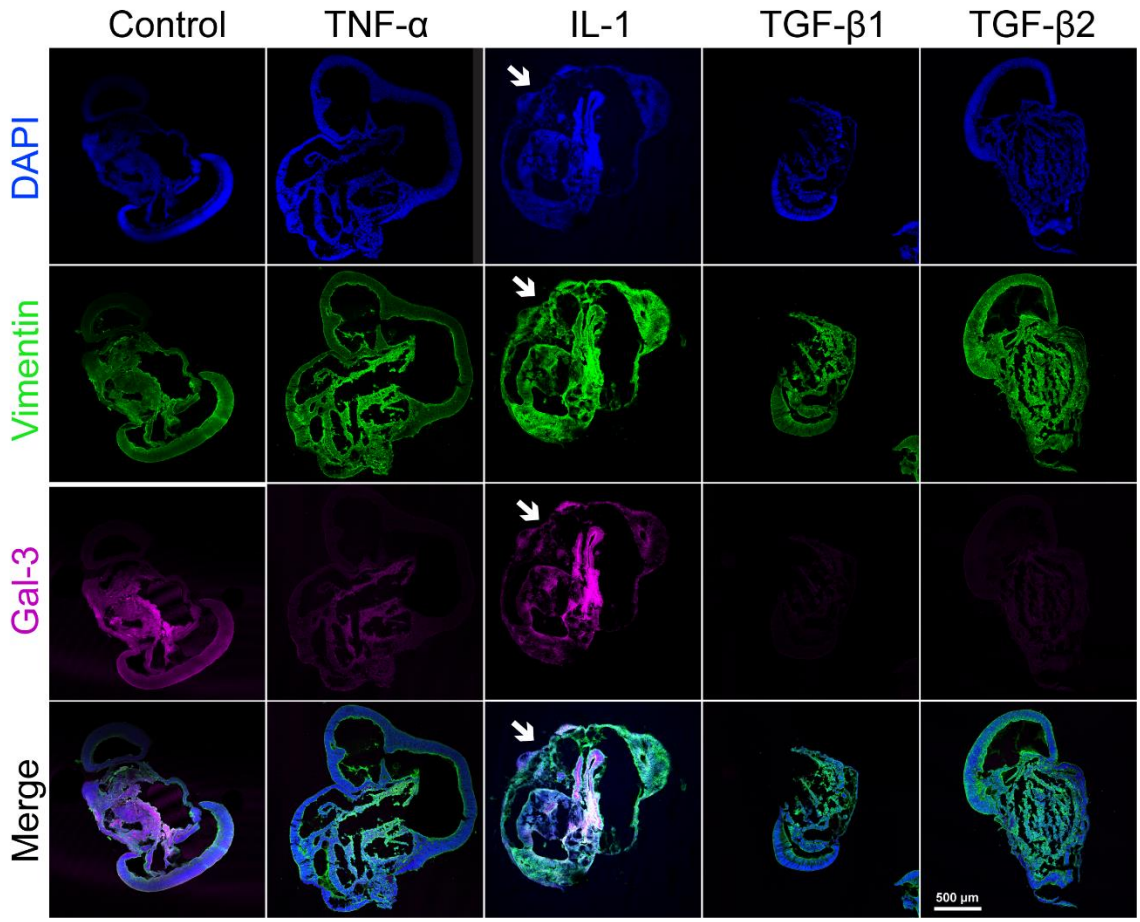

Figure 4-9 The effect of cytokines on Gal-3 expression within retinal organoids. TNF-α treatment resulted in a reduction of Gal-3 expression as well as significant thinning of retinal mantles within retinal organoids. Areas of retinal degeneration were present following IL-1 treatment (arrows) TGF-β1 or -β2 treatment caused more marked reductions in Gal-3 expressions as compared to TNF-α. (n=11-13 per group)

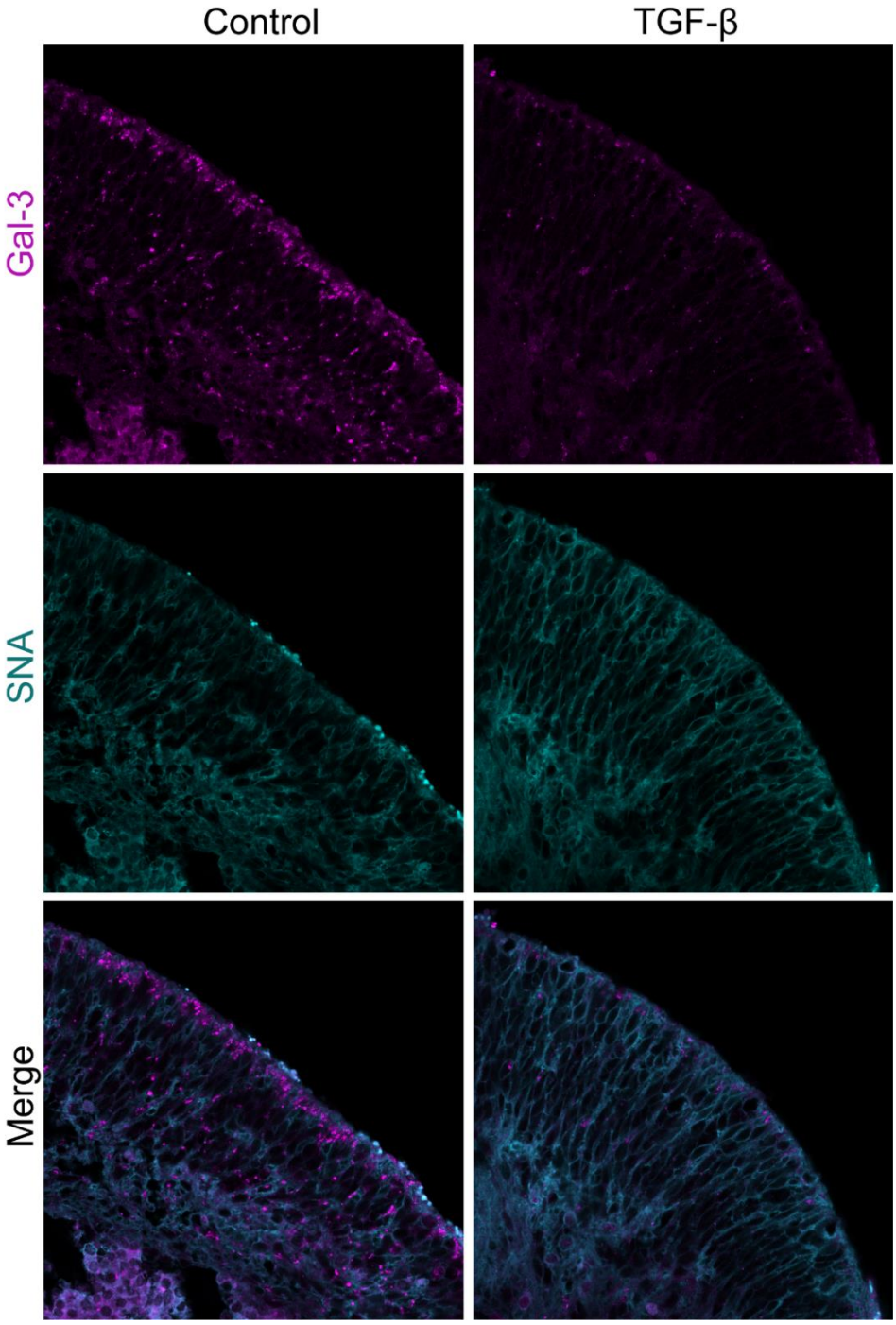

Figure 4-10 High magnification images showing distribution of increased Gal-3 expression in the outer portion of retinal mantles. TGF-β treatment caused a significant decrease in Gal-3 protein expression but had no significant differences in SNA binding were observed.

4.2.5 Expression of TGF-β by Retinal Organoids Derived Müller Glial Cells during Retinal Development

The mRNA expression levels of TGF-β isoforms were analysed from the RNA-Seq data of MGCs isolated from retinal organoids at different stages of differentiation and maturation *in vitro*, as described previously. These MGCs were found to express mRNA coding for both TGF-β1 and -β2 isoforms at different levels, although both isoforms followed a similar pattern of expression: both genes increased their expression rapidly after induction of organoid differentiation (day 10), peaked around day 20, and then gradually decreased to very low levels at day 90 in the mature organoids (Figure 4-11). Upregulation of TGF-β2 expression appeared to be significantly more pronounced when compared to TGF-β1 at days 10 and 20 (Figure 4-11).

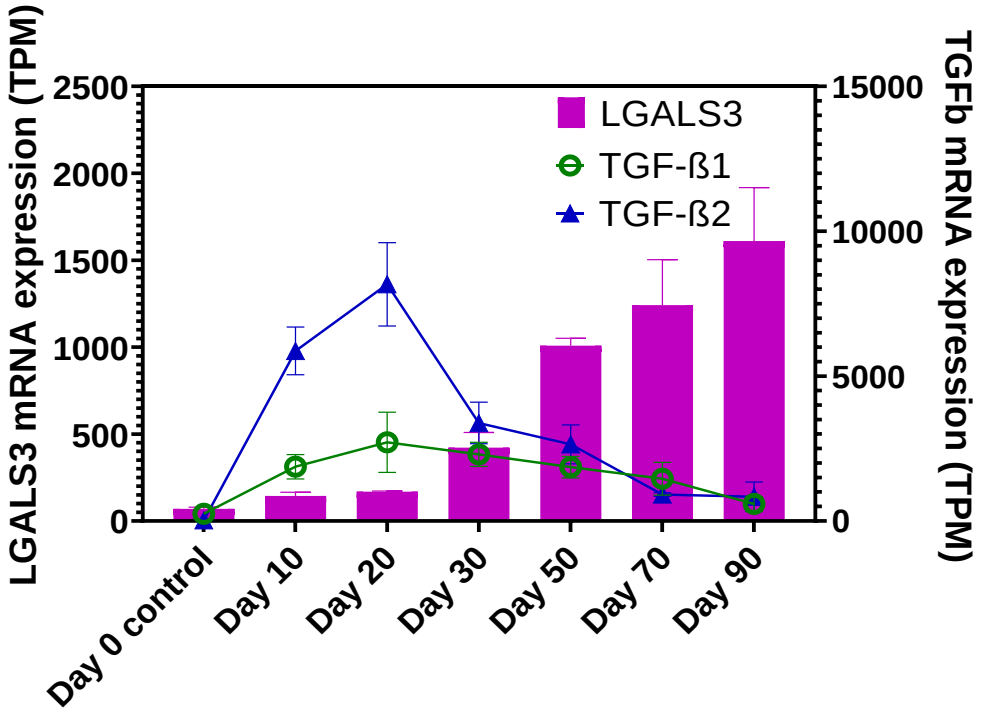

Figure 4-11 Expression of mRNA coding for TGF-β1 and -β2 by MGCs islated from retinal organoids at different stages of differentiation and maturation. TGF-β1 and -β2 expression peaked at day 20, with subsequent gradual decrease during the remaining period of retinal organoid maturation. Gal-3 (LGALS3) expression has also been included for comparison.

4.3 Discussion

4.3.1 Retinal Organoid Differentiation

The differentiation protocol used in this study was successful at developing RC-9 stem cell derived embryonic bodies into viable retinal organoids. RC-9 stem cells consistently formed aggregates within the first 24 hours, and there was little visible variation in the development of these embryonic bodies during the first 12 days of the protocol. During this period, embryonic bodies steadily increased in size and density, and remained roughly spherical in shape. It should be noted that the use of specialist-made low adhesion 96-well v-bottomed plates appeared to be essential at this stage, as the use of alternatives or coating solutions resulted in significantly fewer retinal organoids. This is likely due to the importance of maintaining the cell aggregates, as highlighted by numerous publications, which have subsequently led to the development of various culture mediums and gel scaffolds in order to improve yield and consistency (Wagstaff et al. 2021).

The use of small molecules to manipulate key cell signalling pathways for the induction of stem cell differentiation into retinal organoids has been one of the most ground-breaking discoveries in modern ophthalmological research. In recent years, optimisations tailored for individual stem cell lines and adaptations made to maximise the yield of various retinal cell types have resulted in the development of a large number of distinct protocols (Stanton and Peng 2010). In the present study, ROCK inhibitor and Wnt antagonist were added following stem cell seeding at the beginning of the first phase of development. These reagents were shown to inhibit apoptosis and caudalisation, respectively, and have been used in recent retinal organoid differentiation protocols (Nakano et al. 2012).

At day 12, the embryonic bodies were transferred into larger, 25-well square plates. The culturing media was replaced without the addition of ROCK inhibitor and Wnt antagonist, but instead, smoothened agonist (SAG) was

added to activate the hedgehog signalling pathway, which has been shown to be a central player in the determination of cell fate during development of the CNS (Yang, Qi, and Sun 2021). Previous studies elucidated the ability for the hedgehog pathway to exert mitogenic as well as differentiating effects on retinal progenitors (Stanton and Peng 2010). Whilst these findings may seem contradictory, more recent evidence have indicated that specific consequences of hedgehog pathway activation likely depends on a multitude of factors, the intricacies of which remain to be elucidated (Yang, Qi, and Sun 2021). In addition to the important roles played during development, the organisational effects of the hedgehog pathway are also apparent within the mature eye. This is most readily seen within the ciliary marginal zone, where activation of the hedgehog pathway has been shown to increase proliferation of retinal progenitors which reside in the periphery (Moshiri, McGuire, and Reh 2005), whilst simultaneously inducing the central migration of more differentiated cells (Stadler, Shkumatava, and Neumann 2004).

BMP activators have been shown to be useful in other protocols in stimulating neural differentiation (Nakano et al. 2012), although it was not used in the current study. Notch signalling inhibitors have been shown to improve the yield of photoreceptor cells, and were not used in these experiments, as they were not the primary cells of interest in the current study (Garita-Hernandez et al. 2020).

Between day 15 and day 30, in addition to the embryonic bodies continuing to increase in size, characteristic retinal mantles started to appear as outpouchings in a proportion of samples. In the current study, this occurred in around 30-40% of embryonic bodies. Interestingly, multiple mantles tended to develop on successful embryonic bodies, whilst the remaining 60-70% of embryonic bodies exhibited a complete lack of retinal mantle formation. It has been suggested that the ability for the retinal mantle to develop is dependent on the state of a particular embryonic body as a whole, rather than only specific regions. This finding is consistent with existing literature, although the

intricacies of specific structural and molecular requirements for retinal mantle formation remains to be fully elucidated.

Dissection of the retinal mantle away from its originating embryonic body appeared to be an important step in the cultivating process of retinal organoids. A variety of techniques have been employed to accomplish this goal. In this experiment, dissection was performed using micro-scissors, along boundaries as illustrated in Figure 4-1. Particular attention was paid to dissect slightly away from the base of retinal mantles, so as to minimise the amount of non-retinal tissue carried over to the new wells. In cases where a significant portion of undifferentiated stem cells were carried over post-dissection, these cells often formed dense aggregates centrally which continued to proliferate, and thereby hindered the continuing development of retinal organoids.

The procedure of retinal organoid dissection is relatively subjective and operator dependent. Sufficient material must be obtained in order for the dissected mantles to reorganise into retinal organoids, whilst the dissected sample should ideally contain as little non-retinal material as possible, as this could hinder the full development of retinal organoids. In addition, care must be taken to preserve the delicate tissues of the retinal mantles. For these reasons, some newer protocols have emerged which aimed to bypass dissection altogether as a step via the use of agarose moulds (Rashidi et al. 2022), or to replace the labour intensive dissection process with simpler alternatives such as scraping early retinal organoids from their adherent plates (Regent et al. 2020). These techniques open up the possibility of greatly increasing the throughput of retinal organoid production for both investigative and therapeutic use in the future.

4.3.2 Expression of Gal-1/3 and Related Sialylation Molecules in Retinal Organoids during Development and Maturation

The availability of RNA-Seq data has provided comprehensive insight into the transcriptome of MGCs at various stages of retinal organoid development. In this study, particular focus was placed on Galectins and their potentially related glycosylation enzymes.

Gal-1 and -3 mRNA expression levels were both found to be relatively low in RC-9 stem cells, which were used as day 0 controls. During embryoid body and early retinal organoid development between day 0 and day 30, Gal-1 mRNA expression increased rapidly, reaching its peak around day 20. This coincided with the period of rapid stem cell proliferation and is in keeping with existing studies which have identified Gal-1 as a potent mitogen during development and within malignant tissues (Camby et al. 2006). Although currently there is a lack of understanding for the role of Galectins in the development of the human retina, studies in regenerating zebrafish retina have shown Gal-1 to be upregulated during this process that requires cell growth (Craig et al. 2010). Following day 30, there was a gradual decline in Gal-1 mRNA expression levels until the end of the 90-day period. Assuming that the level of Gal-1 expression correlated with the rate of cell proliferation, its decline following day 30 may be accounted for by the overall slower rate of growth in retinal organoids during maturation as compared to embryoid bodies prior to day 30.

In contrast to Gal-1, Gal-3 mRNA expression remained relatively low during the first 30 days of retinal organoid formation, followed by a steady increase between days 30 and 90. The relatively high levels of Gal-3 expression towards the end of the 90-day retinal organoid differentiation period coincided with the maturation of different cell types, as evident from the increasing density of radially distributed vimentin in mature ROs. Whilst the presence of Gal-3 has been relatively well documented in the mature retina, principally in MGCs and RPE cells, its function during development remains poorly

understood. Given the current observations and existing evidence, it may be possible that Gal-3 acts to bind appropriately glycosylated regions of cell surface proteins to perform a stabilising function. This effect has previously been demonstrated on RPE derived CD147 and Integrin-β1 (Priglinger et al. 2013), as well as the glycocalyx of the cornea (Argueso 2013).

The mRNA expression levels of Gal-1 from MGCs obtained from RNASeq correlated well with the expression of this protein as shown by immunohistochemical staining (Figure 4-4 and Figure 4-5). In these images, changes in Gal-1 protein expression appeared to peak at day 30. Similarly, Gal-3 protein expression in retinal organoids also correlated well with mRNA expression in retinal organoid derived MGCs, as it appeared to significantly increase after day 30, reaching its peak at the end of the 90-day culture period. The strong correlation seen between MGC mRNA expression of Gal-1/3 with protein expression within the layers of a retinal organoid suggests that either MGCs are the major producers of Gal-1/3 within the retina, or that the changes of Gal-1/3 during retinal organoid development are broadly similar across different subtypes of retinal cells. It would be interesting to correlate these findings with other cell-types present within retinal organoids at corresponding time points.

As reviewed previously (Section 1.2.1), each member of the Galectin family demonstrates distinct binding affinities to patterns of glycosylation. More specifically, α2,3-sialylation appears to preferentially promote Gal-1 binding, whereas α2,6-sialylation has an overall inhibitory effect on the binding of all Galectins. This hypothesis was corroborated by RNA-Seq data in the current experiment, where *ST3GAL1* and *ST6GAL1* mRNA expression levels, which code for the major enzymes of α2,3 and α2,6-sialylation respectively, were analysed against respective Gal-1 and Gal-3 mRNA expression levels. The results revealed that *ST3GAL1* and *LGALS1* mRNA expression levels were closely correlated, whereas an inverse relationship can be seen between *ST6Gal1* and *LGALS3* mRNA expression. These results suggest that MGCs

may co-ordinate their protein sialylation mechanisms to match Galectin production. Specifically, as Gal-1 production increases, so does α2,3-sialylation, whereas α2,6-sialylation has an inverse relationship with Gal-3 production. This is in keeping with previous findings *in vitro* (Section 4.3.2), where the expression of *LGALS1* and *ST3GAL1* were highly correlated in response to the presence of IL-1 (Section 3.2.6).

In order to visualise protein sialylation, biotin conjugated lectins *Maackia amurensis* (MAL) and *Sambucus nigra agglutinin* (SNA) were used to target and visualise target conjugated glycans, as these lectins exhibit preferential affinity for α2,3 and α2,6-sialylation respectively. Unfortunately, no significant differences were found in the fluorescence pattern observed by this lectin labelling technique. There are several possible explanations for this finding. Firstly, the RNA-Seq data was only in reference to MGCs, whereas immunohistochemical labelling used whole retinal organoids; secondly, whilst *ST3GAL1* and *ST6GAL1* are the primary enzymes to perform their respective functions, there is a degree of redundancy within the sialylation enzymes; thirdly, RNA-Seq data does not account for post-transcriptional regulatory mechanism; and finally, binding between sialic groups and Gal-1/-3 may prevent the binding of MAL and SNA, in which case, the immunohistochemistry (IHC) results may not be a true representation of protein sialylation.

4.3.3 Effect of Cytokines on Retinal Organoid Expression of Gal-1

The addition of IL-1 to retinal organoids resulted in distinct areas of cellular damage; these areas were characterised by disintegration of the organised layers within the retinal architecture, coinciding with a loss DAPI staining, likely as a result of cell death.

Cytokines of the IL-1 family are major regulators of inflammation and have been shown to be important initiators and propagators of inflammation in AMD, DR and glaucoma (Wooff et al. 2019). Much of the existing literature

pertaining to the IL-1 family are centred around their relationship with the formation and function of the inflammasome. However, in this study, it appears that the presence of IL-1 alone was sufficient to cause cellular damage in retinal organoids which lack circulating immune effector cells.

In the previous chapter, *in vitro* experiments found IL-1 to significantly upregulate Gal-1 production in MGCs (Section 3.2.6). This finding can be confirmed within retinal organoids, where areas of damage following the addition of IL-1 showed significantly increased Gal-1 immunofluorescence signal. Furthermore, these areas also demonstrated increased MAL fluorescence co-localising with Gal-1, as seen more clearly on higher magnification images (Figure 4-7). MAL has a binding preference for α2,3-sialylation, which in turn is a consequence of ST3GAL1 mRNA upregulation. The findings here corroborate with both the results from previous *in vitro* studies which showed simultaneous upregulation of LGALS1 and ST3GAL1 mRNA following exposure to IL-1 (Section 2.2.3), as well as the findings of early embryoid body development where these two genes were similarly upregulated (Section 4.2.2).

In the healthy retinal organoid, MAL immunofluorescence staining showed increased signal on the inner boundaries, which would be analogous to the ILM *in vivo*. However, in the IL-1 treated samples, MAL staining was present throughout the damaged areas. It would be interesting to ascertain the specific function of α2,3-sialylation and the reasons for its preference to the inner limiting membrane. One possibility is that α2,3-sialylation may perform specific functions in relation to the RGCs, which are found adjacent to the ILM. Indeed, evidence from an animal study suggests that diminished α2,3-sialylation may result in aberrant ERG responses (Ahuja 2017).

4.3.4 Effect of Cytokines on Gal-3 Expression in Organoids

Immunohistochemical staining showed Gal-3 expression throughout the retinal organoids, showing higher intensity within the central, non-retinal group of cells likely comprised of non-differentiated progenitors. High magnification images of the retinal layers showed that Gal-3 protein was present in small aggregates, which appeared to be more concentrated towards the outermost portion of the retinal layers. In comparison, SNA staining appeared to delineate the extracellular spaces of the characteristic radial arrangement of the neuroretina.

Similar to findings *in vitro* in the previous chapter, the addition of TGF-β resulted in significantly decreased Gal-3 protein expression throughout the layers of the retinal organoids. Addition of TNF-α also appeared to reduce Gal-3 protein expression, although the effect appeared to be less obvious. These findings confirm that Gal-3 production within the retina responds rapidly to the presence of cytokines, specifically TGF-β and TNF-α.

The role of TGF-β and TNF-α within the retina, particularly in the context of reactive gliosis, was reviewed briefly previously (Section 1.1.4). Although the presence of TGF-β exerts well-established anti-inflammatory roles in the healthy retina (Walshe, Leach, and D'Amore 2011), its expression has also been linked to key pathogenic processes such as neovascularisation in AMD (Wang et al. 2019) and fibrosis in glaucoma (Murphy-Ullrich and Downs 2015). Similarly, TNF-α has been linked to both pro-inflammatory roles (Mirshahi et al. 2012) as well as being found to exert possible neuroprotective effects on RGCs from recent experimental evidence (Mac Nair et al. 2014). The discovery that each cytokine may mediate multiple effects, which are often apparently discordant, is a common theme in recent investigations. The reconciliation of these differences is a difficult but necessary step in understanding the specific molecular mechanisms of ocular diseases. Given the evidence presented in these chapters, it may be that the presence of Gal-

3 is a factor contributing to the determination of which set of effects are mediated by TGF-β.

4.3.5 Expression of TGF-β by Retinal Organoids

Given that TGF-β has potent down-regulatory effects on Gal-3 in MGCs, RNA-Seq data was re-examined which showed that TGF-β expression was increased between days 10 and 30, coinciding with the period where Gal-3 expression levels remained relatively low. This pattern was particularly apparent for the ocular specific TGF-β2 isoform, which showed a significant peak at day 20.

These results suggest that the expression of Gal-3 from MGCs during organoid development may be in part due to the release of TGF-β isoforms from the MGCs themselves. The period of early organoid development between days 10 and 30 corresponds to the emergence of RGCs (Cepko 2014); high TGF-β expression during this time is concordant with existing evidence that this molecule is required for the differentiation and maintenance of RGCs (Walshe, Leach, and D'Amore 2011) as well as prevention of apoptosis (Braunger et al. 2013). Gal-3 has also been shown to be involved in both intrinsic and extrinsic apoptosis pathways, although the exact mechanisms of its function remains to be elucidated (Nangia-Makker et al. 2007). Taken together, these results suggest that regulation of the TGF-β/Gal-3 axis may be an important factor during retinal development. As such, manipulation of these molecules during retinal development may be an interesting avenue to pursue in future experiments.

4.3.6 Summary

In summary, experiments in this chapter described the spatial-temporal distribution of Gal-1 and -3 expression as retinal organoids develop, as well as their response to exogenous cytokines. The results support existing evidence that MGCs are the major producer of these proteins within the neuroretina. Furthermore, the data presented revealed good agreement between mRNA and protein expression. Culturing of mature retinal organoids in the presence of cytokines revealed changes in Gal-1 and -3 expression similar to those found in the previous chapter.

5. Galectins in Animal Models of Glaucoma and Optic Neuropathy

5.1 Introduction

5.1.1 Rodent Models of Glaucoma and Optic Neuropathy

Glaucoma consists of a broad range of pathogenic processes which ultimately converges on a final pathway of optic nerve degeneration with characteristic changes of the optic nerve head, often due to high intraocular pressure (IOP, Section 1.3). Whilst a range of animal models for glaucoma and optic neuropathy are currently available, each has its own advantages and disadvantages, as well as significant variation across different species (Section 1.3.4) (Biswas and Wan 2018). As such, it was important to conduct preliminary experiments comparing different experimental models which induce glaucoma-like damage, in order to identify an appropriate model which would maximise the likelihood of obtaining high quality data.

As increased IOP constitutes a key part of the majority of glaucoma subtypes, a large proportion of modern animal models of glaucoma are based on inducing IOP elevation. This is generally achieved through the injection of IOP elevating substances, such as viscoelastic, ferromagnetic microbeads, or saline (Section 1.3.4). Whilst models which include IOP elevation should in theory be more faithful to the pathogenesis of glaucoma in humans, this approach also introduces a significant source of variation. Furthermore, the causal relationship between IOP rise and optic nerve damage in animals can be unreliable. To mitigate the potential shortcomings of IOP elevation, models of optic neuropathy have also been frequently used. These models are particularly well suited to the investigation of potential neuro-protective agents

and have the advantage of being generalisable to other forms of optic neuropathies in addition to glaucoma.

When choosing the most appropriate model to use for retinal research, it is important to take into consideration the principles of Replacement, Reduction, and Refinement as laid out by the governing bodies of animal research (Sneddon, Halsey, and Bury 2017). In terms of Reduction and Refinement, care should be taken prior to proceeding with an experiment to ensure appropriate preliminary studies are carried out to minimise the number of animals needed. A study power calculation using preliminary or pre-existing data would be useful for this purpose.

Widely accepted primary outcome measures in glaucoma research are based upon the structure and functional evaluation of RGCs. In rodents, this primarily takes the form of electroretinogram (ERG) measurements, where the scotopic threshold response appears to be particularly sensitive (Saszik, Robson, and Frishman 2002). Post-mortem examination of the optic nerve also plays a role for this purpose in terms of quantifying axon loss. In models of IOP elevation, the measurement of IOP is also important, although it can be difficult to take into account diurnal IOP variation in these animals, as this appears to be an independent predictor of glaucoma progression (Caprioli and Coleman 2008).

5.1.2 Cell-based Therapy in Glaucoma

Previous investigations in the host laboratory have shown the efficacy of injecting Müller glial cells (MGCs) to ameliorate RGC damage in both feline and rodent models of NMDA induced excitatory neurotoxicity (Becker et al. 2016; Eastlake et al. 2019). As integration from the injected MGCs was not observed during these experiments, the current hypotheses for the observed effect include structural, metabolic or paracrine mediated mechanisms.

A potential route via which these observed neuroprotective effects were mediated is through the release of extracellular vesicles (EVs, Section 1.5.2).

Techniques to extract EVs from stem cell derived MGCs have recently been refined in the host laboratory to produce purified populations of EVs (PhD Thesis, Lamb, 2021). As such, the next step in this avenue of research was to assess the effects of these EVs on an animal model.

One key difference when comparing the injection of EVs with the injection of whole cells is the need for immunosuppression. Whilst both local and systemic immunosuppression is needed in animals that undergo injections of whole cells, EVs alone do not appear to induce a significant immune response based on preliminary studies within the host laboratory. As such, only local immunosuppression in the form of glucocorticoid steroid triamcinolone was needed at the time of injection.

5.1.3 Gal-1 and -3 Expression in Rodent Models of Glaucoma and Optic Neuropathy

Previous studies have associated the upregulation of Gal-1 with retinal degeneration in human PVR samples, as well as regenerating zebrafish retina, as summarised previously (Section 1.2.5). The role of Gal-1 during retinal degeneration remains relatively poorly understood, although findings from the previous chapters suggest potential participation of this protein in gliotic processes.

Similarly, Gal-3 in animal models of retinal disease also remains largely unexplored. Given the known roles played by Gal-3 in fibrotic diseases (Section 1.2.4), which is supported by findings from the previous chapters. Its expression during animal models of glaucoma would be of particular interest. In particular, it would be interesting to investigate both the anterior chamber and retinal sections of animal tissue to determine whether any similarities can be observed.

5.1.4 Objectives

The specific objectives of this chapter were as follows:

- To validate the use of different intraocular pressure elevating agents following injection into the anterior chamber of rats, including saline, viscoelastic, and ferromagnetic beads.
- To establish the effect of rat models using anterior chamber injection using the agents above on visual function as measured by electroretinogram.
- To perform a power calculation using the preliminary data on IOP elevation models and previously obtained data on the NMDA excitotoxicity model to determine the more appropriate model for subsequent experiments.
- To evaluate the effects of extracellular vesicles on retinal function during a rodent model of disease.
- To characterise Gal-1 and -3 expression in the iridocorneal angle and retina of rats from the control group which underwent anterior chamber ferrous magnetic beads injection and intravitreal NMDA injection models.

5.2 Results

5.2.1 Validation of Rodent Models of Intraocular Pressure Elevation

For this study, three different types of agents were injected into the anterior chamber of Norway Brown rats to induce IOP elevation. On this basis, experimental animals were divided into three treatment groups, with animals receiving either 2% hydroxypropyl methylcellulose (HPMC), 5µm ferromagnetic microbeads, or a combination of 2% HPMC with 5µm microbeads. Saline (0.9%) was injected in the control group. Animals were anaesthetised prior to anterior chamber injections, and all groups received 20µL in volume of the respective substrate.

5.2.1.1 Effect of Viscoelastic and Ferromagnetic Beads Injections into the Anterior Chamber on Intraocular Pressure

Measurements of the intraocular pressure were carried out between 9am and 11am on all occasions. The results showed increases of IOP in all treatment groups at day 1 post injection, which appeared to diminish by day 7, but subsequently increased again to reach significance in all 3 treatment groups at day 21 (Figure 5-1), as compared to IOP measured prior to the injections. The variation of IOP readings between animals of the same group were significantly higher in treatment groups when compared to control, as demonstrated by the size of error bars as shown in Figure 5-1.

5.2.1.2 Negative Scotopic Threshold Response Measurements in Models of Intraocular Pressure Elevation

Measurements of negative scotopic threshold responses (nSTR) were carried out at 4 weeks after anterior chamber injections of HPMC viscoelastic, ferromagnetic beads or a combination of both. In the treatment group which underwent anterior chamber injection of HPMC only, a statistically significant

difference in nSTR was found at -4.0 $cd \cdot s \cdot m^{-2}$ stimulus intensity (ANOVA, $p = 0.0189$). In the treatment group which underwent anterior chamber injection of ferromagnetic beads only, statistically significant differences in nSTR were found at -4.25 and -4.0 $cd \cdot s \cdot m^{-2}$ stimulus intensities (ANOVA, $p = 0.0001$). In the treatment group which underwent anterior chamber injection of both HPMC and ferromagnetic beads, no significant differences were seen at any of the stimulus intensities tested (Figure 5-2).

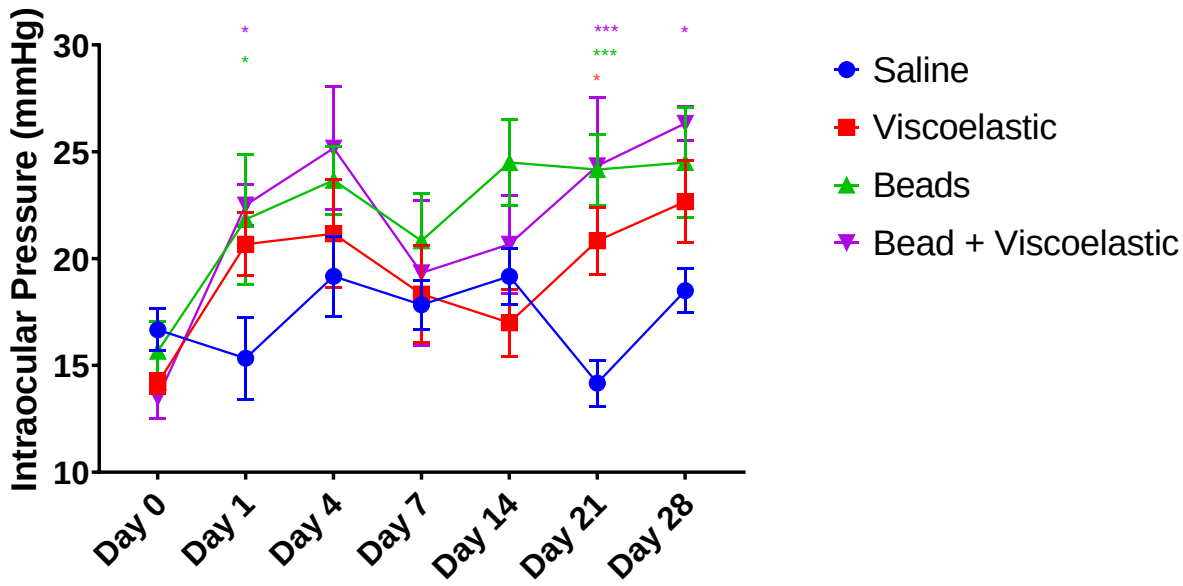

Figure 5-1 The effect of magnetic microbead and/or viscoelastic injection on intraocular pressure. Error bars represent SEM; ANOVA, p<0.0001; post-hoc statistical significance of individual differences from control are labelled in respective colours; n=6 per group.

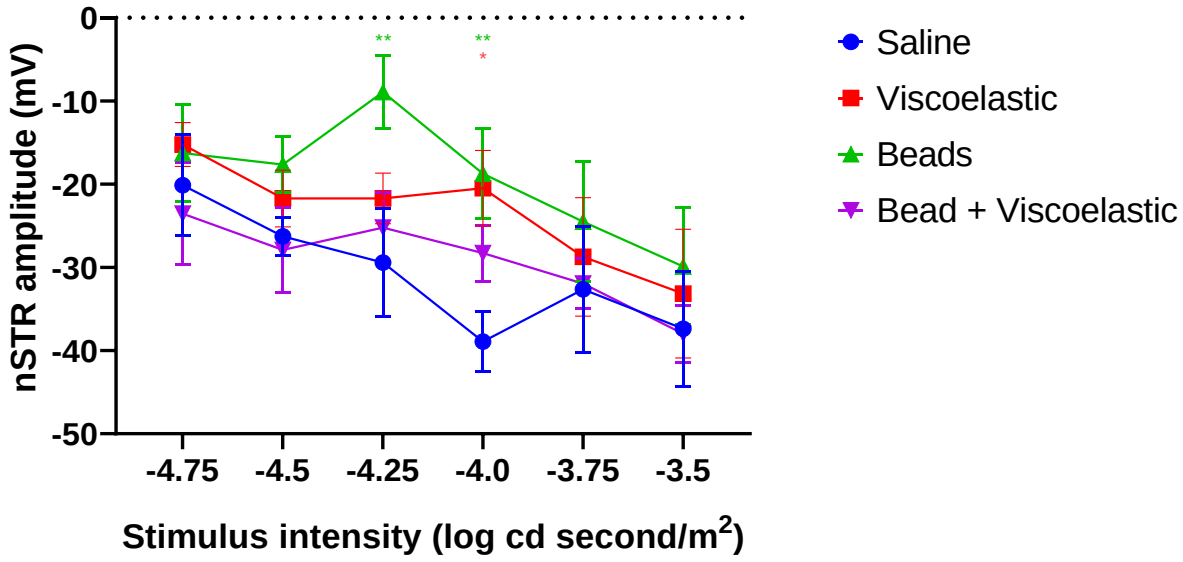

Figure 5-2 The effect of magnetic microbead and/or viscoelastic injection on the negative scotopic threshold response of the ERG at 4 weeks. Error bars represent SEM; ANOVA, p<0.0001; post-hoc statistical significance of individual comparison differences from control are labelled in respective colours; * - p<0.05, ** - p<0.01 n=6 per group.

5.2.2 Effect of Extracellular Vesicles on Rodent Model of NMDA Neurotoxicity

5.2.2.1 Study Power Calculation

The results of these preliminary experiments demonstrated that whilst all three groups were able to achieve significant increases in IOP when compared to the control group, injection of ferromagnetic beads alone appeared to result in the most significant attenuation of nSTR measurements. To ascertain the feasibility of utilising this model in testing the potential effects of EVs in rescuing RGC damage as compared to the NMDA neurotoxicity model, study effect coefficients obtained from these preliminary experiments were combined with known coefficients from previous NMDA studies and incorporated into power calculations.

As shown in Table 5-1, the total number of animals required for an 80% chance of detecting a difference with a p-value below 0.05 are 28 and 46 for the NMDA and magnetic bead models, respectively. The main contributing factor for this discrepancy is due to the difference in effect size, which is a function of both the mean reduction in the magnitude of nSTR values as well as the associated standard deviation of these measurements. In other words, the fact that the magnetic bead model was more variable and resulted in a smaller change in nSTR values was responsible for a higher number of required experimental animals to achieve the same study power as the NMDA model.

Power Calculation

	NMDA model	Magnetic bead model
Anticipated effect size*	0.43	0.33
α error probability	0.05	0.05
Power (1 – β error probability)	0.80	0.80
Number of groups	2	2
Number of measurements	6	6
Total sample size	28	46

Table 5-1 Power calculations to determine required sample sizes for NMDA and magnetic bead models; * - effect size calculated from preliminary and previous experiments of respective models.

Given the above findings and taking into account the importance of *reduction* in the "3Rs" principle outlined previously, it was decided that the main experiment to investigate the effect of EVs was to be conducted using the NMDA model. On this basis, 32 animals were used in total, which were divided equally between control and treatment groups. The slight surplus of animals as compared to the power calculation was in anticipation of any potential experimental complications and based on previous experience in the host laboratory.

5.2.2.2 Effects of Intravitreal Injection of Müller Cell Derived Extracellular Vesicles on Visual Function

Intravitreal injections of EVs were performed at 1 week following NMDA induced excitatory neurotoxicity which consisted of 3 x 10^9 EVs suspended in 2µL sterile PBS. After excluding for experimental complications, 14 animals from the EV group and 12 animals from the control group were included for analysis. At two weeks after the intravitreal injection of EVs, ERG studies

demonstrated a statistically significant improvement of nSTR values in the treatment group when compared to the control group (ANOVA, p = 0.0004). However, ERG studies at week 4 showed severely diminished nSTR values in both groups when compared to baseline, but not significantly different from each other (ANOVA, p = 0.78. Figure 5-3). This clearly indicated that the effect of EVs observed at 2 weeks was transitory.

5.2.2.3 Evaluation of Potential Experimental Confounders

In order to ensure that the ERG outcomes were not influenced by unintended confounders, the potential effects of experimental factors on STR measurements were examined using multiple regression analysis (Table 5-2). None of the p-value for these covariates reached statistical significance, as such, no meaningful effects were detected for these factors on the nSTR outcome measure.

Covariate Multiple Regression Analysis

Variable	Coefficient	P-value
Gender	0.187	0.467
Weight	-0.256	0.308
Day of NMDA injection	0.053	0.596
Day of EV/Saline injection	0.198	0.348
Day of ERG measurement	0.02	0.903

Table 5-2 Covariate multiple regression analysis of experimental factors. No statistically significant effects were detected for these factors on the nSTR outcome measure.

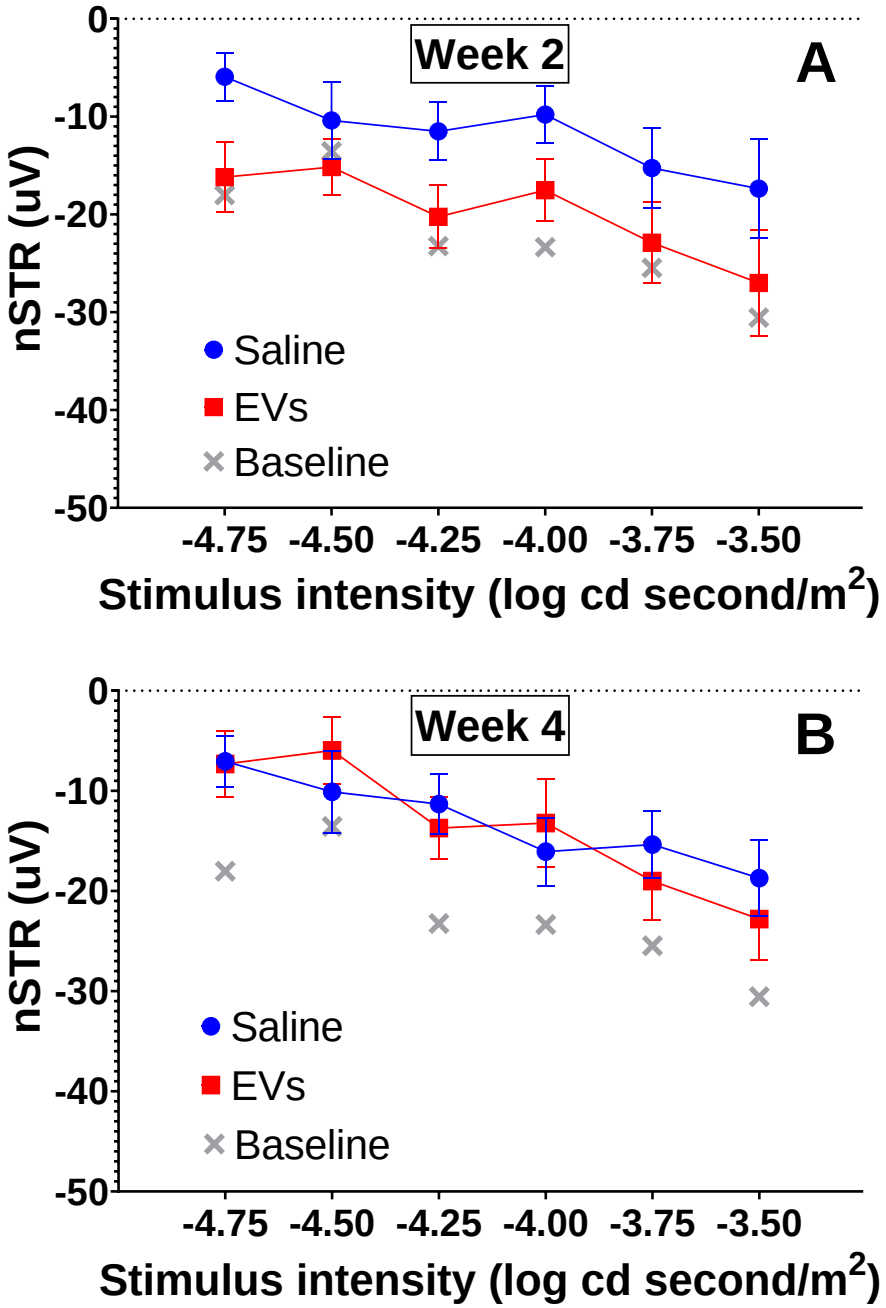

Figure 5-3 Effect of EVs injection on the negative scotopic threshold response (nSTR) of the ERG in the rat NMDA model. (A) At 2 weeks, there was preservation of nSTR in the treatment group, which was significantly improved when compared to the control group (ANOVA, p = 0.0004); (B) At 4 weeks, both groups demonstrated diminished nSTR as compared to baseline, but did not significantly differ from each other (ANOVA, p = 0.78); error bars represent SEM.

5.2.3 Galectin Expression in the Rodent Bead Model

5.2.3.1 Galectin-3 Expression within the Anterior Chamber

Anterior segment tissues were obtained from animals of the control group within the ferromagnetic bead model experiment at 4 weeks following induction of IOP elevation. Immunohistochemical staining was carried out in order to characterise changes in Gal-3 and related proteins within the iridocorneal angle of the anterior chamber. Transmission microscopy examination of these tissues confirmed aggregates of microbeads localised at the iridocorneal angle of these treated animals (Figure 5-4). Immuno-staining for the presence of macrophages using anti-CD68 antibodies showed an increased expression of this marker in animals injected with microbeads as compared to controls. Interestingly, CD68 staining was prominent in cells which appeared to infiltrate the ferromagnetic bead aggregates.

Staining of these sections for Gal-3 showed significantly increased expression of this molecule in the iridocorneal angle with co-localisation with ferromagnetic beads as compared to controls (Figure 5-5). In addition, Gal-3 expression was also significantly increased within the iris tissues. Finally, αSMA expression was increased within the iris tissue of the treated group, visible as circular structures most likely representing blood vessels, in keeping with the observation that prominent blood vessels can be seen on the iris surface of some animals.

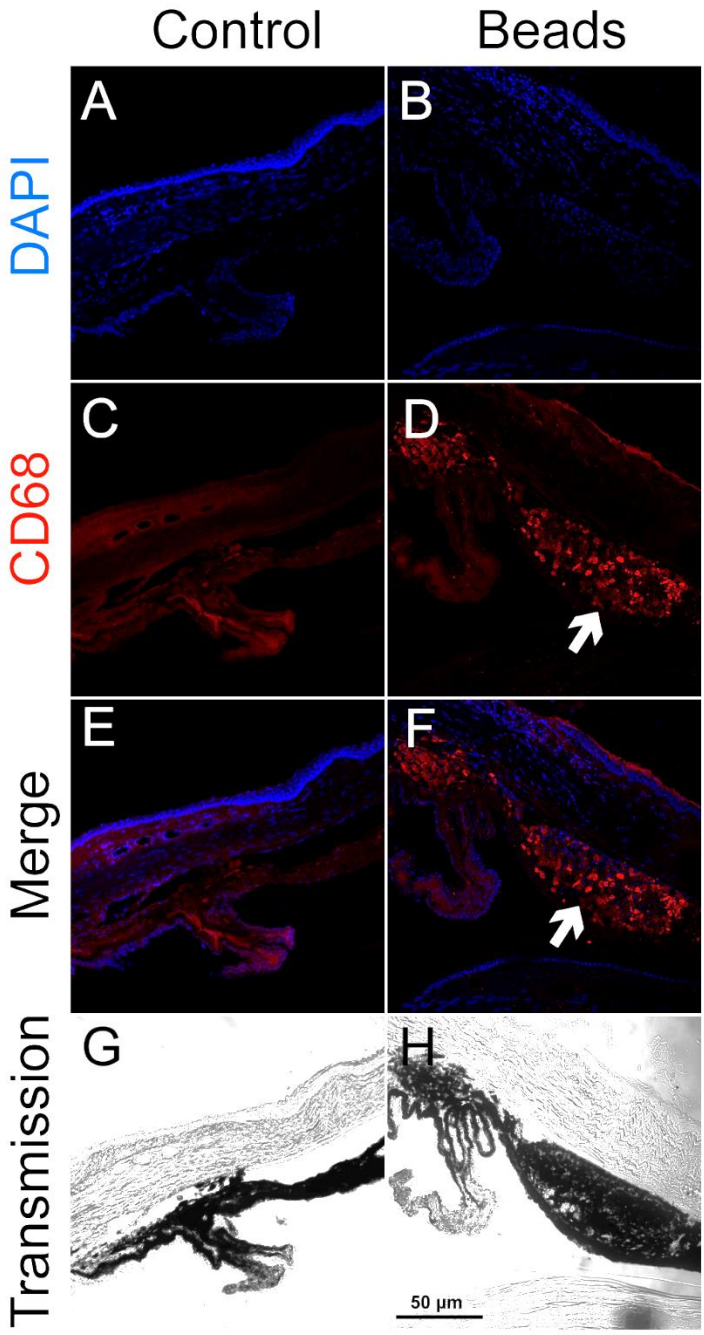

Figure 5-4 Immunohistochemical staining of anterior chamber tissue from 4 weeks after ferromagnetic bead induced intraocular pressure elevation. (A, B) DAPI staining ca be seen along the corneal epithelium, ciliary body and iris. Transmission microscopy (H) showed aggregates of beads within the angle (arrow), which co-localises with CD68 staining (F), which were not present in respective images of control animals (E, G).

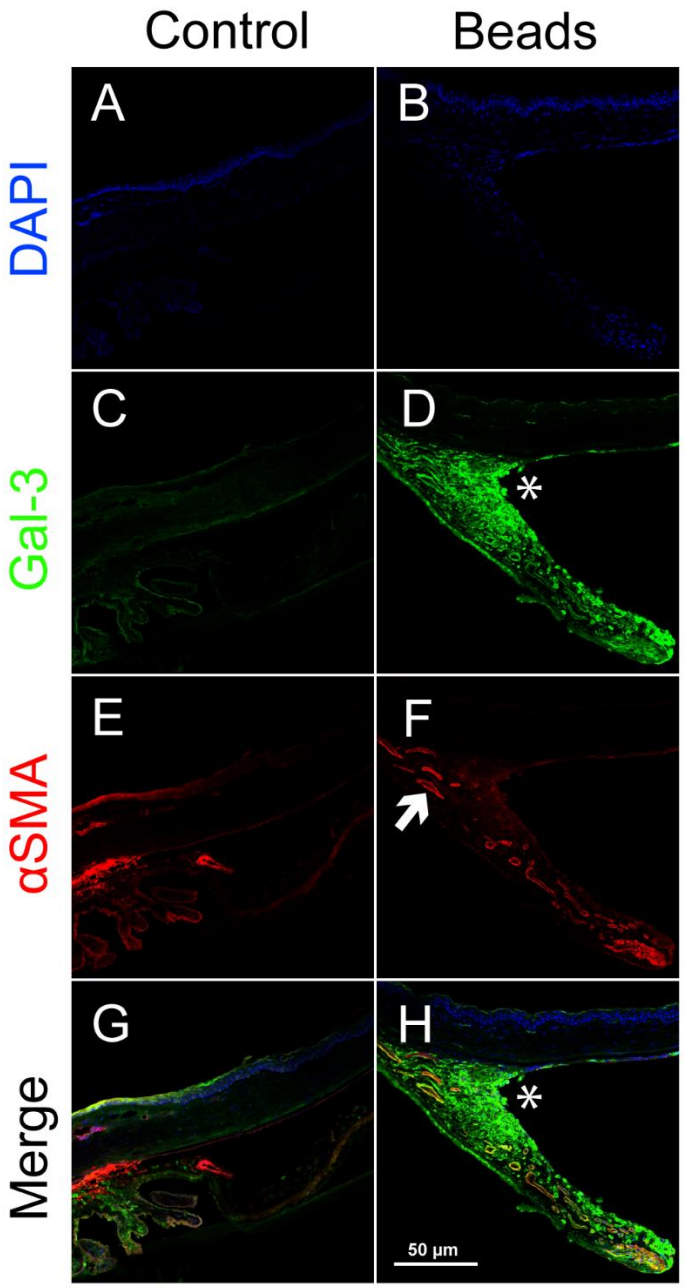

Figure 5-5 Immunohistochemical staining of anterior chamber tissue from 4 weeks after ferromagnetic bead induced intraocular pressure elevation. (A, B) DAPI staining ca be seen along the corneal epithelium, ciliary body and iris. Galectin-3 expression was significantly increased both in the iridocorneal angle (*) as well as and within iris tissue itself (D) when compared to control (C). αSMA expression was also significantly increased within iris tissue in circular structures most likely representing blood vessels (arrow, F) which were not present in control animals (E).

Aqueous fluid was obtained from control group of rodents at 5 weeks after undergoing intravitreal NMDA injection; the contralateral eyes were used as

the control group. Gal-3 protein concentration analysis as quantified by enzyme-linked immunosorbent assay (ELISA) showed increased concentration of Gal-3 as compared to control (p = 0.0027, Figure 5-6).

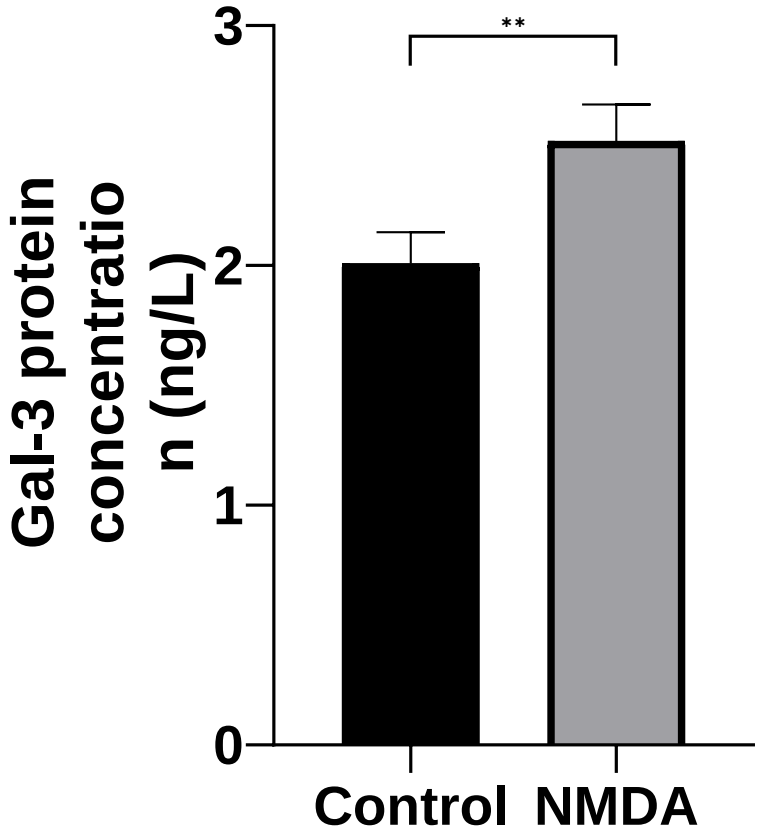

Figure 5-6 Gal-3 concentration of aqueous samples obtained from the anterior chamber of rodent eyes which underwent NMDA model was significantly increased when compared to contralateral eyes used as control at 5 weeks a measured by ELISA. N=13, ** - p<0.01.

5.2.3.2 Galectin-1 Expression within the Retina

Immunohistochemical staining of retinal sections obtained from animals at 5 weeks following the induction of NMDA and magnetic bead models was carried out (Figure 5-7). There was noticeable thinning of the overall retinal thickness in samples from the magnetic bead group (Figure 5-7, right column). Quantification of the retinal thickness measured at 500μm from the optic nerve head showed a significant reduction when comparing animals which underwent magnetic bead injection with controls (258.8 ± 20.9 vs 223.3 ± 19.76, $p = 0.013$, $n = 6$, Figure 5-9).

Vimentin staining showed typical radial distribution of MGCs. Gal-1 staining appeared to show higher intensity in the non-nuclear layers of the retina, particularly in the inner retina. There was also significant Gal-1 staining in the outermost layer of the neuro-retina composed of photoreceptor outer segments. Samples from the magnetic bead model also showed increased Gal-1 staining in the inner retinal layers when compared to the other groups (Figure 5-7, Figure 5-9).

MAL staining followed a similar distribution to Gal-1 in the inner and middle retinal layers. In contrast to Gal-1, there was little in the way of MAL staining within the layer of photoreceptor outer segments, although there was a high intensity edge at the outer boundary of this layer. In the magnetic beads group, there was increased MAL intensity in the inner retinal layers, similar to the findings seen for Gal-1.

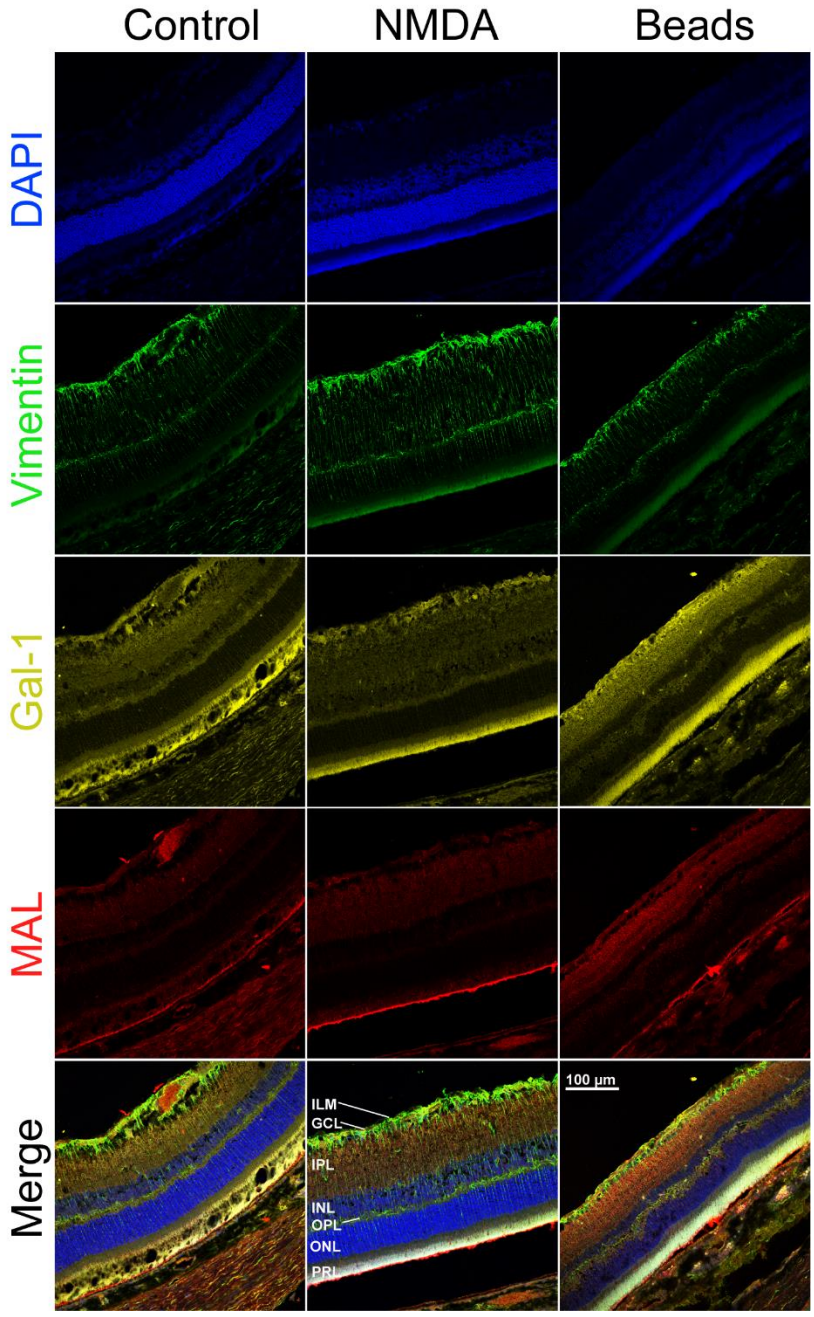

Figure 5-7 Immunohistochemical staining of retinal sections from rodents in control, NMDA and magnetic bead groups. The magnetic bead group (right column) demonstrated significant thinning of the overall retinal thickness, as well as increased Gal-1 and MAL expression in the inner retinal layers as compared to the other two groups. ILM, internal limiting membrane; GCL, ganglion cell layer; OPL/IPL, outer/inner plexiform layer; ONL/INL, outer/inner nuclear layer; PRL, photoreceptor layer.

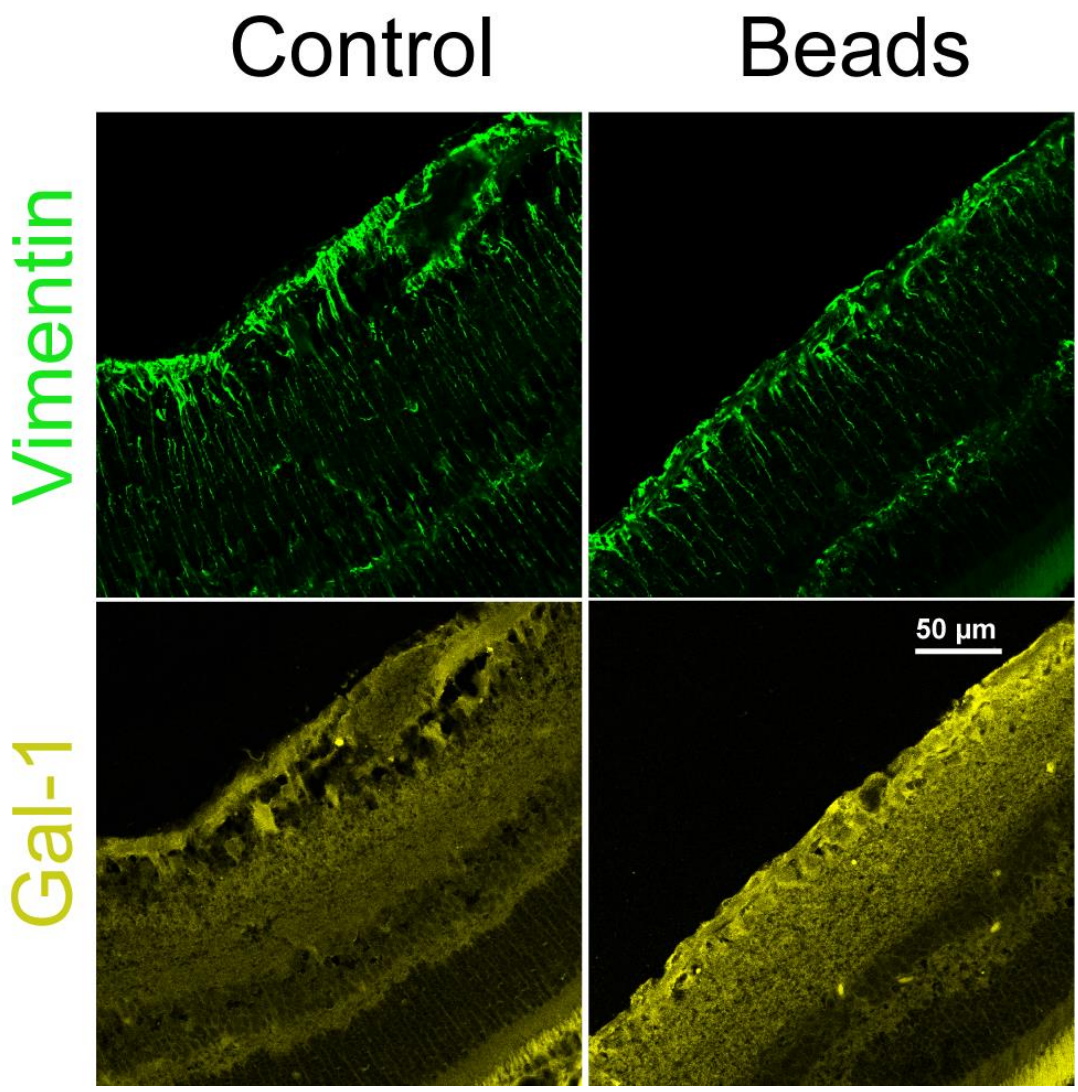

Figure 5-8 Higher magnification image showing increased Gal-1 expression within the inner retinal layers of animals which underwent anterior chamber magnetic bead injection when compared to control.

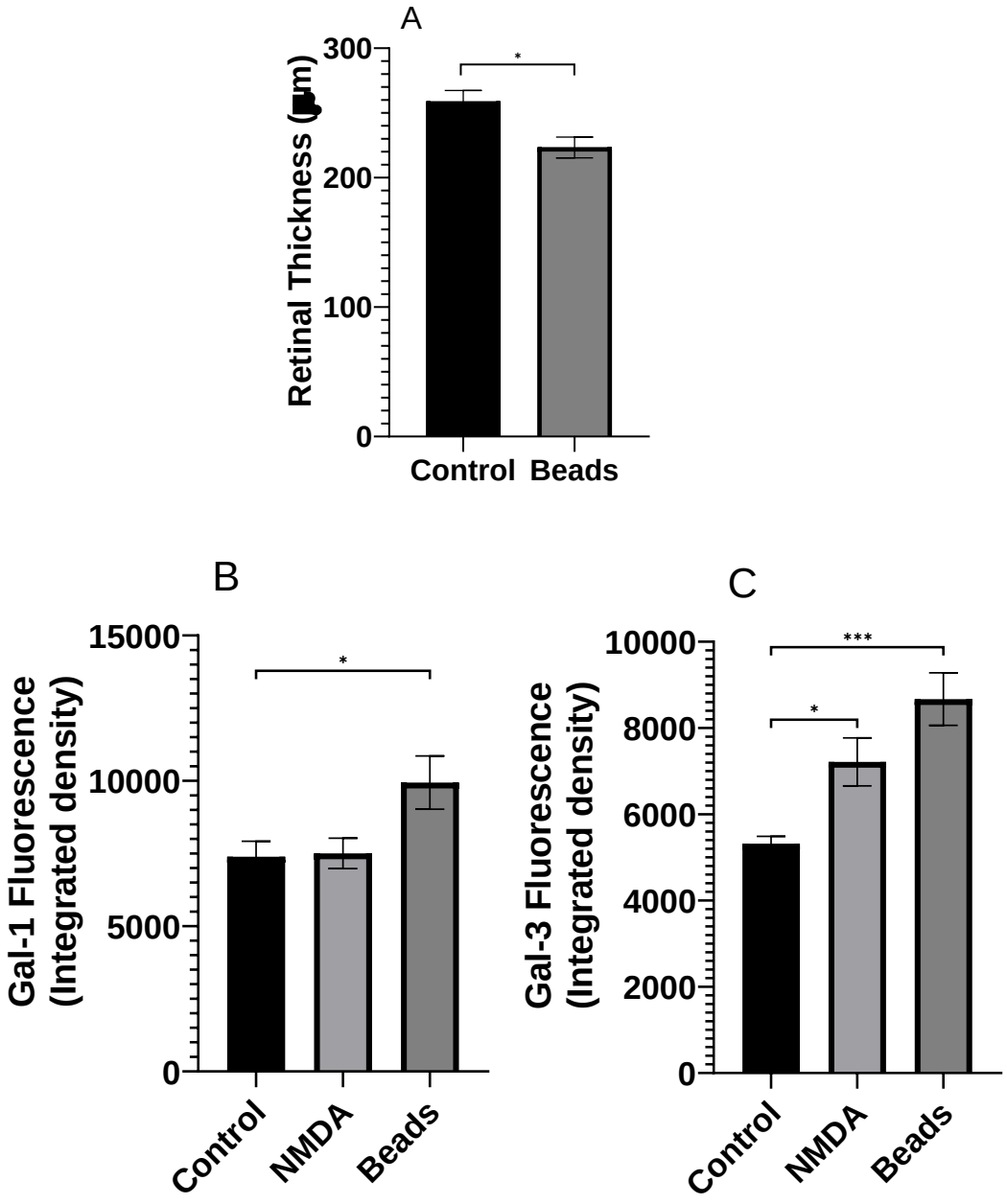

Figure 5-9 Comparison of retinal thickness and Gal-1/-3 expression between experimental animal groups. (A) Animals which underwent magnetic bead injection into the anterior chamber showed significantly decreased retinal thickness when compared to control animals (unpaired t-test, $p < 0.05$, $n = 6$). (B) Gal-1 expression in the retina of animals which underwent magnetic bead injection into the anterior chamber was significantly increased when compared to the control group (ANOVA, $p < 0.05$, $n = 6$). (C) Gal-3 expression in the retina of both groups of animals which underwent intravitreal NMDA injection (ANOVA, $p < 0.05$, $n = 6$) and magnetic bead injection into the anterior chamber (ANOVA, $p < 0.001$, $n = 6$) were significantly increased when compared to the control group.

5.2.3.3 Galectin-3 Expression within the Retina

Immunohistochemical staining for Gal-3 within the retinal sections showed increased expression of this protein in the NMDA and magnetic bead models (Figure 5-9, Figure 5-10). This increase was visible throughout the layers of the retina but was particularly apparent in the photoreceptor outer segment layer. In the retina of the magnetic beads model, there were also focal areas of increased Gal-3 expression, which coincided with areas of disruption to the layered retinal structure. These may be indicative of infiltrating cells of the immune system. Conversely, SNA staining appeared to be slightly decreased for the NMDA and magnetic bead models.

It was also noted that in retinal samples of the control group which contain cross-sections of the optic nerve (Figure 5-12), that Gal-3 expression was significantly increased within the optic nerve itself when compared to the retinal layers.

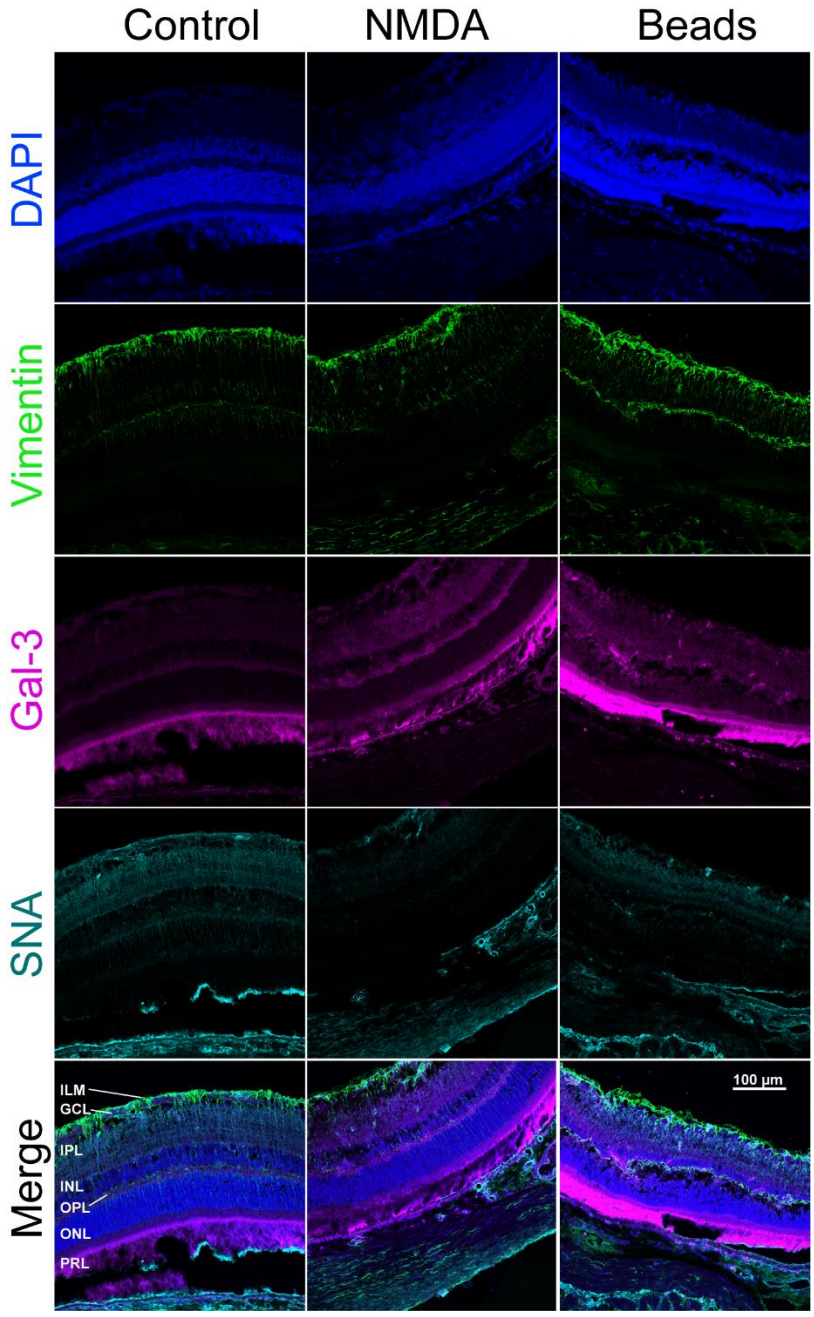

Figure 5-10 Immunohistochemical staining of retinal sections from rodents in control, NMDA and magnetic bead groups. Gal-3 expression was increased in both NMDA and magnetic bead models when compared to control. SNA expression appeared to be decreased in both models as compared to control. ILM, internal limiting membrane; GCL, ganglion cell layer; OPL/IPL, outer/inner plexiform layer; ONL/INL, outer/inner nuclear layer; PRL, photoreceptor layer.

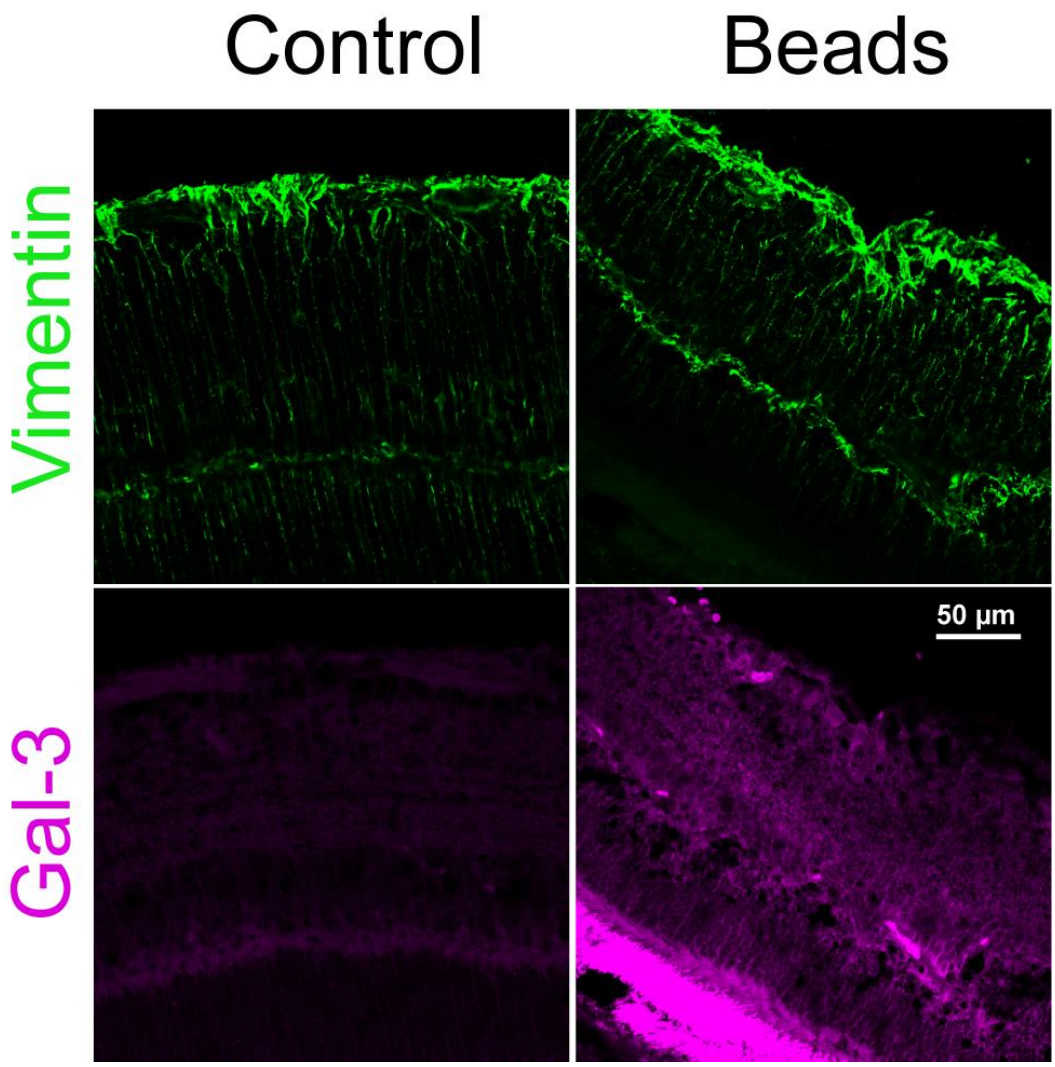

Figure 5-11 Higher magnification image showing increased Gal-3 expression throughout the retinal layers of animals which underwent anterior chamber magnetic bead injection. There also appears to be some general disruption of retinal architecture as shown by vimentin staining when compared to control.

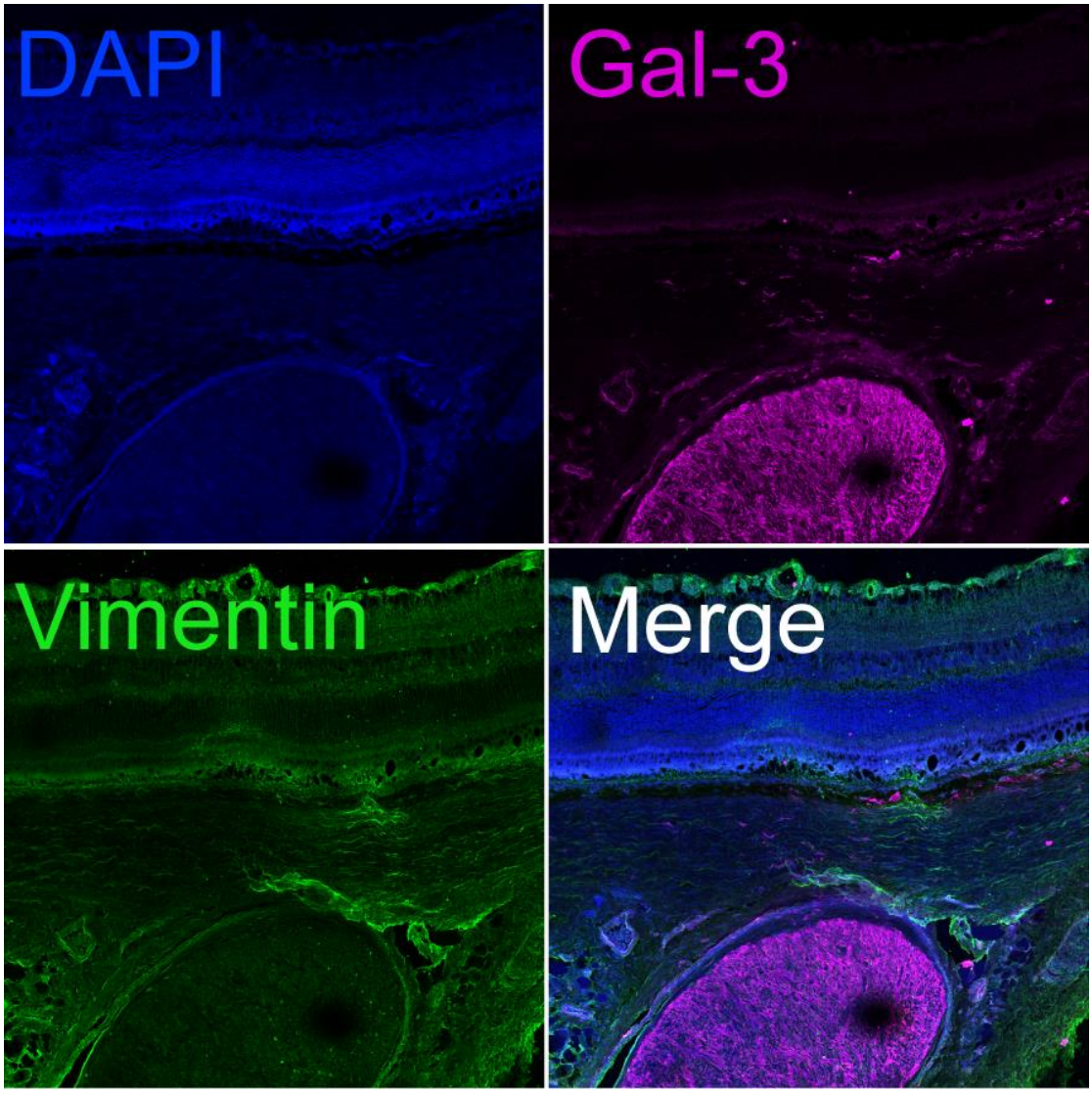

Figure 5-12 Immunohistochemical staining of a retinal section of an animal from the control group containing the optic nerve, demonstrating significantly increased expression of Gal-3 within the optic nerve.

5.3 Discussion

5.3.1 Comparison of Rodent Glaucoma Models

This study examined three candidate models of intraocular pressure elevation by injection of viscoelastic, ferromagnetic microbeads, or a combination of both. The use of viscoelastic agents is an integral part of modern ophthalmic surgery, as these substances are ideal for creating space within the eye to facilitate the manipulation of delicate tissues (Higashide and Sugiyama 2008). It has also been noted that a major side effect of the use of viscoelastic reagents is increased intraocular pressure (IOP) if left unremoved at the end of surgical procedures (Rainer et al. 2001). This observation has since led to the use of viscoelastic in animal models of IOP elevation (Biswas and Wan 2018).

Rodent models of elevated IOP by chamber injection of viscoelastic agents into the anterior chamber offers some advantages, such as the ease with which these reagents can be obtained and the simplicity of the procedure itself. However, it can have some disadvantages, such as high IOP variation, shorter duration of IOP elevation effect when compared with other models, possibly due to enzymatic degradation of viscoelastic agents, which often necessitates repeated injections to maintain elevated IOP levels. Data from the current experiments can confirm these findings, as the standard deviation of the group which underwent viscoelastic injection was the largest of the groups tested, and the overall IOP increase was lower than the other two experimental groups after day 7. This raises the possibility of administering repeated viscoelastic injections at 7-day intervals. However, given the timing of required ERG testing, and the limitation of only one procedure over a 7-day period due to animal welfare considerations, viscoelastic injection does not appear to be a viable alternative.

The use of microbeads to achieve IOP elevation has increased in popularity over the last decade, as these models can achieve controlled and sustained

IOP increase. These methods have been refined by the use of ferromagnetic beads, to allow for their directed placement into the iridocorneal angle within the anterior chamber with the use of a magnet. Using the optimal size and number of beads are key to achieving effective IOP elevation. Based on previous experiments at the host laboratory, 5µm diameter microbeads suspended in sterile saline at 10mg/ml were used. Furthermore, the Norway Brown strain of rats were used based on previous studies which demonstrated significant variations in the Lister Hooded strain (Eastlake, Jayaram, et al. 2021). The use of magnetic beads combined with a viscoelastic agent was attempted as this was thought to potentiate the elevation of IOP, by allowing the viscoelastic to stabilise the position of the beads within the anterior chamber following their injection and subsequent placement.

Overall, all three treatment groups were able to achieve elevated IOP as compared to control. However, nSTR measurements were only significantly lowered in the group which underwent ferromagnetic bead injection. This lack of correlation between induced IOP elevation and nSTR measurements may be ascribed to several possible factors.

Firstly, there may be significant variations of IOP outside of the intervals measured within this experiment, both between days and due to diurnal variation within each day. This explanation is supported by existing evidence that injection of ferromagnetic beads causes larger IOP increases when animals are kept in the dark as compared to animals kept in the light (Fu et al. 2018). It is also worth considering previous studies which suggest that peak IOP may be more predictive of glaucoma progression than mean IOP (Gardiner, Johnson, and Demirel 2012). Therefore, single daily measurements of IOP in animals undergoing models of ocular hypertension is likely insufficient, as night time IOP may be a better predictor of disease severity (Fu et al. 2018).

Secondly, the injection of beads can elicit a pro-inflammatory immune response, as observed in this study, severe macrophage reactivity was

present in the anterior chamber of animals undergoing this procedure. This response may ultimately lead to decreased retinal function through mechanisms independent of IOP elevation. Studies concerning the wide immunogenic effects of intraocular pressure elevation using these models are currently lacking and may represent a relatively overlooked weakness of these models.

Finally, significant experimental variation may have caused the discrepancy in ERG measurements. Whilst a sizable number of studies exist using similar rodent models, it has been well recognised that significant variations can be found in the outcome of studies conducted between different laboratories and indeed animal species, despite similar methodologies (Biswas and Wan 2018; Eastlake, Jayaram, et al. 2021).

A major challenge in conducting glaucoma research using animal models is the paucity of reliable outcome measurements. In humans, the most commonly used investigation to establish and monitor the diagnosis of glaucoma is visual fields testing (Weinreb and Khaw 2004), which requires a high degree of cooperation and therefore not possible to be carried out in rodents. As such, electrophysiological testing has been used in experimental rodent studies to measure the function of RGCs. In particular, the negative scotopic threshold (nSTR) component of the electroretinogram (ERG) has been widely used, whilst other components of the ERG including the positive scotopic threshold (pSTR) and pattern ERG (PERG) have also been shown to correlate with RGC function (Porciatti 2015). However, there are differing opinions with regards to the optimal approach, therefore, each investigator needs to utilize a model that is feasible and reproducible in their own laboratory, and that allows the investigation of specific scientific questions.

In the current study, nSTR was used as the measurement for RGC function in models of IOP elevation. The results were comparable to previous studies conducted in the host laboratory using the NMDA model of RGC damage and appeared to be a faithful indication of RGC function. In future studies, it may

be worth validating the pSTR and PERG as potential outcome measures, as well as Optic coherence tomography (OCT) of the optic nerve (Allen et al. 2020). The use of these outcome measures has gained popularity in recent years and may provide additional sensitivity and structural-functional correlation.

5.3.2 Potential Neuroprotective Effects of Intravitreal EV Injections

Müller cell transplantation into animal models of RGC damage have proved to induce neuroprotection (Eastlake et al. 2019), but as with any tissue transplantation, the ensuing immunological and inflammatory reactions need to be controlled with immunosuppressant drugs if they are to be translated into the clinic. On this basis, substituting whole cell transplants with either soluble cell products or extracellular vesicles, known to carry important neuroprotective agents, will facilitate the implementation of regenerative therapies in the future.

This study aimed to examine whether EVs as a derivative of MGCs would have similar neuroprotective effects on RGC function as the cells themselves. The results showed that EVs appeared to have a neuroprotective effect, as judged by improvement in the nSTR, two weeks after neurotoxic RGC damage in the rat retina. However, this effect proved to be only transient as a decline in RGC function was later observed in these animals at four weeks. This is in contrast with the improvement of RGC function observed at 4 weeks when MGC are injected into the vitreous of animals in which RGC damage had been induced with NMDA. These effects could be ascribed to EVs having a relatively short half-life following injection, as they are endocytosed by cells relatively rapidly. Although the number of EVs ($3x\ 10^4$) used in the current study was estimated to be the number released by 1×10^5 MGCs previously shown to induce neuroprotection, it might be possible that not all EVs contain the same neuroprotective molecules, and that a larger number of EVs may be needed to obtain prolonged effect.

Nevertheless, these results suggest that the effect of EVs reflects a proportion of the beneficial effect observed when whole MGCs are injected into the vitreous of these animals. This is in support of existing data using mesenchymal stem cell (MSC) derived EVs, which have been the most extensively tested cell source for EVs for application in glaucoma models (Mead, Amaral, and Tomarev 2018). In these studies, the authors ascribed much of the beneficial effects to miRNA contained within the MSC derived EVs, although further studies to confirm this hypothesis is awaited. Understanding of the precise roles played by EVs and miRNAs remains a relatively new field, as each miRNA may cause a host of cascading effects in the target cell, whilst a collection of EVs would contain a host of different miRNAs. RNA-Seq techniques to evaluate the contents of EVs would provide some useful insight in this regard and are currently under way at several institutions including the host laboratory (Qian et al. 2016).

The finding that EVs potentially have neuroprotective effects is encouraging, both in terms of demonstrating a potential mechanism of action for MGC-mediated neuroprotection, but also puts forward the possibility of EV injections as a potential therapeutic option in its own right. The use of purified EVs has its advantages and disadvantages as compared to whole cell therapies. One major advantage is that EVs are far less immunogenic, as demonstrated by the fact that the only form of anti-inflammatory therapy used in the present study was intravitreal triamcinolone, whereas whole cell studies conducted previously required post-natal tolerization of the animals, as well as relatively high doses of oral immunosuppressants following treatment.

Further studies are needed to improve the effect of EVs, both in terms of understanding the miRNA and protein content of these organelles, as well as investigating whether repeated injections may be required to achieve the same effect as whole cells, perhaps similar to the treatment regimen currently being used for various anti-VEGF agents in neovascular retinal diseases (Ferrara and Adamis 2016). The short acting nature of potential EV therapy,

however, may make it ideal for acute injuries which threaten RGCs, such as ischaemic optic neuropathies and acute angle closure attacks.

5.3.3 Galectin Expression in the Anterior Segment and the Retina Experimental Rodent Models

Previous studies of the role of Galectins in glaucoma have shown that Gal-3 is significantly upregulated in the anterior segment of human specimens (Section 1.2.5.2). This is consistent with fibrotic diseases of other organs, especially the lungs and kidneys where proprietary Gal-3 inhibitors are currently being investigated in early clinical trials (Hirani et al. 2020).

This study showed that at 4 weeks after injection of ferromagnetic microbeads into the anterior chamber, intense immunostaining for Gal-3 was observed within the aggregates of beads localised in the iridocorneal angle, as well as within iris body. The aggregates of microbeads were also associated with increases in CD68, which is a surface glycoprotein expressed by macrophages and circulating monocytes (Chistiakov et al. 2017). This indicates that the injection of microbeads induced a significant inflammatory reaction, where macrophages were most likely recruited via the blood stream. Blood vessel proliferation and dilatation can also be observed during this period, a finding which was supported by significantly increased immunohistochemical staining of αSMA in animals that underwent microbeads injections. This finding suggests that significant proliferation of iris blood vessels may have occurred, as αSMA is highly expressed in capillary pericytes (Alarcon-Martinez et al. 2018).

Since Gal-3 can be found at high concentrations within macrophages, this protein was initially named Mac-2 (Lakshminarayan et al. 2014). As such, it is unsurprising that Gal-3 was upregulated along with markers for macrophages in this model. However, it is unclear whether the upregulation of Gal-3 seen in this experiment purely originated from the recruited macrophages or whether resident cells found within the anterior chamber angle also contributed to this.

Although it is not possible to compare tissues and fluids from different experimental models, it was interesting that Gal3 was upregulated in the anterior chamber of animals injected with magnetic beads, and that increase in the levels of this molecule was also observed in the anterior chamber fluid of animals injected with NMDA as compared to controls. As the NMDA model did not involve the introduction of any experimental reagents into the anterior chamber, this increase in Gal-3 concentration most likely arose from a different mechanism, which would be interesting to elucidate.

Examination of tissue sections from the rodent models used in this study showed that animals in which IOP elevation was induced by microbead injections exhibited significant thinning of the retina when compared to the controls. They also exhibited increased expression of Gal-1 and MAL in the inner retinal layers. In terms of the distribution of Gal-1 expression increase along the inner retinal layers, this may be due to the damage of RGCs and their associated neurons within these layers. As outlined previously, Gal-1 appears to be upregulated during periods of inflammation, often in synchronisation with increased *α-2,3-sialyltransferase* expression associated with MAL binding (Section 3.2.6). A major mediator of this process is likely to be TNF-α, as there is extensive existing evidence for the upregulation of TNF-α during the pathogenesis of glaucoma (Tezel 2008). Interestingly, increase in Gal-1 expression or MAL binding were not observed in the NMDA group.

Increased expression of Gal-3 was observed in retinal sections of both NMDA and microbead injection models, in keeping with findings from the anterior chamber. At the same time, SNA binding appeared to be slightly reduced for both models as well, which suggests decreased *α-2,6-sialyltransferase* expression. These observations have not been noted previously in existing literature. Based on the known functions of Gal-3, possible explanations for their function in these models include binding of exposed glycoproteins during apoptosis and the stabilisation of receptor complexes to potentiate signalling pathways (Section 1.2.4). However, a significant contribution of the increased

Gal-3 expression may be due to infiltrating pro-inflammatory immune cells. As such, it would therefore be important to elucidate the exact mechanisms of action of Gal-1/-3 and sialylation proteins in the context of these models of optic neuropathy and intraocular pressure elevation, which merits further investigations.

5.3.4 Summary

The experiments shown in this chapter validated NMDA excitotoxicity and anterior chamber magnetic bead injection as reproducible models for assessing RGC function in optic neuropathy and IOP elevation, respectively. It was concluded that viscoelastic injection into the anterior chamber was not a suitable model to achieve reproducible IOP elevation, given its variability and its requirement for frequent re-injections.

In vivo experiments also demonstrated that MGC derived EVs appeared to exert potentially neuroprotective effects following RGC injury, albeit limited in duration as compared to whole-cell therapy. Furthermore, significant changes in Gal-1 and -3 were found in tissues from the anterior chamber and the retina of the two animal models examined. In particular, the consistent changes in tissue *α-2,3- and α-2,6-sialylation* deserve further investigations.

6. GENERAL DISCUSSION

6.1 Galectin-1 Functions within the Retina

Previous proteomic studies conducted in the host laboratory observed Galectin-1 to be highly upregulated in both degenerated zebrafish retina and human retinectomy samples (Eastlake et al. 2018; Eastlake et al. 2017). These observations, along with existing literature showing that Gal-1 has immunosuppressive, pro-proliferative and pro-angiogenic properties, formed the starting point of the current project. Although the role of Gal-1 within the retina most likely extend beyond these facets.

Using the ferromagnetic bead model of glaucoma, this study showed Gal-1 to be upregulated in the inner layers of the neuroretina (Section 5.2.3.2). Since these layers harbour high concentrations of neurons, including RGCs, amacrine cells and bipolar cells (Section 1.1.1), increased Gal-1 expression was likely to have been driven by the response of these neurons to injury, potentially via cytokines such as TNF-α, which is well known to increase in the acute phase of neuronal damage (Mac Nair et al. 2014). This hypothesis was supported by the finding that TNF-α induced Gal-1 production by MGCs *in vitro* (Section 3.2.6). Furthermore, the induction of inflammation within the anterior chamber in this model was demonstrated by immunohistochemistry, as evident by the presence of CD68+ cells (Section 5.2.3.1). Taken together, these observations suggest that the inflammatory effects observed in the retina may have been induced by pro-inflammatory cytokines such as IL-1 travelling from the anterior chamber through the vitreous to induce MGC derived Gal-1 production in the retina.

In contrast to the responses observed in the anterior chamber upon magnetic bead injection, injection of NMDA into the vitreous to elicit RGC damage did not demonstrate any visible increase in Gal-1 expression in the retina, as judged by immunohistochemical staining (Section 5.2.3.2). A likely reason for this may be experimental timing. As mentioned previously, there is extensive

evidence that neuronal injury leads to an immediate increase in TNF-α expression (Woodcock and Morganti-Kossmann 2013). Since this study analysed retinal sections following 5 weeks after the intravitreal injection of NMDA neurotoxin, any significant changes of Gal-1 expression in the acute phase may have subsided by this time point. The rationale behind the timing of the NMDA model experiments was to mirror similar experiments in the past for testing the efficacy of whole cell therapies. As maximising the statistical power of ERG measurements at 4 weeks was the main goal in experimental design (Section 5.2.2.1), animals were not sacrificed at earlier time points.

Following the theme of the relationship between TNF-α and Gal-1, *in vitro* experiments showed that both molecules appeared to participate in the STAT3 signalling pathway (Section 3.3.4). This is in keeping with existing hypotheses of Gal-1 function, as activation of STAT3 has been associated with pro-proliferative states and an early marker of cancer progression (Gu, Mohammad, and Liu 2020), which may be mediated through its binding to integrin-β1 (Nam et al. 2017). In the current study, Gal-1 inhibition reduced STAT3 activation within MGCs in both control samples and following TNF-α activation (Section 3.3.4). Given the additional result that TNF-α can directly upregulate Gal-1 expression in MGCs (Section 3.2.6), it is possible that Gal-1 may play an important role in the potentiation of STAT3 activation in MGC during reactive gliosis.

Within retinal organoids, Gal-1 was found to be most highly expressed between days 10 and 30 during development (Section 4.2.2). Whilst existing literature and the current findings do not directly elucidate the molecular mechanisms of Gal-1 during this period of retinal organoid development, the observed peak of Gal-1 expression may be a reflection of its involvement in pathways relating to cellular differentiation and proliferation. It was also noteworthy that the upregulation of Gal-1 in response to IL-1 within retinal organoids was comparable to the findings of MGCs in culture (Section 4.2.4). This finding further supports existing evidence that MGCs are the major

producer of Gal-1 within the retina, and act as a central regulator of pathways involving this molecule.

In summary, the current observations suggest that expression of Gal-1 within the retina is actively regulated by MGCs. Gal-1 expression was found to be upregulated during early organogenesis of the retina as well as in models of injury, both *in vitro* and in rodent animal models. In addition, it is possible that the effects of Gal-1 may be partially mediated through the STAT pathway.

6.2 Galectin-3 Functions within the Retina and Anterior Chamber

In contrast to Gal-1, Gal-3 has generally been associated with inflammation and fibrosis, and results from the current study support these hypotheses. Gal-3 demonstrated the ability to increase TGF-β induced migration and contraction of MGCs *in vitro*, which suggests that Gal-3 may be a potentiator of these processes. The other major finding was that TGF-β itself downregulates Gal-3 production within MGCs (Section 3.2.6). Taken together, these findings could explain the relatively high concentration of intraocular TGF-β during normal function without inducing migration and contraction of MGCs. Given that certain cells of the immune system, such as macrophages, produce high concentrations of Gal-3, it may be possible that Gal-3 acts as a modulator of certain TGF-β signalling processes within the retina.

In the rodent magnetic bead model, Gal-3 protein was found to be expressed at a high concentration within the anterior chamber. Localisation of Gal-3 protein expression coincided with the infiltration of inflammatory cells of monocyte lineage in the angle of the anterior chambers, which formed aggregates around the injected beads (Section 5.2.3.1). This clearly demonstrated an association between the recruitment of active immune cells and increases in Gal-3 protein expression. It is likely Gal-3 produced in the anterior chamber may be transported towards the posterior segment of the eye through the vitreous cavity to reach the retina. Should the previous

hypothesis of Gal-3 being a gatekeeper of TGF-β mediated inflammation be correct, it may be possible that the observed changes within the anterior chamber could be partially responsible for the degenerative changes seen within the retina of these animals.

The pro-fibrotic properties of Gal-3 also has important implications in a number of retinal diseases. Existing evidence have shown Gal-3 to be upregulated in conditions including diabetic retinopathy (Li et al. 2022) and proliferative vitreoretinopathy (Priglinger et al. 2013), whilst the lack of Gal-3 has proved to inhibit the inflammatory and degenerative sequelae of diabetic retinopathy in an animal model (Mendonca et al. 2018). Whilst much of the potential detrimental effects of Gal-3 have been attributed to the release of this protein by infiltrating cells of the immune system, it is also worth noting the current study has demonstrated MGCs to be potent producers of Gal-3 *in vitro*, it is therefore possible that under normal physiological conditions, the production of Gal-3 by MGCs is supressed by TGF-β, and that this balance may be disturbed in diseased states.

Previous studies identified Gal-3 to be present during organogenesis of the pig retina (Kim et al. 2009), supporting the current observations that Gal-3 expression gradually increased towards day 90 of retinal organoid development *in vitro*. The role of Gal-3 within retinal organoids remains unclear, but its expression may reflect the importance of this factor in retinal development processes. This is substantiated by the close relationship between Gal-3 with TGF-β, a cytokine known to play a central part during retina development and appeared to potently counter-regulate Gal-3 both in MGCs *in vitro* and within retinal organoids in the current study.

6.3 Galectins -1 and -3 and Tissue Sialylation

The ability to bind specific carbohydrates is the defining characteristic of lectins. This is reflected in the structure of Galectin monomers, as the molecules are centred around a specialised carbohydrate binding region, the

centremost of which is specific to galactose. Therefore, there is a general assumption that most of the effects exerted by Galectins are a result of the binding of specific carbohydrate sequences. In particular, there appears to be a particular affinity for members of the Galectin family towards polylactosamine (polyLacNAc), where particular sialylation patterns appeared to influence the binding of specific Galectins (Section 1.2.1).

In the current study, the possibility of these carbohydrate-Galectin interactions was investigated by qPCR and immunohistochemical methods. These were indirect methods of ascertaining the sialylation state of MGCs and retinal tissues, as qPCR allowed measurement of the sialylation enzymes whilst plant lectins, Maackia amurensis lectin-II (MAL) and Sambucus nigra agglutinin (SNA), were used to indicate the degree of α2-3 and α2-6 sialylation respectively.

In general, mRNA gene expression results matched pre-existing hypotheses of the affinity between Gal-1 and α2-3 sialylation (Section 3.2.6 and 4.2.2), as well as the inverse relationship between Gal-3 and α2-6 sialylation (Section 4.2.2). In contrast, whilst immuno-staining with MAL and SNA lectins revealed some interesting co-localisation patterns with Gal-1 and -3 within retinal organoids and animal tissues (Sections 4.2.4 and 5.2.3), the overall appearances of these images did not reveal any striking relationship with gene expression (Sections 4.2.3).

The potential interactions between Galectins and protein glycosylation form a part of a larger concept known as “the Sugar Code” (Section 1.2.1), which postulates that the glycans expressed by cells contain important information and lead to specific biochemical changes upon the binding of corresponding carbohydrate binding molecules such as Galectins. Whilst this is an interesting theory to explore, advances in this field have been constrained by technological limitations, mainly due to the difficulty of carbohydrate “sequencing”.

There are two major challenges in glycomics when compared to the well-established and reliable genomic methods; firstly, there are many carbohydrate monomers when compared to the four nucleotides which form nucleic acids, secondly, carbohydrates monomers can bind in several positions, which can result in highly branched structures. Consequently, traditional approaches of carbohydrate sequencing have consisted of relatively laborious methods such as nuclear magnetic resonance imaging. In more recent years, high throughput methods are being developed and refined (de Haan et al. 2022), and these exciting advances look to propel the field of glycobiology forwards and will provide valuable insight in our understanding of these ubiquitous molecules.

6.4 Potential Clinical Applications of Galectin -1 and -3

Overall, studies into the functions of Galectins within the retina remain at relatively early stages. As such, significant investigations are required before we understand whether clinical studies can be realistically pursued. However, several potential applications have emerged from data presented, and it is conceivable to envisage the following areas becoming promising avenues of research.

6.4.1 Galectin-1 and -3 as Biomarkers of Disease

Whilst the molecular mechanisms of Gal-1 and -3 remain to be elucidated, there is already sufficient evidence that Gal-1 and -3 levels closely correlate to the severity of certain diseases. Furthermore, these associations were found to not just be limited to local concentrations of these proteins, but serum concentrations as well (Section 1.2.4). On this basis, the most immediately translatable use of Gal-1 and -3 in the clinical setting would be to use the measurable concentration of these proteins within accessible fluid compartments such as the tears, aqueous or blood as predictive biomarkers of diseases such as diabetic retinopathy and glaucoma.

6.4.2 Regulation of Cellular Proliferation and Regeneration by Galectins -1 and -3

As shown in this study, Gal-1 and -3 appear to modify cellular proliferation and gliosis-associated intracellular pathways. Therefore, it may be possible that regulation of these proteins may constitute effective therapeutic strategies for ocular diseases. Approaches to achieve this regulation could involve the use of recombinant Gal-1/-3 or their inhibitors, as well as of genetic methods of promoting or inhibiting their production. In the event that these molecules may be used to induce endogenous regeneration, strategies which may ultimately be successful will likely include a range of factors which interact with these molecules. From the data provided in the current study, in addition to existing evidence, it could be suggested that Galectins may well play a key part in the development of such therapies.

6.4.3 Galectin-3 Inhibitors as Potential Anti-fibrotic Agents

Scarring and fibrosis are important processes common to a range of conditions, including trauma, inflammation, and surgical intervention. Gal-3 has been demonstrated to be an important factor in fibrotic processes in organs such as the lungs, heart and kidneys (Section 1.2.4). Data presented in the current study suggest that Gal-3 may play a similar role in fibrotic diseases of the retina. Further investigations using different ocular cell types such as keratocytes and conjunctival fibroblasts may reveal additional areas of application such as in corneal scarring or glaucoma surgery.

6.5 Models of Glaucoma and Optic Neuropathy

Representative and reliable experimental models are central to the investigation of diseases. In the context of glaucoma, establishing such a model is particularly challenging, due to both the breadth of diseases which can ultimately result in glaucomatous optic neuropathy, as well as the

complexity of the pathogenic process within each individual disease subtype (Section 1.3).

In the current study, various methods of raising intraocular pressure were compared, which revealed injection of anterior chamber ferrous magnetic beads to be the most reliable in inducing optic nerve damage as measured by ERG. However, there remained a significant degree of variability in this method, which was reflected in an increased number of animals needed to achieve the required statistical power as compared to NMDA injections. The source of this variability is likely due to several factors, since the procedure of anterior chamber injections is somewhat operator dependent, and it is difficult to ensure equal distribution of magnetic beads throughout the anterior chamber angle. On the other hand, NMDA injections is a proven method used in numerous existing studies and is reliable from the point of view of statistical variation. However, NMDA injections cause neuronal excitotoxicity, which recapitulates optic nerve degeneration, but not other parts of glaucoma pathogenesis. Therefore, NMDA injection is model of optic neuropathy and not specific to glaucoma. This distinction was highlighted in the current study, as no significant changes in the anterior chamber was detected for the NMDA injection group, whereas the magnetic beads group demonstrated significant inflammatory activity as well as evidence of new vessel formation within the iris.

The presence of significant anterior chamber inflammation casts further doubts on the validity of magnetic bead injections as a model of glaucoma (Section 5.2.3.1). There is increasing evidence of an important role for neuroinflammation in glaucoma, a disease which was traditionally viewed as a degenerative condition (Wei et al. 2019). Additionally, emerging evidence have brought to attention the involvement of inflammatory components in other degenerative conditions such as Alzheimer's disease (Heneka et al. 2015) and age-related macular degeneration (Kauppinen et al. 2016). However, the type of inflammation seen in these conditions tend to be chronic,

indolent processes, in contrast to the acute, macrophage driven inflammation seen in the magnetic bead model within the current study. Furthermore, the process of obstructing the anterior chamber angle is incompatible with the majority of subtypes of human glaucoma, which tend to exhibit open angles.

These reservations regarding existing models of glaucoma and optic neuropathy are shared by many within the field of glaucoma research. As such, there is an urgent need for reliable glaucoma models which accurately recapitulates the disease in order to conduct research which more closely resemble human pathogenic processes.

6.6 Retinal Organoids as Models of Retinal Development and Disease

In addition to the need of better animal models, there is also a notable disagreement between *in vivo* and *in vitro* approaches to disease models. Cells *in vitro* can often respond differently to stimuli as compared to being within their natural microenvironment. Furthermore, it is often difficult to reconcile *in vitro* experiments to reach conclusions that are generalisable to complex tissues and organs as a whole. Retinal organoids represent a promising tool to modelling retinal development as well as a variety of ocular diseases such as AMD and glaucoma (O'Hara-Wright and Gonzalez-Cordero 2020), and appear to be well placed to bridge the gap between *in vitro* and animal experimentation.

Data from the current study successfully replicated established methods of retinal organoid differentiation. Further refinement of this retinal based model could provide valuable insight into key disease processes responsible for degenerative retinal diseases such as gliosis (Fligor et al. 2018). In the context of glaucoma, use of retinal organoids currently remains somewhat limited, due to challenges in replicating the complex pathogenic processes of this disease as mentioned previously. In particular, there are no currently existing protocols for retinal organoids to develop anterior chambers or a

formed optic nerve. Consequently, investigations in the current study were limited to within the retinal layers. Nevertheless, further adaptation and refinement of retinal organoid development could provide valuable insight into the behaviour of cells such as MGCs or RGCs in their neuroretinal microenvironment. A clear advantage of the use of retinal organoids is the ability to produce large quantities of retina-like tissue and perform investigations which would otherwise be difficult to undertake in animal models or human tissue.

6.7 Cell-based Therapies for Retinal Diseases

The current landscape of cell-based therapies for retinal diseases has been previously reviewed (Section 1.3.4). Therefore, the current study aimed to further explore additional approaches that could potentially be used for implementing new regenerative and neuro-protective approaches.

Observations from the current study support existing evidence that Galectins are involved in the regenerative capacity of the zebrafish retina. Gal-1 and -3 were both expressed during the development of retinal organoids and were shown to interact with cytokines and intracellular pathways that are associated with regenerative processes. Although further studies are needed, it is possible that the successful induction of retinal regeneration may involve therapeutic modification of the expression of these molecules in key cells involved in retinal regeneration.

An additional aim of this study was to advance our current knowledge of the role of MGC derived EVs. Using the rodent NMDA model, injection of MGC derived EVs were found to partially aid in the restoration of RGC function at two weeks following induction of RGC damage. However, this effect appeared to be transitory and was not maintained at four weeks. The difference in effect duration between the current study using EVs and previous comparable studies using whole MGCs may be due to the shorter half-life of EVs. Whilst the exact mechanism of these neuroprotective effects remains under

investigation, these initial experiments suggest that EVs may be a feasible therapeutic vehicle.

6.8 Summary and Future Directions

A summary of the salient findings from the current study is shown in . Whilst these results have added to our existing understanding of Gal-1 and -3 functions within the eye, they have also raised more questions.

The present observations have provided evidence that Gal-1 and -3 modify important cell proliferation and migratory functions in MGCs *in vitro* and therefore they may influence the behaviour and functionality of these cells within the retina. It would be worthwhile exploring these effects further, both by *in vitro* using retinal organoids and *in vivo* using experimental disease models. This would lead to a better understanding of the functional roles of these molecules during health and disease.

Given that in MIO-M1 monoculture, cytokines appear to be potent regulators of Gal-1/3 production, it would be interesting to extend these findings to more complex models, such as retinal organoids, and observe whether similar changes in cytokine-Galectin-sialylation also occur in tandem, and whether the addition of cytokines results in Galectin regulation within the retina as a whole. More permanent methods of over- and under-expression of Galectins may also need to be established, such as the use of clustered regularly interspaced short palindromic repeats (CRSPR) techniques, as the siRNA transfection techniques employed in the current study would most likely be unable to achieve adequate penetration and longevity in retinal organoids.

Staining using MAL and SNA lectins did not reveal any noticeable patterns during retinal organoid development, nor following incubation with cytokines. More specialised techniques for the quantification and visualisation of protein glycosylation may be useful in further investigating this apparent discrepancy between mRNA expression data and images from lectins-based staining.

Summary of Results

Galectin-1		
Context	Finding	Section
MIO-M1 cells	Upregulated by TNF-α and IL-1	3.2.6
MIO-M1 cells	Promotes TNF-α mediated STAT3 phosphorylation	3.2.7
CD29+/CD44+ cells within Retinal organoids	Highly expressed during first 30 days of development	4.2.2
CD29+/CD44+ cells within Retinal organoids	Upregulated by IL-1	4.2.4
Magnetic bead rodent glaucoma model	Increased expression in the inner retinal layers	5.1.3
Galectin-3		
Context	Finding	
MIO-M1 cells	Promotes proliferation	3.2.3
MIO-M1 cells	Inhibits TGF-β mediated migration	3.2.4
MIO-M1 cells	Inhibits TGF-β mediated contraction	3.2.5
MIO-M1 cells	Downregulated by TNF-α and TGF-β1/2	3.2.6
MIO-M1 cells	Promotes TGF-β mediated SMAD phosphorylation	3.2.7
MIO-M1 cells	Promotes TGF-β mediated β-catenin activation	3.2.7
CD29+/CD44+ cells within Retinal organoids	Slowly increases in expression between days 30 and 90	4.2.2
CD29+/CD44+ cells within Retinal organoids	Downregulated by TNF-α and TGF-β	4.2.4
CD29+/CD44+ cells within Retinal organoids	Inversely correlates with TGF-β mRNA expression	4.3.5
Magnetic bead rodent glaucoma model	Increased expression in the anterior chamber and retina	5.1.3

Table 6-1 Summary of results from the current study and the corresponding section

In terms of retinal organoids research, future investigations could include an exploration of the effect of cytokines and Gal-1/-3 on retinal development. This would require a more detailed characterization of the cell types present in the retinal organoids at each stage of development, in order to determine whether alteration of these protein significantly impact retinal formation and maturation. Single cell RNASeq may represent a potential solution to ascertain this information.

This study was successful in making use of a rodent glaucoma model to investigate the neuroprotective properties of EVs. However, there are some caveats to these findings and the results bring about further questions which are not easily addressable by methods outlined in this chapter.

From a purely statistical perspective, the ideal scenario would be to compare the effect of EVs with the MGCs from which they derived, in identical experimental conditions. This could be carried out using a number of different animal models to differentiate the efficacy of these treatment options in various settings, and the sample sizes should be sufficiently large to detect small changes. Of course, this is not possible due to resource limitations and ethical considerations. As such, it would be preferable to explore the unknown aspects of the results, such as differences in duration of effect between EVs and whole MGCs, using a method such as retinal organoids that is of lower cost, allows higher throughput and avoids or drastically reduces the use of animals. Of course, further development of RO based retinal disease models would be required for this approach to be successful.

Finally, given that Gal-3 has consistently been observed to aggregate around damaged cellular membranes both intra- and extra-cellularly, it would be interesting to investigate whether the presence of Gal-3 could influence EV production, or the effectiveness of EV therapy.

7. REFERENCES

Abreu, C. A., S. V. De Lima, H. R. Mendonca, C. O. Goulart, and A. M. Martinez. 2017. 'Absence of galectin-3 promotes neuroprotection in retinal ganglion cells after optic nerve injury', *Histol Histopathol*, 32: 253-62.

Abu El-Asrar, A. M., A. Ahmad, E. Allegaert, M. M. Siddiquei, K. Alam, P. W. Gikandi, G. De Hertogh, and G. Opdenakker. 2020. 'Galectin-1 studies in proliferative diabetic retinopathy', *Acta Ophthalmol*, 98: e1-e12.

Abu El-Asrar, A. M., L. Missotten, and K. Geboes. 2011. 'Expression of myofibroblast activation molecules in proliferative vitreoretinopathy epiretinal membranes', *Acta Ophthalmol*, 89: e115-21.

'The Advanced Glaucoma Intervention Study (AGIS): 7. The relationship between control of intraocular pressure and visual field deterioration.The AGIS Investigators'. 2000. *Am J Ophthalmol*, 130: 429-40.

Ahmad, N., H. J. Gabius, S. Andre, H. Kaltner, S. Sabesan, R. Roy, B. Liu, F. Macaluso, and C. F. Brewer. 2004. 'Galectin-3 precipitates as a pentamer with synthetic multivalent carbohydrates and forms heterogeneous cross-linked complexes', *J Biol Chem*, 279: 10841-7.

Ahuja, S. 2017. 'Possible role of sialylation of retinal protein glycans in the regulation of electroretinogram response in mice', *Int J Ophthalmol*, 10: 1217-22.

Aires, I. D., A. F. Ambrosio, and A. R. Santiago. 2017. 'Modeling Human Glaucoma: Lessons from the in vitro Models', *Ophthalmic Res*, 57: 77-86.

Alarcon-Martinez, L., S. Yilmaz-Ozcan, M. Yemisci, J. Schallek, K. Kilic, A. Can, A. Di Polo, and T. Dalkara. 2018. 'Capillary pericytes express alpha-smooth muscle actin, which requires prevention of filamentous-actin depolymerization for detection', *Elife*, 7.

Alge-Priglinger, C. S., S. Andre, H. Schoeffl, A. Kampik, R. W. Strauss, M. Kernt, H. J. Gabius, and S. G. Priglinger. 2011. 'Negative regulation of RPE cell attachment by carbohydrate-dependent cell surface binding of galectin-3 and inhibition of the ERK-MAPK pathway', *Biochimie*, 93: 477-88.

Alge, C. S., S. G. Priglinger, D. Kook, H. Schmid, C. Haritoglou, U. Welge-Lussen, and A. Kampik. 2006. 'Galectin-1 influences migration of retinal pigment epithelial cells', *Invest Ophthalmol Vis Sci*, 47: 415-26.

Allen, R. S., K. Bales, A. Feola, and M. T. Pardue. 2020. 'In vivo Structural Assessments of Ocular Disease in Rodent Models using Optical Coherence Tomography', *J Vis Exp*.

Almasieh, M., A. M. Wilson, B. Morquette, J. L. Cueva Vargas, and A. Di Polo. 2012. 'The molecular basis of retinal ganglion cell death in glaucoma', *Prog Retin Eye Res*, 31: 152-81.

Amin, H. Z., L. Z. Amin, and I. P. Wijaya. 2017. 'Galectin-3: a novel biomarker for the prognosis of heart failure', *Clujul Med*, 90: 129-32.

Anderson, A. J., C. A. Johnson, M. Fingeret, J. L. Keltner, P. G. Spry, M. Wall, and J. S. Werner. 2005. 'Characteristics of the normative database for the Humphrey matrix perimeter', *Invest Ophthalmol Vis Sci*, 46: 1540-8.

Aparicio, J. G., H. Hopp, A. Choi, J. Mandayam Comar, V. C. Liao, N. Harutyunyan, and T. C. Lee. 2017. 'Temporal expression of CD184(CXCR4) and CD171(L1CAM) identifies distinct early developmental stages of human retinal ganglion cells in embryonic stem cell derived retina', *Exp Eye Res*, 154: 177-89.

Argueso, P. 2013. 'Glycobiology of the ocular surface: mucins and lectins', *Jpn J Ophthalmol*, 57: 150-5.

Argueso, P., A. Guzman-Aranguez, F. Mantelli, Z. Cao, J. Ricciuto, and N. Panjwani. 2009. 'Association of cell surface mucins with galectin-3 contributes to the ocular surface epithelial barrier', *J Biol Chem*, 284: 23037-45.

Arthur, C. M., M. D. Baruffi, R. D. Cummings, and S. R. Stowell. 2015. 'Evolving mechanistic insights into galectin functions', *Methods Mol Biol*, 1207: 1-35.

Baberg, F., S. Geyh, D. Waldera-Lupa, A. Stefanski, C. Zilkens, R. Haas, T. Schroeder, and K. Stuhler. 2019. 'Secretome analysis of human bone marrow derived mesenchymal stromal cells', *Biochim Biophys Acta Proteins Proteom*, 1867: 434-41.

Bae, K. S., J. B. Park, H. S. Kim, D. S. Kim, D. J. Park, and S. J. Kang. 2011. 'Neuron-like differentiation of bone marrow-derived mesenchymal stem cells', *Yonsei Med J*, 52: 401-12.

Balaratnasingam, C., W. H. Morgan, L. Bass, L. Ye, C. McKnight, S. J. Cringle, and D. Y. Yu. 2008. 'Elevated pressure induced astrocyte damage in the optic nerve', *Brain Res*, 1244: 142-54.

Balaratnasingam, C., D. Pham, W. H. Morgan, L. Bass, S. J. Cringle, and D. Y. Yu. 2009. 'Mitochondrial cytochrome c oxidase expression in the central nervous system is elevated at sites of pressure gradient elevation but not absolute pressure increase', *J Neurosci Res*, 87: 2973-82.

Baneke, A. J., J. Aubry, A. C. Viswanathan, and G. T. Plant. 2020. 'The role of intracranial pressure in glaucoma and therapeutic implications', *Eye (Lond)*, 34: 178-91.

Bartolazzi, A. 2018. 'Galectins in Cancer and Translational Medicine: From Bench to Bedside', *Int J Mol Sci*, 19.

Becker, S., K. Eastlake, H. Jayaram, M. F. Jones, R. A. Brown, G. J. McLellan, D. G. Charteris, P. T. Khaw, and G. A. Limb. 2016. 'Allogeneic Transplantation of Muller-Derived Retinal Ganglion Cells Improves Retinal Function in a Feline Model of Ganglion Cell Depletion', *Stem Cells Transl Med*, 5: 192-205.

Belmares, R., U. Raychaudhuri, S. Maansson, and A. F. Clark. 2018. 'Histological investigation of human glaucomatous eyes: Extracellular fibrotic changes and galectin 3 expression in the trabecular meshwork and optic nerve head', *Clin Anat*, 31: 1031-49.

Bera, A., F. Das, N. Ghosh-Choudhury, M. M. Mariappan, B. S. Kasinath, and G. Ghosh Choudhury. 2017. 'Reciprocal regulation of miR-214 and PTEN by high

glucose regulates renal glomerular mesangial and proximal tubular epithelial cell hypertrophy and matrix expansion', *Am J Physiol Cell Physiol*, 313: C430-C47.

Bernardos, R. L., L. K. Barthel, J. R. Meyers, and P. A. Raymond. 2007. 'Late-stage neuronal progenitors in the retina are radial Muller glia that function as retinal stem cells', *J Neurosci*, 27: 7028-40.

Bertaud, J., Z. Qin, and M. J. Buehler. 2010. 'Intermediate filament-deficient cells are mechanically softer at large deformation: a multi-scale simulation study', *Acta Biomater*, 6: 2457-66.

Bhatia, B., S. Singhal, J. M. Lawrence, P. T. Khaw, and G. A. Limb. 2009. 'Distribution of Muller stem cells within the neural retina: evidence for the existence of a ciliary margin-like zone in the adult human eye', *Exp Eye Res*, 89: 373-82.

Biedermann, B., A. Bringmann, and A. Reichenbach. 2002. 'High-affinity GABA uptake in retinal glial (Muller) cells of the guinea pig: electrophysiological characterization, immunohistochemical localization, and modeling of efficiency', *Glia*, 39: 217-28.

Biswas, S., and K. H. Wan. 2018. 'Review of rodent hypertensive glaucoma models', *Acta Ophthalmol*.

Blanchard, H., K. Bum-Erdene, M. H. Bohari, and X. Yu. 2016. 'Galectin-1 inhibitors and their potential therapeutic applications: a patent review', *Expert Opin Ther Pat*, 26: 537-54.

Blazevits, O., Y. G. Mideksa, M. Solman, A. Ligabue, N. Ariotti, H. Nakhaeizadeh, E. K. Fansa, A. C. Papageorgiou, A. Wittinghofer, M. R. Ahmadian, and D. Abankwa. 2016. 'Galectin-1 dimers can scaffold Raf-effectors to increase H-ras nanoclustering', *Sci Rep*, 6: 24165.

Bobadilla, A. V. P., J. Arevalo, E. Sarro, H. M. Byrne, P. K. Maini, T. Carraro, S. Balocco, A. Meseguer, and T. Alarcon. 2019. 'In vitro cell migration quantification method for scratch assays', *J R Soc Interface*, 16: 20180709.

Bonomi, L., G. Marchini, M. Marraffa, P. Bernardi, I. De Franco, S. Perfetti, A. Varotto, and V. Tenna. 1998. 'Prevalence of glaucoma and intraocular pressure distribution in a defined population. The Egna-Neumarkt Study', *Ophthalmology*, 105: 209-15.

Boscher, C., J. W. Dennis, and I. R. Nabi. 2011. 'Glycosylation, galectins and cellular signaling', *Curr Opin Cell Biol*, 23: 383-92.

Bouhenni, R. A., J. Dunmire, A. Sewell, and D. P. Edward. 2012. 'Animal models of glaucoma', *J Biomed Biotechnol*, 2012: 692609.

Braunger, B. M., S. Pielmeier, C. Demmer, V. Landstorfer, D. Kawall, N. Abramov, M. Leibinger, I. Kleiter, D. Fischer, H. Jagle, and E. R. Tamm. 2013. 'TGF-beta signaling protects retinal neurons from programmed cell death during the development of the mammalian eye', *J Neurosci*, 33: 14246-58.

Bringmann, A., T. Pannicke, J. Grosche, M. Francke, P. Wiedemann, S. N. Skatchkov, N. N. Osborne, and A. Reichenbach. 2006. 'Muller cells in the healthy and diseased retina', *Prog Retin Eye Res*, 25: 397-424.

Bringmann, L. F., N. Vissers, M. Wichers, N. Geschwind, P. Kuppens, F. Peeters, D. Borsboom, and F. Tuerlinckx. 2013. 'A network approach to psychopathology: new insights into clinical longitudinal data', *PLoS One*, 8: e60188.

Burgoyne, C. F., J. C. Downs, A. J. Bellezza, J. K. Suh, and R. T. Hart. 2005. 'The optic nerve head as a biomechanical structure: a new paradigm for understanding the role of IOP-related stress and strain in the pathophysiology of glaucomatous optic nerve head damage', *Prog Retin Eye Res*, 24: 39-73.

Burguillos, M. A., M. Svensson, T. Schulte, A. Boza-Serrano, A. Garcia-Quintanilla, E. Kavanagh, M. Santiago, N. Viceconte, M. J. Oliva-Martin, A. M. Osman, E. Salomonsson, L. Amar, A. Persson, K. Blomgren, A. Achour, E. Englund, H. Leffler, J. L. Venero, B. Joseph, and T. Deierborg. 2015. 'Microglia-Secreted Galectin-3 Acts as a Toll-like Receptor 4 Ligand and Contributes to Microglial Activation', *Cell Rep*, 10: 1626-38.

Burns, S. A., A. E. Elsner, K. A. Sapoznik, R. L. Warner, and T. J. Gast. 2019. 'Adaptive optics imaging of the human retina', *Prog Retin Eye Res*, 68: 1-30.

Burton, M. J., J. Ramke, A. P. Marques, R. R. A. Bourne, N. Congdon, I. Jones, B. A. M. Ah Tong, S. Arunga, D. Bachani, C. Bascaran, A. Bastawrous, K. Blanchet, T. Braithwaite, J. C. Buchan, J. Cairns, A. Cama, M. Chagunda, C. Chuluunkhuu, A. Cooper, J. Crofts-Lawrence, W. H. Dean, A. K. Denniston, J. R. Ehrlich, P. M. Emerson, J. R. Evans, K. D. Frick, D. S. Friedman, J. M. Furtado, M. M. Gichangi, S. Gichuhi, S. S. Gilbert, R. Gurung, E. Habtamu, P. Holland, J. B. Jonas, P. A. Keane, L. Keay, R. C. Khanna, P. T. Khaw, H. Kuper, F. Kyari, V. C. Lansingh, I. Mactaggart, M. M. Mafwiri, W. Mathenge, I. McCormick, P. Morjaria, L. Mowatt, D. Muirhead, G. V. S. Murthy, N. Mwangi, D. B. Patel, T. Peto, B. M. Qureshi, S. R. Salomao, V. Sarah, B. R. Shilio, A. W. Solomon, B. K. Swenor, H. R. Taylor, N. Wang, A. Webson, S. K. West, T. Y. Wong, R. Wormald, S. Yasmin, M. Yusufu, J. C. Silva, S. Resnikoff, T. Ravilla, C. E. Gilbert, A. Foster, and H. B. Faal. 2021. 'The Lancet Global Health Commission on Global Eye Health: vision beyond 2020', *Lancet Glob Health*, 9: e489-e551.

Caberoy, N. B., G. Alvarado, J. L. Bigcas, and W. Li. 2012. 'Galectin-3 is a new MerTK-specific eat-me signal', *J Cell Physiol*, 227: 401-7.

Cai, J., X. Liu, J. Cheng, Y. Li, X. Huang, Y. Li, X. Ma, H. Yu, H. Liu, and R. Wei. 2012. 'MicroRNA-200 is commonly repressed in conjunctival MALT lymphoma, and targets cyclin E2', *Graefes Arch Clin Exp Ophthalmol*, 250: 523-31.

Camby, I., M. Le Mercier, F. Lefranc, and R. Kiss. 2006. 'Galectin-1: a small protein with major functions', *Glycobiology*, 16: 137R-57R.

Cao, Z., N. Said, S. Amin, H. K. Wu, A. Bruce, M. Garate, D. K. Hsu, I. Kuwabara, F. T. Liu, and N. Panjwani. 2002. 'Galectins-3 and -7, but not galectin-1, play a role in re-epithelialization of wounds', *J Biol Chem*, 277: 42299-305.

Cao, Z., N. Said, H. K. Wu, I. Kuwabara, F. T. Liu, and N. Panjwani. 2003. 'Galectin-7 as a potential mediator of corneal epithelial cell migration', *Arch Ophthalmol*, 121: 82-6.

Cao, Z., H. K. Wu, A. Bruce, K. Wollenberg, and N. Panjwani. 2002. 'Detection of differentially expressed genes in healing mouse corneas, using cDNA microarrays', *Invest Ophthalmol Vis Sci*, 43: 2897-904.

Caprioli, J., and A. L. Coleman. 2008. 'Intraocular pressure fluctuation a risk factor for visual field progression at low intraocular pressures in the advanced glaucoma intervention study', *Ophthalmology*, 115: 1123-29 e3.

Cepko, C. 2014. 'Intrinsically different retinal progenitor cells produce specific types of progeny', *Nat Rev Neurosci*, 15: 615-27.

Chakraborty, D., B. Sumova, T. Mallano, C. W. Chen, A. Distler, C. Bergmann, I. Ludolph, R. E. Horch, K. Gelse, A. Ramming, O. Distler, G. Schett, L. Senolt, and J. H. W. Distler. 2017. 'Activation of STAT3 integrates common profibrotic pathways to promote fibroblast activation and tissue fibrosis', *Nat Commun*, 8: 1130.

Chan, M. P. Y., D. C. Broadway, A. P. Khawaja, J. L. Y. Yip, D. F. Garway-Heath, J. M. Burr, R. Luben, S. Hayat, N. Dalzell, K. T. Khaw, and P. J. Foster. 2017. 'Glaucoma and intraocular pressure in EPIC-Norfolk Eye Study: cross sectional study', *BMJ*, 358: j3889.

Chan, Y. C., H. Y. Lin, Z. Tu, Y. H. Kuo, S. D. Hsu, and C. H. Lin. 2018. 'Dissecting the Structure-Activity Relationship of Galectin-Ligand Interactions', *Int J Mol Sci*, 19.

Chao, M. V. 2003. 'Neurotrophins and their receptors: a convergence point for many signalling pathways', *Nat Rev Neurosci*, 4: 299-309.

Chatterjee, A., G. Villarreal, Jr., and D. J. Rhee. 2014. 'Matricellular proteins in the trabecular meshwork: review and update', *J Ocul Pharmacol Ther*, 30: 447-63.

Chen, H. Y., Y. J. Ho, H. C. Chou, E. C. Liao, Y. T. Tsai, Y. S. Wei, L. H. Lin, M. W. Lin, Y. S. Wang, M. L. Ko, and H. L. Chan. 2020. 'The Role of Transforming Growth Factor-Beta in Retinal Ganglion Cells with Hyperglycemia and Oxidative Stress', *Int J Mol Sci*, 21.

Chen, Q., H. Wang, S. Liao, Y. Gao, R. Liao, P. J. Little, J. Xu, Z. P. Feng, Y. Zheng, and W. Zheng. 2015. 'Nerve growth factor protects retinal ganglion cells against injury induced by retinal ischemia-reperfusion in rats', *Growth Factors*, 33: 149-59.

Chen, W. S., Z. Cao, S. Sugaya, M. J. Lopez, V. G. Sendra, N. Laver, H. Leffler, U. J. Nilsson, J. Fu, J. Song, L. Xia, P. Hamrah, and N. Panjwani. 2016. 'Pathological lymphangiogenesis is modulated by galectin-8-dependent crosstalk between podoplanin and integrin-associated VEGFR-3', *Nat Commun*, 7: 11302.

Chen, W. S., Z. Cao, L. Truong, S. Sugaya, and N. Panjwani. 2015. 'Fingerprinting of galectins in normal, P. aeruginosa-infected, and chemically burned mouse corneas', *Invest Ophthalmol Vis Sci*, 56: 515-25.

Chen, X. L., J. O. Nam, C. Jean, C. Lawson, C. T. Walsh, E. Goka, S. T. Lim, A. Tomar, I. Tancioni, S. Uryu, J. L. Guan, L. M. Acevedo, S. M. Weis, D. A. Cheresh, and D. D. Schlaepfer. 2012. 'VEGF-induced vascular permeability is mediated by FAK', *Dev Cell*, 22: 146-57.

Chiariotti, L., P. Salvatore, R. Frunzio, and C. B. Bruni. 2002. 'Galectin genes: regulation of expression', *Glycoconj J*, 19: 441-9.

Ching, R. C., M. Wiberg, and P. J. Kingham. 2018. 'Schwann cell-like differentiated adipose stem cells promote neurite outgrowth via secreted exosomes and RNA transfer', *Stem Cell Res Ther*, 9: 266.

Chistiakov, D. A., M. C. Killingsworth, V. A. Myasoedova, A. N. Orekhov, and Y. V. Bobryshev. 2017. 'CD68/macrosialin: not just a histochemical marker', *Lab Invest*, 97: 4-13.

Choi, J., K. H. Kim, J. Jeong, H. S. Cho, C. H. Lee, and M. S. Kook. 2007. 'Circadian fluctuation of mean ocular perfusion pressure is a consistent risk factor for normal-tension glaucoma', *Invest Ophthalmol Vis Sci*, 48: 104-11.

Chou, F. C., H. Y. Chen, C. C. Kuo, and H. K. Sytwu. 2018. 'Role of Galectins in Tumors and in Clinical Immunotherapy', *Int J Mol Sci*, 19.

Cone, F. E., S. E. Gelman, J. L. Son, M. E. Pease, and H. A. Quigley. 2010. 'Differential susceptibility to experimental glaucoma among 3 mouse strains using bead and viscoelastic injection', *Exp Eye Res*, 91: 415-24.

Craig, S. E., R. Thummel, H. Ahmed, G. R. Vasta, D. R. Hyde, and P. F. Hitchcock. 2010. 'The zebrafish galectin Drgal1-l2 is expressed by proliferating Muller glia and photoreceptor progenitors and regulates the regeneration of rod photoreceptors', *Invest Ophthalmol Vis Sci*, 51: 3244-52.

Cruzat, A., M. Gonzalez-Andrades, J. Mauris, D. B. AbuSamra, P. Chidambaram, K. R. Kenyon, J. Chodosh, C. H. Dohlman, and P. Argueso. 2018. 'Colocalization of Galectin-3 With CD147 Is Associated With Increased Gelatinolytic Activity in Ulcerating Human Corneas', *Invest Ophthalmol Vis Sci*, 59: 223-30.

Cui, Z., Y. Guo, Y. Zhou, S. Mao, X. Yan, Y. Zeng, C. Ding, H. F. Chan, S. Tang, L. Tang, and J. Chen. 2020. 'Transcriptomic Analysis of the Developmental Similarities and Differences Between the Native Retina and Retinal Organoids', *Invest Ophthalmol Vis Sci*, 61: 6.

Cummings, R. D. 2009. 'The repertoire of glycan determinants in the human glycome', *Mol Biosyst*, 5: 1087-104.

D'Haene, N., S. Sauvage, C. Maris, I. Adanja, M. Le Mercier, C. Decaestecker, L. Baum, and I. Salmon. 2013. 'VEGFR1 and VEGFR2 involvement in extracellular galectin-1- and galectin-3-induced angiogenesis', *PLoS One*, 8: e67029.

da Cruz, L., K. Fynes, O. Georgiadis, J. Kerby, Y. H. Luo, A. Ahmado, A. Vernon, J. T. Daniels, B. Nommiste, S. M. Hasan, S. B. Gooljar, A. F. Carr, A. Vugler, C. M. Ramsden, M. Bictash, M. Fenster, J. Steer, T. Harbinson, A. Wilbrey, A. Tufail, G. Feng, M. Whitlock, A. G. Robson, G. E. Holder, M. S. Sagoo, P. T. Loudon, P. Whiting, and P. J. Coffey. 2018. 'Phase 1 clinical study of an embryonic stem cell-derived retinal pigment epithelium patch in age-related macular degeneration', *Nat Biotechnol*, 36: 328-37.

da Silva-Junior, A. J., L. A. Mesentier-Louro, G. Nascimento-Dos-Santos, L. C. Teixeira-Pinheiro, J. F. Vasques, L. Chimeli-Ormonde, V. Bodart-Santos, L. R. P. de Carvalho, M. F. Santiago, and R. Mendez-Otero. 2021. 'Human mesenchymal stem cell therapy promotes retinal ganglion cell survival and target reconnection after optic nerve crush in adult rats', *Stem Cell Res Ther*, 12: 69.

de Haan, N., M. Pucic-Bakovic, M. Novokmet, D. Falck, G. Lageveen-Kammeijer, G. Razdorov, F. Vuckovic, I. Trbojevic-Akmacic, O. Gornik, M. Hanic, M. Wuhrer, G. Lauc, and Project The Human Glycome. 2022. 'Developments and perspectives in high-throughput protein glycomics: enabling the analysis of thousands of samples', *Glycobiology*, 32: 651-63.

Di Polo, A., L. J. Aigner, R. J. Dunn, G. M. Bray, and A. J. Aguayo. 1998. 'Prolonged delivery of brain-derived neurotrophic factor by adenovirus-infected Muller cells temporarily rescues injured retinal ganglion cells', *Proc Natl Acad Sci U S A*, 95: 3978-83.

Diskin, S., Z. Cao, H. Leffler, and N. Panjwani. 2009. 'The role of integrin glycosylation in galectin-8-mediated trabecular meshwork cell adhesion and spreading', *Glycobiology*, 19: 29-37.

Eastlake, K., W. E. Heywood, P. Banerjee, E. Bliss, K. Mills, P. T. Khaw, D. Charteris, and G. A. Limb. 2018. 'Comparative proteomic analysis of normal and gliotic PVR retina and contribution of Muller glia to this profile', *Exp Eye Res*, 177: 197-207.

Eastlake, K., W. E. Heywood, D. Tracey-White, E. Aquino, E. Bliss, G. R. Vasta, K. Mills, P. T. Khaw, M. Moosajee, and G. A. Limb. 2017. 'Comparison of proteomic profiles in the zebrafish retina during experimental degeneration and regeneration', *Sci Rep*, 7: 44601.

Eastlake, K., H. Jayaram, J. Luis, M. Hayes, P. T. Khaw, and G. A. Limb. 2021. 'Strain Specific Responses in a Microbead Rat Model of Experimental Glaucoma', *Curr Eye Res*, 46: 387-97.

Eastlake, K., W. D. B. Lamb, J. Luis, P. T. Khaw, H. Jayaram, and G. A. Limb. 2021. 'Prospects for the application of Muller glia and their derivatives in retinal regenerative therapies', *Prog Retin Eye Res*: 100970.

Eastlake, K., J. Luis, and G. A. Limb. 2019. 'Potential of Muller Glia for Retina Neuroprotection', *Curr Eye Res*: 1-10.

Eastlake, K., W. Wang, H. Jayaram, C. Murray-Dunning, A. J. F. Carr, C. M. Ramsden, A. Vugler, K. Gore, N. Clemo, M. Stewart, P. Coffey, P. T. Khaw, and G. A. Limb. 2019. 'Phenotypic and Functional Characterization of Muller Glia Isolated from Induced Pluripotent Stem Cell-Derived Retinal Organoids: Improvement of Retinal Ganglion Cell Function upon Transplantation', *Stem Cells Transl Med*, 8: 775-84.

Eiraku, M., N. Takata, H. Ishibashi, M. Kawada, E. Sakakura, S. Okuda, K. Sekiguchi, T. Adachi, and Y. Sasai. 2011. 'Self-organizing optic-cup morphogenesis in three-dimensional culture', *Nature*, 472: 51-6.

Esteban-Martinez, L., and P. Boya. 2018. 'BNIP3L/NIX-dependent mitophagy regulates cell differentiation via metabolic reprogramming', *Autophagy*, 14: 915-17.

Fajka-Boja, R., V. S. Urban, G. J. Szebeni, A. Czibula, A. Blasko, E. Kriston-Pal, I. Makra, A. Hornung, E. Szabo, F. Uher, N. G. Than, and E. Monostori. 2016. 'Galectin-1 is a local but not systemic immunomodulatory factor in mesenchymal stromal cells', *Cytotherapy*, 18: 360-70.

Fautsch, M. P., A. O. Silva, and D. H. Johnson. 2003. 'Carbohydrate binding proteins galectin-1 and galectin-3 in human trabecular meshwork', *Exp Eye Res*, 77: 11-6.

Fenwick, N., G. Griffin, and C. Gauthier. 2009. 'The welfare of animals used in science: how the "Three Rs" ethic guides improvements', *Can Vet J*, 50: 523-30.

Ferrara, N., and A. P. Adamis. 2016. 'Ten years of anti-vascular endothelial growth factor therapy', *Nat Rev Drug Discov*, 15: 385-403.

Fimbel, S. M., J. E. Montgomery, C. T. Burket, and D. R. Hyde. 2007. 'Regeneration of inner retinal neurons after intravitreal injection of ouabain in zebrafish', *J Neurosci*, 27: 1712-24.

Fini, M. E., A. Bauskar, S. Jeong, and M. R. Wilson. 2016. 'Clusterin in the eye: An old dog with new tricks at the ocular surface', *Exp Eye Res*, 147: 57-71.

Fischer, A. J., and T. A. Reh. 2003. 'Potential of Muller glia to become neurogenic retinal progenitor cells', *Glia*, 43: 70-6.

Fligor, C. M., K. B. Langer, A. Sridhar, Y. Ren, P. K. Shields, M. C. Edler, S. K. Ohlemacher, V. M. Sluch, D. J. Zack, C. Zhang, D. M. Suter, and J. S. Meyer. 2018. 'Three-Dimensional Retinal Organoids Facilitate the Investigation of Retinal Ganglion Cell Development, Organization and Neurite Outgrowth from Human Pluripotent Stem Cells', *Sci Rep*, 8: 14520.

Franze, K., J. Grosche, S. N. Skatchkov, S. Schinkinger, C. Foja, D. Schild, O. Uckermann, K. Travis, A. Reichenbach, and J. Guck. 2007. 'Muller cells are living optical fibers in the vertebrate retina', *Proc Natl Acad Sci U S A*, 104: 8287-92.

Fu, L., J. S. M. Lai, A. C. Y. Lo, and K. C. Shih. 2018. 'Induction of significant intraocular pressure diurnal fluctuation in rats using a modified technique of microbead occlusion', *Int J Ophthalmol*, 11: 1114-19.

Fujimura, N. 2016. 'WNT/beta-Catenin Signaling in Vertebrate Eye Development', *Front Cell Dev Biol*, 4: 138.

Fukushima, A., T. Sumi, K. Fukuda, N. Kumagai, T. Nishida, K. Okumura, H. Akiba, H. Yagita, and H. Ueno. 2008. 'Roles of galectin-9 in the development of experimental allergic conjunctivitis in mice', *Int Arch Allergy Immunol*, 146: 36-43.

Gabius, H. J. 2018. 'The sugar code: Why glycans are so important', *Biosystems*, 164: 102-11.

Gabius, H. J., H. C. Siebert, S. Andre, J. Jimenez-Barbero, and H. Rudiger. 2004. 'Chemical biology of the sugar code', *Chembiochem*, 5: 740-64.

Gardiner, S. K., C. A. Johnson, and S. Demirel. 2012. 'Factors predicting the rate of functional progression in early and suspected glaucoma', *Invest Ophthalmol Vis Sci*, 53: 3598-604.

Garita-Hernandez, M., F. Routet, L. Guibbal, H. Khabou, L. Toualbi, L. Riancho, S. Reichman, J. Duebel, J. A. Sahel, O. Goureau, and D. Dalkara. 2020. 'AAV-Mediated Gene Delivery to 3D Retinal Organoids Derived from Human Induced Pluripotent Stem Cells', *Int J Mol Sci*, 21.

Garnham, R., E. Scott, K. E. Livermore, and J. Munkley. 2019. 'ST6GAL1: A key player in cancer', *Oncol Lett*, 18: 983-89.

Garway-Heath, D. F., D. P. Crabb, C. Bunce, G. Lascaratos, F. Amalfitano, N. Anand, A. Azuara-Blanco, R. R. Bourne, D. C. Broadway, I. A. Cunliffe, J. P. Diamond, S. G. Fraser, T. A. Ho, K. R. Martin, A. I. McNaught, A. Negi, K. Patel, R. A. Russell, A. Shah, P. G. Spry, K. Suzuki, E. T. White, R. P. Wormald, W. Xing, and T. G. Zeyen. 2015. 'Latanoprost for open-angle glaucoma (UKGTS): a randomised, multicentre, placebo-controlled trial', *Lancet*, 385: 1295-304.

Ghasemi, M., E. Alizadeh, K. Saei Arezoumand, B. Fallahi Motlagh, and N. Zarghami. 2018. 'Ciliary neurotrophic factor (CNTF) delivery to retina: an overview of current research advancements', *Artif Cells Nanomed Biotechnol*, 46: 1694-707.

Goldman, D. 2014. 'Muller glial cell reprogramming and retina regeneration', *Nat Rev Neurosci*, 15: 431-42.

Gonen, T., P. Donaldson, and J. Kistler. 2000. 'Galectin-3 is associated with the plasma membrane of lens fiber cells', *Invest Ophthalmol Vis Sci*, 41: 199-203.

Gonnermann, D., H. H. Oberg, M. Lettau, M. Peipp, D. Bauerschlag, S. Sebens, D. Kabelitz, and D. Wesch. 2020. 'Galectin-3 Released by Pancreatic Ductal Adenocarcinoma Suppresses gammadelta T Cell Proliferation but Not Their Cytotoxicity', *Front Immunol*, 11: 1328.

Gorsuch, R. A., and D. R. Hyde. 2014. 'Regulation of Muller glial dependent neuronal regeneration in the damaged adult zebrafish retina', *Exp Eye Res*, 123: 131-40.

Graca, A. B., C. Hippert, and R. A. Pearson. 2018. 'Muller Glia Reactivity and Development of Gliosis in Response to Pathological Conditions', *Adv Exp Med Biol*, 1074: 303-08.

Gu, Y., I. S. Mohammad, and Z. Liu. 2020. 'Overview of the STAT-3 signaling pathway in cancer and the development of specific inhibitors', *Oncol Lett*, 19: 2585-94.

Guenther, M. G., G. M. Frampton, F. Soldner, D. Hockemeyer, M. Mitalipova, R. Jaenisch, and R. A. Young. 2010. 'Chromatin structure and gene expression programs of human embryonic and induced pluripotent stem cells', *Cell Stem Cell*, 7: 249-57.

Guo, J., G. S. Lin, C. Y. Bao, Z. M. Hu, and M. Y. Hu. 2007. 'Anti-inflammation role for mesenchymal stem cells transplantation in myocardial infarction', *Inflammation*, 30: 97-104.

Guzman-Aranguez, A., and P. Argueso. 2010. 'Structure and biological roles of mucin-type O-glycans at the ocular surface', *Ocul Surf*, 8: 8-17.

Hagstrom, S. A., G. S. Ying, G. J. Pauer, G. M. Sturgill-Short, J. Huang, M. G. Maguire, D. F. Martin, and Group Comparison of Age-Related Macular Degeneration Treatments Trials Research. 2014. 'VEGFA and VEGFR2 gene polymorphisms and response to anti-vascular endothelial growth factor therapy: comparison of age-related macular degeneration treatments trials (CATT)', *JAMA Ophthalmol*, 132: 521-7.

Hallam, D., G. Hilgen, B. Dorgau, L. Zhu, M. Yu, S. Bojic, P. Hewitt, M. Schmitt, M. Uteng, S. Kustermann, D. Steel, M. Nicholds, R. Thomas, A. Treumann, A. Porter, E. Sernagor, L. Armstrong, and M. Lako. 2018. 'Human-Induced Pluripotent Stem Cells Generate Light Responsive Retinal Organoids with Variable and Nutrient-Dependent Efficiency', *Stem Cells*, 36: 1535-51.

Harada, C., A. Kimura, X. Guo, K. Namekata, and T. Harada. 2019. 'Recent advances in genetically modified animal models of glaucoma and their roles in drug repositioning', *Br J Ophthalmol*, 103: 161-66.

Harper, M. M., S. D. Grozdanic, B. Blits, M. H. Kuehn, D. Zamzow, J. E. Buss, R. H. Kardon, and D. S. Sakaguchi. 2011. 'Transplantation of BDNF-secreting

mesenchymal stem cells provides neuroprotection in chronically hypertensive rat eyes', *Invest Ophthalmol Vis Sci*, 52: 4506-15.

Harrison, S. A., S. R. Marri, N. Chalasani, R. Kohli, W. Aronstein, G. A. Thompson, W. Irish, M. V. Miles, S. A. Xanthakos, E. Lawitz, M. Noureddin, T. D. Schiano, M. Siddiqui, A. Sanyal, B. A. Neuschwander-Tetri, and P. G. Traber. 2016. 'Randomised clinical study: GR-MD-02, a galectin-3 inhibitor, vs. placebo in patients having non-alcoholic steatohepatitis with advanced fibrosis', *Aliment Pharmacol Ther*, 44: 1183-98.

Hawkins, B. T., and T. P. Davis. 2005. 'The blood-brain barrier/neurovascular unit in health and disease', *Pharmacol Rev*, 57: 173-85.

He, J., and L. G. Baum. 2006. 'Galectin interactions with extracellular matrix and effects on cellular function', *Methods Enzymol*, 417: 247-56.

Heavner, W., and L. Pevny. 2012. 'Eye development and retinogenesis', *Cold Spring Harb Perspect Biol*, 4.

Henderson, N. C., A. C. Mackinnon, S. L. Farnworth, F. Poirier, F. P. Russo, J. P. Iredale, C. Haslett, K. J. Simpson, and T. Sethi. 2006. 'Galectin-3 regulates myofibroblast activation and hepatic fibrosis', *Proc Natl Acad Sci U S A*, 103: 5060-5.

Heneka, M. T., M. J. Carson, J. El Khoury, G. E. Landreth, F. Brosseron, D. L. Feinstein, A. H. Jacobs, T. Wyss-Coray, J. Vitorica, R. M. Ransohoff, K. Herrup, S. A. Frautschy, B. Finsen, G. C. Brown, A. Verkhratsky, K. Yamanaka, J. Koistinaho, E. Latz, A. Halle, G. C. Petzold, T. Town, D. Morgan, M. L. Shinohara, V. H. Perry, C. Holmes, N. G. Bazan, D. J. Brooks, S. Hunot, B. Joseph, N. Deigendesch, O. Garaschuk, E. Boddeke, C. A. Dinarello, J. C. Breitner, G. M. Cole, D. T. Golenbock, and M. P. Kummer. 2015. 'Neuroinflammation in Alzheimer's disease', *Lancet Neurol*, 14: 388-405.

Hernandez, M. R. 2000. 'The optic nerve head in glaucoma: role of astrocytes in tissue remodeling', *Prog Retin Eye Res*, 19: 297-321.

Hertz, J., B. Qu, Y. Hu, R. D. Patel, D. A. Valenzuela, and J. L. Goldberg. 2014. 'Survival and integration of developing and progenitor-derived retinal ganglion cells following transplantation', *Cell Transplant*, 23: 855-72.

Higashide, T., and K. Sugiyama. 2008. 'Use of viscoelastic substance in ophthalmic surgery - focus on sodium hyaluronate', *Clin Ophthalmol*, 2: 21-30.

Hirani, N., A. C. MacKinnon, L. Nicol, P. Ford, H. Schambye, A. Pedersen, U. J. Nilsson, H. Leffler, T. Sethi, S. Tantawi, L. Gavelle, R. J. Slack, R. Mills, U. Karmakar, D. Humphries, F. Zetterberg, L. Keeling, L. Paul, P. L. Molyneaux, F. Li, W. Funston, I. A. Forrest, A. J. Simpson, M. A. Gibbons, and T. M. Maher. 2020. 'Target-inhibition of Galectin-3 by Inhaled TD139 in Patients with Idiopathic Pulmonary Fibrosis', *Eur Respir J*.

Hirose, I., A. Kanda, K. Noda, and S. Ishida. 2019. 'Glucocorticoid receptor inhibits Muller glial galectin-1 expression via DUSP1-dependent and -independent deactivation of AP-1 signalling', *J Cell Mol Med*, 23: 6785-96.

Hollander, H., F. Makarov, F. H. Stefani, and J. Stone. 1995. 'Evidence of constriction of optic nerve axons at the lamina cribrosa in the normotensive eye in humans and other mammals', *Ophthalmic Res*, 27: 296-309.

Hrdlickova-Cela, E., J. Plzak, K. Smetana, Jr., Z. Melkova, H. Kaltner, M. Filipec, F. T. Liu, and H. J. Gabius. 2001. 'Detection of galectin-3 in tear fluid at disease states and immunohistochemical and lectin histochemical analysis in human corneal and conjunctival epithelium', *Br J Ophthalmol*, 85: 1336-40.

Huang, E. J., and L. F. Reichardt. 2001. 'Neurotrophins: roles in neuronal development and function', *Annu Rev Neurosci*, 24: 677-736.

Huang, J. G., C. B. Shen, W. B. Wu, J. W. Ren, L. Xu, S. Liu, and Q. Yang. 2014. 'Primary cilia mediate sonic hedgehog signaling to regulate neuronal-like differentiation of bone mesenchymal stem cells for resveratrol induction in vitro', *J Neurosci Res*, 92: 587-96.

Huat, T. J., A. A. Khan, S. Pati, Z. Mustafa, J. M. Abdullah, and H. Jaafar. 2014. 'IGF-1 enhances cell proliferation and survival during early differentiation of mesenchymal stem cells to neural progenitor-like cells', *BMC Neurosci*, 15: 91.

Ingensiep, C., K. Schaffrath, P. Walter, and S. Johnen. 2022. 'Effects of Hydrostatic Pressure on Electrical Retinal Activity in a Multielectrode Array-Based ex vivo Glaucoma Acute Model', *Front Neurosci*, 16: 831392.

Inohara, H., S. Akahani, and A. Raz. 1998. 'Galectin-3 stimulates cell proliferation', *Exp Cell Res*, 245: 294-302.

Ishida, K., N. Panjwani, Z. Cao, and J. W. Streilein. 2003. 'Participation of pigment epithelium in ocular immune privilege. 3. Epithelia cultured from iris, ciliary body, and retina suppress T-cell activation by partially non-overlapping mechanisms', *Ocul Immunol Inflamm*, 11: 91-105.

Iwabe, S., N. A. Moreno-Mendoza, F. Trigo-Tavera, C. Crowder, and G. A. Garcia-Sanchez. 2007. 'Retrograde axonal transport obstruction of brain-derived neurotrophic factor (BDNF) and its TrkB receptor in the retina and optic nerve of American Cocker Spaniel dogs with spontaneous glaucoma', *Vet Ophthalmol*, 10 Suppl 1: 12-9.

Jadhav, A. P., K. Roesch, and C. L. Cepko. 2009. 'Development and neurogenic potential of Muller glial cells in the vertebrate retina', *Prog Retin Eye Res*, 28: 249-62.

Jarrett, S. G., and M. E. Boulton. 2012. 'Consequences of oxidative stress in age-related macular degeneration', *Mol Aspects Med*, 33: 399-417.

Jayaram, H., M. F. Jones, K. Eastlake, P. B. Cottrill, S. Becker, J. Wiseman, P. T. Khaw, and G. A. Limb. 2014. 'Transplantation of photoreceptors derived from human Muller glia restore rod function in the P23H rat', *Stem Cells Transl Med*, 3: 323-33.

Ji, J. Z., W. Elyaman, H. K. Yip, V. W. Lee, L. W. Yick, J. Hugon, and K. F. So. 2004. 'CNTF promotes survival of retinal ganglion cells after induction of ocular hypertension in rats: the possible involvement of STAT3 pathway', *Eur J Neurosci*, 19: 265-72.

Johannes, L., R. Jacob, and H. Leffler. 2018. 'Galectins at a glance', *J Cell Sci*, 131.

Johnson, T. V., N. D. Bull, D. P. Hunt, N. Marina, S. I. Tomarev, and K. R. Martin. 2010. 'Neuroprotective effects of intravitreal mesenchymal stem cell transplantation in experimental glaucoma', *Invest Ophthalmol Vis Sci*, 51: 2051-9.

Ju, W. K., K. Y. Kim, J. D. Lindsey, M. Angert, A. Patel, R. T. Scott, Q. Liu, J. G. Crowston, M. H. Ellisman, G. A. Perkins, and R. N. Weinreb. 2009. 'Elevated

hydrostatic pressure triggers release of OPA1 and cytochrome C, and induces apoptotic cell death in differentiated RGC-5 cells', *Mol Vis*, 15: 120-34.

Juszczynski, P., J. Ouyang, S. Monti, S. J. Rodig, K. Takeyama, J. Abramson, W. Chen, J. L. Kutok, G. A. Rabinovich, and M. A. Shipp. 2007. 'The AP1-dependent secretion of galectin-1 by Reed Sternberg cells fosters immune privilege in classical Hodgkin lymphoma', *Proc Natl Acad Sci U S A*, 104: 13134-9.

Kamili, N. A., C. M. Arthur, C. Gerner-Smidt, E. Tafesse, A. Blenda, M. Dias-Baruffi, and S. R. Stowell. 2016. 'Key regulators of galectin-glycan interactions', *Proteomics*, 16: 3111-25.

Kanda, A., Y. Dong, K. Noda, W. Saito, and S. Ishida. 2017. 'Advanced glycation endproducts link inflammatory cues to upregulation of galectin-1 in diabetic retinopathy', *Sci Rep*, 7: 16168.

Kanda, A., K. Noda, W. Saito, and S. Ishida. 2015. 'Aflibercept Traps Galectin-1, an Angiogenic Factor Associated with Diabetic Retinopathy', *Sci Rep*, 5: 17946.

Kang, M. H., D. J. Oh, J. H. Kang, and D. J. Rhee. 2013. 'Regulation of SPARC by transforming growth factor beta2 in human trabecular meshwork', *Invest Ophthalmol Vis Sci*, 54: 2523-32.

Kang, W., and J. M. Hebert. 2011. 'Signaling pathways in reactive astrocytes, a genetic perspective', *Mol Neurobiol*, 43: 147-54.

Karlsson, A., K. Christenson, M. Matlak, A. Bjorstad, K. L. Brown, E. Telemo, E. Salomonsson, H. Leffler, and J. Bylund. 2009. 'Galectin-3 functions as an opsonin and enhances the macrophage clearance of apoptotic neutrophils', *Glycobiology*, 19: 16-20.

Kass, M. A., D. K. Heuer, E. J. Higginbotham, C. A. Johnson, J. L. Keltner, J. P. Miller, R. K. Parrish, 2nd, M. R. Wilson, and M. O. Gordon. 2002. 'The Ocular Hypertension Treatment Study: a randomized trial determines that topical ocular hypotensive medication delays or prevents the onset of primary open-angle glaucoma', *Arch Ophthalmol*, 120: 701-13; discussion 829-30.

Kassumeh, S., G. R. Weber, M. Nobl, S. G. Priglinger, and A. Ohlmann. 2021. 'The neuroprotective role of Wnt signaling in the retina', *Neural Regen Res*, 16: 1524-28.

Kauppinen, A., J. J. Paterno, J. Blasiak, A. Salminen, and K. Kaarniranta. 2016. 'Inflammation and its role in age-related macular degeneration', *Cell Mol Life Sci*, 73: 1765-86.

Kilbride, S. M., and J. H. Prehn. 2013. 'Central roles of apoptotic proteins in mitochondrial function', *Oncogene*, 32: 2703-11.

Kim, J., C. Moon, M. Ahn, H. G. Joo, J. K. Jin, and T. Shin. 2009. 'Immunohistochemical localization of galectin-3 in the pig retina during postnatal development', *Mol Vis*, 15: 1971-6.

Kim, S., A. Lowe, R. Dharmat, S. Lee, L. A. Owen, J. Wang, A. Shakoor, Y. Li, D. J. Morgan, A. A. Hejazi, A. Cvekl, M. M. DeAngelis, Z. J. Zhou, R. Chen, and W. Liu. 2019. 'Generation, transcriptome profiling, and functional validation of cone-rich human retinal organoids', *Proc Natl Acad Sci U S A*, 116: 10824-33.

Klingeborn, M., W. M. Dismuke, C. Bowes Rickman, and W. D. Stamer. 2017. 'Roles of exosomes in the normal and diseased eye', *Prog Retin Eye Res*, 59: 158-77.

Kobayashi, W., A. Onishi, H. Y. Tu, Y. Takihara, M. Matsumura, K. Tsujimoto, M. Inatani, T. Nakazawa, and M. Takahashi. 2018. 'Culture Systems of Dissociated Mouse and Human Pluripotent Stem Cell-Derived Retinal Ganglion Cells Purified by Two-Step Immunopanning', *Invest Ophthalmol Vis Sci*, 59: 776-87.

Kondo, T., A. J. Matsuoka, A. Shimomura, K. R. Koehler, R. J. Chan, J. M. Miller, E. F. Srour, and E. Hashino. 2011. 'Wnt signaling promotes neuronal differentiation from mesenchymal stem cells through activation of Tlx3', *Stem Cells*, 29: 836-46.

Kruczek, K., A. Gonzalez-Cordero, D. Goh, A. Naeem, M. Jonikas, S. J. I. Blackford, M. Kloc, Y. Duran, A. Georgiadis, R. D. Sampson, R. N. Maswood, A. J. Smith, S. Decembrini, Y. Arsenijevic, J. C. Sowden, R. A. Pearson, E. L. West, and R. R. Ali. 2017. 'Differentiation and Transplantation of Embryonic Stem Cell-Derived Cone Photoreceptors into a Mouse Model of End-Stage Retinal Degeneration', *Stem Cell Reports*, 8: 1659-74.

Kruczek, K., and A. Swaroop. 2020. 'Pluripotent stem cell-derived retinal organoids for disease modeling and development of therapies', *Stem Cells*, 38: 1206-15.

La Torre, A., D. A. Lamba, A. Jayabalu, and T. A. Reh. 2012. 'Production and transplantation of retinal cells from human and mouse embryonic stem cells', *Methods Mol Biol*, 884: 229-46.

Lahne, M., M. Nagashima, D. R. Hyde, and P. F. Hitchcock. 2020. 'Reprogramming Muller Glia to Regenerate Retinal Neurons', *Annu Rev Vis Sci*, 6: 171-93.

Laine, R. A. 1994. 'A calculation of all possible oligosaccharide isomers both branched and linear yields 1.05 x 10(12) structures for a reducing hexasaccharide: the Isomer Barrier to development of single-method saccharide sequencing or synthesis systems', *Glycobiology*, 4: 759-67.

Lakshminarayan, R., C. Wunder, U. Becken, M. T. Howes, C. Benzing, S. Arumugam, S. Sales, N. Ariotti, V. Chambon, C. Lamaze, D. Loew, A. Shevchenko, K. Gaus, R. G. Parton, and L. Johannes. 2014. 'Galectin-3 drives glycosphingolipid-dependent biogenesis of clathrin-independent carriers', *Nat Cell Biol*, 16: 595-606.

Lambiase, A., M. Coassin, P. Tirassa, F. Mantelli, and L. Aloe. 2009. 'Nerve growth factor eye drops improve visual acuity and electrofunctional activity in age-related macular degeneration: a case report', *Ann Ist Super Sanita*, 45: 439-42.

Lane, A., K. Jovanovic, C. Shortall, D. Ottaviani, A. B. Panes, N. Schwarz, R. Guarascio, M. J. Hayes, A. Palfi, N. Chadderton, G. J. Farrar, A. J. Hardcastle, and M. E. Cheetham. 2020. 'Modeling and Rescue of RP2 Retinitis Pigmentosa Using iPSC-Derived Retinal Organoids', *Stem Cell Reports*, 15: 67-79.

Langer, K. B., S. K. Ohlemacher, M. J. Phillips, C. M. Fligor, P. Jiang, D. M. Gamm, and J. S. Meyer. 2018. 'Retinal Ganglion Cell Diversity and Subtype Specification from Human Pluripotent Stem Cells', *Stem Cell Reports*, 10: 1282-93.

Lawrence, J. M., S. Singhal, B. Bhatia, D. J. Keegan, T. A. Reh, P. J. Luthert, P. T. Khaw, and G. A. Limb. 2007. 'MIO-M1 cells and similar muller glial cell lines derived from adult human retina exhibit neural stem cell characteristics', *Stem Cells*, 25: 2033-43.

Lee, H. J., J. H. Kim, S. Hong, I. Hwang, S. J. Park, T. I. Kim, W. H. Kim, J. W. Yu, S. W. Kim, and J. H. Cheon. 2019. 'Proteomics-based functional studies reveal that

galectin-3 plays a protective role in the pathogenesis of intestinal Behcet's disease', *Sci Rep*, 9: 11716.

Lee, Y. J., S. W. Kang, J. K. Song, J. J. Park, Y. D. Bae, E. Y. Lee, E. B. Lee, and Y. W. Song. 2007. 'Serum galectin-3 and galectin-3 binding protein levels in Behcet's disease and their association with disease activity', *Clin Exp Rheumatol*, 25: S41-5.

Leffler, H., S. Carlsson, M. Hedlund, Y. Qian, and F. Poirier. 2002. 'Introduction to galectins', *Glycoconj J*, 19: 433-40.

Leite, C., N. T. Silva, S. Mendes, A. Ribeiro, J. P. de Faria, T. Lourenco, F. dos Santos, P. Z. Andrade, C. M. Cardoso, M. Vieira, A. Paiva, C. L. da Silva, J. M. Cabral, J. B. Relvas, and M. Graos. 2014. 'Differentiation of human umbilical cord matrix mesenchymal stem cells into neural-like progenitor cells and maturation into an oligodendroglial-like lineage', *PLoS One*, 9: e111059.

Lenkowski, J. R., Z. Qin, C. J. Sifuentes, R. Thummel, C. M. Soto, C. B. Moens, and P. A. Raymond. 2013. 'Retinal regeneration in adult zebrafish requires regulation of TGFbeta signaling', *Glia*, 61: 1687-97.

Levkovitch-Verbin, H. 2015. 'Retinal ganglion cell apoptotic pathway in glaucoma: Initiating and downstream mechanisms', *Prog Brain Res*, 220: 37-57.

Levkovitch-Verbin, H., D. Makarovsky, and S. Vander. 2013. 'Comparison between axonal and retinal ganglion cell gene expression in various optic nerve injuries including glaucoma', *Mol Vis*, 19: 2526-41.

Levkovitch-Verbin, H., H. A. Quigley, K. R. Martin, D. Valenta, L. A. Baumrind, and M. E. Pease. 2002. 'Translimbal laser photocoagulation to the trabecular meshwork as a model of glaucoma in rats', *Invest Ophthalmol Vis Sci*, 43: 402-10.

Levkovitch-Verbin, H., O. Sadan, S. Vander, M. Rosner, Y. Barhum, E. Melamed, D. Offen, and S. Melamed. 2010. 'Intravitreal injections of neurotrophic factors secreting mesenchymal stem cells are neuroprotective in rat eyes following optic nerve transection', *Invest Ophthalmol Vis Sci*, 51: 6394-400.

Lewis, G. P., E. A. Chapin, G. Luna, K. A. Linberg, and S. K. Fisher. 2010. 'The fate of Muller's glia following experimental retinal detachment: nuclear migration, cell division, and subretinal glial scar formation', *Mol Vis*, 16: 1361-72.

Leydhecker, W., K. Akiyama, and H. G. Neumann. 1958. '[Intraocular pressure in normal human eyes]', *Klin Monbl Augenheilkd Augenarztl Fortbild*, 133: 662-70.

Li, L. C., J. Li, and J. Gao. 2014. 'Functions of galectin-3 and its role in fibrotic diseases', *J Pharmacol Exp Ther*, 351: 336-43.

Li, M., W. Zhao, Y. Gao, P. Hao, J. Shang, H. Duan, Z. Yang, and X. Li. 2019. 'Differentiation of Bone Marrow Mesenchymal Stem Cells into Neural Lineage Cells Induced by bFGF-Chitosan Controlled Release System', *Biomed Res Int*, 2019: 5086297.

Li, R., Y. Jin, Q. Li, X. Sun, H. Zhu, and H. Cui. 2018. 'MiR-93-5p targeting PTEN regulates the NMDA-induced autophagy of retinal ganglion cells via AKT/mTOR pathway in glaucoma', *Biomed Pharmacother*, 100: 1-7.

Li, Y., T. Li, Z. Zhou, and Y. Xiao. 2022. 'Emerging roles of Galectin-3 in diabetes and diabetes complications: A snapshot', *Rev Endocr Metab Disord*, 23: 569-77.

Limb, G. A., T. E. Salt, P. M. Munro, S. E. Moss, and P. T. Khaw. 2002. 'In vitro characterization of a spontaneously immortalized human Muller cell line (MIO-M1)', *Invest Ophthalmol Vis Sci*, 43: 864-9.

Liu, C. Y., Y. Yang, W. N. Ju, X. Wang, and H. L. Zhang. 2018. 'Emerging Roles of Astrocytes in Neuro-Vascular Unit and the Tripartite Synapse With Emphasis on Reactive Gliosis in the Context of Alzheimer's Disease', *Front Cell Neurosci*, 12: 193.

Long, Q., Q. Luo, K. Wang, A. Bates, and A. K. Shetty. 2017. 'Mash1-dependent Notch Signaling Pathway Regulates GABAergic Neuron-Like Differentiation from Bone Marrow-Derived Mesenchymal Stem Cells', *Aging Dis*, 8: 301-13.

Lundkvist, A., A. Reichenbach, C. Betsholtz, P. Carmeliet, H. Wolburg, and M. Pekny. 2004. 'Under stress, the absence of intermediate filaments from Muller cells in the retina has structural and functional consequences', *J Cell Sci*, 117: 3481-8.

Luo, L. H., D. M. Li, Y. L. Wang, K. Wang, L. X. Gao, S. Li, J. G. Yang, C. L. Li, W. Feng, and H. Guo. 2017. 'Tim3/galectin-9 alleviates the inflammation of TAO patients via suppressing Akt/NF-kB signaling pathway', *Biochem Biophys Res Commun*, 491: 966-72.

Mac Nair, C. E., K. A. Fernandes, C. L. Schlamp, R. T. Libby, and R. W. Nickells. 2014. 'Tumor necrosis factor alpha has an early protective effect on retinal ganglion cells after optic nerve crush', *J Neuroinflammation*, 11: 194.

Mackinnon, A. C., M. A. Gibbons, S. L. Farnworth, H. Leffler, U. J. Nilsson, T. Delaine, A. J. Simpson, S. J. Forbes, N. Hirani, J. Gauldie, and T. Sethi. 2012. 'Regulation of transforming growth factor-beta1-driven lung fibrosis by galectin-3', *Am J Respir Crit Care Med*, 185: 537-46.

Madeira, M. H., F. Elvas, R. Boia, F. Q. Goncalves, R. A. Cunha, A. F. Ambrosio, and A. R. Santiago. 2015. 'Adenosine A2AR blockade prevents neuroinflammation-induced death of retinal ganglion cells caused by elevated pressure', *J Neuroinflammation*, 12: 115.

Manouchehrian, O., K. Arner, T. Deierborg, and L. Taylor. 2015. 'Who let the dogs out?: detrimental role of Galectin-3 in hypoperfusion-induced retinal degeneration', *J Neuroinflammation*, 12: 92.

Markowska, A. I., K. C. Jefferies, and N. Panjwani. 2011. 'Galectin-3 protein modulates cell surface expression and activation of vascular endothelial growth factor receptor 2 in human endothelial cells', *J Biol Chem*, 286: 29913-21.

Markowska, A. I., F. T. Liu, and N. Panjwani. 2010. 'Galectin-3 is an important mediator of VEGF- and bFGF-mediated angiogenic response', *J Exp Med*, 207: 1981-93.

Martire, A., F. B. Bedada, S. Uchida, J. Poling, M. Kruger, H. Warnecke, M. Richter, T. Kubin, S. Herold, and T. Braun. 2016. 'Mesenchymal stem cells attenuate inflammatory processes in the heart and lung via inhibition of TNF signaling', *Basic Res Cardiol*, 111: 54.

Masuda, T., M. Shimazawa, and H. Hara. 2017. 'Retinal Diseases Associated with Oxidative Stress and the Effects of a Free Radical Scavenger (Edaravone)', *Oxid Med Cell Longev*, 2017: 9208489.

Mauris, J., A. M. Woodward, Z. Cao, N. Panjwani, and P. Argueso. 2014. 'Molecular basis for MMP9 induction and disruption of epithelial cell-cell contacts by galectin-3', *J Cell Sci*, 127: 3141-8.

Mead, B., Z. Ahmed, and S. Tomarev. 2018. 'Mesenchymal Stem Cell-Derived Small Extracellular Vesicles Promote Neuroprotection in a Genetic DBA/2J Mouse Model of Glaucoma', *Invest Ophthalmol Vis Sci*, 59: 5473-80.

Mead, B., J. Amaral, and S. Tomarev. 2018. 'Mesenchymal Stem Cell-Derived Small Extracellular Vesicles Promote Neuroprotection in Rodent Models of Glaucoma', *Invest Ophthalmol Vis Sci*, 59: 702-14.

Mead, B., and S. Tomarev. 2017. 'Bone Marrow-Derived Mesenchymal Stem Cells-Derived Exosomes Promote Survival of Retinal Ganglion Cells Through miRNA-Dependent Mechanisms', *Stem Cells Transl Med*, 6: 1273-85.

Meldolesi, J. 2017. 'Neurotrophin receptors in the pathogenesis, diagnosis and therapy of neurodegenerative diseases', *Pharmacol Res*, 121: 129-37.

Melo, F. H., D. Butera, S. Junqueira Mde, D. K. Hsu, A. M. da Silva, F. T. Liu, M. F. Santos, and R. Chammas. 2011. 'The promigratory activity of the matricellular protein galectin-3 depends on the activation of PI-3 kinase', *PLoS One*, 6: e29313.

Mendonca, H. R., J. N. A. Carvalho, C. A. Abreu, D. Mariano de Souza Aguiar Dos Santos, J. R. Carvalho, S. A. Marques, K. da Costa Calaza, and A. M. B. Martinez. 2018. 'Lack of Galectin-3 attenuates neuroinflammation and protects the retina and optic nerve of diabetic mice', *Brain Res*, 1700: 126-37.

Meyer-Franke, A., M. R. Kaplan, F. W. Pfrieger, and B. A. Barres. 1995. 'Characterization of the signaling interactions that promote the survival and growth of developing retinal ganglion cells in culture', *Neuron*, 15: 805-19.

Mirshahi, A., R. Hoehn, K. Lorenz, C. Kramann, and H. Baatz. 2012. 'Anti-tumor necrosis factor alpha for retinal diseases: current knowledge and future concepts', *J Ophthalmic Vis Res*, 7: 39-44.

Mitsuhiro, M. R., S. Eguchi, and H. Yamashita. 2003. 'Regulation mechanisms of retinal pigment epithelial cell migration by the TGF-beta superfamily', *Acta Ophthalmol Scand*, 81: 630-8.

Mochizuki, M., S. Sugita, and K. Kamoi. 2013. 'Immunological homeostasis of the eye', *Prog Retin Eye Res*, 33: 10-27.

Moiseeva, E. P., B. Williams, and N. J. Samani. 2003. 'Galectin 1 inhibits incorporation of vitronectin and chondroitin sulfate B into the extracellular matrix of human vascular smooth muscle cells', *Biochim Biophys Acta*, 1619: 125-32.

Moore, D., A. Harris, D. Wudunn, N. Kheradiya, and B. Siesky. 2008. 'Dysfunctional regulation of ocular blood flow: A risk factor for glaucoma?', *Clin Ophthalmol*, 2: 849-61.

Morgan, J. E. 2000. 'Optic nerve head structure in glaucoma: astrocytes as mediators of axonal damage', *Eye (Lond)*, 14 (Pt 3B): 437-44.

Morgan, J. E., and J. R. Tribble. 2015. 'Microbead models in glaucoma', *Exp Eye Res*, 141: 9-14.

Morrison, J. C., W. O. Cepurna Ying Guo, and E. C. Johnson. 2011. 'Pathophysiology of human glaucomatous optic nerve damage: insights from rodent models of glaucoma', *Exp Eye Res*, 93: 156-64.

Morrison, J. C., C. G. Moore, L. M. Deppmeier, B. G. Gold, C. K. Meshul, and E. C. Johnson. 1997. 'A rat model of chronic pressure-induced optic nerve damage', *Exp Eye Res*, 64: 85-96.

Morrison, J., S. Farrell, E. Johnson, L. Deppmeier, C. G. Moore, and E. Grossmann. 1995. 'Structure and composition of the rodent lamina cribrosa', *Exp Eye Res*, 60: 127-35.

Moshiri, A., C. R. McGuire, and T. A. Reh. 2005. 'Sonic hedgehog regulates proliferation of the retinal ciliary marginal zone in posthatch chicks', *Dev Dyn*, 233: 66-75.

Mozaffarieh, M., and J. Flammer. 2013. 'New insights in the pathogenesis and treatment of normal tension glaucoma', *Curr Opin Pharmacol*, 13: 43-9.

Murphy-Ullrich, J. E., and J. C. Downs. 2015. 'The Thrombospondin1-TGF-beta Pathway and Glaucoma', *J Ocul Pharmacol Ther*, 31: 371-5.

Nagae, M., N. Nishi, T. Murata, T. Usui, T. Nakamura, S. Wakatsuki, and R. Kato. 2009. 'Structural analysis of the recognition mechanism of poly-N-acetyllactosamine by the human galectin-9 N-terminal carbohydrate recognition domain', *Glycobiology*, 19: 112-7.

Nakano, T., S. Ando, N. Takata, M. Kawada, K. Muguruma, K. Sekiguchi, K. Saito, S. Yonemura, M. Eiraku, and Y. Sasai. 2012. 'Self-formation of optic cups and storable stratified neural retina from human ESCs', *Cell Stem Cell*, 10: 771-85.

Nam, K., S. H. Son, S. Oh, D. Jeon, H. Kim, D. Y. Noh, S. Kim, and I. Shin. 2017. 'Binding of galectin-1 to integrin beta1 potentiates drug resistance by promoting survivin expression in breast cancer cells', *Oncotarget*, 8: 35804-23.

Nangia-Makker, P., S. Nakahara, V. Hogan, and A. Raz. 2007. 'Galectin-3 in apoptosis, a novel therapeutic target', *J Bioenerg Biomembr*, 39: 79-84.

Nelson, C. M., K. M. Ackerman, P. O'Hayer, T. J. Bailey, R. A. Gorsuch, and D. R. Hyde. 2013. 'Tumor necrosis factor-alpha is produced by dying retinal neurons and is required for Muller glia proliferation during zebrafish retinal regeneration', *J Neurosci*, 33: 6524-39.

Nelson, C. M., R. A. Gorsuch, T. J. Bailey, K. M. Ackerman, S. C. Kassen, and D. R. Hyde. 2012. 'Stat3 defines three populations of Muller glia and is required for initiating maximal muller glia proliferation in the regenerating zebrafish retina', *J Comp Neurol*, 520: 4294-311.

Newman, E. A. 1993. 'Inward-rectifying potassium channels in retinal glial (Muller) cells', *J Neurosci*, 13: 3333-45.

Newman, E., and A. Reichenbach. 1996. 'The Muller cell: a functional element of the retina', *Trends Neurosci*, 19: 307-12.

Nie, X. G., D. S. Fan, Y. X. Huang, Y. Y. He, B. L. Dong, and F. Gao. 2018. 'Downregulation of microRNA-149 in retinal ganglion cells suppresses apoptosis through activation of the PI3K/Akt signaling pathway in mice with glaucoma', *Am J Physiol Cell Physiol*, 315: C839-C49.

Nielsen, M. I., J. Stegmayr, O. C. Grant, Z. Yang, U. J. Nilsson, I. Boos, M. C. Carlsson, R. J. Woods, C. Unverzagt, H. Leffler, and H. H. Wandall. 2018. 'Galectin binding to cells and glycoproteins with genetically modified glycosylation reveals galectin-glycan specificities in a natural context', *J Biol Chem*, 293: 20249-62.

Nishi, Y., H. Sano, T. Kawashima, T. Okada, T. Kuroda, K. Kikkawa, S. Kawashima, M. Tanabe, T. Goto, Y. Matsuzawa, R. Matsumura, H. Tomioka, F. T. Liu, and K. Shirai. 2007. 'Role of galectin-3 in human pulmonary fibrosis', *Allergol Int*, 56: 57-65.

Niwa, M., H. Aoki, A. Hirata, H. Tomita, P. G. Green, and A. Hara. 2016. 'Retinal Cell Degeneration in Animal Models', *Int J Mol Sci*, 17.

Nolte-'t Hoen, E., T. Cremer, R. C. Gallo, and L. B. Margolis. 2016. 'Extracellular vesicles and viruses: Are they close relatives?', *Proc Natl Acad Sci U S A*, 113: 9155-61.

O'Hara-Wright, M., and A. Gonzalez-Cordero. 2020. 'Retinal organoids: a window into human retinal development', *Development*, 147.

Obermann, J., C. S. Priglinger, J. Merl-Pham, A. Geerlof, S. Priglinger, M. Gotz, and S. M. Hauck. 2017. 'Proteome-wide Identification of Glycosylation-dependent Interactors of Galectin-1 and Galectin-3 on Mesenchymal Retinal Pigment Epithelial (RPE) Cells', *Mol Cell Proteomics*, 16: 1528-46.

Pan, D., X. Chang, M. Xu, M. Zhang, S. Zhang, Y. Wang, X. Luo, J. Xu, X. Yang, and X. Sun. 2019. 'UMSC-derived exosomes promote retinal ganglion cells survival in a rat model of optic nerve crush', *J Chem Neuroanat*, 96: 134-39.

Pan, D., X. X. Xia, H. Zhou, S. Q. Jin, Y. Y. Lu, H. Liu, M. L. Gao, and Z. B. Jin. 2020. 'COCO enhances the efficiency of photoreceptor precursor differentiation in early human embryonic stem cell-derived retinal organoids', *Stem Cell Res Ther*, 11: 366.

Pang, I. H., and A. F. Clark. 2007. 'Rodent models for glaucoma retinopathy and optic neuropathy', *J Glaucoma*, 16: 483-505.

Pardue, M. T., and R. S. Allen. 2018. 'Neuroprotective strategies for retinal disease', *Prog Retin Eye Res*, 65: 50-76.

Park, K. K., K. Liu, Y. Hu, P. D. Smith, C. Wang, B. Cai, B. Xu, L. Connolly, I. Kramvis, M. Sahin, and Z. He. 2008. 'Promoting axon regeneration in the adult CNS by modulation of the PTEN/mTOR pathway', *Science*, 322: 963-6.

Partridge, E. A., C. Le Roy, G. M. Di Guglielmo, J. Pawling, P. Cheung, M. Granovsky, I. R. Nabi, J. L. Wrana, and J. W. Dennis. 2004. 'Regulation of cytokine receptors by Golgi N-glycan processing and endocytosis', *Science*, 306: 120-4.

Pearson, R. A., A. Gonzalez-Cordero, E. L. West, J. R. Ribeiro, N. Aghaizu, D. Goh, R. D. Sampson, A. Georgiadis, P. V. Waldron, Y. Duran, A. Naeem, M. Kloc, E. Cristante, K. Kruczek, K. Warre-Cornish, J. C. Sowden, A. J. Smith, and R. R. Ali. 2016. 'Donor and host photoreceptors engage in material transfer following transplantation of post-mitotic photoreceptor precursors', *Nat Commun*, 7: 13029.

Peng, H., Y. B. Sun, J. L. Hao, C. W. Lu, M. C. Bi, and E. Song. 2019. 'Neuroprotective effects of overexpressed microRNA-200a on activation of glaucoma-related retinal glial cells and apoptosis of ganglion cells via downregulating FGF7-mediated MAPK signaling pathway', *Cell Signal*, 54: 179-90.

Perillo, N. L., K. E. Pace, J. J. Seilhamer, and L. G. Baum. 1995. 'Apoptosis of T cells mediated by galectin-1', *Nature*, 378: 736-9.

Petrenko, Y., I. Vackova, K. Kekulova, M. Chudickova, Z. Koci, K. Turnovcova, H. Kupcova Skalnikova, P. Vodicka, and S. Kubinova. 2020. 'A Comparative Analysis of Multipotent Mesenchymal Stromal Cells derived from Different Sources, with a Focus on Neuroregenerative Potential', *Sci Rep*, 10: 4290.

Pfeiffer, R. L., J. R. Anderson, J. Dahal, J. C. Garcia, J. H. Yang, C. L. Sigulinsky, K. Rapp, D. P. Emrich, C. B. Watt, H. A. Johnstun, A. R. Houser, R. E. Marc, and B. W. Jones. 2020. 'A pathoconnectome of early neurodegeneration: Network changes in retinal degeneration', *Exp Eye Res*, 199: 108196.

Pittenger, M. F., A. M. Mackay, S. C. Beck, R. K. Jaiswal, R. Douglas, J. D. Mosca, M. A. Moorman, D. W. Simonetti, S. Craig, and D. R. Marshak. 1999. 'Multilineage potential of adult human mesenchymal stem cells', *Science*, 284: 143-7.

Poitry-Yamate, C. L., S. Poitry, and M. Tsacopoulos. 1995. 'Lactate released by Muller glial cells is metabolized by photoreceptors from mammalian retina', *J Neurosci*, 15: 5179-91.

Popa, S. J., S. E. Stewart, and K. Moreau. 2018. 'Unconventional secretion of annexins and galectins', *Semin Cell Dev Biol*, 83: 42-50.

Porciatti, V. 2015. 'Electrophysiological assessment of retinal ganglion cell function', *Exp Eye Res*, 141: 164-70.

Priglinger, C. S., J. Obermann, C. M. Szober, J. Merl-Pham, U. Ohmayer, J. Behler, F. Gruhn, T. C. Kreutzer, C. Wertheimer, A. Geerlof, S. G. Priglinger, and S. M. Hauck. 2016. 'Epithelial-to-Mesenchymal Transition of RPE Cells In Vitro Confers Increased beta1,6-N-Glycosylation and Increased Susceptibility to Galectin-3 Binding', *PLoS One*, 11: e0146887.

Priglinger, C. S., C. M. Szober, S. G. Priglinger, J. Merl, K. N. Euler, M. Kernt, G. Gondi, J. Behler, A. Geerlof, A. Kampik, M. Ueffing, and S. M. Hauck. 2013. 'Galectin-3 induces clustering of CD147 and integrin-beta1 transmembrane glycoprotein receptors on the RPE cell surface', *PLoS One*, 8: e70011.

Qian, X., C. Xu, S. Fang, P. Zhao, Y. Wang, H. Liu, W. Yuan, and Z. Qi. 2016. 'Exosomal MicroRNAs Derived From Umbilical Mesenchymal Stem Cells Inhibit Hepatitis C Virus Infection', *Stem Cells Transl Med*, 5: 1190-203.

Qin, Z., L. K. Barthel, and P. A. Raymond. 2009. 'Genetic evidence for shared mechanisms of epimorphic regeneration in zebrafish', *Proc Natl Acad Sci U S A*, 106: 9310-5.

Quigley, H. A., and E. M. Addicks. 1980. 'Chronic experimental glaucoma in primates. I. Production of elevated intraocular pressure by anterior chamber injection of autologous ghost red blood cells', *Invest Ophthalmol Vis Sci*, 19: 126-36.

Quigley, H. A., and A. T. Broman. 2006. 'The number of people with glaucoma worldwide in 2010 and 2020', *Br J Ophthalmol*, 90: 262-7.

Quigley, H. A., S. J. McKinnon, D. J. Zack, M. E. Pease, L. A. Kerrigan-Baumrind, D. F. Kerrigan, and R. S. Mitchell. 2000. 'Retrograde axonal transport of BDNF in retinal ganglion cells is blocked by acute IOP elevation in rats', *Invest Ophthalmol Vis Sci*, 41: 3460-6.

Rabesandratana, O., A. Chaffiol, A. Mialot, A. Slembrouck-Brec, C. Joffrois, C. Nanteau, A. Rodrigues, G. Gagliardi, S. Reichman, J. A. Sahel, A. Chedotal, J. Duebel, O. Goureau, and G. Orieux. 2020. 'Generation of a Transplantable Population of Human iPSC-Derived Retinal Ganglion Cells', *Front Cell Dev Biol*, 8: 585675.

Rainer, G., R. Menapace, O. Findl, B. Kiss, V. Petternel, M. Georgopoulos, and B. Schneider. 2001. 'Intraocular pressure rise after small incision cataract surgery: a randomised intraindividual comparison of two dispersive viscoelastic agents', *Br J Ophthalmol*, 85: 139-42.

Ramirez, A. I., R. de Hoz, E. Salobrar-Garcia, J. J. Salazar, B. Rojas, D. Ajoy, I. Lopez-Cuenca, P. Rojas, A. Trivino, and J. M. Ramirez. 2017. 'The Role of Microglia in Retinal Neurodegeneration: Alzheimer's Disease, Parkinson, and Glaucoma', *Front Aging Neurosci*, 9: 214.

Rashidi, H., Y. C. Leong, K. Venner, H. Pramod, Q. Z. Fei, O. J. R. Jones, D. Moulding, and J. C. Sowden. 2022. 'Generation of 3D retinal tissue from human pluripotent stem cells using a directed small molecule-based serum-free microwell platform', *Sci Rep*, 12: 6646.

Raymond, P. A., L. K. Barthel, R. L. Bernardos, and J. J. Perkowski. 2006. 'Molecular characterization of retinal stem cells and their niches in adult zebrafish', *BMC Dev Biol*, 6: 36.

Regent, F., H. Y. Chen, R. A. Kelley, Z. Qu, A. Swaroop, and T. Li. 2020. 'A simple and efficient method for generating human retinal organoids', *Mol Vis*, 26: 97-105.

Reichenbach, A., J. U. Stolzenburg, W. Eberhardt, T. I. Chao, D. Dettmer, and L. Hertz. 1993. 'What do retinal muller (glial) cells do for their neuronal 'small siblings'?', *J Chem Neuroanat*, 6: 201-13.

Reichenbach, Andreas, and Andreas Bringmann. 2010. *Müller cells in the healthy and diseased retina* (Springer: New York).

Ren, R., J. B. Jonas, G. Tian, Y. Zhen, K. Ma, S. Li, H. Wang, B. Li, X. Zhang, and N. Wang. 2010. 'Cerebrospinal fluid pressure in glaucoma: a prospective study', *Ophthalmology*, 117: 259-66.

Rhee, D. J., R. N. Fariss, R. Brekken, E. H. Sage, and P. Russell. 2003. 'The matricellular protein SPARC is expressed in human trabecular meshwork', *Exp Eye Res*, 77: 601-7.

Rhee, D. J., R. I. Haddadin, M. H. Kang, and D. J. Oh. 2009. 'Matricellular proteins in the trabecular meshwork', *Exp Eye Res*, 88: 694-703.

Ridano, M. E., P. V. Subirada, M. C. Paz, V. E. Lorenc, J. C. Stupirski, A. L. Gramajo, J. D. Luna, D. O. Croci, G. A. Rabinovich, and M. C. Sanchez. 2017. 'Galectin-1 expression imprints a neurovascular phenotype in proliferative retinopathies and delineates responses to anti-VEGF', *Oncotarget*, 8: 32505-22.

Ritchie, S., D. Neal, H. Shlevin, A. Allgood, and P. Traber. 2017. 'A phase 2a, open-label pilot study of the galectin-3 inhibitor GR-MD-02 for the treatment of moderate-to-severe plaque psoriasis', *J Am Acad Dermatol*, 77: 753-55.

Romero, M. D., J. C. Muino, G. A. Bianco, M. Ferrero, C. P. Juarez, J. D. Luna, and G. A. Rabinovich. 2006. 'Circulating anti-galectin-1 antibodies are associated with the

severity of ocular disease in autoimmune and infectious uveitis', *Invest Ophthalmol Vis Sci*, 47: 1550-6.

Saijilafu, E. M. Hur, C. M. Liu, Z. Jiao, W. L. Xu, and F. Q. Zhou. 2013. 'PI3K-GSK3 signalling regulates mammalian axon regeneration by inducing the expression of Smad1', *Nat Commun*, 4: 2690.

Sampson, J. F., E. Hasegawa, L. Mulki, A. Suryawanshi, S. Jiang, W. S. Chen, G. A. Rabinovich, K. M. Connor, and N. Panjwani. 2015. 'Galectin-8 Ameliorates Murine Autoimmune Ocular Pathology and Promotes a Regulatory T Cell Response', *PLoS One*, 10: e0130772.

Sampson, J. F., A. Suryawanshi, W. S. Chen, G. A. Rabinovich, and N. Panjwani. 2016. 'Galectin-8 promotes regulatory T-cell differentiation by modulating IL-2 and TGFbeta signaling', *Immunol Cell Biol*, 94: 213-9.

Santos-Ferreira, T., S. Llonch, O. Borsch, K. Postel, J. Haas, and M. Ader. 2016. 'Retinal transplantation of photoreceptors results in donor-host cytoplasmic exchange', *Nat Commun*, 7: 13028.

Saravanan, C., F. T. Liu, I. K. Gipson, and N. Panjwani. 2009. 'Galectin-3 promotes lamellipodia formation in epithelial cells by interacting with complex N-glycans on alpha3beta1 integrin', *J Cell Sci*, 122: 3684-93.

Sardar Pasha, S. P. B., R. Munch, P. Schafer, P. Oertel, A. M. Sykes, Y. Zhu, and M. O. Karl. 2017. 'Retinal cell death dependent reactive proliferative gliosis in the mouse retina', *Sci Rep*, 7: 9517.

Saszik, S. M., J. G. Robson, and L. J. Frishman. 2002. 'The scotopic threshold response of the dark-adapted electroretinogram of the mouse', *J Physiol*, 543: 899-916.

Sayed, D., M. He, C. Hong, S. Gao, S. Rane, Z. Yang, and M. Abdellatif. 2010. 'MicroRNA-21 is a downstream effector of AKT that mediates its antiapoptotic effects via suppression of Fas ligand', *J Biol Chem*, 285: 20281-90.

Schuettauf, F., C. Vorwerk, R. Naskar, A. Orlin, K. Quinto, D. Zurakowski, N. S. Dejneka, R. L. Klein, E. M. Meyer, and J. Bennett. 2004. 'Adeno-associated viruses containing bFGF or BDNF are neuroprotective against excitotoxicity', *Curr Eye Res*, 29: 379-86.

Sehrawat, S., A. Suryawanshi, M. Hirashima, and B. T. Rouse. 2009. 'Role of Tim-3/galectin-9 inhibitory interaction in viral-induced immunopathology: shifting the balance toward regulators', *J Immunol*, 182: 3191-201.

Sharma, U. C., S. Pokharel, T. J. van Brakel, J. H. van Berlo, J. P. Cleutjens, B. Schroen, S. Andre, H. J. Crijns, H. J. Gabius, J. Maessen, and Y. M. Pinto. 2004. 'Galectin-3 marks activated macrophages in failure-prone hypertrophied hearts and contributes to cardiac dysfunction', *Circulation*, 110: 3121-8.

Shen, H., J. Wang, J. Min, W. Xi, Y. Gao, L. Yin, Y. Yu, K. Liu, J. Xiao, Y. F. Zhang, and Z. N. Wang. 2018. 'Activation of TGF-beta1/alpha-SMA/Col I Profibrotic Pathway in Fibroblasts by Galectin-3 Contributes to Atrial Fibrosis in Experimental Models and Patients', *Cell Physiol Biochem*, 47: 851-63.

Shimmura-Tomita, M., M. Wang, H. Taniguchi, H. Akiba, H. Yagita, and J. Hori. 2013. 'Galectin-9-mediated protection from allo-specific T cells as a mechanism of immune privilege of corneal allografts', *PLoS One*, 8: e63620.

Sieving, P. A., R. C. Caruso, W. Tao, H. R. Coleman, D. J. Thompson, K. R. Fullmer, and R. A. Bush. 2006. 'Ciliary neurotrophic factor (CNTF) for human retinal degeneration: phase I trial of CNTF delivered by encapsulated cell intraocular implants', *Proc Natl Acad Sci U S A*, 103: 3896-901.

Siew, J. J., H. M. Chen, H. Y. Chen, H. L. Chen, C. M. Chen, B. W. Soong, Y. R. Wu, C. P. Chang, Y. C. Chan, C. H. Lin, F. T. Liu, and Y. Chern. 2019. 'Galectin-3 is required for the microglia-mediated brain inflammation in a model of Huntington's disease', *Nat Commun*, 10: 3473.

Silva, A. O., C. E. Ercole, and S. C. McLoon. 2003. 'Regulation of ganglion cell production by Notch signaling during retinal development', *J Neurobiol*, 54: 511-24.

Singhal, S., B. Bhatia, H. Jayaram, S. Becker, M. F. Jones, P. B. Cottrill, P. T. Khaw, T. E. Salt, and G. A. Limb. 2012. 'Human Muller glia with stem cell characteristics differentiate into retinal ganglion cell (RGC) precursors in vitro and partially restore RGC function in vivo following transplantation', *Stem Cells Transl Med*, 1: 188-99.

Sluch, V. M., C. H. Davis, V. Ranganathan, J. M. Kerr, K. Krick, R. Martin, C. A. Berlinicke, N. Marsh-Armstrong, J. S. Diamond, H. Q. Mao, and D. J. Zack. 2015. 'Differentiation of human ESCs to retinal ganglion cells using a CRISPR engineered reporter cell line', *Sci Rep*, 5: 16595.

Sneddon, L. U., L. G. Halsey, and N. R. Bury. 2017. 'Considering aspects of the 3Rs principles within experimental animal biology', *J Exp Biol*, 220: 3007-16.

Soria, J., A. Acera, J. A. Duran, A. Boto-de-Los-Bueis, A. Del-Hierro-Zarzuelo, N. Gonzalez, R. Reigada, and T. Suarez. 2018. 'The analysis of human conjunctival epithelium proteome in ocular surface diseases using impression cytology and 2D-DIGE', *Exp Eye Res*, 167: 31-43.

Sridhar, A., A. Hoshino, C. R. Finkbeiner, A. Chitsazan, L. Dai, A. K. Haugan, K. M. Eschenbacher, D. L. Jackson, C. Trapnell, O. Bermingham-McDonogh, I. Glass, and T. A. Reh. 2020. 'Single-Cell Transcriptomic Comparison of Human Fetal Retina, hPSC-Derived Retinal Organoids, and Long-Term Retinal Cultures', *Cell Rep*, 30: 1644-59 e4.

Stadler, J. A., A. Shkumatava, and C. J. Neumann. 2004. 'The role of hedgehog signaling in the development of the zebrafish visual system', *Dev Neurosci*, 26: 346-51.

Stanton, B. Z., and L. F. Peng. 2010. 'Small-molecule modulators of the Sonic Hedgehog signaling pathway', *Mol Biosyst*, 6: 44-54.

Starossom, S. C., I. D. Mascanfroni, J. Imitola, L. Cao, K. Raddassi, S. F. Hernandez, R. Bassil, D. O. Croci, J. P. Cerliani, D. Delacour, Y. Wang, W. Elyaman, S. J. Khoury, and G. A. Rabinovich. 2012. 'Galectin-1 deactivates classically activated microglia and protects from inflammation-induced neurodegeneration', *Immunity*, 37: 249-63.

Stout, J. T., and P. J. Francis. 2011. 'Surgical approaches to gene and stem cell therapy for retinal disease', *Hum Gene Ther*, 22: 531-5.

Stowell, S. R., C. M. Arthur, P. Mehta, K. A. Slanina, O. Blixt, H. Leffler, D. F. Smith, and R. D. Cummings. 2008. 'Galectin-1, -2, and -3 exhibit differential recognition of sialylated glycans and blood group antigens', *J Biol Chem*, 283: 10109-23.

Sugaya, S., W. S. Chen, Z. Cao, K. R. Kenyon, T. Yamaguchi, M. Omoto, P. Hamrah, and N. Panjwani. 2015. 'Comparison of galectin expression signatures in rejected and accepted murine corneal allografts', *Cornea*, 34: 675-81.

Suryawanshi, A., Z. Cao, T. Thitiprasert, T. S. Zaidi, and N. Panjwani. 2013. 'Galectin-1-mediated suppression of Pseudomonas aeruginosa-induced corneal immunopathology', *J Immunol*, 190: 6397-409.

Suthahar, N., W. C. Meijers, H. H. W. Sillje, J. E. Ho, F. T. Liu, and R. A. de Boer. 2018. 'Galectin-3 Activation and Inhibition in Heart Failure and Cardiovascular Disease: An Update', *Theranostics*, 8: 593-609.

Takahashi, K., K. Okita, M. Nakagawa, and S. Yamanaka. 2007. 'Induction of pluripotent stem cells from fibroblast cultures', *Nat Protoc*, 2: 3081-9.

Takahashi, K., K. Tanabe, M. Ohnuki, M. Narita, T. Ichisaka, K. Tomoda, and S. Yamanaka. 2007. 'Induction of pluripotent stem cells from adult human fibroblasts by defined factors', *Cell*, 131: 861-72.

Tang, Z., S. Zhang, C. Lee, A. Kumar, P. Arjunan, Y. Li, F. Zhang, and X. Li. 2011. 'An optic nerve crush injury murine model to study retinal ganglion cell survival', *J Vis Exp*.

Taniguchi, T., A. M. Woodward, P. Magnelli, N. M. McColgan, S. Lehoux, S. M. P. Jacobo, J. Mauris, and P. Argueso. 2017. 'N-Glycosylation affects the stability and barrier function of the MUC16 mucin', *J Biol Chem*, 292: 11079-90.

Tassew, N. G., J. Charish, A. P. Shabanzadeh, V. Luga, H. Harada, N. Farhani, P. D'Onofrio, B. Choi, A. Ellabban, P. E. B. Nickerson, V. A. Wallace, P. D. Koeberle, J. L. Wrana, and P. P. Monnier. 2017. 'Exosomes Mediate Mobilization of Autocrine Wnt10b to Promote Axonal Regeneration in the Injured CNS', *Cell Rep*, 20: 99-111.

Taylor, S., B. Srinivasan, R. J. Wordinger, and R. S. Roque. 2003. 'Glutamate stimulates neurotrophin expression in cultured Muller cells', *Brain Res Mol Brain Res*, 111: 189-97.

Teixeira, F. G., M. M. Carvalho, K. M. Panchalingam, A. J. Rodrigues, B. Mendes-Pinheiro, S. Anjo, B. Manadas, L. A. Behie, N. Sousa, and A. J. Salgado. 2017. 'Impact of the Secretome of Human Mesenchymal Stem Cells on Brain Structure and Animal Behavior in a Rat Model of Parkinson's Disease', *Stem Cells Transl Med*, 6: 634-46.

Tezel, G. 2008. 'TNF-alpha signaling in glaucomatous neurodegeneration', *Prog Brain Res*, 173: 409-21.

Tham, Y. C., X. Li, T. Y. Wong, H. A. Quigley, T. Aung, and C. Y. Cheng. 2014. 'Global prevalence of glaucoma and projections of glaucoma burden through 2040: a systematic review and meta-analysis', *Ophthalmology*, 121: 2081-90.

Thanos, C. G., W. J. Bell, P. O'Rourke, K. Kauper, S. Sherman, P. Stabila, and W. Tao. 2004. 'Sustained secretion of ciliary neurotrophic factor to the vitreous, using the encapsulated cell therapy-based NT-501 intraocular device', *Tissue Eng*, 10: 1617-22.

Thiemann, S., and L. G. Baum. 2016. 'Galectins and Immune Responses-Just How Do They Do Those Things They Do?', *Annu Rev Immunol*, 34: 243-64.

Tielsch, J. M., J. Katz, K. Singh, H. A. Quigley, J. D. Gottsch, J. Javitt, and A. Sommer. 1991. 'A population-based evaluation of glaucoma screening: the Baltimore Eye Survey', *Am J Epidemiol*, 134: 1102-10.

Toscano, M. A., A. G. Commodaro, J. M. Ilarregui, G. A. Bianco, A. Liberman, H. M. Serra, J. Hirabayashi, L. V. Rizzo, and G. A. Rabinovich. 2006. 'Galectin-1 suppresses autoimmune retinal disease by promoting concomitant Th2- and T regulatory-mediated anti-inflammatory responses', *J Immunol*, 176: 6323-32.

Tripathi, R. C., J. Li, W. F. Chan, and B. J. Tripathi. 1994. 'Aqueous humor in glaucomatous eyes contains an increased level of TGF-beta 2', *Exp Eye Res*, 59: 723-7.

Trivli, A., I. Koliarakis, C. Terzidou, G. N. Goulielmos, C. S. Siganos, D. A. Spandidos, G. Dalianis, and E. T. Detorakis. 2019. 'Normal-tension glaucoma: Pathogenesis and genetics', *Exp Ther Med*, 17: 563-74.

Uchino, Y. 2018. 'The Ocular Surface Glycocalyx and its Alteration in Dry Eye Disease: A Review', *Invest Ophthalmol Vis Sci*, 59: DES157-DES62.

Uchino, Y., A. M. Woodward, J. Mauris, K. Peterson, P. Verma, U. J. Nilsson, J. Rajaiya, and P. Argueso. 2018. 'Galectin-3 is an amplifier of the interleukin-1beta-mediated inflammatory response in corneal keratinocytes', *Immunology*, 154: 490-99.

Uehara, F., N. Ohba, and M. Ozawa. 2001. 'Isolation and characterization of galectins in the mammalian retina', *Invest Ophthalmol Vis Sci*, 42: 2164-72.

Ulyanova, T., A. Szel, R. K. Kutty, B. Wiggert, A. R. Caffe, G. J. Chader, and T. van Veen. 2001. 'Oxidative stress induces heme oxygenase-1 immunoreactivity in Muller cells of mouse retina in organ culture', *Invest Ophthalmol Vis Sci*, 42: 1370-4.

van der Leij, J., A. van den Berg, T. Blokzijl, G. Harms, H. van Goor, P. Zwiers, R. van Weeghel, S. Poppema, and L. Visser. 2004. 'Dimeric galectin-1 induces IL-10 production in T-lymphocytes: an important tool in the regulation of the immune response', *J Pathol*, 204: 511-8.

van Reyk, D. M., M. C. Gillies, and M. J. Davies. 2003. 'The retina: oxidative stress and diabetes', *Redox Rep*, 8: 187-92.

Varki, A. 1993. 'Biological roles of oligosaccharides: all of the theories are correct', *Glycobiology*, 3: 97-130.

Vilela, C. A. P., A. Messias, R. T. Calado, R. C. Siqueira, M. J. L. Silva, D. T. Covas, and J. S. Paula. 2021. 'Retinal function after intravitreal injection of autologous bone marrow-derived mesenchymal stromal cells in advanced glaucoma', *Doc Ophthalmol*.

Vogler, S., A. Grosche, T. Pannicke, E. Ulbricht, P. Wiedemann, A. Reichenbach, and A. Bringmann. 2013. 'Hypoosmotic and glutamate-induced swelling of bipolar cells in the rat retina: comparison with swelling of Muller glial cells', *J Neurochem*, 126: 372-81.

Volkner, M., M. Zschatzsch, M. Rostovskaya, R. W. Overall, V. Busskamp, K. Anastassiadis, and M. O. Karl. 2016. 'Retinal Organoids from Pluripotent Stem Cells Efficiently Recapitulate Retinogenesis', *Stem Cell Reports*, 6: 525-38.

Wagstaff, P. E., A. Heredero Berzal, C. J. F. Boon, P. M. J. Quinn, Alma Ten Asbroek, and A. A. Bergen. 2021. 'The Role of Small Molecules and Their Effect on the Molecular Mechanisms of Early Retinal Organoid Development', *Int J Mol Sci*, 22.

Wahlin, K. J., J. A. Maruotti, S. R. Sripathi, J. Ball, J. M. Angueyra, C. Kim, R. Grebe, W. Li, B. W. Jones, and D. J. Zack. 2017. 'Photoreceptor Outer Segment-like Structures in Long-Term 3D Retinas from Human Pluripotent Stem Cells', *Sci Rep*, 7: 766.

Walshe, T. E., L. L. Leach, and P. A. D'Amore. 2011. 'TGF-beta signaling is required for maintenance of retinal ganglion cell differentiation and survival', *Neuroscience*, 189: 123-31.

Walton, K. L., K. E. Johnson, and C. A. Harrison. 2017. 'Targeting TGF-beta Mediated SMAD Signaling for the Prevention of Fibrosis', *Front Pharmacol*, 8: 461.

Wan, J., X. F. Zhao, A. Vojtek, and D. Goldman. 2014. 'Retinal injury, growth factors, and cytokines converge on beta-catenin and pStat3 signaling to stimulate retina regeneration', *Cell Rep*, 9: 285-97.

Wang, B., K. A. Lucy, J. S. Schuman, I. A. Sigal, R. A. Bilonick, C. Lu, J. Liu, I. Grulkowski, Z. Nadler, H. Ishikawa, L. Kagemann, J. G. Fujimoto, and G. Wollstein. 2018. 'Tortuous Pore Path Through the Glaucomatous Lamina Cribrosa', *Sci Rep*, 8: 7281.

Wang, J., A. Harris, M. A. Prendes, L. Alshawa, J. C. Gross, S. M. Wentz, A. B. Rao, N. J. Kim, A. Synder, and B. Siesky. 2017. 'Targeting Transforming Growth Factor-beta Signaling in Primary Open-Angle Glaucoma', *J Glaucoma*, 26: 390-95.

Wang, K., H. Li, R. Sun, C. Liu, Y. Luo, S. Fu, and Y. Ying. 2019. 'Emerging roles of transforming growth factor beta signaling in wet age-related macular degeneration', *Acta Biochim Biophys Sin (Shanghai)*, 51: 1-8.

Wang, X., X. Zhang, X. P. Ren, J. Chen, H. Liu, J. Yang, M. Medvedovic, Z. Hu, and G. C. Fan. 2010. 'MicroRNA-494 targeting both proapoptotic and antiapoptotic proteins protects against ischemia/reperfusion-induced cardiac injury', *Circulation*, 122: 1308-18.

Wanner, I. B., M. A. Anderson, B. Song, J. Levine, A. Fernandez, Z. Gray-Thompson, Y. Ao, and M. V. Sofroniew. 2013. 'Glial scar borders are formed by newly proliferated, elongated astrocytes that interact to corral inflammatory and fibrotic cells via STAT3-dependent mechanisms after spinal cord injury', *J Neurosci*, 33: 12870-86.

Wdowiak, K., T. Francuz, E. Gallego-Colon, N. Ruiz-Agamez, M. Kubeczko, I. Grochola, and J. Wojnar. 2018. 'Galectin Targeted Therapy in Oncology: Current Knowledge and Perspectives', *Int J Mol Sci*, 19.

Wei, X., K. S. Cho, E. F. Thee, M. J. Jager, and D. F. Chen. 2019. 'Neuroinflammation and microglia in glaucoma: time for a paradigm shift', *J Neurosci Res*, 97: 70-76.

Weinreb, R. N., T. Aung, and F. A. Medeiros. 2014. 'The pathophysiology and treatment of glaucoma: a review', *JAMA*, 311: 1901-11.

Weinreb, R. N., and P. T. Khaw. 2004. 'Primary open-angle glaucoma', *Lancet*, 363: 1711-20.

Wernig, M., A. Meissner, R. Foreman, T. Brambrink, M. Ku, K. Hochedlinger, B. E. Bernstein, and R. Jaenisch. 2007. 'In vitro reprogramming of fibroblasts into a pluripotent ES-cell-like state', *Nature*, 448: 318-24.

Woodcock, T., and M. C. Morganti-Kossmann. 2013. 'The role of markers of inflammation in traumatic brain injury', *Front Neurol*, 4: 18.

Woodward, A. M., J. Mauris, and P. Argueso. 2013. 'Binding of transmembrane mucins to galectin-3 limits herpesvirus 1 infection of human corneal keratinocytes', *J Virol*, 87: 5841-7.

Wooff, Y., S. M. Man, R. Aggio-Bruce, R. Natoli, and N. Fernando. 2019. 'IL-1 Family Members Mediate Cell Death, Inflammation and Angiogenesis in Retinal Degenerative Diseases', *Front Immunol*, 10: 1618.

Wu, D., A. Kanda, Y. Liu, S. Kase, K. Noda, and S. Ishida. 2019. 'Galectin-1 promotes choroidal neovascularization and subretinal fibrosis mediated via epithelial-mesenchymal transition', *FASEB J*, 33: 2498-513.

Xia, X., Y. Li, W. Wang, F. Tang, J. Tan, L. Sun, Q. Li, L. Sun, B. Tang, and S. He. 2015. 'MicroRNA-1908 functions as a glioblastoma oncogene by suppressing PTEN tumor suppressor pathway', *Mol Cancer*, 14: 154.

Yafai, Y., I. Iandiev, J. Lange, J. D. Unterlauft, P. Wiedemann, A. Bringmann, A. Reichenbach, and W. Eichler. 2014. 'Muller glial cells inhibit proliferation of retinal endothelial cells via TGF-beta2 and Smad signaling', *Glia*, 62: 1476-85.

Yamanaka, S., J. Li, G. Kania, S. Elliott, R. P. Wersto, J. Van Eyk, A. M. Wobus, and K. R. Boheler. 2008. 'Pluripotency of embryonic stem cells', *Cell Tissue Res*, 331: 5-22.

Yang, C., Y. Qi, and Z. Sun. 2021. 'The Role of Sonic Hedgehog Pathway in the Development of the Central Nervous System and Aging-Related Neurodegenerative Diseases', *Front Mol Biosci*, 8: 711710.

Yang, N., W. Zhang, T. He, and Y. Xing. 2017. 'Suppression of Retinal Neovascularization by Inhibition of Galectin-1 in a Murine Model of Oxygen-Induced Retinopathy', *J Ophthalmol*, 2017: 5053035.

Yang, R. Y., D. K. Hsu, and F. T. Liu. 1996. 'Expression of galectin-3 modulates T-cell growth and apoptosis', *Proc Natl Acad Sci U S A*, 93: 6737-42.

Youssef, P. N., N. Sheibani, and D. M. Albert. 2011. 'Retinal light toxicity', *Eye (Lond)*, 25: 1-14.

Yu, D. Y., S. J. Cringle, C. Balaratnasingam, W. H. Morgan, P. K. Yu, and E. N. Su. 2013. 'Retinal ganglion cells: Energetics, compartmentation, axonal transport, cytoskeletons and vulnerability', *Prog Retin Eye Res*, 36: 217-46.

Yu, Q., L. Liu, Y. Duan, Y. Wang, X. Xuan, L. Zhou, and W. Liu. 2013. 'Wnt/beta-catenin signaling regulates neuronal differentiation of mesenchymal stem cells', *Biochem Biophys Res Commun*, 439: 297-302.

Zanon Cde, F., N. M. Sonehara, A. P. Girol, C. D. Gil, and S. M. Oliani. 2015. 'Protective effects of the galectin-1 protein on in vivo and in vitro models of ocular inflammation', *Mol Vis*, 21: 1036-50.

Zhang, K., J. J. Hopkins, J. S. Heier, D. G. Birch, L. S. Halperin, T. A. Albini, D. M. Brown, G. J. Jaffe, W. Tao, and G. A. Williams. 2011. 'Ciliary neurotrophic factor delivered by encapsulated cell intraocular implants for treatment of geographic atrophy in age-related macular degeneration', *Proc Natl Acad Sci U S A*, 108: 6241-5.

Zhang, L. Q., H. Cui, Y. B. Yu, H. Q. Shi, Y. Zhou, and M. J. Liu. 2019. 'MicroRNA-141-3p inhibits retinal neovascularization and retinal ganglion cell apoptosis in glaucoma mice through the inactivation of Docking protein 5-dependent mitogen-activated protein kinase signaling pathway', *J Cell Physiol*, 234: 8873-87.

Zhang, S., and W. Cui. 2014. 'Sox2, a key factor in the regulation of pluripotency and neural differentiation', *World J Stem Cells*, 6: 305-11.

Zhang, X. M., and X. J. Yang. 2001. 'Regulation of retinal ganglion cell production by Sonic hedgehog', *Development*, 128: 943-57.

Zhang, X., K. Tenerelli, S. Wu, X. Xia, S. Yokota, C. Sun, J. Galvao, P. Venugopalan, C. Li, A. Madaan, J. L. Goldberg, and K. C. Chang. 2020. 'Cell transplantation of retinal ganglion cells derived from hESCs', *Restor Neurol Neurosci*, 38: 131-40.

Zhang, Z., X. Luo, S. Ding, J. Chen, T. Chen, X. Chen, H. Zha, L. Yao, X. He, and H. Peng. 2012. 'MicroRNA-451 regulates p38 MAPK signaling by targeting of Ywhaz and suppresses the mesangial hypertrophy in early diabetic nephropathy', *FEBS Lett*, 586: 20-6.

Zhong, X., X. Qian, G. Chen, and X. Song. 2019. 'The role of galectin-3 in heart failure and cardiovascular disease', *Clin Exp Pharmacol Physiol*, 46: 197-203.

Zhou, S., A. Flamier, M. Abdouh, N. Tetreault, A. Barabino, S. Wadhwa, and G. Bernier. 2015. 'Differentiation of human embryonic stem cells into cone photoreceptors through simultaneous inhibition of BMP, TGFbeta and Wnt signaling', *Development*, 142: 3294-306.

8. APPENDIX

8.1 Primary Antibodies

Primary Antibodies Used

Target	Species	Cat no.	Titres		Supplier
			IHC	WB	
Gal-1	goat	AF1152	1/200	1/1000	ThermoFisher
Gal-3	Rabbit	ab76245	1/200	1/1000	Abcam
Gal-3	goat	AF1197	1/100	1/500	R&D Systems
aSMA	Rabbit	ab5694	1/200		Abcam
CD68	Mouse	ab31630	1/200		Abcam
Phospho-p44/42	Rabbit	4370		1/1000	Cell Signaling
p44/42	Rabbit	4695		1/1000	Cell Signaling
Phospho-SMAD2/3	Rabbit	3108S		1/250	Cell Signaling
SMAD2/3	Rabbit	3102		1/250	Cell Signaling
Phospho-STAT3	Rabbit	9145S		1/500	Cell Signaling
STAT3	Rabbit	4904S		1/500	Cell Signaling
Non-phospho-β-Catenin	Rabbit	8814S		1/500	Cell Signaling
β-Catenin	Rabbit	58480S		1/500	Cell Signaling

Table 8-1 Primary antibodies used, their titres for immunohistochemistry (IHC), and western blot (WB).

8.2 Original Immunoblots

This section includes original western blot membranes included in previous sections.

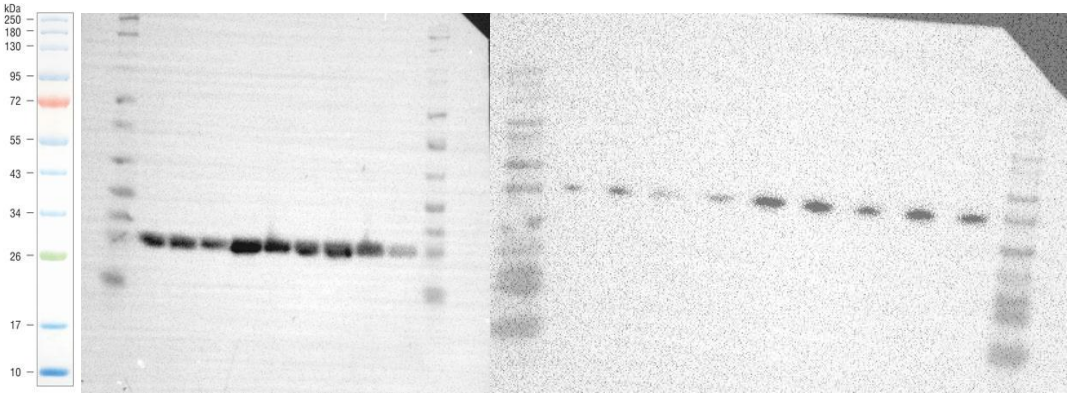

Figure 8-1 Immunoblots demonstrating Gal-1 downregulation following siRNA transfection, showing Gal-1 protein (left) and β-Actin (right), section 3.2.2.

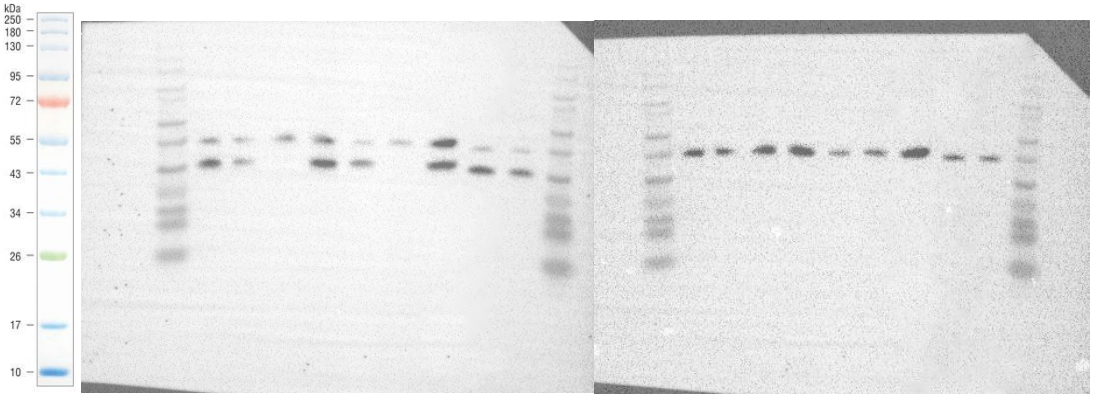

Figure 8-2 Immunoblots demonstrating Gal-3 downregulation following siRNA transfection, showing Gal-3 protein (left) and β-Actin (right), section 3.2.2.

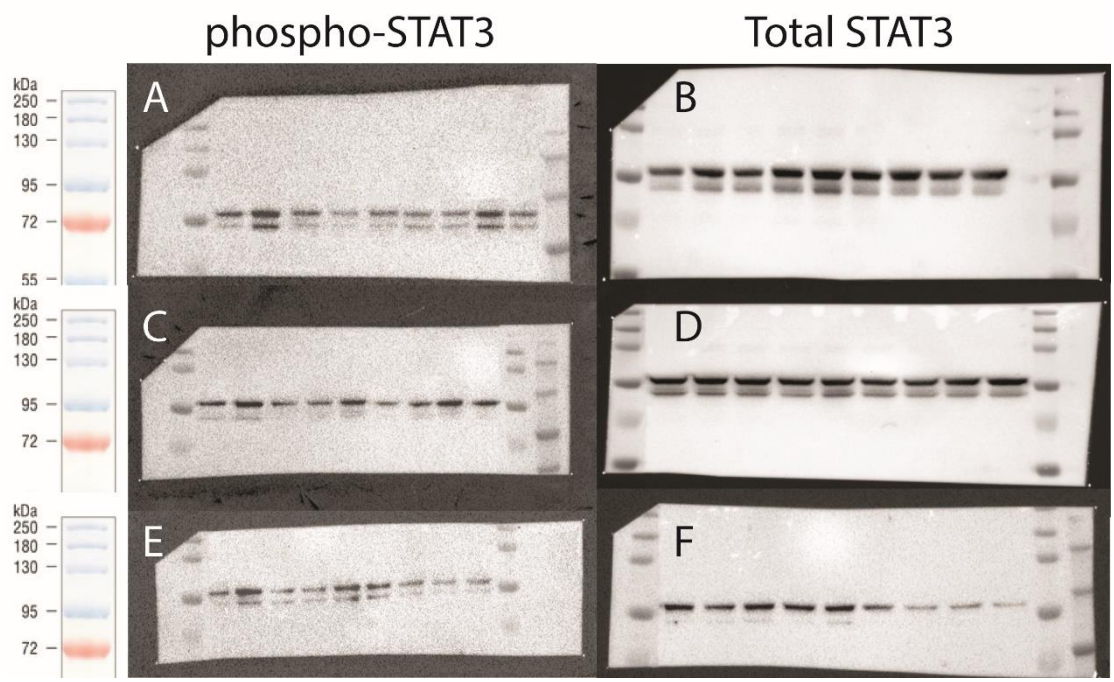

Figure 8-3 Immunoblots demonstrating STAT3 protein phosphorylation at 60 minutes following TNF-α treatment, (A, C, E) phospho-STAT3 protein, (B, D, F) total STAT3 protein, section 3.2.7.

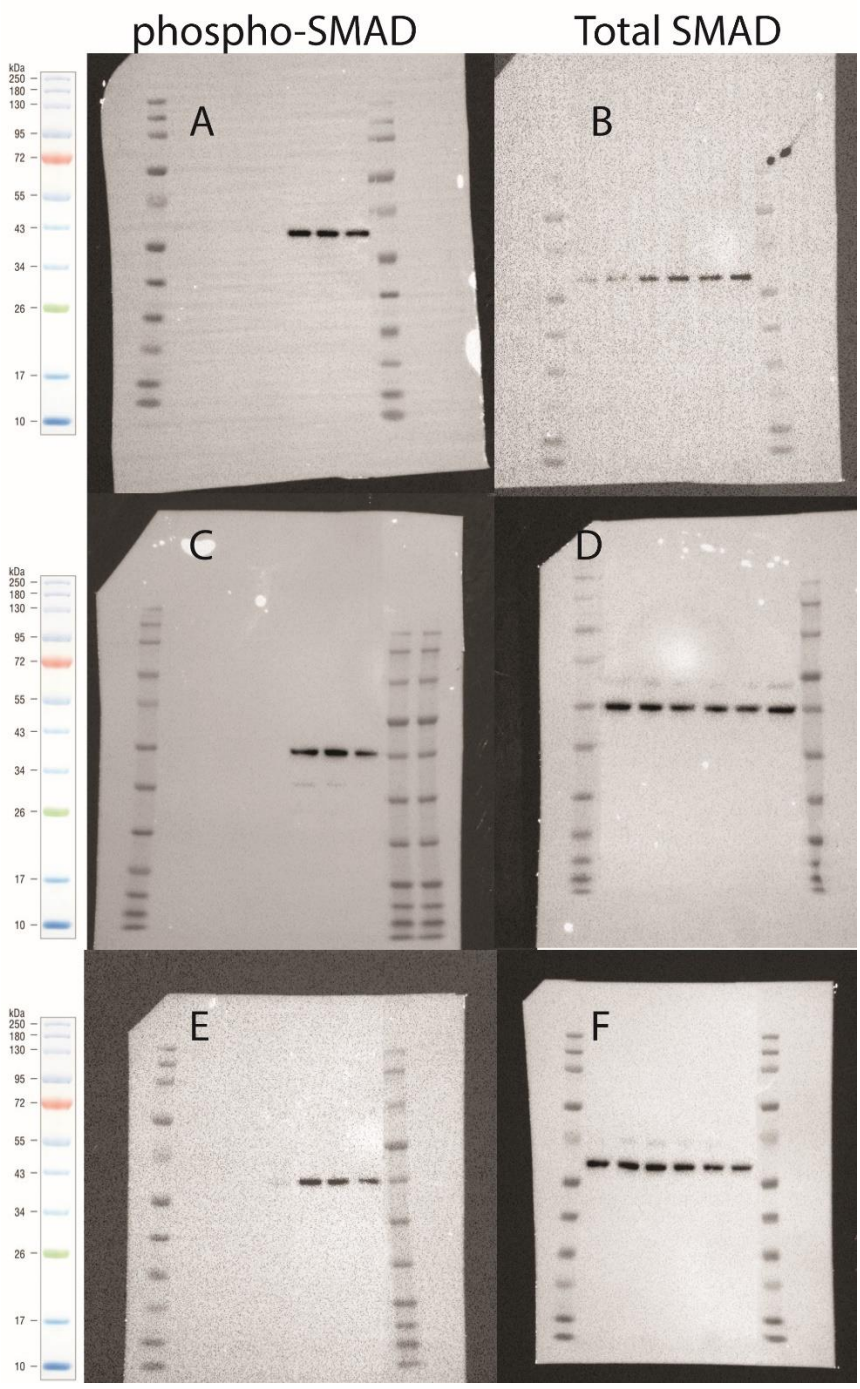

Figure 8-4 Immunoblots demonstrating SMAD protein phosphorylation at 60 minutes following TNF-α treatment, (A, C, E) phospho-SMAD protein, (B, D, F) total SMAD protein, section 3.2.7.

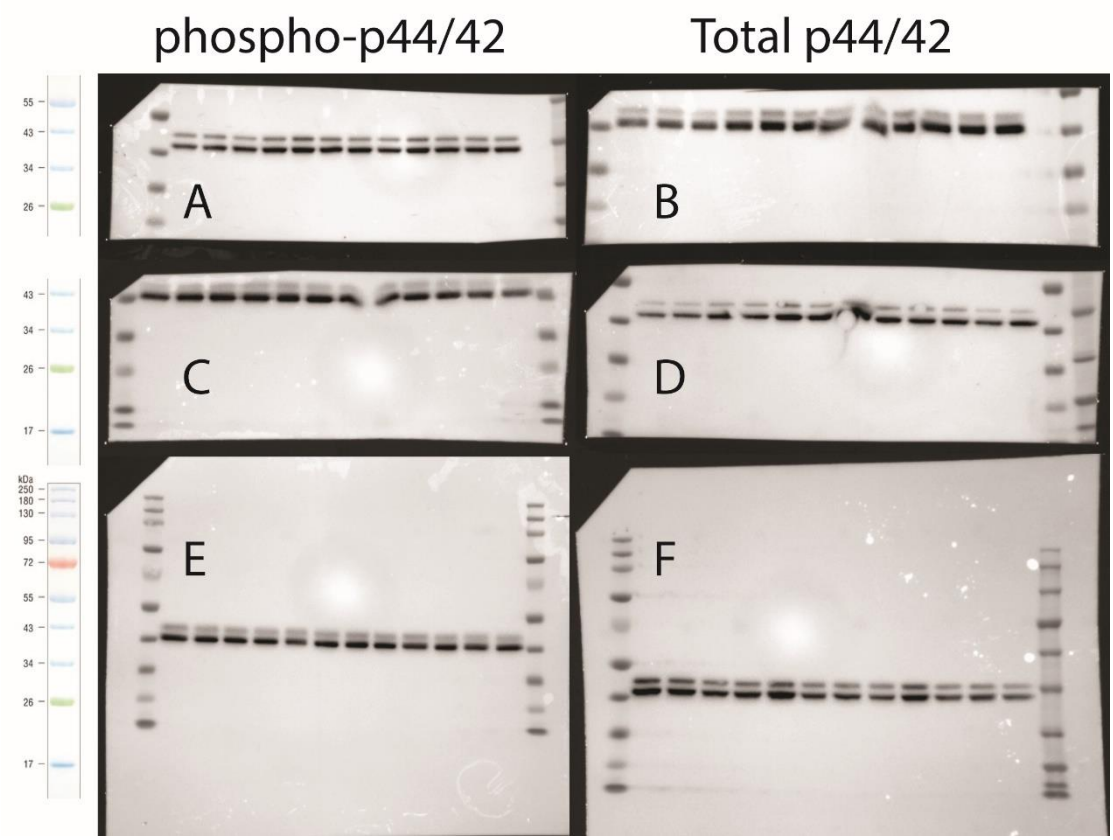

Figure 8-5 Immunoblots demonstrating p44/42 protein phosphorylation at 60 minutes following TGF-β treatment, (A, C, E) phospho-p44/42 protein, (B, D, F) total p44/42 protein, section 3.2.7.

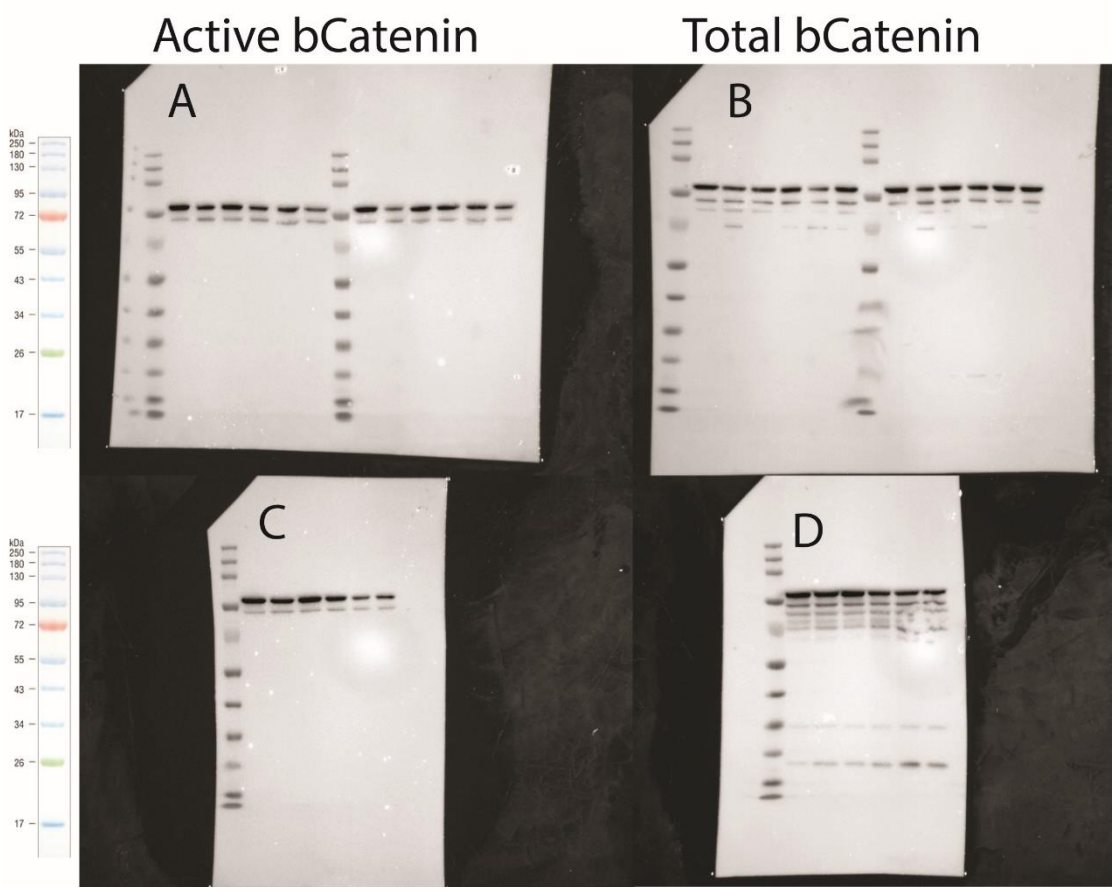

Figure 8-6 Immunoblots demonstrating β-catenin protein phosphorylation at 24 hours following Wnt antagonist treatment, (A, C) active (non-phosphorylated) β-catenin protein, (B, D) total β-catenin protein, section 3.2.7.